DEEP-SEA OCTOCORALS:

DATING METHODS, STABLE ISOTOPIC COMPOSITION, AND PROXY RECORDS OF THE SLOPEWATERS OFF NOVA SCOTIA

by

Owen A. Sherwood, B.Sc., M.Sc.

Submitted in partial fulfillment of the requirements for the degree of
Doctor of Philosophy

at

Dalhousie University
Halifax, Nova Scotia
June 2006

Distribution License

DalSpace requires agreement to this non-exclusive distribution license before your item can appear on DalSpace.

NON-EXCLUSIVE DISTRIBUTION LICENSE

You (the author(s) or copyright owner) grant to Dalhousie University the non-exclusive right to reproduce and distribute your submission worldwide in any medium.

You agree that Dalhousie University may, without changing the content, reformat the submission for the purpose of preservation.

You also agree that Dalhousie University may keep more than one copy of this submission for purposes of security, back-up and preservation.

You agree that the submission is your original work, and that you have the right to grant the rights contained in this license. You also agree that your submission does not, to the best of your knowledge, infringe upon anyone's copyright.

If the submission contains material for which you do not hold copyright, you agree that you have obtained the unrestricted permission of the copyright owner to grant Dalhousie University the rights required by this license, and that such third-party owned material is clearly identified and acknowledged within the text or content of the submission.

If the submission is based upon work that has been sponsored or supported by an agency or organization other than Dalhousie University, you assert that you have fulfilled any right of review or other obligations required by such contract or agreement.

Dalhousie University will clearly identify your name(s) as the author(s) or owner(s) of the submission, and will not make any alteration to the content of the files that you have submitted.

If you have questions regarding this license please contact the repository manager at dalspace@dal.ca.

Grant the distribution license by signing and dating below.

_____ _____

Name of signatory Date

DALHOUSIE UNIVERSITY
DEPARTMENT OF EARTH SCIENCE

The undersigned hereby certify that they have read and recommend to the Faculty of Graduate Studies for acceptance a thesis entitled:

"DEEP-SEA OCTOCORALS: DATING METHODS, STABLE ISOTOPIC COMPOSITION, AND PROXY RECORDS OF THE SLOPEWATERS OFF NOVA SCOTIA"

by Owen A. Sherwood

in partial fulfillment of the requirements for the degree of Doctor of Philosophy.

Dated: June 17, 2006

Supervisor: _____

Readers: _____

_____

_____

_____

_____

_____

DALHOUSIE UNIVERSITY

DATE: June 16, 2006

AUTHOR: Owen A. Sherwood

TITLE: DEEP-SEA OCTOCORALS: DATING METHODS, STABLE ISOTOPIC COMPOSITION, AND PROXY RECORDS OF THE SLOPEWATERS OFF NOVA SCOTIA

DEPARTMENT OR SCHOOL: Department of Earth Sciences

DEGREE: Ph.D. CONVOCATION: October YEAR: 2006

For Grandma,

who was always interested.

TABLE OF CONTENTS

LIST OF TABLES

LIST OF FIGURES

ABSTRACT

For generations, fishermen in Atlantic Canada have known about corals or "trees" growing in the deep waters along the shelf break. Scientific interest dates back to the 1880s, when Gloucester Fisheries collected specimens for the Smithsonian. In recent years, growing concern about the rate and scale of climate change has prompted an examination of climate records encoded in deep-sea coral skeletons.

Focusing on the gorgonian species *Primnoa resedaeformis*, this thesis examines the paleoceanographic utility of deep-sea octocorals. With a lifespan of 700+ years, *P. resedaeformis* is the longest-living octocoral, and one of the oldest animals in the sea. Unlike their aragonitic counterparts, the scleractinians, octocorals secrete a 2-part skeleton of calcite and gorgonin, a protein. The calcite is derived from dissolved inorganic carbon at depth, while the gorgonin is derived from recently exported particulate organic matter. The gorgonin is resistant to organic diagenesis, as revealed by the amino acid composition of a nearly 2000 year old sub-fossil specimen. Clues about past environmental conditions are encoded in the chemical make-up of annual rings secreted over the lifetime of the coral. The 2-part skeleton calcite and gorgonin thus constitutes a record of surface- and deep- water properties alike.

Development of calcite- and gorgonin-based proxy records from *P. resedaeformis* sheds new light on the slopewater system off the Scotian Shelf/Gulf of Maine. From the skeletal calcite, a record of $\Delta^{14}C$ documents decadal-scale shifts in ^{14}C reservoir age of

upper intermediate waters. From the skeletal gorgonin, stable C and N isotopic composition presents a more complicated picture of the surface water environment. Following nearly 2000 years of relatively constant values, $\delta^{15}N$ rapidly decreased during the 20th century. As a possible cause for the observed trend, a weakening of the Labrador Current is suggested, but a trophic cascade presents a plausible alternative hypothesis. Methods developed herein may be expanded to other oceanographic regions where proxy climate data are lacking.

LIST OF ABBREVIATIONS USED

AAR	Amino Acid Racemization
AAIW	Antarctic Intermediate Water
AMS	Accelerator Mass Spectrometry
AOU	Apparent Oxygen Utilization
B/P	Benthic Foraminifera-Planktic Foraminifera dating method
CSWS	Coupled Slope Water System
COC	Centre of Calcification
DIC	Dissolved Inorganic Carbon
DOM	Dissolved Organic Matter
ECF	Extracellular Calcifying Fluid
ENSO	El Niño / Southern Oscillation
IRMS	Isotope Ratio Mass Spectrometry
LA-ICP-MS	Laser-Ablation Inductively Coupled Plasma Mass Spectrometry
LShW	Labrador Shelf Water
LSW	Labrador Slope Water
NAO	North Atlantic Oscillation
POM	Particulate Organic Matter
SEM	Scanning electron microscope
SOM	Sedimentary organic matter
TL	Trophic Level
WSW	Warm Slope Water

ACKNOWLEDGEMENTS

This thesis would not have been completed without the help of many people. My supervisor, Dave Scott, provided constant support, encouragement. Mike Risk got me interested in corals in first place, and helped me to focus on the bigger picture. Several people offered advice and constructive criticism over the years: Kumiko Azetsu-Scott, Evan Edinger, Hermann Ehrlich, John Gosse, Jeff Heikoop, Claude Hillaire-Marcel, Brian Petrie, Dan Sinclair and Branwen Williams. For laboratory analyses, I am especially indebted to Steve deVogel, Bassam Ghaleb, Tom Guilderson, Moritz Lehmann, Jennifer McKay and Patricia Stoffyn. Lawrence Plug helped with Matlab programming. The pioneers of Canadian deep-sea coral research - Sanford Atwood, Derek Jones, Ronnie Wolkins - kindly donated many priceless chunks of coral. To my friends in Halifax - Jane, Russ, Myles, Laurie, Flavia, Hawkes, Joyia, Tony, Jim, Barb, Jeremiah, Anastasia, Anne, Saka, Sophie - thanks for the good times. My family back maintained an interest in my weird specialty, and their support was invaluable. Finally, my biggest thanks go to Christine, with whom there's never a dull moment!

CHAPTER 1

GENERAL INTRODUCTION

In the 1990s, Nova Scotia fishermen forced deep-sea corals onto the radar screens of Canadian scientists. Knowing full-well the link between coral habitat and fishing success, their interest was in saving deep-sea corals from bottom dragging. Their efforts ultimately led to the establishment in 2002 of a 424 km^2 Coral Conservation Area[1] in the Northeast Channel, a 250 m deep canyon southwest of Cape Sable, Nova Scotia. This area is noted for dense thickets of gorgonian corals (Breeze et al., 1997; MacIssac et al., 2001), structurally unlike the *Lophelia* reefs characterizing the NE Atlantic (e.g. Fössa et al., 2002), but important fish habitat nonetheless. Conservation concerns propelled deep-sea corals into the media spotlight; but, for earth scientists, deep-sea corals present a fascinating new archive of climate change.

We hear how global warming could trigger unexpected changes in the North Atlantic thermohaline circulation, with uncertain consequences for the stability of global climate (IPCC, 2001; Bryden et al., 2005; Overpeck et al., 2006). The geologic record, upon which climate predictions largely rely, provides us with long term averages. What happened in the past on shorter timescales, the human timescale, constitutes a major gap in knowledge. On land, the gap is partly filled by tree rings and ice cores providing annually-resolved records in the form of tree rings or ice layers. In the oceans, tropical reef corals do much the same, in the form of annually-banded carbonate skeletons.

[1] DFO Backgrounder on Coral Research and Conservation: http://www.mar.dfo-mpo.gc.ca/communications/maritimes/back02e/B-MAR-02-(5E).html

Outside the warm, shallow tropics, high resolution marine proxy records are virtually absent.

Several studies on deep scleractinian (aragonite-secreting) corals firmly establish this group as a key tool in paleoceanographic studies (e.g. Smith et al., 1997; Robinson et al., 2005). This thesis explores the paleoceanographic potential of the deep-sea gorgonian coral *Primnoa resedaeformis*. This species looks and grows very much like a tree, with an unusual 2-part skeleton of calcite and gorgonin, the latter being a durable protein. The presence of skeletal growth rings of presumed annual timing suggested earlier on that records of ambient environmental conditions may be encoded in the skeletons, year by year, over the centuries (Heikoop et al., 2002; Risk et al., 2002; Sherwood 2002).

The promise of new and exciting climate records notwithstanding, several basic questions about *Primnoa* had yet to be answered, for instance, "How long do they live?", "Are the skeletal growth rings really annual?", and "What do they eat?". This thesis addresses several basic questions about the biology and geochemistry of *Primnoa*. The focus is primarily on the skeletal gorgonin fraction, as its geochemical link to the surface water environment, via the sinking of plankton, presented novel research. The scope of the research presented here was largely driven by sample availability: specimens were donated by fishermen or obtained from limited scientific surveys.

Each chapter is presented as a stand-alone manuscript. Three of the chapters have been published at the time of this writing; another is due for publication in autumn 2006.

Parts of Chapters 6 and 7 were presented as abstracts at meetings. The ordering of chapters strives for a smooth flow of logic, each chapter building on previous chapters. This was not always possible, however, as the desire to submit publishable results took precedence over the execution of each project in an orderly sequence.

Chapter 2, “Deep-Sea Corals: New Insights to Paleoceanography” was prepared as a chapter on deep-sea corals for a special volume on methods in late Cenozoic paleoceanography, to be published in autumn, 2006. This chapter reviews applications of deep-sea corals in paleoceanography, with a focus on methodological aspects. Most of the attention is given to scleractinians, as opposed to octocorals, as the number of studies on the former far outweighs the latter. As the manuscript is intended for publication, some of the material is reproduced from later chapters of this thesis.

Chapter 3, "Radiocarbon Evidence for Annual Growth Rings in a Deep-Sea Octocoral (*Primnoa resedaeformis*)” was published in the journal Marine Ecology Progress Series in October, 2005. This manuscript presents incontrovertible proof for the annual timing of growth ring formation in the inner, organic-rich regions of *Primnoa* skeletons. Indeed, this was the first solid proof for annual ring timing in any octocoral species, whereas previous studies relied on more circumstantial evidence.

Chapter 4, “Stable Isotopic Composition of Deep-Sea Gorgonian Corals (*Primnoa* spp.): a new archive of surface processes” was published as a companion to Chapter 3 in the journal Marine Ecology Progress Series in October, 2005. This manuscript

investigates the stable C and N isotopic composition among *Primnoa* spp. collected in the Atlantic and Pacific Oceans and the Sea of Japan. Special attention is paid to the intra- and inter-colony reproducibility of $\delta^{13}C$ and $\delta^{15}N$, and in elucidating the trophic level of *Primnoa* with $\delta^{15}N$.

Chapter 5, "Late Holocene Radiocarbon and Aspartic Acid Racemization Dating of Deep-Sea Octocorals" was published in the journal Geochimica et Cosmochimica Acta in June, 2006. Some of these data were also published as an abstract in the 2005 Proceedings of the North American Paleontology Conference. This study into amino acid racemization (AAR) dating of corals was undertaken as a side-project funded through a Geological Society of America student grant. The results of the AAR dating were not encouraging. On the other hand, one of the sub-fossil corals had a radiocarbon-dated lifespan of 700 years, the longest-lived octocoral ever documented.

Chapter 6, "Carbon-14 Records From the Calcite Phase of Deep-Sea Octocorals" has not been submitted for publication at the time of this writing. Whereas most of the thesis explores the geochemistry of the organic fraction of *Primnoa*, this chapter explores the proxy records from the calcite fraction. Much attention is given towards chronological aspects (bomb-^{14}C dating and ^{210}Pb) because growth banding in the skeletal calcite is poorly defined. Accurate reconstruction of the anthropogenic Pb pulse demonstrates that useful proxy information is encoded in the trace elemental profiles from the calcite. Profiles of $\Delta^{14}C$ track shifts in slopewater reservoir age over time.

Chapter 7, "Stable C and N Isotopic Records from Deep-Sea Octocorals Parallel Recent Changes in the Slopewater System off Nova" focuses on recent and longer term patterns in stable C and N records. Parts of these data were presented at the 3rd International Symposium on Deep-Sea Corals in November, 2005, and at the May, 2006 meeting of the Geological Association of Canada. Several records of $\delta^{13}C$ and $\delta^{15}N$ are patched together to cover most of the last ~300 years, with additional data from ~ 400 AD. The recent trends are correlated with the presence of warm vs. cold slopewaters, while the longer term trend is towards isotopic depletion in the 20th century. Competing hypotheses regarding the cause of observed correlations are presented, including a decline in the relative strength of the Labrador Current, and a trophic cascade brought on by overfishing.

With rare exception, the conceptualization, sample preparation, data analysis, and writing of this thesis was completed entirely by O. Sherwood. M. Risk drafted the introductory paragraphs of Chapter 2. J. Heikoop initiated some of the ideas, and performed some of the isotopic measurements presented in Chapter 4. All chemical analyses were outsourced to other laboratories.

CHAPTER 2

DEEP-SEA CORALS: NEW INSIGHTS TO PALEOCEANOGRAPHY

Owen A. Sherwood [1], Michael J. Risk [2]

[1] Centre for Environmental and Marine Geology, Dalhousie University, Halifax, Canada

[2] School of Geography and Geology, McMaster University, Hamilton, Canada

Manuscript prepared for: "Late Cenozoic Paleoceanography Volume 1: Methods"

(for publication in autumn 2006)

2.1 INTRODUCTION

Deep-sea corals were first described from the coast of Norway, and the first species identified by Linnaeus (1758). Since then, at least until recently, interest in the group has waxed and waned, seemingly in concert with the frequency of their relationship with fishing efforts on the continental shelves.

In recent years, two critical concerns have heightened interest in deep-sea corals. Worldwide decline of coastal fisheries, especially off the shelves on eastern North America, has prompted a re-examination of the role of deep-sea corals as habitat for fishes. In addition, concern about the rate and scale of climate change has combined with the growing realisation that this process can best be measured by using the records encoded in coral skeletons. Instrumental records are not sufficiently widespread or long-standing to allow predictive models to be constructed, and proxy records have to be consulted. Other than deep-sea corals, few archives offer the combination of global distribution (Fig. 2.1), temporal resolution, and duration of record. In this chapter, when we speak of deep-sea "corals", we are referring not only to the true corals, the Scleractinia (which date from the Triassic) but any coelenterate that makes a hard skeleton capable of recording climate data (Fig. 2.2). This would include several orders that secrete a horny skeleton, such as Octocorals, (Ordovician-recent), Antipatharians (Miocene-recent) and Zoanthids (recent).

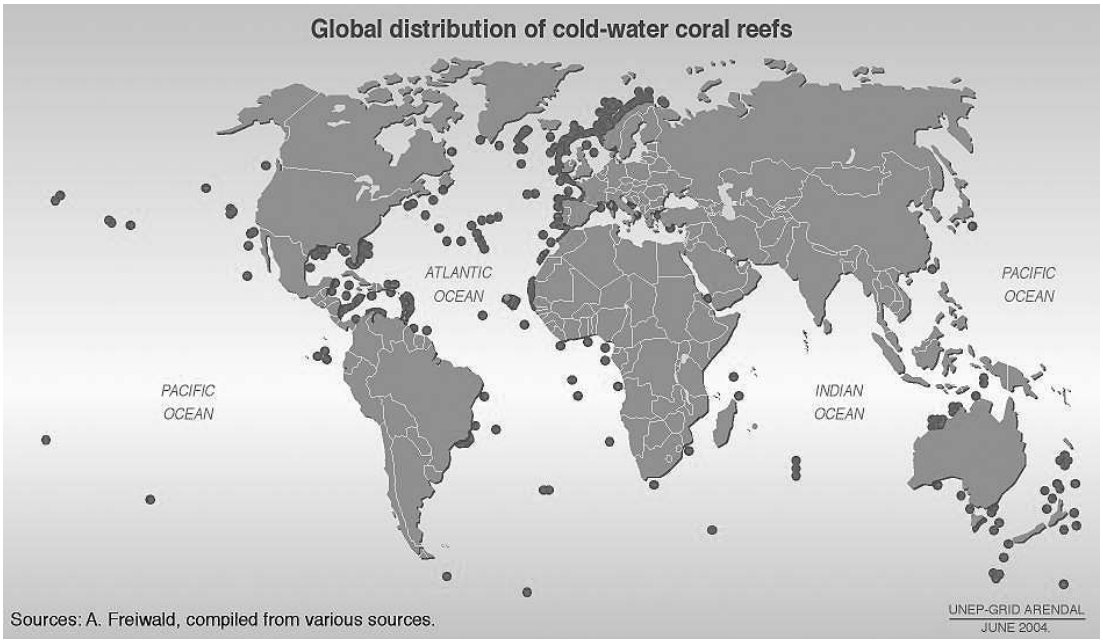

Fig. 2.1: Global distribution of deep-sea coral reefs. Points on the map indicate observed reefs of varying size and stages of development but not the actual area covered. The high density of reefs shown in the North Atlantic reflects the intensity of research in this region. Further discoveries are expected worldwide, particularly in the deeper waters of subtropical and tropical regions. Figure from André Freiwald.

2.1.1 Overview of past work on geochemistry of deep-sea corals

Previous attempts several decades ago to decipher the climate record in deep-sea corals from stable isotope analyses were overshadowed by the upsurge in interest in records from shallow-water reef corals. Weber (1973) found that deep-sea corals were generally less depleted in $\delta^{18}O$ and $\delta^{13}C$ than were reef corals; Emiliani et al. (1978) described a series of analyses of subsamples of corals from the Blake Plateau, off Florida, and found a progressive up-polyp closer approach to equilibrium values.

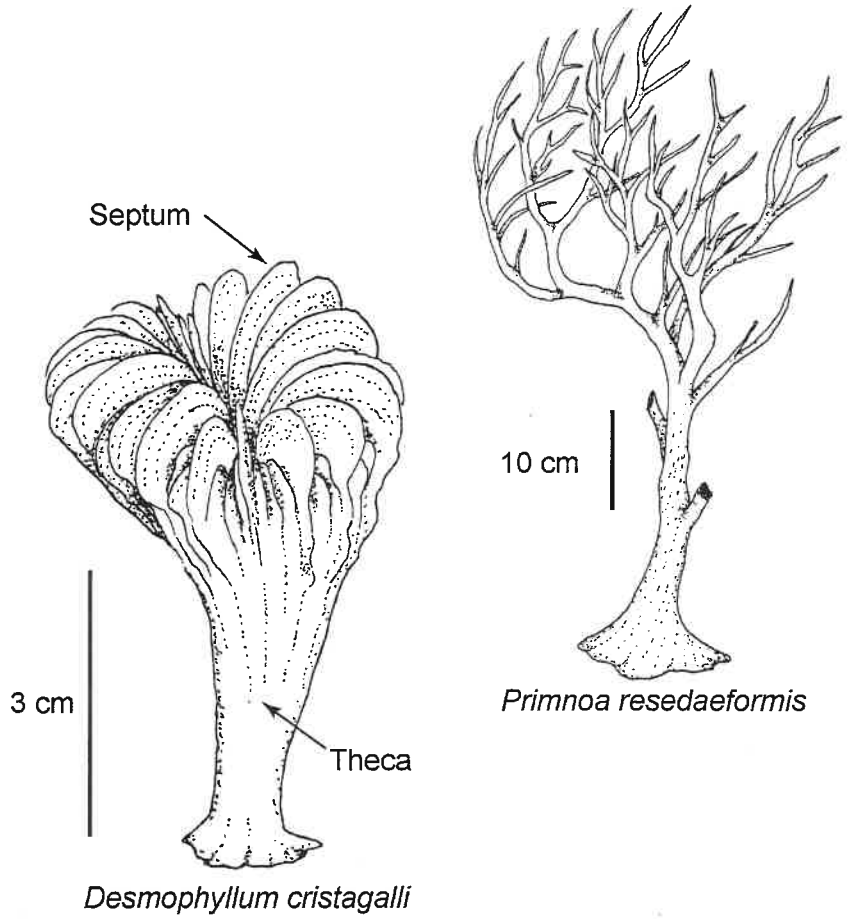

Fig. 2.2: Two of the deep-sea scleractinian (*D. cristagalli*, a.k.a. *D. dianthus;* redrawn from Cairns, 1981) and horny corals (*P. resedaeformis*) discussed in this chapter.

Since the early 1970's, paleoceanographic studies have relied heavily on cores from reef corals. Two examples, from hundreds of papers, involve our understanding of El Niño-Southern Oscillation (ENSO) events. Carriquiry et al. (1988) were the first to establish the record of the timing and intensity of such an event, working up the stable isotopic record in reef corals from the west coast of Costa Rica. Tudhope et al. (2001) analysed cores from the superbly-exposed and preserved reef terraces of Papua New

Guinea, and found that ENSO events have existed for at least the past 130,000 years, and that they continued even through glacial times. They also found that ENSO events of the 20th century were stronger than in past glacial or interglacial times. Cores from reef corals can frequently span centuries: Hendy et al. (2002) were able to go back in time more than 400 years.

Most of the work on reef coral cores has emphasized temperature determinations, using the $\delta^{18}O$ paleothermometer. More than temperature can be determined from these cores, however: Fallon et al. (2002) used reef coral cores to determine the impact of mining on the waters around Misima Island, Papua New Guinea, and Heikoop et al. (1996) found the hydrothermal pulse associated with a volcanic eruption in the Banda islands, Indonesia, recorded in corals near the eruption site. As useful and as flexible as the reef coral record is, however, it suffers from severe geographical restrictions. To state the obvious, reef coral records may only be obtained where reef corals grow: warm, shallow waters. The most dynamic oceanographic processes are frequently located deeper in the water column and further toward the poles.

The mid-90's saw increased interest in the records from deep-sea corals, sparked by two key papers. Druffel et al. (1995) determined an age of approximately 1800 years for an individual *Gerardia* (zoanthid) collected off Little Bahama Bank, suggesting that these organisms were perhaps the oldest living species in the ocean, rivaling Bristlecone Pines for the title of longest-lived organisms on the planet. They further suggested (p. 5031) "there is potential for *Gerardia* to serve as a millennial-scale integrator of upper

ocean particle flux, and possibly reveal past changes in the productivity of the surface ocean." Smith et al. (1997) analysed a suite of *Desmophyllum dianthus* from off Orphan Knoll, off the Newfoundland slope. The record of one pseudocolony captured a rapid cooling of intermediate waters at the onset of the Younger Dryas (~13 ka BP). Their analyses showed that this took place in as little as five years, a startling find for the time.

The field has expanded dramatically in the past decade. At the Third International Symposium on Deep-Sea Corals, held in Miami in Nov-Dec 2005, there were climate-related papers from authors from almost 20 different countries.

2.1.2 Advantages of the deep-sea coral archive

To be accepted as dependable, any climate proxy extracted from organisms or sediments must be diagenetically stable, reproducible among specimens, and must faithfully record data of climatic significance. Advantages would be longevity, wide geographic and depth ranges, ease of analysis and abundance. Deep-sea corals fulfill all these criteria, with the possible exception of abundance. So-called deep-sea corals in fact range from depths of only a few metres (in places like Alaska and Chile), to > 4 km, and in all oceans, but they are by no means abundant. In many cases, such as much of our own work, adventitious or opportunistic samples may be obtained from cultivating good relationships with fishermen, or from accidental trawl hauls. Samples specific to a given research project may be collected using deep submersibles, all of which are very expensive, and the use of which is mostly restricted to developed nations.

Although Scleractinians are relatively common and widespread in the deep-sea, obtaining long, coherent climate records from their skeletons can be challenging. They are usually small, less than 5 cm in height, and their growth banding is exceedingly narrow, ca. 10 – 100 microns (Lazier et al., 1999; Sherwood 2002). Recent technological advances, however, such as microsamplers and microprobes, have made small sample sizes much less of a problem, and, whereas a century of reef-coral record could be carried on a strong shoulder (it could weigh ~100 kg), the same length of record in a deep-sea coral could be tucked in a shirt pocket. In the future, it is likely that more research will focus on horny corals, which have tree-like morphologies, and life-spans of several centuries (Druffel et al., 1990; Druffel et al., 1995; Risk et al., 2002; Sherwood et al., 2006).

In summary, deep-sea corals provide a widespread archive of oceanographic processes, with annual- to decadal-resolution records spanning several centuries in length. They are ideally suited to the study of rapid changes, such as that which characterized the Pleistocene-Holocene transition.

2.2 METHODS AND INTERPRETATIONS

2.2.1 Growth and sclerochronology in deep-sea scleractinians

Deep-sea scleractinians exhibit a wide variety of growth forms, from simple, solitary cup corals to complex, branching colonies (Fig. 2.2). A brief introduction to skeletal nomenclature is provided here, to facilitate the discussion of sclerochronology.

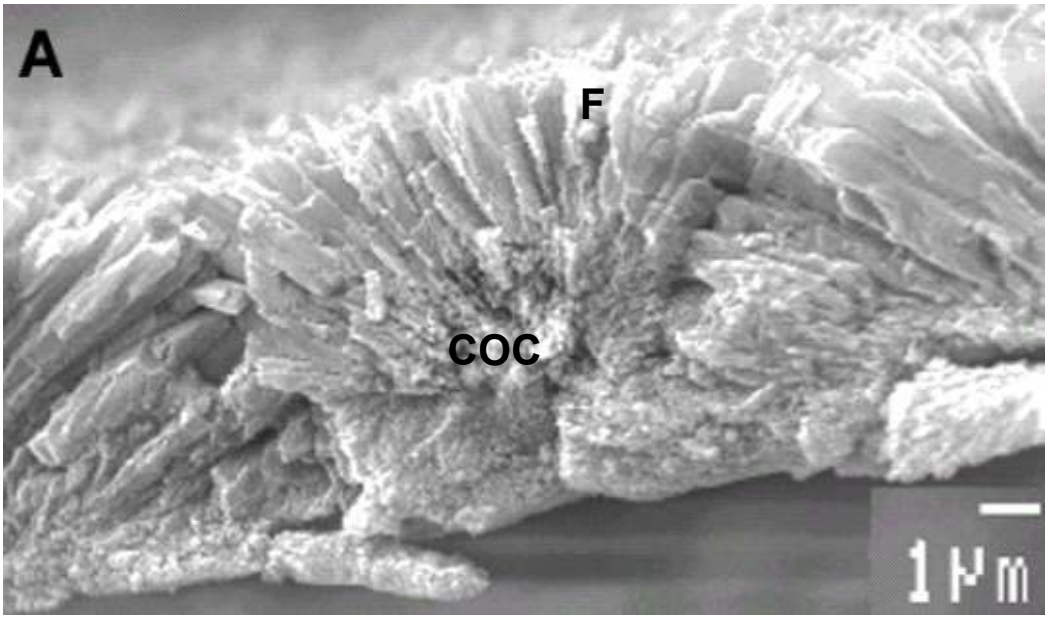

Fig 2.3: SEM image of centers of calcification (COC) and crystal fibres (F) in the (shallow-water) scleractinian coral *Porites lutea*. Note occlusion of crystal fibres at points of lateral interference. Image from Cohen and McConnaughey (2003).

The animal itself, the polyp, ranges from a few mm to several cm in diameter. The polyp sits atop a vertical calcified tube, the corallite, supported by a thin horizontal plate called the dissepiment. The corallite is lengthened by periodic uplift of the polyp and formation of a new dissepiment. The wall of the corallite is called the theca. A series of thin vertical sheets, the septa, radiate from the theca into the center of the corallite.

At the microscopic scale, all the coral structures share a common mode of crystal nucleation and growth. The extending tips of structures comprise so-called "centers of calcification" (COCs; see review in Cohen and McConnaughey, 2003). Crystal nucleation occurs in the COCs, producing randomly-oriented microgranules. In thin

section, COCs appear opaque. Thickening of the skeletal structures is achieved by the growth of crystal fibres (Fig. 2.3). Fan-shaped bundles of fibres (spherulites) compete for space as they elongate (Barnes, 1970; Gladfelter, 1982). The fibres thus take on an increasingly preferred orientation further away from the COCs. Micro-banding on the growing fibres occurs with a periodicity of ca. 1 micron (Sorauf and Jell, 1977; Cuif and Dauphin, 2005). The fibrous region appears translucent in transmitted light, even though the crystals are more densely packed (Cohen et al., unpubl.). Crystal fibres comprise the bulk of coral skeletons.

Growth couplets consisting of alternating opaque-translucent band pairs (Fig. 2.4) are found in many deep-sea scleractinians, ranging from 0.1 to 0.75 mm in width (Mortensen and Rapp, 1998; Lazier et al., 1999, Cheng et al., 2000; Adkins et al., 2004; Cohen et al., unpubl.). The delicate, sheet-like septae usually exhibit the clearest banding where they have not been secondarily thickened (Lazier et al., 1999). Growth bands are visible in transverse and longitudinal sections of the theca, but these may be susceptible to dissolution where the living tissue does not envelop the outer skeleton (Lazier et al., 1999). Cohen et al. (unpubl.) relate opaque-translucent growth banding observed in *Lophelia pertusa* to the repetition of crystal nucleation and growth events. They suggest that the process of crystal nucleation and growth occurs quickly in succession, and that it may reflect a seasonal growth spurt followed by a dormant period. Obviously, this has an important consequence for the continuity of geochemical proxy records.

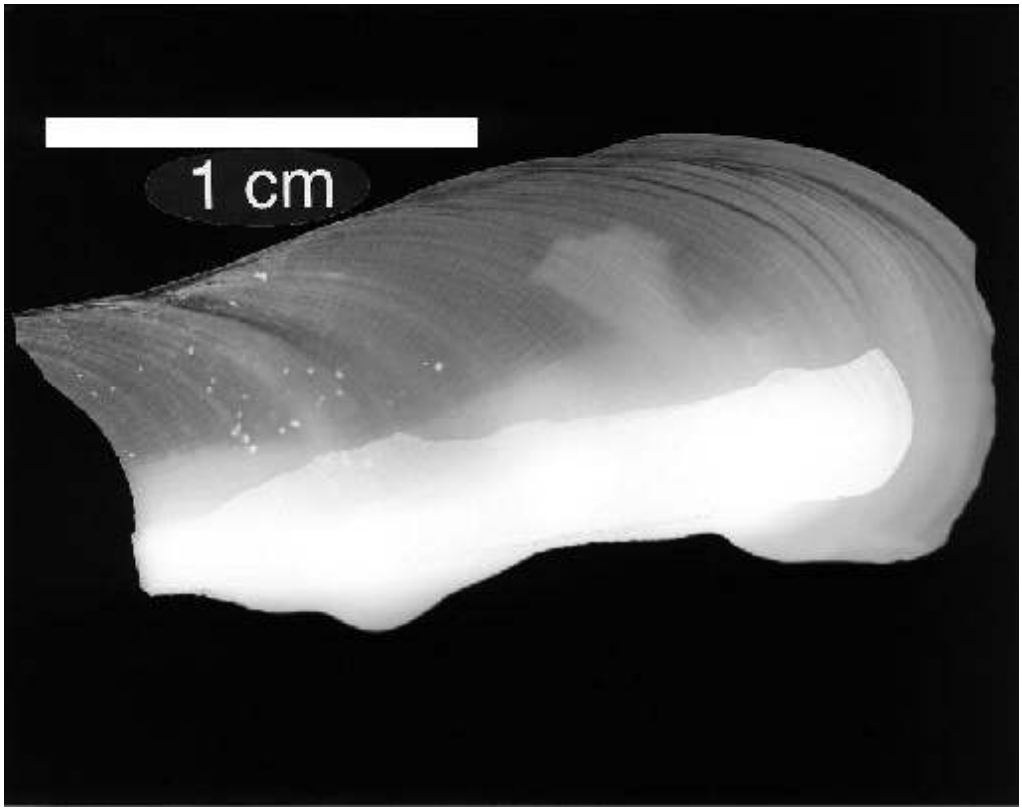

Fig. 2.4: Example of growth banding in a septum of the scleractinian coral *Desmophyllum dianthus*. White patch at bottom of image is where the theca was attached. Figure from Cheng et al. (2000).

The key utility of corals in paleoceanography is that long records of ambient conditions are locked into the growing skeleton in successive layers. When dealing with tropical reef scleractinians, massive colonies are selected for climate reconstructions because of the simplicity of their growth banding. Deep-sea scleractinians have more complicated cup and branching morphologies, making it difficult to visualize and sample the growth layers. The solitary cup corals are easier to deal with because they grow as one corallite over their 100+ year life-spans (Smith et al., 1997; Adkins et al., 1998; Cheng et al., 2000). Thus, the septa and theca exhibit the full complement of growth

layers over the lifespan of the coral (Fig. 2.4), provided that dissolution has not removed some of these layers (Lazier et al., 1999). Branching species are much more difficult to analyze because the individual corallites are relatively short lived. Although there are visible growth layers in the septa and theca of *Lophelia pertusa*, for example, they usually number < 10 (Mortensen and Rapp, 1998; Cohen et al., unpubl.). Theoretically, extended chronologies could be developed by tracking successive growth layers into younger corallites, but this has not been demonstrated. Also, Pons-Branchu et al. (2005) raise the possibility that growth in *L. pertusa* occurs in relatively short bursts, separated by long hiatuses.

In most cases deep-sea corals cannot be observed growing in their natural habitat (but see Mortensen and Rapp, 1998), so growth rates must be determined with radiometric dating techniques (e.g. U/Th, ^{226}Ra/Ba, ^{210}Pb or ^{14}C). Vertical growth rates range between 0.1 and 3 mm/yr for solitary corals (Cheng et al., 2000; Adkins et al., 2002; Adkins et al., 2004) and 2 and 5 mm/yr for branching corals (Mortensen and Rapp 1998, Adkins et al. 2004). Corresponding periodicities of growth banding range from 0.3 to 3 bands/yr in *Desmophyllum dianthus* (Cheng et al. 2000) to ~ 0.1 bands/yr in *Enallopsammia rostrata* (Adkins et al. 2004). Banding periodicity probably varies within and among different species depending on depth and environmental conditions. For this reason, banding periodicity should be assessed on a case-by-case basis. Since they often live in near-constant physical conditions, the causes of growth banding in deep-sea scleractinians remains "quite literally, in the dark" (Lazier et al., 1999). Overall, it appears that growth banding in deep-sea scleractinians is not a reliable chronometer in

most cases, and that skeletal chronologies must instead be established by radiometric dating methods.

2.2.2 Growth and sclerochronology in horny corals

Several genera of deep-sea fans (Octocorallia: Order Gorgonacea) form durable, long-lived, tree-like skeletons (Fig. 2.2). Compositionally, they differ from scleractinians in two key aspects. First, the carbonate phase is usually high magnesium calcite; but some species may deposit carbonate hydroxyapatite (Mcintyre et al., 2000). Relative to aragonite, the smaller lattice geometry of calcite favours co-precipitation of small cations such as Mg, and discriminates against larger cations, such as Sr and U. Second, the skeleton also contains a horny, fibrillar protein called gorgonin. The function of gorgonin is to lend flexibility to the otherwise stiff calcified skeleton (Grasshoff and Zibrowius, 1983; Lewis et al., 1992). Different regions of the skeleton may be composed of 'massive' (100%) calcite, 100% gorgonin, or a combination of both. For example, the Bamboo Corals (family Isididae) deposit gorgonin nodes, like the joints of a finger, between internodes of massive calcite. Red tree corals (family Primnoidae) deposit a 2-part calcite-gorgonin "horny axis" towards the inner part of the axial skeleton, and a massive calcite cortex later on.

At the microscopic scale, massive calcite structures in octocorals appear almost identical to the aragonite in scleractinians (Lewis et al. 1992; Sherwood, 2002; Bond et al. 2005). Calcite fibres grow in spherulitic fashion, the fibres nucleating on

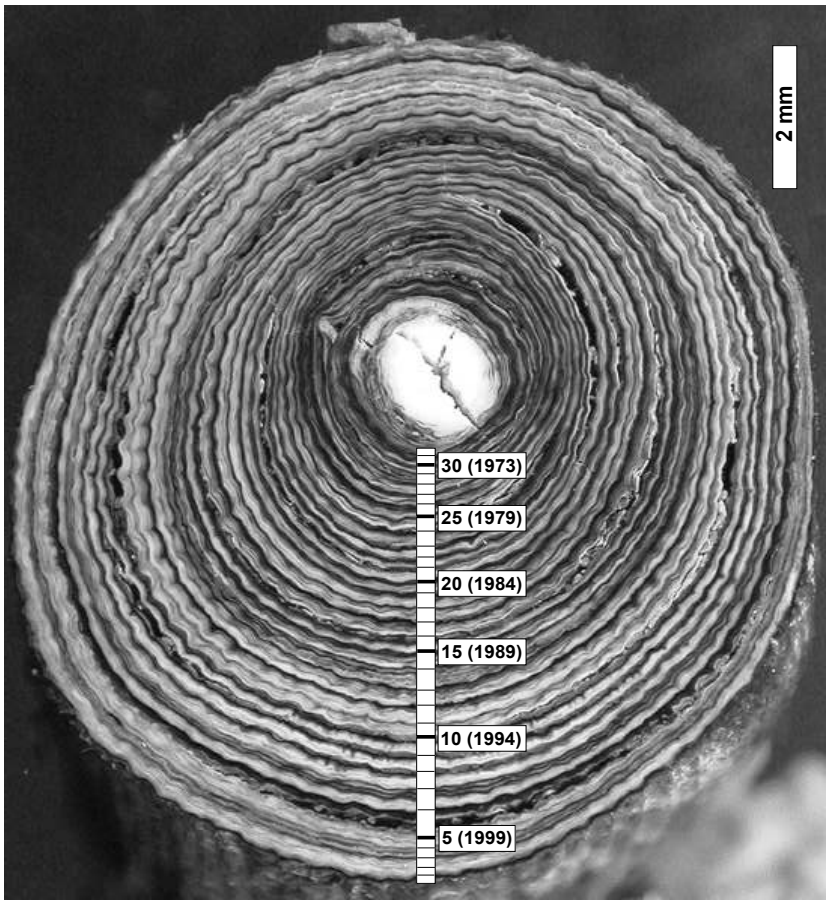

Fig. 2.5: Example of the annual growth rings in a young (30 year old) axial skeleton of the deep-sea gorgonian *Primnoa resedaeformis*. Markings show individual rings isolated for analysis, with corresponding calendar age (in brackets), as determined by amateur growth ring counters. Figure from Sherwood et al. (2005a).

gorgonin surfaces or COCs. Micro-banding on the growing fibres occurs with a periodicity of ca. 1 micron (Sherwood, 2002). Where calcite is embedded with gorgonin, the calcite fibres take on stubbier morphologies, perhaps indicating a different process or rate of biomineralization (Sherwood, 2002).

Growth rings in octocorals may be observed in either the massive calcite or horny regions of the skeleton (Fig. 2.5). In the massive calcite, the rings probably relate to the repetition of crystal growth and nucleation events. In the horny regions, the rings are produced by alternations in the ratio of gorgonin:calcite (Risk et al., 2002; Sherwood, 2002; Marschal et al., 2004), perhaps compounded by variations in the extent of protein tanning (Szmant-Froelich, 1974). Using bomb-^{14}C (Sherwood et al., 2005a) and ^{210}Pb-dating (Andrews et al., 2002) annual ring periodicity in the red tree coral *Primnoa resedaeformis* has been proven (Fig. 2.6). Finer-scale growth rings, possibly lunar in origin, have also been described in *P. resedaeformis* (Risk et al., 2002; Sherwood, 2002) making this species perhaps the highest resolution deep water archive in the world. Thresher et al. (2004) verified annual ring formation in the calcite internodes of the bamboo coral *Keratoisis spp.* Other studies report more diffuse banding patterns, with ambiguous periodicities (Druffel et al., 1990; Roark et al. 2005; Andrews et al. 2005). As with scleractinians, it is highly likely that the appearance and timing of rings depends on local environmental factors, such as the downward flux of organic matter from spring plankton blooms (Sherwood, 2002). In regions of the ocean where seasonal variability is attenuated, growth rings may not be as prominently developed.

Life-spans of octocorals often exceed several hundreds of years (Druffel et al., 1990; Risk et al., 2002; Andrews et al. 2002; Thresher et al. 2004; Roark et al. 2005), the oldest reported lifespan being a 700 yr old specimen of *P. resedaeformis* (Sherwood et al., 2006). Compared with deep-sea scleractinian corals, obtaining centuries-long

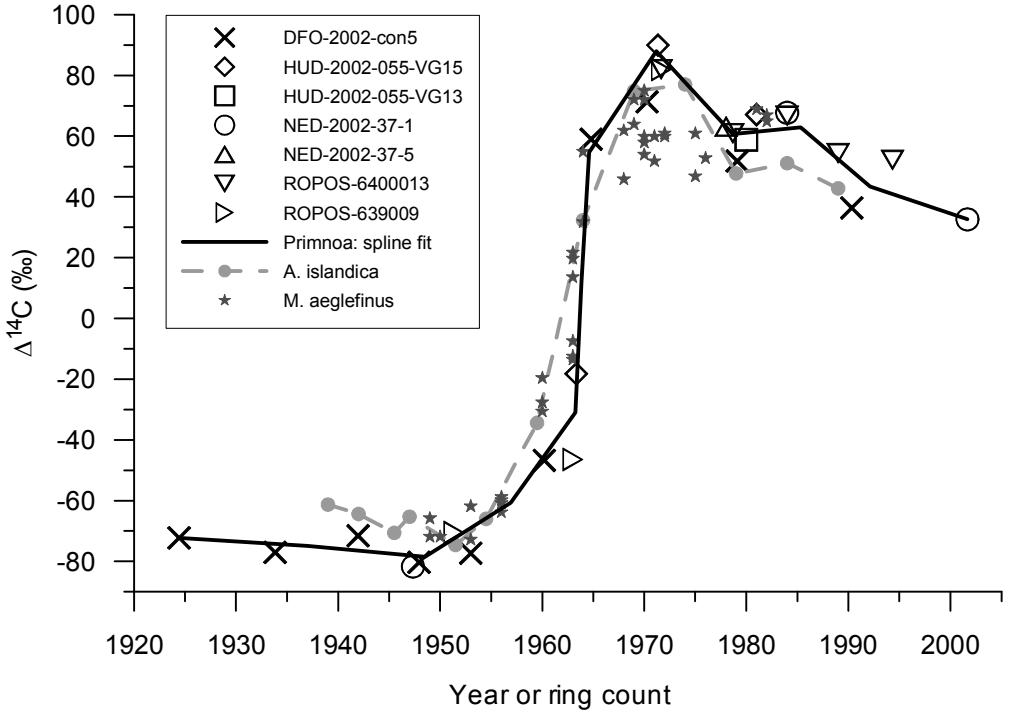

Fig. 2.6: Timeseries $\Delta^{14}C$ of annual horny rings (after decalcification) of *Primnoa resedaeformis*. Data are from 7 different colonies collected from 250-475m in the NW Atlantic Ocean. Accurate reconstruction of the bomb-^{14}C signal proves annual ring periodicity. Reference curves for clam shell (*Arctica islandica*; Weidman and Jones, 1993) and haddock otoliths (*Melanogrammus aeglefinus*; Campana 1997) also shown. Figure from Sherwood et al. (2005a).

geochemical records from octocorals is simplified by the ability to sample across the growth rings of the axial skeletal.

Zoanthids and antipatharians (black corals) also show great promise as marine archives. These corals also form arborescent, concentrically banded skeletons composed of a horny protein much like the gorgonin found in octocorals (Goldberg, 1991; Druffel et al., 1995). The skeletons are not calcified, so the fossil record is sparse. However, these organisms have some of the longest life-spans of any corals. Druffel et al's (1995) 1800-

year old *Gerardia* is a case in point. Antipatharians may live for several hundreds of years (Williams et al., 2005), and their growth rings, demarcated by dark-coloured protein "glue" (Goldberg, 1991), also appear to form annually (Williams et al., 2005).

2.2.3 Fossil preservation

The degree of diagenetic stability of deep-sea corals seems excellent (Teichert 1958). Repeated scanning electron microscope examination of deep-sea scleractinians from various depths (a few hundred metres to >2 km) and various oceans shows that they remain the original aragonite, with virtually no recrystallisation, since the early Pleistocene (Titschak and Freiwald, 2005; Remia and Taviani, 2004). The massive calcite structures in gorgonians have more durable and compact skeletons; Cretaceous-aged specimens are excellently preserved (Grasshoff and Zibrowius, 1983). The organic phase of horny corals has poorer preservation potential, but amino acid and stable isotopic analyses suggest that it is stable over at least the last few thousand years (Goodfriend, 1997; Sherwood et al., 2006).

Both the reef coral record and the deep-sea coral record, at least in the case of the scleractinian record, may be compromised by bioerosion. All corals, from all depths, are bored by a variety of organisms, of which the most prevalent are sponges and, in shallow water, algae. In deep-sea corals, the major bioeroders are sponges, fungi, bryozoa and polychaetes (Boerboom et al., 1998; Bromley, 2005; Beuck and Freiwald, 2005; Wisshak et al., 2005). The effects of bioerosion may range from complete removal of the record to selective dissolution of aragonite COCs (Titschak and Freiwald, 2005) and subtle

alterations of the trace element composition of the skeleton (Pons-Branchu et al., 2005; Robinson et al., 2006). Virtually nothing is known of the process by which climate records are distorted by bioerosion.

2.2.4 Sources of carbon to deep-sea corals

Based on radiocarbon measurements, Griffin and Druffel (1989) originally established that the carbonate fraction of deep-sea scleractinians and octocorals is mostly derived from ambient dissolved inorganic carbon (DIC) at depth. Other authors have noted a 1:1 relationship in the $\Delta^{14}C$ of coral carbonate and seawater DIC (Goldstein et al. 2001; Adkins et al. 2002; Frank et al., 2004; Roark et al. 2005). Radiocarbon evidence limits the amount of respiratory CO_2 incorporated into the carbonate to < 10% (Adkins et al. 2002); however, $\delta^{13}C$ data indicate that the amount of respired CO_2 may be somewhat higher in select species (e.g. Fig 2.7).

In contrast to the carbonate, the organic fraction of horny corals is synthesized from food sources sinking out of surface waters, a conclusion based on the presence of bomb-^{14}C in deep-dwelling specimens (Fig. 2.6; Griffin and Druffel, 1989; Druffel et al., 1995; Roark et al., 2005; Sherwood et al., 2005a). The actual food sources are mostly unknown because field monitoring is prohibitively expensive, and specimens usually die when raised to the surface. Studies on relatively shallow-dwelling octocorals consistently point to detrital particulate organic matter (POM) and zooplankton (in a ~ 50:50 ratio) as the main food sources (Ribes et al., 1999; 2003; Orejas et al., 2003). The sinking, rather than suspended fraction of detrital POM is likely to be more important to deeper-dwelling

taxa, as the nutritional value of the latter decreases with depth. Our $\Delta^{14}C$ and $\delta^{15}N$ data support a sinking POM and/or zooplankton (as both have approximately the same $\Delta^{14}C$ and $\delta^{15}N$) diet in deep-sea gorgonians and antipatharians, while ruling out deep suspended POM and dissolved organic matter (DOM) as important food sources (Heikoop et al., 2002; Sherwood et al., 2005a; 2005b; Williams et al., 2005).

2.2.5 Biocalcification models

A debate on the mechanism of coral calcification has persisted for 40 years (see review in Cohen and McConnaughey 2003). A brief overview of this debate seems appropriate, as it frames our discussion of isotopic and trace elemental variability in coral carbonate. In the "organic matrix" model crystal growth is initiated, directed and terminated by organic secretions (Goreau, 1959; Johnston, 1980). Support for this idea is provided by localization of sulphur-containing organic matter within COCs and crystal fibres (Cuif and Dauphin, 2005). In the "physicochemical" model (Barnes, 1970; Constanz, 1986) crystal growth occurs freely within pockets of enzymatically-modified seawater beneath the ectodermal tissue. This idea is rooted in the similarity of spherulitic crystal morphology in corals to that in mineral specimens (Bryan and Hill, 1941).

One of the advantages of the physicochemical model is that, being grounded in the principles of inorganic (thermodynamic and kinetic) solution/crystal chemistry, it may be quantitatively evaluated against a growing body of isotopic and trace elemental data from coral skeletons (Sinclair and Risk, in press). These data indicate that isotopic and trace elemental compositions of corals almost always depart from thermodynamic

equilibrium (i.e. 'vital effects'). In most cases, physicochemical-based models can account for the isotopic and trace elemental disequilibria in corals through biological manipulation of calcification fluids (McConnaughey 1998b; Adkins et al., 2003; Sinclair, 2005; Sinclair and Risk, in press).

In the classic model of calcification physiology (e.g.: McConnaughey, 1989b; Cohen and McConnaughey, 2003) calcification occurs in a thin (~10 micron), extracellular calcifying fluid (ECF) between the coral tissue and the skeleton. The ECF is isolated from cell fluids by a membrane which is permeable to small, uncharged molecules only. CO_2 passively diffuses across the cell membrane where it reacts with H_2O or OH^- to form HCO_3^-. The enzyme Ca-ATPase pumps Ca^{++} into the ECF in exchange for 2 protons, to maintain charge neutrality. Proton removal increases the pH of the ECF, and converts HCO_3^- to CO_3^{--}, which precipitates with Ca^{++}. Small amounts of seawater HCO_3^- and $CO_3^{=}$, as well as trace elements, enter the ECF through leaky membranes or by passage of invaginated vacuoles across the cell membrane (Furla et al., 1998).

2.2.6 Stable isotopic disequilibria in deep-sea corals

Oxygen and carbon isotope analysis of biogenic carbonates has been a cornerstone of paleoceanography for over 50 years. The $\delta^{18}O$ of carbonate is used to infer past temperatures (Epstein et al., 1953) and the extent of continental glaciation (e.g.:

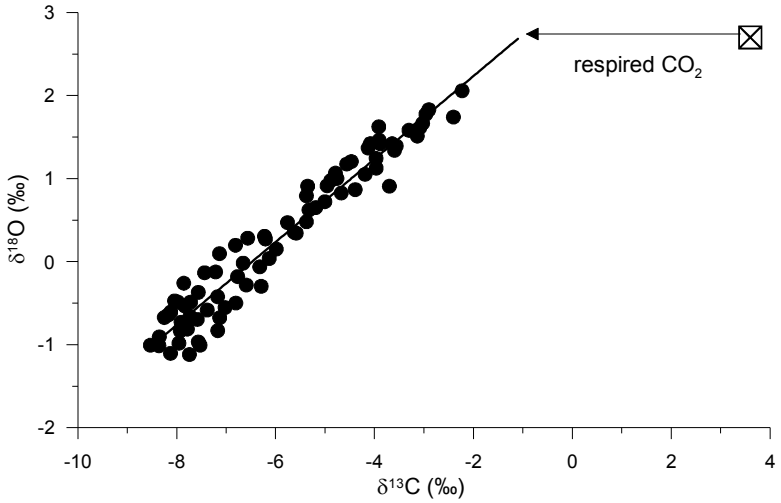

Fig. 2.7: Stable isotopic data from a specimen of *Lophelia pertusa* collected from the NE Atlantic. Isotopic data plot along a straight line extending roughly to theoretical aragonite-seawater isotopic equilibrium (boxed cross). Horizontal offset from equilibrium is caused by skeletal incorporation of $\delta^{13}C$-depleted respired CO_2 (i.e. metabolic effects). Data from Risk et al. (2005).

Shackleton, 1967), and $\delta^{13}C$ is used to identify water masses in the deep ocean (e.g.: Sarnthein et al., 1994). Many biogenic carbonates that exhibit a "vital effect" have consistent offsets from isotopic equilibrium. Deep-sea scleractinians are a special case: the extent of disequilibrium is highly variable within an individual coral (Emiliani et al., 1978; McConnaughey, 1989a; Smith et al., 2000; 2002). When plotted in $\delta^{18}O$ vs. $\delta^{13}C$ space (Fig. 2.7), isotopic data plot along straight lines extending roughly from equilibrium to a point up to 5 ‰ depleted for $\delta^{18}O$, and up to 15 ‰ depleted for $\delta^{13}C$. The slopes of these lines average about 1/3. Octocoral calcites show similar patterns, though the extent of disequilibria is somewhat less (Druffel et al., 1990; Heikoop et al., 1998).

According to McConnaughey's kinetic model (1998b, 2003), strong isotopic depletions are mainly caused by hydration and hydroxylation of CO_2 within the ECF, although the pathways of $\delta^{18}O$ and $\delta^{13}C$ fractionation differ. For oxygen, both H_2O and OH^- are strongly depleted in $\delta^{18}O$: about -30 ‰ and -69 ‰, respectively. Since 1/3 of the oxygen atoms in HCO_3^- come from H_2O or OH^-, McConnaughey's (2003) calculations predict a DIC with a $\delta^{18}O$ composition well below that of aragonite in equilibrium with seawater. For carbon, the reaction of CO_2 with H_2O and OH^- strongly fractionates $\delta^{13}C$, about -7 ‰ and -27 ‰, respectively. Again, the resulting DIC takes on a $\delta^{13}C$ content much depleted compared with equilibrium aragonite. Hydroxylation of CO_2 predominates at pH > 8, where most calcification occurs; thus the stronger $\delta^{18}O$ and $\delta^{13}C$ depletions associated with hydroxylation dominate the isotopic composition of the coral skeleton (McConnaughey, 2003).

McConnuaghey (1989b) calculated that HCO_3^- can precipitate with Ca^{++} much faster than it can attain equilibrium with H_2O in the ECF, so the $\delta^{18}O$ depletion is buried in the precipitating aragonite. Furthermore, equilibration of HCO_3^- occurs through a CO_2 intermediate, which diffuses back and forth across the cell membrane and equilibrates with cell H_2O at lower pH. Some of the carbon in the ECF is carried with the CO_2 molecule, allowing it to equilibrate within the cell also. Strong depletions in $\delta^{13}C$ incurred during hydration and hydroxylation are thereby partly "eroded" (Cohen and McConnaughey, 2003). The CO_2 molecule carries both C and O atoms across the cell membrane, allowing simultaneous equilibration of $\delta^{13}C$ and $\delta^{18}O$ in the cell. This

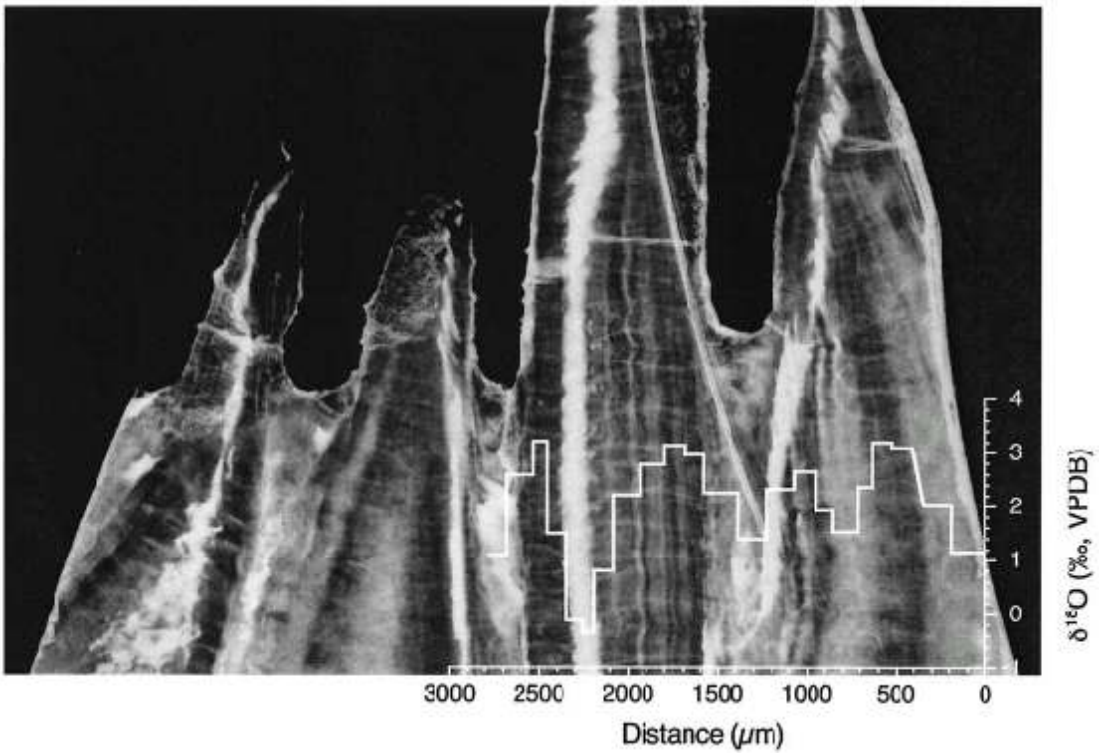

Fig. 2.8: Transmitted light image of the thecal region of *Desmophyllum dianthus*, overlain with $\delta^{18}O$ results obtained with a high spatial resolution microsampler. Vertical line of COCs (lightest region) is associated with the lowest $\delta^{18}O$. Figure from Adkins et al. (2003).

accounts for the $\delta^{18}O - \delta^{13}C$ correlations in deep corals. In addition to 'kinetic effects', a small amount of the CO_2 entering the ECF is derived from metabolism, and is about 2 ‰ depleted in $\delta^{13}C$ (McConnuaghey, 1989a). Thus, the lines in $\delta^{18}O - \delta^{13}C$ space extend to a point roughly 2 ‰ depleted in $\delta^{13}C$ compared to equilibrium.

In recent years, a new aspect of isotopic disequilibria in deep-sea corals has emerged. High resolution microsampling reveals that COCs are more isotopically depleted than crystal fibres (Fig. 2.8; Adkins et al., 2003; Rollion-Bard et al., 2003).

Moreover, isotopic data from COCs may even fall off the $\delta^{18}O$ vs. $\delta^{13}C$ lines, where $\delta^{18}O$ continues to decrease but $\delta^{13}C$ does not. Such anomalous data went unnoticed in earlier studies because the dental drills used in sampling could not be used to separate fibres from COCs (Lutringer et al., 2005). To account for these observations, Adkins et al. (2003) developed a "carbonate model" of isotopic disequilibrium. In their model, $\delta^{18}O$ and $\delta^{13}C$ disequilibria are driven by thermodynamic response to a biologically-induced pH gradient in the ECF. While McConnaughey's (1989b) kinetic model and Adkins et al's (2003) carbonate model are fundamentally different, both agree that isotopic depletions in COCs are an indication of a faster rate of calcification.

2.2.7 Overcoming isotopic disequilibria: the "lines technique"

Smith et al. (2000) proposed the "lines technique" as a way to overcome vital effects in deep-sea scleractinian corals. Their approach makes use of the fact that the lighter ends of $\delta^{18}O - \delta^{13}C$ regression lines for any one coral extend towards isotopic equilibrium (Fig. 2.9). If $\delta^{13}C$ at equilibrium is known (from $\delta^{13}C$ of seawater or coeval benthic foraminifera), then, with a small correction for respiratory $\delta^{13}C$ (about 2 ‰), the corresponding value of $\delta^{18}O$ at equilibrium, and hence temperature, can be calculated. Using 35 modern corals, Smith et al. (2000) showed that even if $\delta^{13}C$ is not known, the intercepts of $\delta^{18}O - \delta^{13}C$ regression lines were strongly correlated with temperature:

$$(\delta^{18}O_c - \delta^{18}O_w) = -0.21\ T\ (^oC) + 4.51 \quad (1)$$

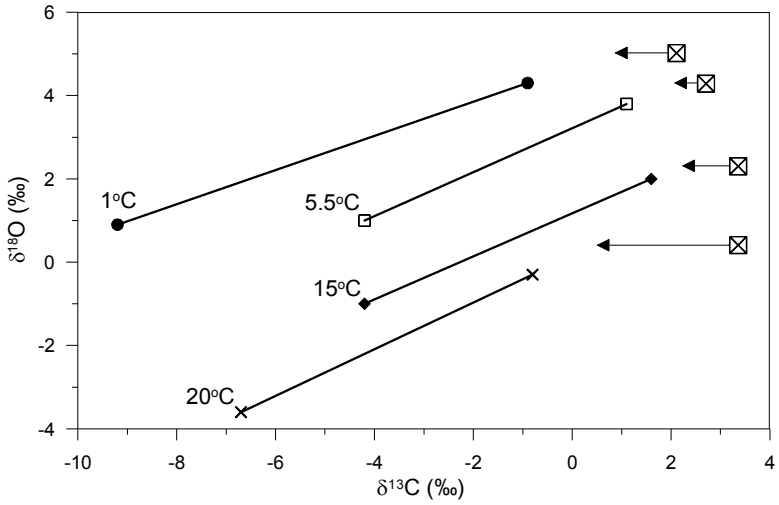

Fig. 2.9: Isotopic data for 4 coral specimens collected from: Antarctic shores, 410m (solid circles); NW Atlantic slope, 1025m (open squares); NE Atlantic, 310m (solid diamonds); Bahamas, 295m (crosses). For clarity, only the least squares regression lines are shown. Crossed boxes represent theoretical isotopic equilibrium for each of the coral's datasets. Vertical offsets, reflecting temperature dependence of d18O, are the basis for the 'lines technique'. Horizontal arrows point to intersection of regression lines with equilibrium d18O; length of arrows reflects magnitude of theoretical metabolic effect. Figure modified from Smith et al. (2000).

Equation 1 is nearly identical to Grossman and Ku's (1986) experimentally-derived $\delta^{18}O$ vs. temperature equation. This suggests that setting $\delta^{13}C = 0$ is a reasonable approximation for seawater $\delta^{13}C$ minus the respiratory $\delta^{13}C$ correction.

Weaknesses to the lines technique stem from variability in metabolic effects (Adkins et al. 2003), or the slopes of $\delta^{18}O$ vs. $\delta^{13}C$ (Smith et al., 2000). Despite these limitations, Smith et al. (2000) could calculate present day temperatures to a precision of ± 0.36 to ± 1 ^{o}C over a range of 1 – 28 ^{o}C. The lines technique may not work as well with

pre-Holocene corals, however, because seawater $\delta^{13}C$ was more variable, and coral metabolism may have been much different; this is apparent upon re-examination of their earlier results on *Desmophyllum* (Smith et al., 1997). In addition, Smith et al. (2000) used the classic dental drill sampling method, thus they could not resolve the isotopic differences between fibres and COCs. Lutringer et al. (2005) analysed fibres and COCs separately with an ion microprobe and essentially reproduced Smith et al's (2000) findings, albeit with slightly larger estimates of precision (± 0.7 to ± 1.5 ^{o}C). Overall, the lines technique may be useful in tracking relatively large changes in water temperature, such as that which occurs in upper intermediate waters.

2.2.8 Trace element vital effects

A growing body of evidence shows that trace elemental vital effects are a ubiquitous feature of shallow- and deep-water scleractinians alike (Sinclair et al., submitted ms). The mean compositions differ from inorganic carbonate, and the range of variability greatly exceeds that which can be accounted for by temperature-dependent partitioning alone. In scleractinians, different trace elements are strongly correlated with each other, much in the same way that $\delta^{18}O$ and $\delta^{13}C$ are correlated (Fig. 2.10; Montagna et al., 2005; Shirae et al., 2005; Sinclair et al. submitted ms). Moreover, elemental compositions are distinctly different in COCs than in surrounding fibres, with COCs being lower in Sr and U, and higher in Mg (Shirai et al. 2005; Cohen et al., unpubl.; Gagnon and Adkins, 2005; Sinclair et al., submitted ms). A recently developed trace element equilibrium/kinetic model of calcification can account for the apparent vital effects; specifically, Sr and U depletions are predicted at high calcification rates (Sinclair

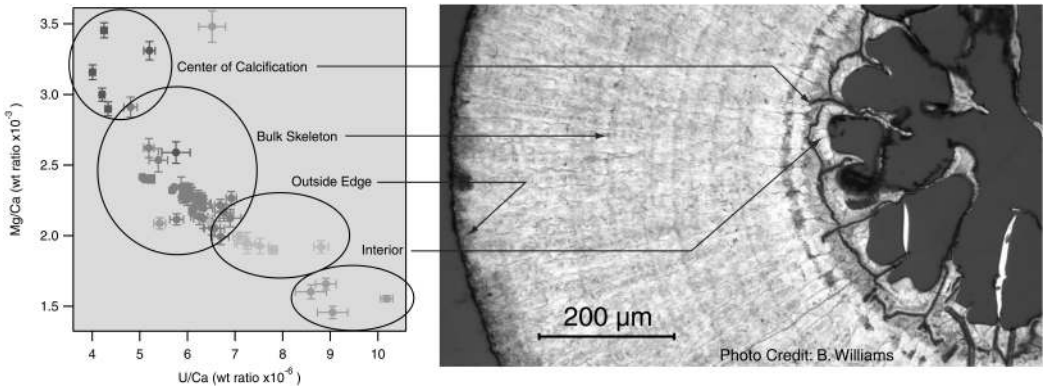

Fig. 2.10: Negative correlation between Mg/Ca and U/Ca across the skeletal micro-structures of *Lophelia pertusa*. Highest Mg and lowest U occurs in the optically dense COC. Conversely, the lowest Mg and highest U occurs in the optically light deposits lining the inside of the calyx. The bulk of the skeleton is a mixture between these 2 end-members. Figure from Sinclair et al. (submitted ms).

and Risk, in press). Cohen et al. (unpubl.) present compelling evidence for a Sr/Ca paleothermometer in *Lophelia*; however, we are still a long way from producing reliable temperature reconstructions from scleractinian corals.

Following the extensive research on foraminiferal calcites, Mg/Ca in octocorals has been proposed as a potential paleothermometer (Weinbauer et al., 2000; Thresher et al., 2004; Bond et al., 2005; Sherwood et al., 2005c). Thresher et al. (2004) present 350 year long records of Mg/Ca from Bamboo corals, which they interpret as evidence for recent cooling in the upper intermediate waters off Australia (Fig. 2.11). More recent studies, however, suggest that Mg/Ca, as well as U/Ca and Sr/Ca, may be poorly reproducible along multiple transects of the same coral (Allard et al. 2005; Fallon et al., 2005; Sinclair et al. 2005). Mg/Ca in particular may be strongly enriched in organic

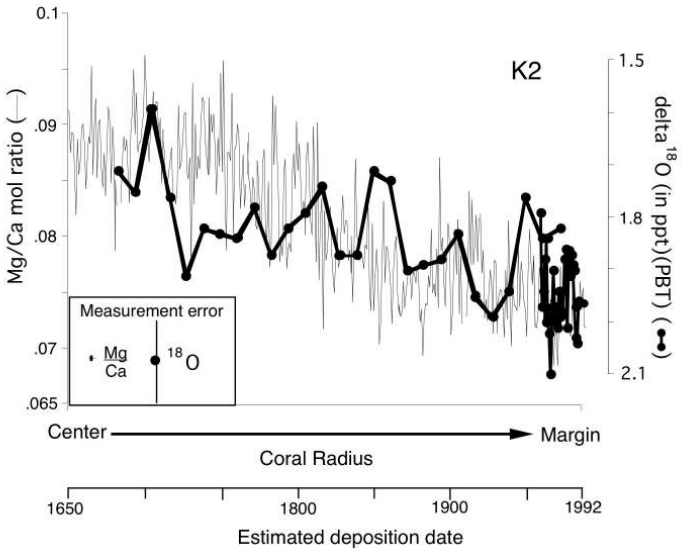

Fig. 2.11: Records of Mg/Ca for two specimens (K2 and K4) of bamboo coral collected from ~1000 m depth off Tasmania. Record of d18O from K2 is also shown. Both datasets indicate a gradual decline in water temperature over the last ~ 350 years. Figure from Thresher et al. (2004).

phases within the calcite, thus masking any temperature effect. On the other hand, Ba/Ca exhibits excellent reproducibility, and is therefore a good candidate as an environmental proxy (Allard et al. 2005; Fallon et al. 2005). Overall, further work is needed to assess the factors controlling elemental partitioning in octocoral calcite before reliable proxy data can be produced.

2.2.9 U-series dating of deep-sea corals

Deep-sea corals are excellent subjects for U-series dating. Scleractinians are easier to date because their aragonite skeletons contain higher levels of U (2-4 ppm) compared with the calcite skeletons of octocorals (3-4 ppb). With modern Multicollector

ICP-MS, high precision U-series ages can be obtained on < 1 g of sample. Here, we provide a brief overview of U-series dating as it applies to deep-sea corals. More detailed treatments are provided in Cheng et al. (2000) and Edwards et al. (2003). Both the ^{238}U-^{234}U-^{230Th} (U/Th) and the ^{235}U-^{231}Pa (U/Pa) decay schemes can be used. U/Th is the method of choice because it is somewhat more precise and covers a longer time range: 0-600 ka vs. 0-250 ka for U/Pa. However, U/Th dating can be used in concert with U/Pa (Goldstein et al. 2001), or even ^{226}Ra/Ba dating (Pons-Branchu et al., 2005), as a check on closed-system behavior and thus on dating accuracy.

In reef corals, it is normally the case that all of the measured ^{230}Th can be accounted for by radioactive in-growth. Deep-sea corals, on the other hand, live in a thorium-rich environment, since thorium increases with depth in the ocean. As a consequence, deep-sea corals may incorporate significant amounts of unsupported or non-radiogenic thorium, leading to older apparent ages. There are 3 sources of unsupported thorium (Cheng et al., 2000; Schröder-Ritzrau et al., 2003): 1) a loosely attached detrital phase; 2) ferromanganese coatings, which adsorb thorium from seawater; and 3) an "initial", lattice-bound fraction incorporated during crystallization. The detritus and coatings can usually be removed by mechanical cleaning and by a series of chemical leaches, respectively (e.g.: Shen and Boyle, 1988). Initial thorium cannot be separated from radiogenic thorium, so it must be accounted for in age calculations. The precision and accuracy of U/Th ages therefore depends on the precision and accuracy of the correction for unsupported thorium (Cheng et al., 2000).

The U/Th age equation, including the term for initial thorium is defined as (Edwards et al., 2003):

$$\{[^{230}U/^{238}U] - [^{232}U/^{238}U][^{230}Th/^{232}Th]_i\,(e^{-\lambda 230t})\}\ -1 =$$
$$-e^{-\lambda 230t} + \{\delta^{234}U_m/1000\}\{\lambda_{230}/(\lambda_{230}-\lambda_{234})\}\{1 - e^{-(\lambda 230 - \lambda 234)t}\} \qquad (2)$$

where: isotope ratios are activity ratios; λ's are decay constants; t is the ^{230}Th age; subscripts i and m represent initial and measured values, respectively; and $\delta^{234}U_m$ is the measured deviation in per mil of the $[^{234}U/^{238}U]$ ratio from secular equilibrium: $\delta^{234}U = ([^{234}U/^{238}U]-1) \times 1000$. The measurement of ^{232}Th provides a check on the extent of unsupported thorium; thus, the only unknowns in Equation 2 are the ^{230}Th age (t) and the initial $[^{230}Th/^{232}Th]_i$ activity.

There are two approaches to estimate $[^{230}Th/^{232}Th]_i$. In the first approach, a constant value is assumed, based on seawater measurements. This approach is suitable for relatively clean samples, with ^{232}Th contents of ca. < 20 ppb. Cheng et al. (2000) showed that $[^{230}Th/^{232}Th]$ measured in modern deep-sea scleractinians from between 400 and 2000 m in the Atlantic and Pacific Oceans was indistinguishable, within error, from seawater measurements. Their estimate of $[^{230}Th/^{232}Th] = 14.8 +/- 14.8$ has been used as a "blanket" correction factor (Adkins et al., 1998; Cheng et al., 2000; Robinson et al., 2005). Alternatively, measurements of seawater $[^{230}Th/^{232}Th]$ specific to the area and depth of interest may be used to narrow the range of possible $[^{230}Th/^{232}Th]_i$ (Schröder-Ritzrau et al., 2003; Frank et al., 2004; 2005). Use of a constant $[^{230}Th/^{232}Th]_i$ correction

assumes that seawater [$^{230}Th/^{232}Th$ was constant in the past, which may not necessarily have been the case. Accordingly, errors in $[^{230}Th/^{232}Th]_i$, of ± 50 % to 100 % are propagated through the age calculations to account for this uncertainty.

The second approach, using the so-called Rosholt-II isochron method (Ludwig et al., 1994), assumes a 2 end-member mixing model between ^{232}Th-free carbonate and the ^{232}Th-rich contaminant (Lomitschka and Mangini, 1999; Schröder-Ritzrau et al., 2003; 2005). This method is suitable for heavily coated samples with ^{232}Th contents > 20 ppb (Shröder-Ritzrau et al., 2005). Two to four fractions of the same sample are prepared and analyzed separately. The first fraction consists of just the coating; the other fractions are subjected to cleanings of increasing intensity, from simple mechanical cleaning to strong chemical leaching in ascorbic acid and Na_2EDTA solution (Lomitschka and Mangini, 1999). When plotted in $[^{230}Th/^{232}Th]$ vs. $[^{238}Th/^{232}Th]$ space, data for the different fractions define an isochron, the y-intercept of which represents the $[^{230}Th/^{232}Th]_i$ correction factor for input to equation 2. A slightly different variation of the isochron approach is outlined in Goldstein et al. (2001).

The relationship between measured and initial $\delta^{234}U$ is defined as (Edwards et al. 2003):

$$\delta^{234}U_m = (\delta^{234}U_i)\, e^{-\lambda 234 t} \qquad (3)$$

If the ^{230}Th age can be solved independently, then Equation 3 can be used to calculate initial $\delta^{234}U$. Knowledge of $\delta^{234}U_i$ is a useful check on diagenetic alteration of the

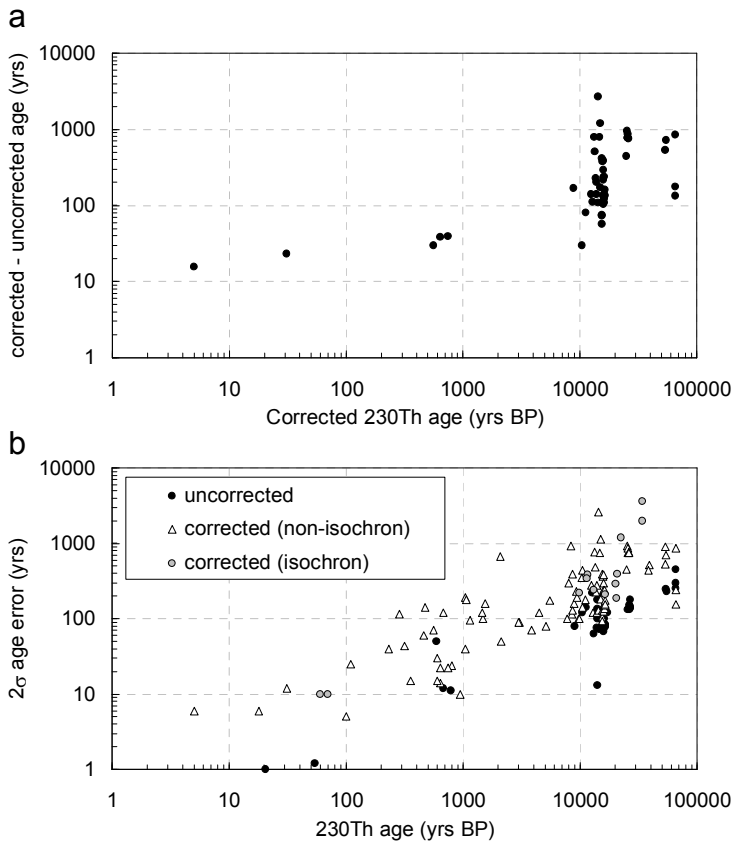

Fig. 2.12: Compilation of all published U/Th dates from deep sea scleractinian corals. Upper panel: Difference between uncorrected and corrected ages averages < 3%. Lower panel: 2σ age errors associated with uncorrected data, and corrected data using either the isochron or non-isochron approaches. See text for explanation.

skeleton and hence open-system behavior, because marine $\delta^{234}U$ is fairly constant in time and space (Cheng et al., 2000; Bard et al., 1991; Henderson, 2002). If uranium is added to the skeleton by diagenetic processes (endolithic borings, secondary mineralization, micro-redox traps, pore water U; Swart and Hubbard, 1982; Pons-Branchu et al., 2005; Robinson et al., 2006), then the U/Th age equation may be invalidated. It is common practice to discard data when $\delta^{234}U_i$ falls outside a defined range of seawater $\delta^{234}U$ (e.g.: 146 ± 7‰; Robinson et al. 2005).

Compilation of all published U/Th dates in deep-sea scleractinians provides an indication of the accuracy and precision of the technique (Fig. 2.12). In general, $^{230}Th/^{232}Th$-corrected ages are younger than uncorrected ages by < 3%. Thus, depending on the dating resolution required, a correction may not be necessary, provided that the ^{232}Th concentration is low. For uncorrected ages, the 2σ dating precision is better than 1%. For corrected data, the 2σ precision is larger, ~ 5 %, owing to uncertainty in the value of initial [$^{230}Th/^{232}Th$]. There are no apparent differences in the precision of the isochron vs. non-isochron dating techniques.

In summary, U/Th dating of deep-sea corals is challenging because of the presence of unsupported Th, which leads to older apparent ages, and possible diagenetic incorporation of U, leading to younger apparent ages. With careful sample pre-treatment, correction for unsupported Th, and screening for diagenetically-altered samples, high precision U/Th dates may be obtained.

2.2.10 Radiocarbon dating and paleo-$\Delta^{14}C$

Seawater $\Delta^{14}C$ has long been recognized as an important tool for tracking water mass circulation (Key, 2001). In the deep North Atlantic, for example, $\Delta^{14}C$ differentiates North Atlantic Deep Water (-65‰) from Antarctic Bottom Water (-165 ‰; Broecker et al., 1960; Stuiver et al., 1983). The relative dominance of these water masses at any one location provides an indication of oceanic circulation patterns. Coral skeletons provide one of the few archives of past seawater $\Delta^{14}C$ variations, since their carbonate skeletons are derived from ambient DIC at depth (Griffin and Druffel, 1989; Adkins et al., 2002).

Coral skeletons contain enough carbonate material to perform both U/Th and ^{14}C dating on the same sample (Adkins et al., 1998; Mangini et al., 1998). Since the U/Th-dating can be used to calculate an absolute age, paired U/Th-^{14}C dating provides a direct measure of the ^{14}C age of the seawater in which the coral grew (Bard et al., 1993; Edwards et al., 1993, Adkins et al., 2002). Adkins et al. (1998) and Mangini et al. (1998) first demonstrated this method on deep-sea corals, analogous to the method of differencing radiocarbon ages from pairs of benthic-planktic foraminifera sampled from the same core interval (B/P-dating; Broecker et al. 1990), but much improved by the fact that bioturbation and foraminiferal species effects are not at issue, and U/Th dating is model independent.

Paleo-$\Delta^{14}C$ may be calculated by (Adkins and Boyle 1997):

$$\Delta^{14}C_{paleo} = \{[\, e\,(-^{14}C \text{ age} / 8033) / e(-\text{cal age} / 8266)] -1 \,\} \times 1000 \qquad (4)$$

where ^{14}C age is the ^{14}C age measured on the coral, cal age is the U/Th age measured on coral, 8033 is the Libby mean life and 8266 is the true ^{14}C mean life in years. Knowledge of paleo-$\Delta^{14}C$ is powerful for tracking past variations in deep and intermediate water mass distributions (Frank et al., 2004; 2005; Robinson et al., 2005). In theory, by projecting paleo-$\Delta^{14}C$ values back in time to their intersection with the atmospheric record, the residence time or ventilation age of deep water masses may be calculated (Adkins et al., 1998; Mangini et al., 1998; Goldstein et al., 2001; Shröder-Ritzrau et al.,

2003); however, this approach may be complicated by the mixing of multiple water masses with different convection histories.

2.2.11 Surface signals from the organic skeletons of horny corals

Some of the more promising paleoceanographic information may found in the skeletons of horny corals. Druffel et al. (1995) originally hypothesized that certain aspects of export of POM may be monitored by studying the isotopic and amino acid chemistry of horny layers, in much the same way that down-core trends in sedimentary organic matter (SOM) is utilized in paleoceanography. In some species the annual rings may be decalcified and gently peeled apart and analyzed separately, without the need for expensive in situ microprobe analyses. Moreover, the amino acid composition of the horny material is stable over at least the last few thousand years, an indication that it is resistant to organic diagenesis (Goodfriend, 1997; Sherwood et al., 2006). Since the horny material is derived from sinking POM and/or zooplankton, annually banded horny corals provide a long-term, high resolution archive of biogeochemical processes occurring in surface waters (Sherwood et al., 2005b).

Accurate reconstruction of 20th century bomb radiocarbon from *Primnoa resedaeformis* (Fig. 2.6) is a good example of the type of data that may be retrieved from horny corals (Sherwood et al., 2005a). As a variation on B/P dating, paired ^{14}C dating of both the carbonate and horny phases may prove to be useful in tracking ventilation rates of ambient water masses. The $\delta^{15}N$ and $\delta^{13}C$ of the horny phase may be another source of paleoceanographic data (Heikoop et al., 2002; Sherwood et al., 2005b; Ward-Paige et al.,

2005; Williams et al., 2005). The $\delta^{15}N$ and $\delta^{13}C$ in gorgonians and antipatharians is correlated with $\delta^{15}N$ and $\delta^{13}C$ in phytoplankton. Moreover, the intra- and inter-colony reproducibility of both isotopes appears to be excellent.

The $\delta^{15}N$ composition of horny corals is controlled by a variety of bottom-up processes, beginning with the isotopic composition of source nutrients, uptake by phytoplankton, and the length and complexity of the food web. The relative influence of denitrification vs. nitrification among different oceanographic regimes has a strong impact, for example, on the $\delta^{15}N$ of NO_3 (Cline and Kaplan, 1975; Altabet et al., 1999; Knapp et al., 2005). Phytoplankton preferentially assimilate $^{14}NO_3$, leading to isotopically depleted biomass. In many regions of the ocean NO_3 is completely consumed, and the $\delta^{15}N$ of phytoplankton and sinking POM converges on the $\delta^{15}N$ of subsurface NO_3 (Altabet and McCarthy, 1985; Altabet, 1988; Altabet et al., 1999; Thunnel 2004). This is the basis for the interpretation of down-core sedimentary $\delta^{15}N$ as a proxy for the $\delta^{15}NO_3$ history of the oceans (Altabet et al., 1995; Ganeshram et al., 1995; Haug et al., 1998). The simple relation between subsurface NO_3 and sinking POM may be confounded by a variety of factors, including incomplete nutrient utilization (Altabet and Francois 1994), alteration of sinking POM during transit through the water column (Saino and Hattori, 1987; Altabet et al., 1991), and the complexity of the plankton food web (Altabet, 1988; Wu et al., 1999a). This latter factor presents the largest source of uncertainty in the

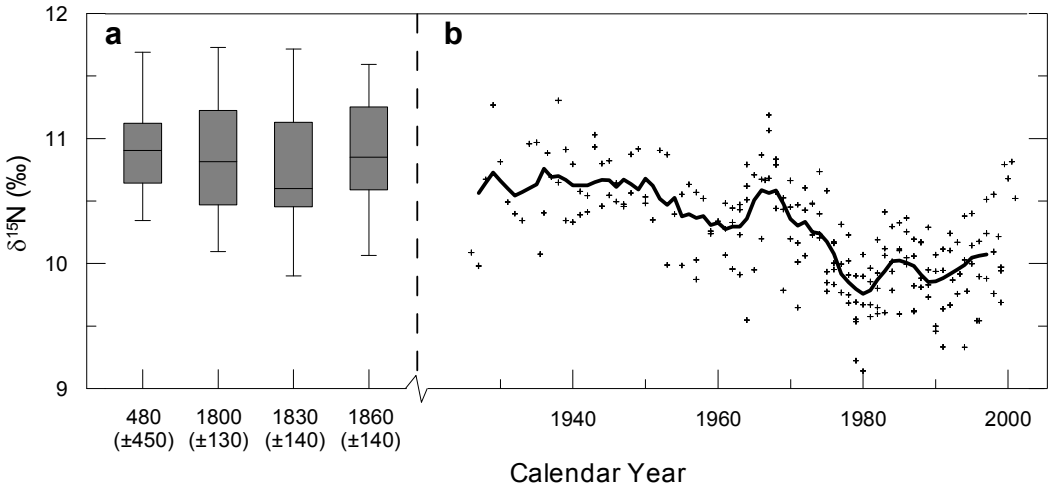

Fig. 2.13: $\delta^{15}N$ measured in the annual horny rings of *Primnoa resedaeformis* (NW Atlantic; 250 - 475m). (a) Data for sub-fossil colonies plotted as box-and-whisker plot because of uncertainties in radiocarbon age calibrations. Each box represents at least 20 annual rings. Ages below boxes indicate mean (± 2σ range), as determined by calibrated ^{14}C-dating and accounting for number of annual rings analyzed. (b) Data for 6 recent colonies plotted against calendar year, as dated by the bomb-^{14}C method and visual counting of annual rings. Bold line indicates 5 yr running mean. The 20th century decline in $\delta^{15}N$ is attributed to isotopic depletion of ambient NO_3, and/or trophic level effects. Data from Chapter 7.

interpretation of $\delta^{15}N$ data from horny corals, since trophic fractionation is large (~3.4 ‰ per trophic level; DeNiro and Epstein, 1981) relative to oceanic $\delta^{15}NO_3$ variability, and the corals may feed opportunistically on a wide range of plankton size classes (Ribes et al., 1999; 2003; Orejas et al., 2003). Future compound-specific isotope analyses will likely allow for the separation of trophic level and source nutrient isotope effects through separate analysis of different amino acids (McClelland and Montoya, 2002).

Specific processes that could be tracked with the $\delta^{15}N$ composition of horny corals include water mass movements, eutrophication, and trophic dynamics. Recent

exploratory studies highlight some of this potential, particularly in assessing anthropogenic perturbations over the last few centuries. Sherwood et al. (Chapter 7) presented a near 2000 year long record of $\delta^{15}N$ from colonies of *P. resedaeformis* collected from the slope water region off eastern Canada (Fig. 2.13). Anomalous decline in $\delta^{15}N$ over the 20th century was interpreted to reflect weakening of isotopically-heavier Labrador Current, or a change in the relative trophic level of the corals. Ward-Paige et al. (2005), using shallow gorgonians, and Williams et al., (2005), using deep antipatharians, presented records of long-term increases in $\delta^{15}N$ off SE USA, which they interpreted as evidence of increasing anthropogenic nutrient inputs.

The $\delta^{13}C$ of horny corals is controlled by a different assortment of bottom-up processes. Variability in the $\delta^{13}C$ of oceanic DIC is only 1-2 ‰ (Kroopnick, 1985), and trophic fractionation averages only about 1‰ per trophic level (DeNiro and Epstein, 1978). The $\delta^{13}C$ of SOM is often used to distinguish between marine and terrestrial inputs (Fry and Sherr, 1984); however this generally does not apply to deep corals because they usually inhabit regions far from terrestrial influences. Most of the variability in $\delta^{13}C$ of phytoplankton and subsequent trophic levels arises from isotopic fractionation during phytoplankton growth. Earlier studies emphasized dissolved CO_2 in determining phytoplankton $\delta^{13}C$, and the use of sedimentary $\delta^{13}C$ as a proxy for paleo-CO_2 (Jasper et al., 1994; Rau, 1994). More recent studies point to growth rate, cell geometry, nutrient and light limitation and active carbon uptake (as opposed to diffusive uptake of CO_2) as equally, if not more important determinants of $\delta^{13}C$ (see review in Laws et al., 2002). Long-term declines in $\delta^{13}C$ measured in octocorals and antipatharians appear to reflect

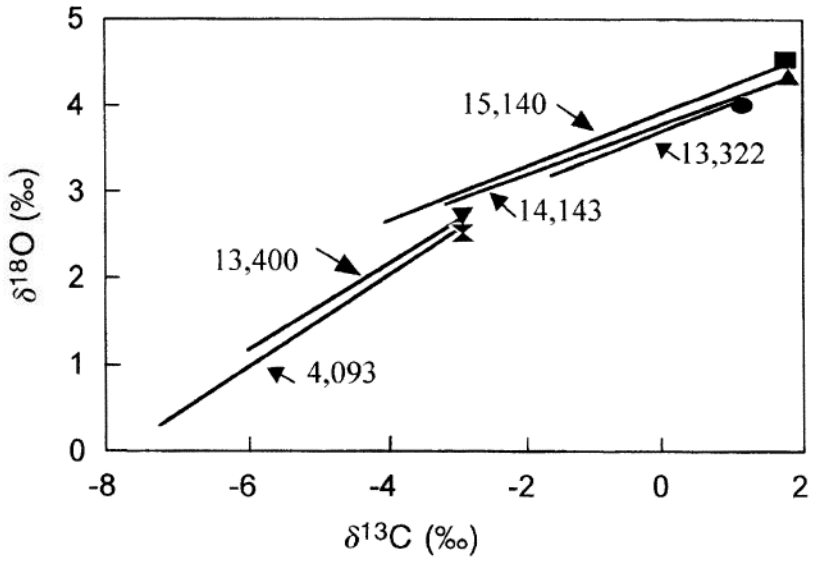

Fig. 2.14: Isotopic data from *D. cristigalli* collected from Orphan Knoll (Labrador Sea). For clarity, only the least squares regression lines are shown. Symbols indicating isotopic maxima for each of the coral's datasets are assumed to approach isotopic equilibrium. Numbers indicate U/Th ages in years BP. The 2 oldest corals (15,140 and 14,143 yrs) grew when the Labrador sea retained much of its glacial character. Corresponding $\delta^{18}O$ maxima average 4.5 ‰. At the base of the next youngest coral (13,400 yrs), $\delta^{18}O$ maxima (2.5 ‰) are much like that of a mid-Holocene coral (4,093 yrs). Further up the same colony (13,322 yrs), data return to that of the oldest-aged corals, indicating a rapid return to glacial-like conditions with the onset of the Younger Dryas. Figure from Smith et al. (1997).

the oceanic Suess effect, that is, the gradual depletion of oceanic $\delta^{13}C$ due to burning of isotopically-light fossil fuels (Chapter 7; Williams et al., 2005). Over shorter time periods, the observed variations are yet to be explained. As with $\delta^{15}N$, future compound-specific analysis may lead to a better understanding of $\delta^{13}C$ records obtained from horny corals.

2.3 LANDMARK STUDIES

Having explored the growth, geochemistry and radiometric dating of deep-sea corals, we now turn our attention to a few studies that have produced operationally useful paleoceanographic data. We focus on papers dealing with the rate of intermediate water mass variability across the Pleistocene-Holocene transition. The central theme of these papers is that climatic transitions occur over very short (decadal) timescales. Under most circumstances decadal-scale events are difficult to reconstruct from marine sediment records because of bioturbation.

Smith et al's (1997) landmark paper focused on *Desmophyllum* corals collected from the top of Orphan Knoll (1800 m), an isolated seamount off the Newfoundland slope. The location and depth of Orphan Knoll allowed for the reconstruction of intermediate water mass variability in the Labrador Sea, an important component of the North Atlantic circulation. Stable isotopic data from these corals exhibited a major difference in the distribution of $\delta^{18}O$ vs. $\delta^{13}C$ lines between warm and cold periods spanning the last 15 ka. (Fig. 2.14). Foreshadowing the 'lines technique' published a few years later (Smith et al., 2000), they assumed that the lighter ends of their $\delta^{18}O$ vs. $\delta^{13}C$ lines approached isotopic equilibrium with seawater, an assumption supported by similarity of $\delta^{18}O$ values measured in contemporaneous foraminifera. One of their corals captured a rapid shift from warmer conditions at the base of the coral (13.400 ka BP), to cooler conditions at the top of the coral (13.322 ka), approximately co-incident with the accepted timing of the onset of the Younger Dryas event (12.9 ka BP). In this specimen,

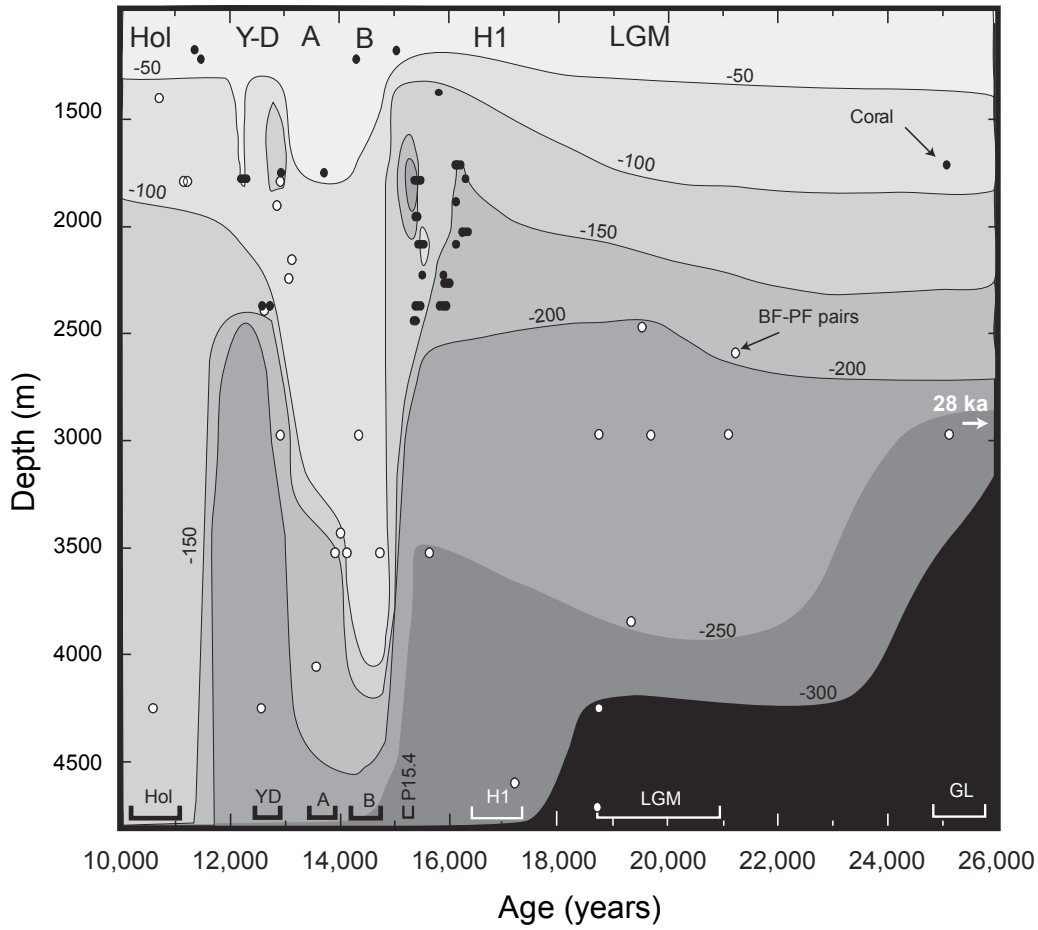

Fig. 2.15: Mid-North Atlantic paleo-$\Delta^{14}C$ reconstructed from deep sea corals (black circles) and foraminifera B/F pairs (white circles). During the last glacial period and Younger Dryas, the deep ocean was dominated by older, $\Delta^{14}C$-depleted southern source waters, indicating cessation of deep water formation in the N. Atlantic. Younger, northern source waters characterize the warmer Bølling-Allerød and Holocene periods. Coral data indicate higher frequency variability in upper intermediate waters. Figure from Robinson et al. (2005).

the shift from full warm to full cold conditions occurred between sub-samples spaced 3mm apart, an equivalent of 5 years in time. This study was the first to demonstrate the utility of deep-sea corals in providing useful paleoceanographic data. Shortly thereafter, a series of papers on paired U/Th-^{14}C dating of deep-sea corals came out, emphasizing

rapid changes in intermediate water ventilation rates across the Pleistocene-Holocene transition (Adkins et al., 1998; Schröder-Ritzrau et al., 2003). The approach outlined in these studies culminated in the recent work of Robinson et al. (2005), with data from some 30 corals recovered from the New England Seamounts (33-39^{o}N). Their reconstructions of paleo-$\Delta^{14}C$ over the interval 11-25 ka (Fig. 2.15) document switches in the relative proportions of southern vs. northern source waters (a "bipolar seesaw"). Switches at intermediate depths occurred more frequently than they did in the abyss, and they coincided with climatic events documented in Greenland and Antarctic ice cores. The 15.4 ka event, in particular, saw a shift from full glacial to full modern-like conditions that took place in less than 100 years.

CHAPTER 3

RADIOCARBON EVIDENCE FOR ANNUAL GROWTH RINGS IN A DEEP-SEA OCTOCORAL (*Primnoa resedaeformis*)

Owen A. Sherwood [1], David B. Scott [1], Michael J. Risk [2], Thomas P. Guilderson [3, 4]

[1] Centre for Environmental and Marine Geology, Dalhousie University, Halifax, Canada

[2] School of Geography and Geology, McMaster University, Hamilton, Canada

[3] Center for Accelerator Mass Spectrometry, LLNL, Livermore, CA, USA

[4] Department of Ocean Sciences & Institute of Marine Sciences, University of California Santa Cruz, Santa Cruz, USA

Published as an article in:

Marine Ecology Progress Series 301: 129-134

(October 2005)

3.1 ABSTRACT

The deep-sea gorgonian octocoral *Primnoa resedaeformis* is distributed throughout the Atlantic and Pacific Oceans at depths of 65 - 3200 m. It has a two-part skeleton of calcite and gorgonin. Towards the inside of the axial skeleton, gorgonin and calcite are deposited in concentric growth rings, similar to tree rings. Colonies were collected from the Northeast Channel (northwest Atlantic Ocean, southwest of Nova Scotia, Canada) from depths of 250 – 475 m. Radiocarbon was measured in individual rings isolated from sections of each colony, after dissolution of calcite. Each $\Delta^{14}C$ measurement was paired with a ring age determined by three amateur ring counters. The precision of ring counts averaged better than ± 2 years. Accurate reconstruction of 20^{th} century bomb-radiocarbon shows that 1) the growth rings are formed annually, 2) the gorgonin is derived from surface particulate organic matter (POM) and 3) useful environmental data are recorded in the organic endoskeletons of deep-sea octocorals. These results support the use of *Primnoa resedaeformis* as a long-term, high resolution monitor of surface ocean conditions, particularly in temperate and boreal environments where proxy data are lacking.

3.2 INTRODUCTION

For generations, fishermen in Atlantic Canada have known about the occurrence of habitat-forming, deep-sea corals offshore (Breeze et al., 1997). There has been recent interest in using these corals as historical monitors of deep and intermediate water mass variability (Smith et al., 1997; Frank et al., 2004). This interest stems from the fact that deep-sea corals generally live for hundreds of years or more and their skeletons contain discrete growth layers (Druffel et al., 1995; Risk et al., 2002; Adkins et al., 2004). Geochemical sampling of these layers may provide long-term, high resolution records of proxy climate information, far beyond the range of instrumental records (Heikoop et al., 2002, Roark et al., 2005).

The deep-sea gorgonian coral *Primnoa resedaeformis* is one of the dominant corals found off eastern Canada, particularly in canyons along the shelf break (Breeze et al., 1997). It is also distributed throughout the Atlantic and Pacific Oceans at depths of 65-3200 m (Smithsonian holdings: http://goode.si.edu/webnew/pages/nmnh/iz/Query.php). The arborescent skeletons of *P. resedaeformis* are made up of calcite and gorgonin, a tough horny protein, deposited in concentric rings (Risk et al., 2002). Three growth zones are evident: 1) an inner "central rod" and 2) "horny axis", both made of calcite and gorgonin, and 3) an outer "calcite cortex", containing practically no gorgonin (Sherwood and Risk, in press). Growth rings in the horny axis are visible as light-dark couplets; the darker parts contain a higher percentage of gorgonin:calcite (Risk et al., 2002). Rings in the calcite cortex are more ambiguous; often they are barely visible as slight differences in translucence. Using ^{210}Pb

dating, Andrews et al. (2002) inferred that the growth rings in an Alaskan *Primnoa* colony were formed annually. Based on radiocarbon (Risk et al., 2002) and U/Th dating (Scott and Risk, 2003) of sub-fossil *P. resedaeformis* specimens collected near Georges Bank, life-spans of individual colonies may exceed several hundreds of years.

In this paper, we use bomb-produced radiocarbon to validate annual ring formation in colonies of *P. resedaeformis* collected off Nova Scotia, Canada. Oceanic uptake of bomb-^{14}C produced by atmospheric nuclear weapons testing in the late 1950s and early 1960s provides a time-varying tracer. In the North Atlantic, the timing of the increase is well constrained from direct measurements of dissolved inorganic carbon (DIC; Nydal et al., 1998) and indirectly, from measurements of ^{14}C in annually-banded reef corals from Bermuda and Florida (Druffel, 1989), and a long-lived quahog (*Arctica islandica*) from Georges Bank (Weidman and Jones, 1993). The initial rise of bomb-^{14}C in the surface ocean provides a unique time-marker which may be used to establish or validate skeletal chronology (Kerr et al., 2005). Additionally, if one knows the year of the post-bomb maximum for a certain location or water-mass the post-bomb peak itself can be used as a reference tie point (e.g. Roark et al., 2005). Since the gorgonin fraction of gorgonian corals is formed from recently exported particulate organic matter (POM; Griffin and Druffel, 1989; Roark et al., 2005; Sherwood et al., 2005b), we expect that living colonies of *P. resedaeformis* incorporated the bomb-^{14}C pulse. We focus on younger colonies (< 75 years), so that rings in the horny axis may be dated more easily.

Table 3.1 Summary of P. resedaeformis sections used on growth ring counting and $\Delta^{14}C$ determinations. Average year and standard error calculated from 3 different ring counters.

Section	Ring no.	Avg. year	SE	CAMS #	$\Delta^{14}C$ (‰)	±
DFO-2002-con5A1	5	1990	1.9	97097	36	5
DFO-2002-con5A1	10	1979	2.4	97098	52	4
DFO-2002-con5A1	16	1970	2.8	97099	71	4
DFO-2002-con5A1	21	1965	2.4	97100	59	4
DFO-2002-con5A1	25	1960	2.1	97101	-47	3
DFO-2002-con5A1	31	1953	2.1	97102	-77	3
DFO-2002-con5A1	37	1948	2.2	97103	-80	3
DFO-2002-con5A1	43	1942	2.8	97104	-72	3
DFO-2002-con5A1	50	1934	3.3	97105	-77	3
DFO-2002-con5A1	58	1924	3.3	97106	-72	3
HUD-2002-055-VG15-A3	10	1981	0.6	111140	67	4
HUD-2002-055-VG15-A3	19	1971	0.7	111142	90	4
HUD-2002-055-VG15-A3	27	1963	1.7	111143	-18	5
HUD-2002-055-VG13-2	22	1980	1.5	111139	59	4
NED-2002-037.46-1A	1	2002	0.3	111328	33	5
NED-2002-037.46-1A	16	1984	0.6	111329	68	5
NED-2002-037.46-1A	58	1947	0.7	111330	-82	4
NED-2002-037.46-5-1	25	1978	1.2	111331	63	4
ROPOS-639009-C4	19	1972	0.9	111623	82	4
ROPOS-639009-C4	27	1963	1.5	111624	-46	4
ROPOS-639009-C4	40	1951	0.3	111625	-70	3
ROPOS-6400013-E1	10	1994	1.2	111626	52	4
ROPOS-6400013-E1	15	1989	1.5	111141	54	4
ROPOS-6400013-E1	20	1984	1.5	111627	67	5
ROPOS-6400013-E1	25	1979	1.9	111628	61	4
ROPOS-6400013-E1	31	1972	3.3	111629	82	4

3.3 MATERIALS AND METHODS

Colonies of *Primnoa resedaeformis* were collected offshore Nova Scotia, Canada, from the Northeast Channel (approx. 42°00 N/ 65°50 W), located between Georges and Browns bank, at depths of 250-475 m. Collections were made in August 2001, during an expedition using the remotely operated submersible ROPOS aboard the CCGS Martha Black, and in the summer of 2002, by trawl, during routine oceanographic surveys conducted by the Bedford Institute of Oceanography. Some of the specimens were frozen at the time of collection, others were air-dried. Skeletal sections were cut from the thickest part of each recovered colony using a rock saw. The sections were ground and polished on a diamond lap wheel and photographed with a digital camera in macro mode under UV light. The UV light improves the appearance of ring couplets and makes it easier to distinguish the rings from cracks in the sections (Fig. 3.1).

To isolate the gorgonin fraction for radiocarbon assays, the sections were dissolved in 5% HCl until reaction ceased, which took up to 3 weeks. The sections were then placed in a Petrie dish filled with distilled water and the rings were picked apart with tweezers and scalpel under a binocular microscope, starting at the outside of each section, and moving in toward the centre. The exact position of each sample on a section was marked on photographic prints overlain with transparency film. The separated rings were placed in 5 ml polyethylene vials, topped with 5 % HCl and left for an additional 2 days to ensure that all of the calcite dissolved. Afterwards, samples were triple-rinsed in de-ionized water and dried at 70 °C overnight. From each colony, anywhere from 1 to 10 rings were selected for ^{14}C analysis, depending on colony age and the ease with which the

annual ring couplets could be identified and counted. Samples were preferentially selected to bridge the expected rise in bomb-^{14}C between 1958 and the early 1970s, because this provides the best constraint on chronology. Samples were combusted in individual quartz tubes and reduced to graphite in the presence of iron catalyst. Delta-^{14}C was determined on graphite targets at the Center for AMS. Results include a background and $\delta^{13}C$ correction and are reported as $\Delta^{14}C$ according to Stuiver and Polach (1977).

To obtain ring counts as objectively as possible, the photographic prints of each section were circulated randomly among departmental colleagues with no prior experience in counting rings in gorgonian corals or any other organism. The prints were overlain with a second layer of transparency film, with the first transparency flipped off. Ring counters were briefed for 5 minutes on how to identify an annual ring. They were then asked to mark the positions of annual rings on the second transparency. This involved drawing a line radially across parts of the sections where rings could be seen the easiest, and marking the annual rings along that line (Fig. 3.1). Each ring identified was assigned to a calendar year based on whether the outermost layer represented 2001 or 2002, depending on the year of collection. In 2 of the 7 colonies, there was tissue necrosis on the outer margin of the skeleton. For these "dead" colonies, a chronological control point was provided by the peak in $\Delta^{14}C$ (see below). Afterwards, the first transparency was replaced, and calendar years were paired with the rings isolated earlier. The counting experiment was repeated three times by different counters.

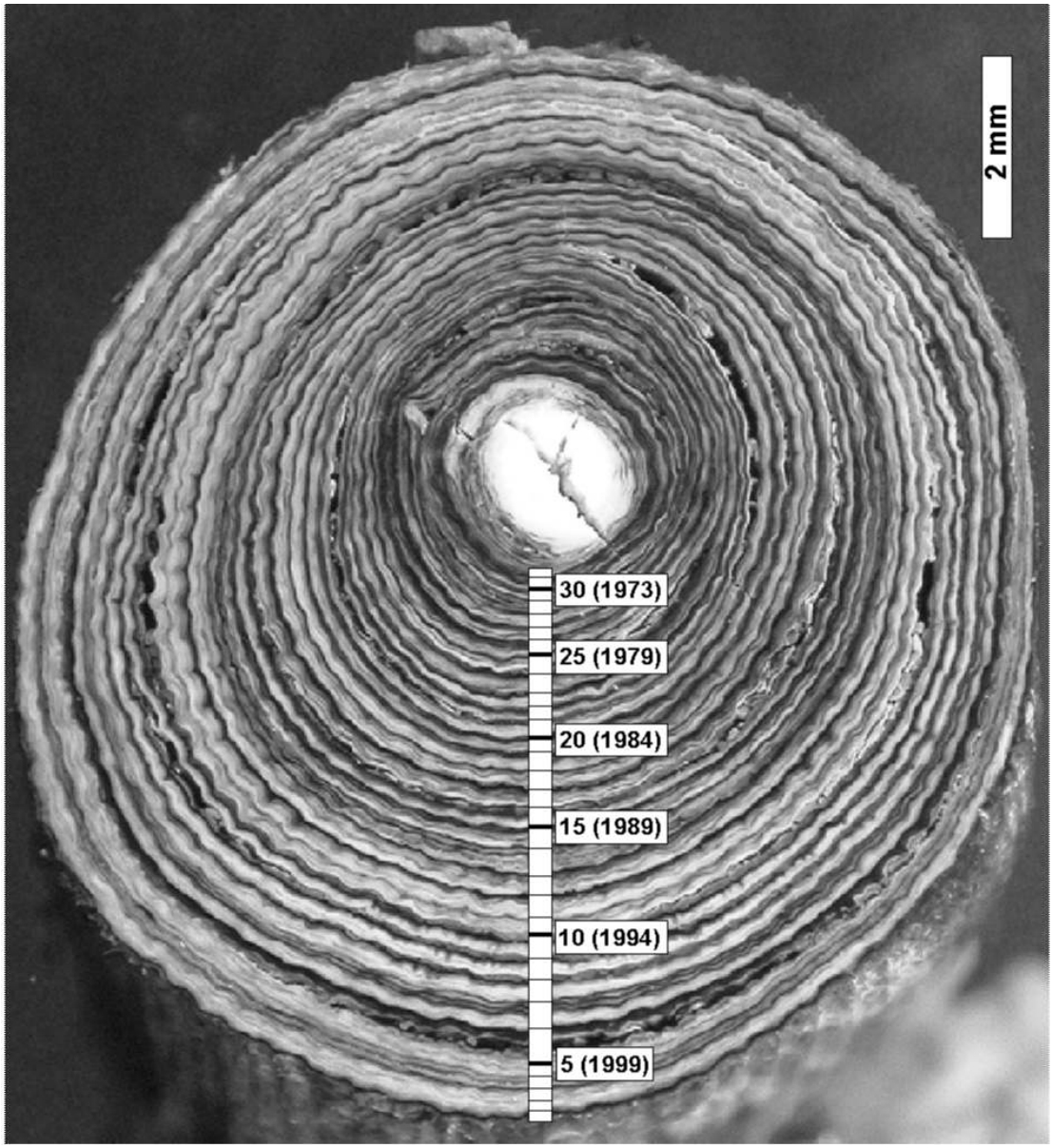

Fig. 3.1: Example section of *Primnoa resedaeformis* (Colony ROPOS-6400013; collected live in 2001). Lighter centre is the central rod, outer banded section is the horny axis. Calcite cortex is not present. Markings show individual rings isolated in preparation, with corresponding calendar age (in brackets) as determined by 3 counters.

3.4 RESULTS

The precision of growth ring counts, as measured by the standard error among three different ring counters, averaged ± 1.2 years (Table 3.1). Ages ranged from 24 - 78 years. The standard error increased slightly with age, as expected, because the chronological error is compounded with increasing age. The spread in values reflected differences in the "quality" of rings viewed in different sections. The least precise age estimates were generated on the older sections; but these were still relatively good (± 3.5 years).

The accuracy of growth ring counts is demonstrated in a plot of $\Delta^{14}C$ against calendar year (Fig. 3.2). Data from the 5 live colonies clearly indicated that the peak in $\Delta^{14}C$ occurred around 1972. Additional data from the two “dead” colonies were added to the figure by using 1972 as a chronological control point. An all-time high of +90 ‰ was measured in one colony, so this point was assigned to the year 1972. In the other specimen, a spline curve was fit through a plot of $\Delta^{14}C$ versus ring number in order to determine which ring number should be assigned to 1972.

The $\Delta^{14}C$ curve for *P. resedaeformis* is identical to that previously measured in an ocean qhahog (*Arctica islandica*) collected at a depth of 75 m on nearby Georges Bank (Weidman and Jones, 1993; Fig. 3.2). A similar curve based on the otoliths of haddock (*Melanogrammus aeglefinus*) collected on the southern Grand Banks has also been published (Campana, 1997; Fig. 3.2). The *P. resedaeformis*, *A. islandica*, and

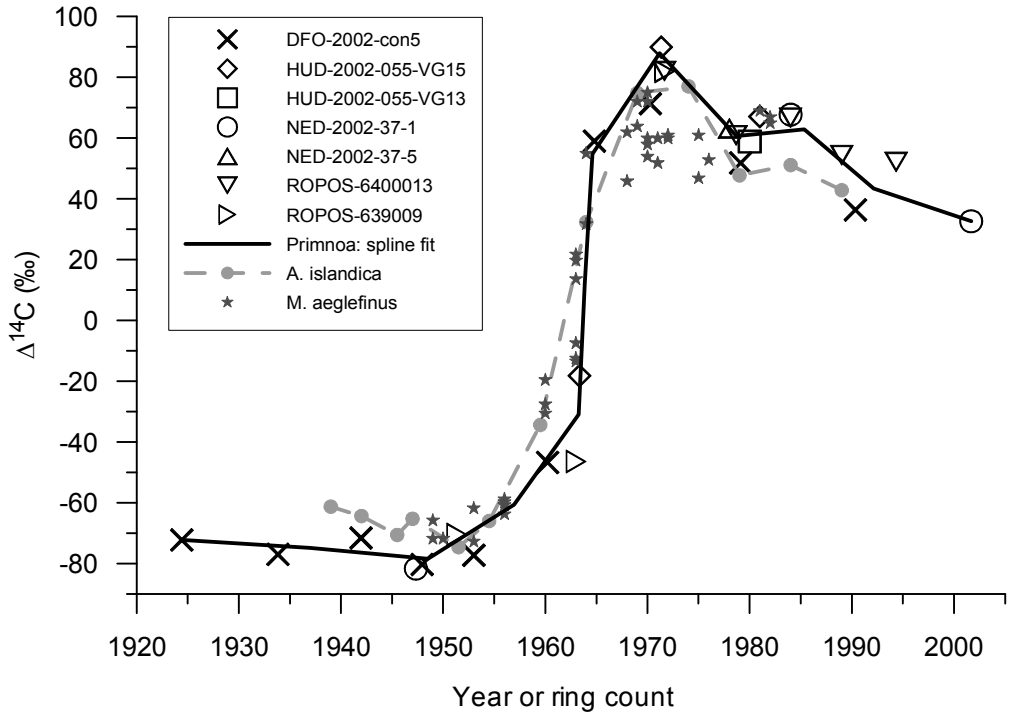

Fig. 3.2: Plot of $\Delta^{14}C$ vs. age for 7 different colonies of *P. resedaeformis* collected in the Northeast Channel. A spline fit is drawn through the data. Also shown are the data from a clam shell (*Arctica islandica*; Weidman and Jones, 1993), collected at a depth of 75 m on Georges Bank, and haddock otoliths (*Melanogrammus aeglefinus*; Campana 1997), collected on the Grand Banks.

M. aeglefinus curves all range from a pre-1958 low of ~ -80 ‰ to an early 1970s peak of ~ +80 ‰, followed by a gradual decrease to ~ +40 ‰ to the present.

3.5 DISCUSSION

The growth ring counting method used here is a relatively simple and effective way to age specimens of *P. resedaeformis* with an acceptable level of precision (SE < 2 years). The counters had no previous training in growth ring counting and were not asked to count any more than 3 specimens each, so no one individual became an expert counter.

The precision of ring counts largely depended on the quality of the sections. In some cases the growth rings were very narrow, making counting difficult. Sub-annual rings (Risk et al., 2002) could have been mistaken for annual rings. In addition, "calcite cortex" material was sometimes inter-layered with the horny material. Gorgonians colonies may bend and twist throughout their lives to keep their fans oriented perpendicularly to prevailing currents (Wainwright and Dillon, 1969). These growth variations affect the appearance of rings. Therefore, future studies involving ageing of *Primnoa* should select for the straightest and highest quality colonies. Similar considerations are routine in dendochronology and sclerochronology.

Samples for $\Delta^{14}C$ and growth ring counts were made on the same sections, such that each $\Delta^{14}C$ measurement had a matching calendar age. Data from eight different colonies were used to establish a twentieth century record of $\Delta^{14}C$. This record was identical to previously published $\Delta^{14}C$ records derived from a mollusc shell (Weidman and Jones, 1993) and haddock otoliths (Campana, 1997) collected from the NW Atlantic. The *P. resedaeformis* $\Delta^{14}C$ curve is also in phase with the record from annually banded reef coral skeletons from Florida and Bermuda (Druffel, 1989), and with direct measurements of surface water DIC (Nydal et al., 1998). The results are consistent with the interpretation that the ring couplets found in the horny axis region of *P. resedaeformis* are formed annually.

Andrews et al., (2002) also validated annual ring formation in an Alaskan *Primnoa*; however, they measured the rate of decay of ^{210}Pb over the length of a colony

to validate growth ring counts. Among shallow water gorgonians, annual growth rings have also been demonstrated by non-radiometric methods. Usually, this has involved the correspondence in age estimated from the height of a colony with the age estimated from growth rings (e.g. Grigg, 1974). The method described here is a more direct way of validating annual growth rings, since $\Delta^{14}C$ and age determinations were made on the same sections.

Similarity in the range and timing of $\Delta^{14}C$ measured in *P. resedaeformis* growing between 250-475 m with *A. islandica* growing at 75 m on Georges Bank suggests that the skeletons of these organisms are derived from the same pool of DIC. The carbonate shell of *A. islandica* incorporates ^{14}C directly from DIC (Weidman and Jones, 1993). The shelf waters on Georges Bank are well mixed; so DIC will have about the same $\Delta^{14}C$ from 0 - 75 m. In contrast to Georges Bank, the slope waters which occupy the Northeast Channel are stratified. If the gorgonin in *P. resedaeformis* were derived from ambient DIC at depth, $\Delta^{14}C$ would be much lower than actually measured (Bauer et al., 2002). As in shallow-water gorgonians that have been studied in situ (e.g. Ribes et al., 1999), zooplankton and sinking POM probably constitute the main diet of this species. Therefore, ^{14}C is assimilated by phytoplankton in surface waters, and is incorporated by *P. resedaeformis* via the plankton food web. The lack of a time lag in peak $\Delta^{14}C$ rules out the possibility that *P. resedaeformis* feeds on older, more refractory POM, as we have found with $\delta^{15}N$ data (Sherwood et al., 2005b). These results corroborate earlier work showing that gorgonin is derived from sinking POM (Griffin and Druffel 1989; Roark et al., 2005).

The range of $\Delta^{14}C$ values measured in *P. resedaeformis*, *A. islandica*, and *M. aeglefinus* (~ -80 to ~ +80 ‰) is depleted compared to reef coral records from Florida and Bermuda (~ -60 to ~ +160 ‰; Druffel, 1989). This difference has been explained by the supply of $\Delta^{14}C$-depleted Labrador Sea water to the NW Atlantic shelf and slope (Weidman and Jones, 1993). In the subtropics, more intense stratification prevents dilution of the bomb signal by $\Delta^{14}C$-depleted deep waters.

From a paleoceanographic standpoint, the formation of annual rings makes *P. resedaeformis* analogous to reef scleractinian corals. Geochemical proxy records from reef corals have been a mainstay of Holocene paleoceanography ever since Knutsen et al. (1972) conclusively demonstrated annual timing of density bands with ^{90}Sr. Accurate reconstruction of 20th century surface water $\Delta^{14}C$ demonstrates that useful environmental data are recorded in the organic fraction of *Primnoa* skeletons. In addition, the stable C and N isotopic composition of gorgonin may reflect surface water productivity (Sherwood et al., 2005b); thus, long term, high resolution reconstructions of surface processes may be feasible (Heikoop et al., 2002). The oldest colony in the present study was 78 years; but, colonies may live for at least 320 years (Risk et al., 2002). Useful information on ambient conditions at depth may also be contained in the skeletal calcite, since this fraction is derived from ambient DIC at depth (Griffin and Druffel, 1989; Roark et al., 2005).

There has been increasing interest in the frequency of climate forcing mechanisms such as the North Atlantic Oscillation. High-resolution proxy reconstructions from *Primnoa* may help to resolve the "spectral gap" issue between instrumental and proxy-based climate records, particularly in temperate and boreal environments, where proxy marine climate data are lacking.

ACKNOWLEDGEMENTS

We thank the *ROPOS* crew and the Bedford Institute of Oceanography for collecting specimens, and Joyia Chakungal, Jeremiah Couey, Flavia Fiorini, Jen McIntosh, Mike Rygel, Myles Thompson, Laurie Tremblay, Christine Ward-Paige and Jane Willenbring-Staiger for counting growth rings. Radiocarbon analyses were performed under the auspices of the U.S. Department of Energy by the University of California's Lawrence Livermore National Laboratory (W-7405-Eng 48). Funding was provided by an NSERC Strategic Grant to Mike Risk and David Scott and an NSERC postgraduate scholarship to Owen Sherwood.

CHAPTER 4

STABLE ISOTOPIC COMPOSITION OF DEEP-SEA GORGONIAN CORALS (*Primnoa* spp.): A NEW ARCHIVE OF SURFACE PROCESSES

Owen A. Sherwood [1], Jeffrey M. Heikoop [2], David B. Scott [1], Michael J. Risk [3], Thomas P. Guilderson [4, 5], Richard A. McKinney [6]

[1] Centre for Environmental and Marine Geology, Dalhousie University, Halifax, Canada

[2] Los Alamos National Laboratory, Los Alamos, USA

[3] School of Geography and Geology, McMaster University, Hamilton, Canada

[4] Center for Accelerator Mass Spectrometry, LLNL, Livermore, USA

[5] Department of Ocean Sciences & Institute of Marine Sciences, University of California Santa Cruz, Santa Cruz, USA

[6] USEPA Atlantic Ecology Division, Narragansett, RI, USA, 02882

Published as an article in:

Marine Ecology Progress Series 301: 135-148

(October 2005)

4. 1 ABSTRACT

The deep-sea gorgonian coral *Primnoa* spp. lives in the Atlantic and Pacific Oceans at depths of 65-3200 m. It has an arborescent growth form with a skeletal axis composed of annual rings made from calcite and gorgonin. Life-spans may exceed several hundreds of years. It has been suggested that isotopic profiles from the gorgonin fraction of the skeleton could be used to reconstruct long-term, annual-scale variations in surface productivity. We tested assumptions about the trophic level, intra- and inter-colony isotopic reproducibility, and preservation of isotopic signatures in a suite of modern and sub-fossil specimens. Measurements of gorgonin $\delta^{15}N$ indicate that *Primnoa* spp. feed mainly on zooplankton and/or sinking particulate organic matter (POM_{SINK}), and not on suspended POM (POM_{SUSP}) or dissolved organic carbon (DOC). Gorgonin $\delta^{13}C$ and $\delta^{15}N$ in specimens from NE Pacific shelf waters, NW Atlantic slope waters, the Sea of Japan, and a South Pacific (Southern Ocean sector) seamount were strongly correlated with Levitus 1994 surface apparent oxygen utilization (AOU; the best available measure of surface productivity), demonstrating coupling between skeletal isotopic ratios and bio-physical processes in surface water. Time-series isotopic profiles from different sections along the same colony, and different colonies inhabiting the same area were identical for $\delta^{13}C$, while $\delta^{15}N$ profiles were less reproducible. Similarity in C:N, $\delta^{13}C$ and $\delta^{15}N$ between modern and sub-fossil specimens suggest that isotopic signatures are preserved over millennial timescales. These results support the use of *Primnoa* spp. as historical recorders of surface water processes such as biological productivity and the isotopic composition of source nutrients.

4.2 INTRODUCTION

Primnoa resedaeformis (Gunnerson) is a deep-sea gorgonian coral with known occurrences in North Atlantic, Arctic and North Pacific waters at depths of 65-3200 m (Breeze et al., 1997; Etnoyer and Morgan, 2003). A subspecies, *Primnoa resedaeformis notialis* (Bayer), occurs on seamounts in the Southern Ocean sector of the Pacific Ocean. *Primnoa willeyi* (Hickson) and *Primnoa pacifica* (Kinoshita) are found in the eastern and western North Pacific, respectively (Smithsonian holdings: http://goode.si.edu/webnew/pages/nmnh/iz/Query.php). These corals have an arborescent growth pattern with a skeleton made of calcite and a proteinaceous material called gorgonin (Goldberg, 1976) arranged in alternating concentric rings around longitudinal growth axes (Risk et al., 2002; Sherwood, 2002). Towards the outer growth surface of older portions of the skeleton the outer cortex may be comprised of just calcite, with gorgonin layers lacking. Based on ^{210}Pb-dating Andrews et al. (2002) inferred that visible growth rings in the skeleton are formed annually. This was subsequently validated with bomb-^{14}C (Sherwood et al., 2005a). Sub-annual banding patterns have also been identified using scanning electron microscopy and Nomarski differential interference imaging (Risk et al., 2002; Sherwood 2002). This coral appears to have lifespans on timescales of up to several centuries (Andrews et al., 2002; Risk et al., 2002; Scott et al., 2005).

Based on ^{14}C analyses, Griffin and Druffel (1989) originally suggested that the main source of carbon to deep-sea corals was sinking particulate organic matter (POM). They further suggested (Druffel et al., 1995) that the carbon and nitrogen isotopic

composition of the proteinaceous layers of the colonial zoanthid *Gerardia* spp. could be a recorder of surface ocean processes (productivity, nutrient sources, etc.). *Primnoa* spp. may also form its gorgonin skeleton from sinking POM, since $\delta^{15}N$ and $\delta^{13}C$ in the polyps and gorgonin show similar regional differences to $\delta^{15}N$ and $\delta^{13}C$ of surface water POM (Heikoop et al., 1998; 2002). Moreover, the $\delta^{15}N$ and $\delta^{13}C$ of the polyps is highly correlated to the $\delta^{15}N$ and $\delta^{13}C$ of associated gorgonin (Heikoop et al., 2002). Together, these results suggest that the isotopic composition of annual gorgonin layers could record the temporal history of processes that control the isotopic composition of POM (Heikoop et al., 2002) including plankton productivity and the $\delta^{15}N$ and $\delta^{13}C$ of nutrient sources (e.g. Ward-Paige et al., 2005). The $\delta^{15}N$ and $\delta^{13}C$ of gorgonin from a suite of corals from Alaskan waters, waters off the eastern shore board of the United States and Canada, and a South Pacific seamount were positively correlated (Heikoop et al., 2002), suggesting that surface ocean productivity relative to nutrient supply may be the primary control on the isotopic composition of gorgonin.

For stable isotopic profiles generated from the annual gorgonin layers of *Primnoa spp.* skeletons to have any meaningful environmental significance, four conditions must be met: (1) the trophic position of *Primnoa* spp. must be known; (2) organic diagenesis must not affect the isotopic composition of the skeleton; isotopic trends must be reproducible among (3) different sections of the same colony; and (4) different colonies inhabiting the same area. The purpose of this paper is to test these assumptions using a suite of recently collected live and sub-fossil specimens from the Atlantic and Pacific oceans.

Table 4.1 *Primnoa* spp. Collection data of samples examined. n/a: not applicable

Sample	Species	Location	Year collected	Lat	Lon	Depth
NW Atlantic						
ROPOS 637052	*P. resedaeformis*	NE Channel	2001	42.048°N	65.577°W	475
ROPOS 639009	*P. resedaeformis*	NE Channel	2001	41.998°N	65.648°W	410
HUD-2000-020-VG2	*P. resedaeformis*	NE Channel	2000	42.047°N	65.610°W	331
HUD-2001-055-VG-15	*P. resedaeformis*	NE Channel	2001	42.021°N	65.682°W	321
DFO-2002-con5	*P. resedaeformis*	NE Channel	2002	42.0°N [d]	-65.6°W [d]	250-500
COHPS-2001-1 [a]	*P. resedaeformis*	NE Channel	2001	42.0°N [d]	-65.6°W [d]	250-500
Fossil-95 [b]	*P. resedaeformis*	NE Channel	1995	42.0°N [d]	-65.6°W [d]	250-500
Smith-54269	*P. resedaeformis*	E. of Virginia Beach	1974	37.060°N	74.410°W	237-385
NE Pacific						
QC-98	*P. willeyi*	E. of Queen Charlotte Islands	1998	54.386°N	132.786°W	378
KIS-02	*P. willeyi*	Knight Inlet sill, BC	2002	50.679°N	126.000°W	65
Smith-51283 [c]	*P. pacifica*	P. William Sound, AK	1941	61.034°N	146.714°W	64
Smith-52199	*P. willeyi*	Chatham Sound, BC	1960	54.5°N [d]	130.5°W [d]	n/a
Smith-1010257	*P. willeyi*	Atka Island, AK	2002	51.9°N [d]	174.1°W [d]	213-220
Smith-1010785	*P. willeyi*	S. of Chirikof Island, AK	2000	55.5°N [d]	155.5°W [d]	235
Sea of Japan						
SOJ-03	*P. pacifica*	S. of Vladivostok, Russia	2003	42.482°N	132.572°E	913
Smith-56993 [c]	*P. pacifica*	West of Hokkaido, Japan	1906	43.000°N	140.175°E	713-783
S Pacific – Southern Ocean Sector						
Smith-58171 [c]	*P. resedae. notialis*	S. Pacific Seamount	1964	54.833°S	129.833°W	604
Smith-87624 [c]	*P. resedae. notialis*	S. Pacific Seamount	1964	54.817°S	119.800°W	549

a Fossil specimen, ca. 150 yrs old based on 210Pb dating
b Fossil specimen, ca. 2000 yrs old based on U-Th dating (Scott et al. 2003)
c preserved in ethanol
d Exact co-ordinates unknown; these are general co-ordinates for the location reported

4.3 MATERIALS AND METHODS

Specimens were obtained during research and fishing expeditions (Table 4.1). Seven additional specimens were obtained from the Smithsonian Institution National Museum of Natural History. *Primnoa resedaeformis* (Gunnerus) was collected from the Northeast Channel, southwest of Halifax, Nova Scotia (Fig. 4.1) and from east of Virginia Beach, USA. *Primnoa willeyi* (Hickson) was collected east of the Queen Charlotte Islands, Chatham Sound and Knight Inlet, British Columbia, and from the Aleutian Islands and Prince William Sound, Alaska. *Primnoa pacifica* (Kinoshita) was collected in the Sea of Japan. The subspecies *Primnoa resedaeformis notialis* was collected from a seamount in the Southern Ocean sector of the South Pacific. Three of the Smithsonian samples were originally reported in Heikoop et al., (2002); these are included here to highlight geographic trends in stable isotopic composition.

All specimens were collected alive, except for Fossil-95 and COHPS-2001-1. These dead-collected specimens were dated radiometrically by B. Ghaleb at GEOTOP-UQAM-McGill, Montreal, Canada (Chapter 6). Samples from COHPS-2001-1 are ca. 150 yrs old, based on ^{210}Pb-^{226}Ra analyses of the outer calcite cortex region of the coral. Fossil-95 is ca. 2000 years old, based on two uranium-series dates on the middle and outer regions of a section of the colony.

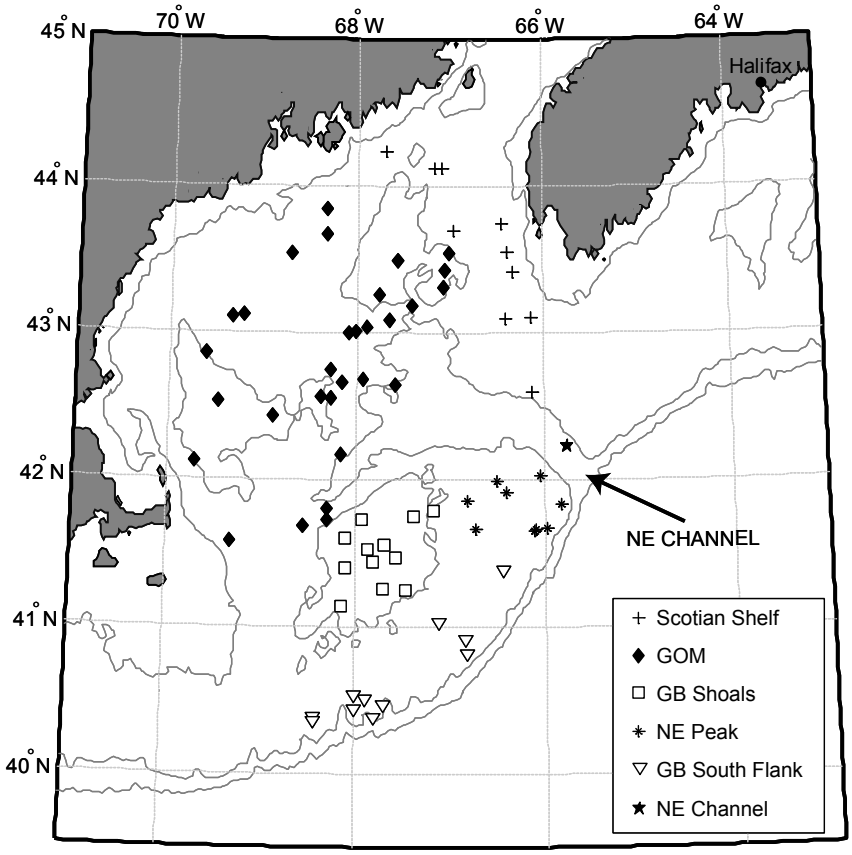

Fig. 4.1: Map of the Gulf of Maine region, NW Atlantic Ocean. Colonies of *Primnoa resedaeformis* were collected from the NE Channel. Symbols show locations of water samples for analysis of POM_{SUSP}.

Colonies for stable isotopic analyses (Fig. 4.2) were sectioned with a rock saw and ground and polished on a diamond lap wheel to a thickness of about 5 mm. Sections were photographed with a Nikon Coolpix digital camera in macro mode. After some trial and error we found that photographing the sections in ultraviolet light gave the clearest image of ring patterns in the horny axis owing to contrast between the calcite-rich (luminescent) and gorgonin-rich (non-luminescent) portions of the annual growth rings (Fig. 4.3).

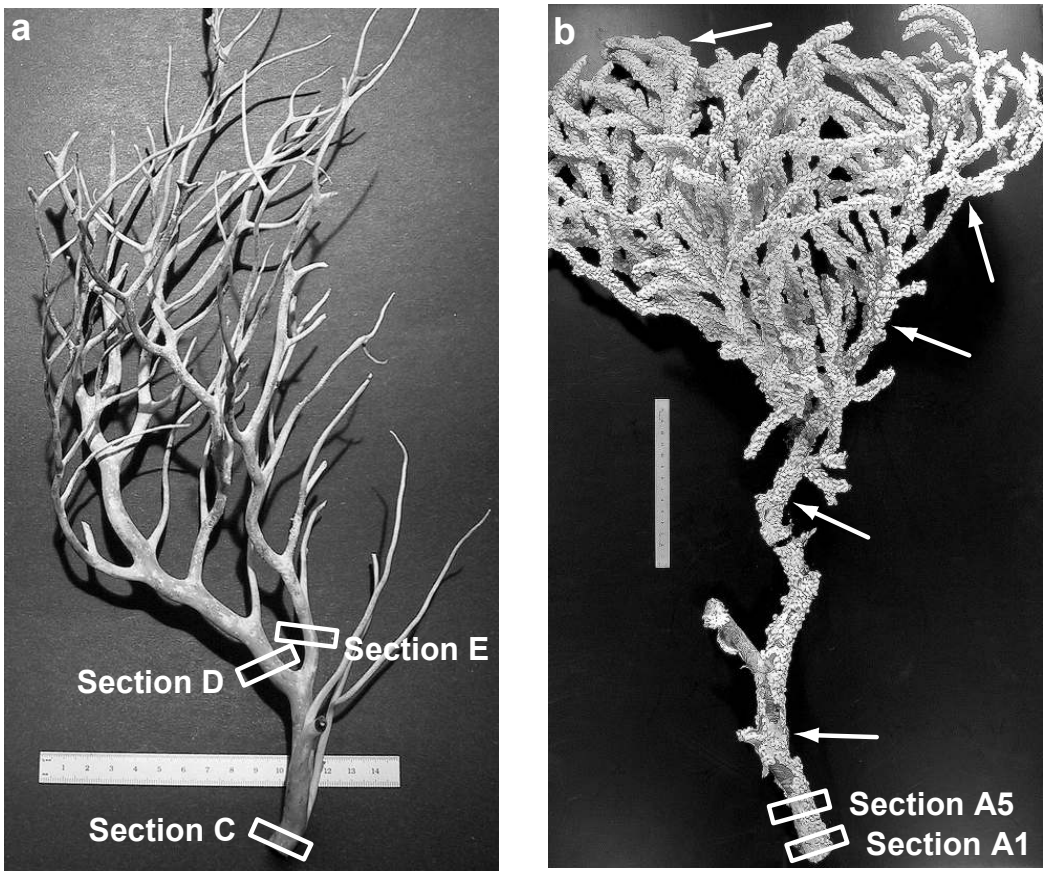

Fig. 4.2: Colonies of *Primnoa resedaeformis* collected from the Northeast Channel: (a) HUD-2001-055-VG15 (tissue missing) and (b) DFO-2002-con5 (tissue present). Sections for isotopic time-series profiles are indicated by boxes, tissue samples are indicated by arrows. Ruler for scale is 15 cm.

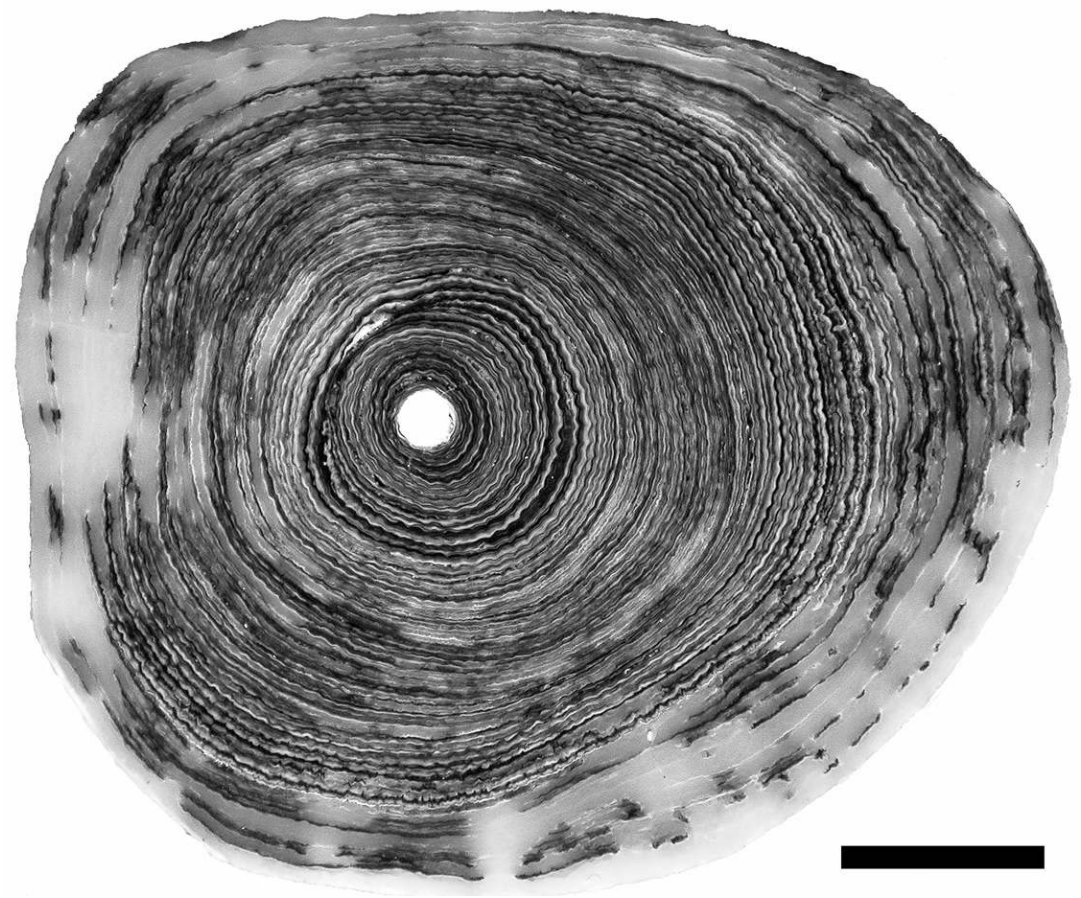

Fig. 4.3: Section A5 from Colony DFO-2002-con5, photographed under ultraviolet light. White portion towards the outside is the inorganic calcite cortex. Darker layers toward middle are annual gorgonin rings isolated for chemical analyses. Specimen is approx. 75 yrs old, based on growth ring counts (Sherwood et al., 2005a). Bar for scale is 0.5 cm.

Annual gorgonin rings were isolated by dissolving sections in 5% HCl for a week (up to three weeks for larger sections). Upon dissolution sections were transferred to a Petrie dish filled with distilled water, and the annual rings were picked apart with tweezers and scalpel under a binocular microscope. Photographs of the sections taken before dissolution were used to guide sampling. Individual rings were placed in 5 ml polyethylene vials with 5 % HCl, for an additional week, to ensure that all the calcite had dissolved. After two more rinses in HCl, the rings were triple rinsed in de-ionized water and dried in a low temperature oven. Rings averaged about 5 mg in weight. Tissue material scraped off the skeletal axes was prepared in the same way.

Isotopic and C:N analyses of gorgonin were performed by Elemental Analyzer/ Continuous Flow Isotope Ratio Mass Spectrometry at GEOTOP-UQAM-McGill. Isotope ratios are reported in conventional delta notation, where (example for carbon): $\delta^{13}C = [(R_{sample}/R_{standard}) - 1] \times 1000$; and $R = {}^{13}C/{}^{12}C$. Standards used were PDB ($\delta^{13}C$) and air ($\delta^{15}N$). Analytical error, as measured by the standard deviation of duplicate measurements, averaged 0.10 ‰ for $\delta^{13}C$ and $\delta^{15}N$, and 0.01 for C:N. Some of the corals obtained from the Smithsonian Institute were preserved in ethanol, which may have affected stable isotopic compositions (Bosley and Wainright, 1999).

Suspended particulate organic matter (POM_{SUSP}) in the Gulf of Maine/Georges Bank region (Fig. 4.1) was sampled as part of the Ecosystems Monitoring Survey at the Northeast Fisheries Science Center, Narragansett, RI, USA. Samples were collected in spring, summer and autumn, between November 2000 and August 2003. In addition, a

vertical transect (depths 3.7 m, 100 m and 215 m) was sampled in the Northeast Channel in August 2004 (Fig. 4.1). Surface samples were obtained with a ship-board, near surface flow–through system. Deeper samples were collected with Niskin bottles attached to a CTD rosette. A volume of 600-1000 ml of water was pre-filtered through 300 μm mesh to remove most zooplankton, then onto a GF/F filter. Samples were immediately frozen and transported to the US Environmental Protection Agency, Atlantic Ecology Division, Narragansett, RI for isotopic analysis. Nitrogen and carbon isotopic composition was determined by continuous flow isotope ratio mass spectrometry using a Carlo-Erba NA 1500 Series II Elemental Analyzer interfaced to a GV Instruments Optima Mass Spectrometer. All samples were analyzed in duplicate with a typical difference of about 0.1 ‰. Sample material was re-analyzed periodically over a several month period and exhibited a precision of 0.30 ‰, calculated as a single sigma standard deviation of all replicate values. This latter estimate of precision is appropriate for POM_{SUSP} $\delta^{15}N$ values determined in this study.

Table 4.2 *Primnoa* spp. Summary of stable isotopic and C:N data (mean ± SD). $\delta^{13}C$'; lipid-normalized $\delta^{13}C$; -; insufficient material for analysis

Sample	Tissue					Gorgonin				
	n	C:N	$\delta^{13}C$	$\delta^{13}C$'	$\delta^{15}N$	n	C:N	$\delta^{13}C$	$\delta^{13}C$'	$\delta^{15}N$
NW Atlantic										
ROPOS 637052	3	7.70 +/- .47	-23.68 +/- .06	-21.50	10.22 +/- .12	16	-	-19.15 +/- .28	-20.3[c]	9.74 +/- .15
ROPOS 639009	3	7.45 +/- .31	-23.92 +/- .20	-21.82	10.12 +/- .05	26	3.17 +/- .04	-19.13 +/- .49	-20.34	9.95 +/- .47
HUD 2000-020-VG2	-	-	-	-	-	12	3.17 +/- .05	-19.38 +/- .27	-20.59	9.50 +/- .51
HUD2001-055-VG-15	-	-	-	-	-	107	3.15 +/- .03	-19.01 +/- .74	-20.25	10.13 +/- .56
DFO-2002-con5	5	7.25 +/- .80	-23.87 +/- .30	-21.84	10.58 +/- .31	99	-	-19.03 +/- .55	-20.18[c]	10.28 +/- .4
COHPS2001-1	-	-	-	-	-	21[b]	3.41 +/- .10	-17.79 +/- .53	-18.59	10.86 +/- .47
Fossil-95	-	-	-	-	-	6	3.46 +/- .07	-18.29 +/- .48	-19.01	10.99 +/- .45
Smith-54269 [a]	4	-	-20.65 +/- .34	-	-	1	-	-18.35	-19.50[c]	11.8
NE Pacific										
QC-98	3	7.67 +/- .57	-21.17 +/- .20	-19.00	13.26 +/- .13	3	3.22 +/- .04	-17.93 +/- .16	-19.04	12.82 +/- .20
KIS-02	1	5.73	-19.42	-18.05	13.80	8	3.26 +/- .06	-16.08 +/- .34	-17.13	12.26 +/- .33
Smith-51283 [a]	5	-	-16.50 +/- .38	-	-	2	-	-16.17 +/- .39	-17.32[c]	13.8
Smith-52199	1	4.06	-18.24	-18.17	12.53	-	-	-	-	-
Smith-1010257	4	6.89 +/- .43	-23.77 +/- .04	-21.87	9.09 +/- .22	-	-	-	-	-
Smith-1010785	3	6.22 +/- .23	-19.49 +/- .15	-17.86	12.75 +/- .18	-	-	-	-	-
Sea of Japan										
SOJ-03	3	4.87 +/- .03	-22.45 +/- .11	-21.64	12.91 +/- .16	2	3.22 +/- .02	-19.46 +/- .11	-20.58	10.45 +/- .37
Smith-56993	3	4.52 +/- .05	-21.24 +/- .38	-20.72	10.67 +/- .09	-	-	-	-	-
S Pacific – Southern Ocean Sector										
Smith-58171	3	4.12 +/- .01	-22.05 +/- .30	-21.91	7.76 +/- .12	3	-	-	-	-
Smith-87624 [a]	3	-	-21.14 +/- .57	-	-	2	-	20.41 +/- .45	-21.56[c]	7.8

[a] Isotopic analyses performed at University of New Mexico; all others at GEOTOP
[b] Only 3 samples were analyzed for C:N
[c] assumes a C:N ratio of 3:2

4.4 RESULTS

4.4.1 Composition of tissue and skeletal gorgonin

Stable isotope and C:N data for *Primnoa* spp. are summarized in Table 4.2. Missing entries reflect cases of insufficient sample material for analyses. There were large differences in the isotopic and elemental composition between tissue and gorgonin. C:N ratios were higher and more variable in tissue (6.1 +/- 1.4, n = 11) than gorgonin (3.3 +/- 0.1, n = 8). $\delta^{13}C$ values were more negative in the tissue by an average of 3.0 +/- 1.7 ‰ (n = 9). Most of this difference in $\delta^{13}C$ may be accounted for by the difference in lipid content of the two fractions. Taking C:N as a proxy for lipid content, lipid-normalized values of $\delta^{13}C$ ($\delta^{13}C$') were calculated from equations in McConnaughey and McRoy (1979). After normalization, $\delta^{13}C$' values were more negative in the tissue by 1.0 +/- 0.6 ‰ (n = 6). Values of $\delta^{15}N$ were more positive in the tissue by 0.9 +/- 0.9 ‰ (n = 6).

The reason for lower $\delta^{13}C$' (even after lipid-normalization) and higher $\delta^{15}N$ in the tissue compared with the gorgonin is not clear, but may be related to differences in tissue turn-over time (Tieszen et al., 1983). Each gorgonin layer integrates seasonal variations over one year, and the average isotopic compositions listed in Table 4.2 integrate inter-annual variations over many years. We expect that the tissue, which turns over in something less than one year, represents a unique seasonal signature. Another possibility relates to differences in the amino acid contents of the two fractions (Sherwood et al., 2006). Different amino acids are known to have unique and widely variable $\delta^{13}C$ (Keil and Fogel, 2001) and $\delta^{15}N$ (McClelland and Montoya, 2002); therefore, the relative

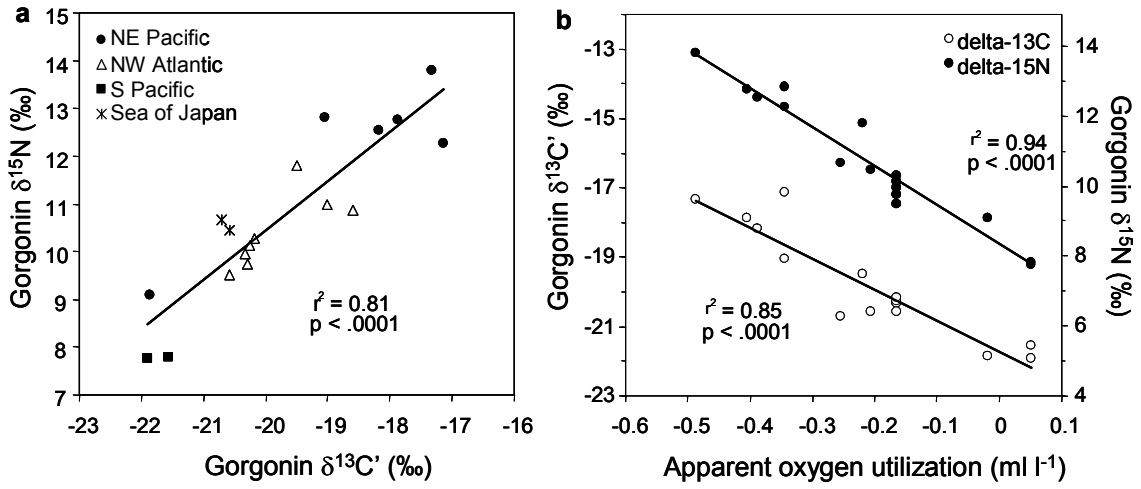

Fig. 4.4: (a) Plot of average $\delta^{15}N$ vs. $\delta^{13}C'$ (lipid normalized $\delta^{13}C$) from the gorgonin fraction of different *Primnoa* spp. colonies. (b) Same data, plotted against Apparent Oxygen Utilization in surface water. Note, where gorgonin was not measured, the tissue isotopic values were plotted instead.

proportion of amino acids between tissue and gorgonin may impart differences in stable isotopic content.

4.4.2 Geographic and interspecific variability

There were significant compositional differences among the different species and geographic areas (Table 4.2). *Primnoa pacifica* and *Primnoa resedaeformis notialis* from the Sea of Japan and South Pacific had the lowest tissue C:N values (4.5 +/- 0.4, n = 3). *Primnoa willeyi* from the NE Pacific had intermediate C:N (6.1 +/- 1.4, n = 5), and *Primnoa resedaeformis* from the NW Atlantic had the highest C:N (7.5 +/- 0.2, n = 3). $\delta^{13}C'$ and $\delta^{15}N$ were positively correlated ($p < 0.001$; Fig. 4.4a), as previously found in Heikoop et al., (2002). Isotope values in $\delta^{15}N$ vs. $\delta^{13}C'$ space were clearly delineated by geography, with highest values in the NE Pacific, intermediate values in the NW Atlantic

and Sea of Japan, and lowest values in the Pacific-Southern Ocean Sector (Fig. 4.4a). The sample from Atka Island in the NE Pacific (Smith-1010257) deviated from this pattern; it had isotopic values more similar to the South Pacific samples.

Isotope values were plotted against apparent oxygen utilization (AOU), selected from the Levitus and Boyer (1994) dataset as the best available measure of surface productivity for open ocean, slope water and shelf sites alike (Fig. 4.4b). Surface-water AOU data were obtained from the 0.5^{o} latitude X 0.5^{o} longitude grid nearest each of the coral collection locations. Both $\delta^{13}C$' and $\delta^{15}N$ significantly increased with more negative AOU (i.e. higher productivity; $p < 0.0001$).

4.4.3 Intra-colony isotopic reproducibility

Specimen HUD2001-055-VG15 was the first colony examined for trends in the isotopic composition of annual gorgonin rings. This colony was collected alive and transferred to an aquarium, where the tissue layer eventually died and sloughed off the skeleton. A 50 cm long main branch was snapped off the colony for geochemical sampling. Sections for stable isotopic analyses were cut from the base of the main branch, and from two divergent branches 10 cm higher up the colony (Fig. 4.2a). The basal section measured 14 mm in diameter. Stable isotope and C:N profiles from this specimen are shown in Fig. 4.5. The $\delta^{13}C$ profiles were identical among the three different sections (correlation coefficients (r) ranged 0.84 to 0.97; $p < 0.0001$), showing trends towards heavier values with increasing age. The amplitude of $\delta^{13}C$ profiles was 3 ‰, much larger than the analytical error (0.10 ‰). $\delta^{15}N$ profiles were less reproducible between the

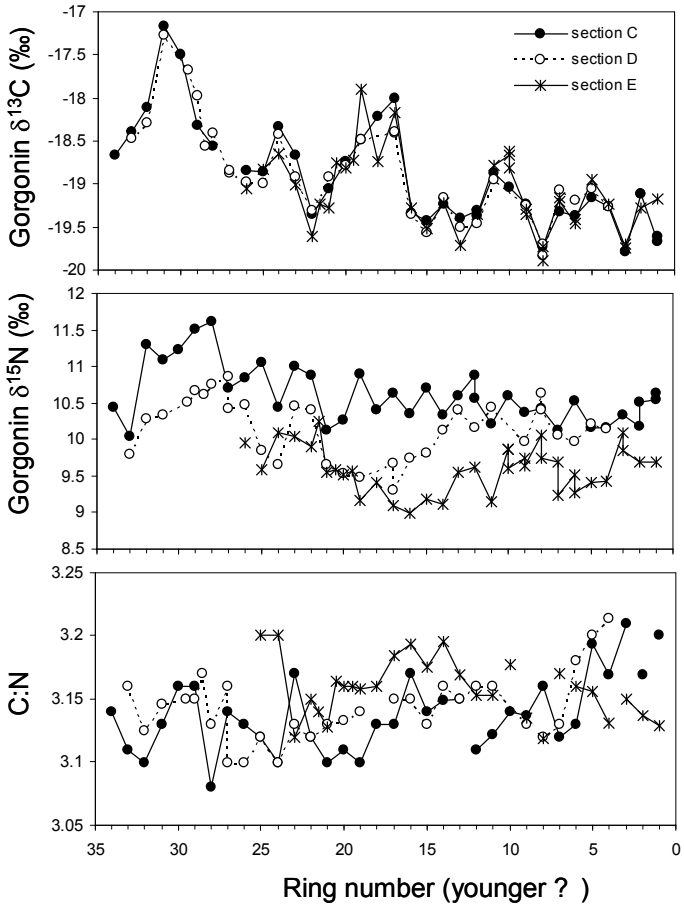

Fig. 4.5: Intra-colony isotopic and C:N profiles from three different section of Colony HUD-2001-055-VG15. (see Fig. 4.2a) for location of sections along colony axis).

different sections (r = 0.38 to 0.48; p = < .01 to .05). Differences among coeval rings, up to 1.5 ‰, were equivalent to the amplitude of the profiles, and cannot be explained by analytical error. C:N profiles were the least reproducible among the different sections (r = -0.23 to 0.44; p = 0.02 to 0.78), with differences among coeval rings (up to 0.07) exceeding the analytical error (0.01).

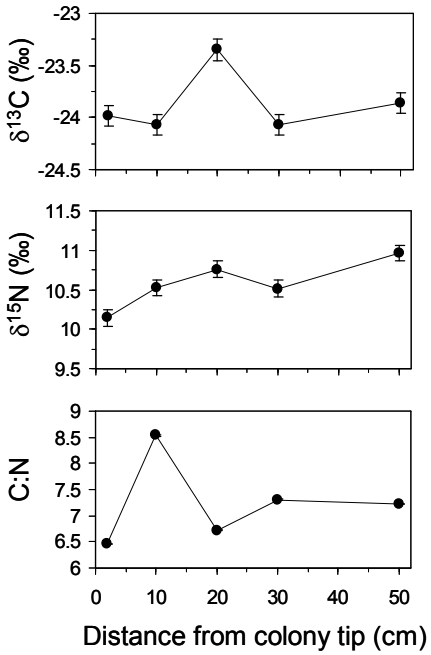

Fig. 4.6: Isotopic and C:N data from the tissue fraction of Colony DFO-2002-con5 (see Fig. 4.2b for location of samples along colony axis). Error bars are 1σ.

A larger colony of *Primnoa resedaeformis* (DFO-2002-con5) was subsequently obtained from the Canadian Department of Fisheries and Oceans and the same experiment was repeated. This colony was completely covered in live tissue and was frozen immediately after collection (Fig. 4.2b). Sections for geochemistry were thawed and air dried in the laboratory. The colony received measured 70 cm in length and had a diameter of 26 mm at the base, which included a thick accumulation of calcite cortex (Fig. 4.3). Analyses of five tissue samples taken along the length of DFO-2002-con5 showed no difference in $\delta^{13}C$, within analytical error (Fig. 4.6). The exception was the tissue sample 20 cm from the top of the colony, which had a value 0.3 ‰ heavier than the

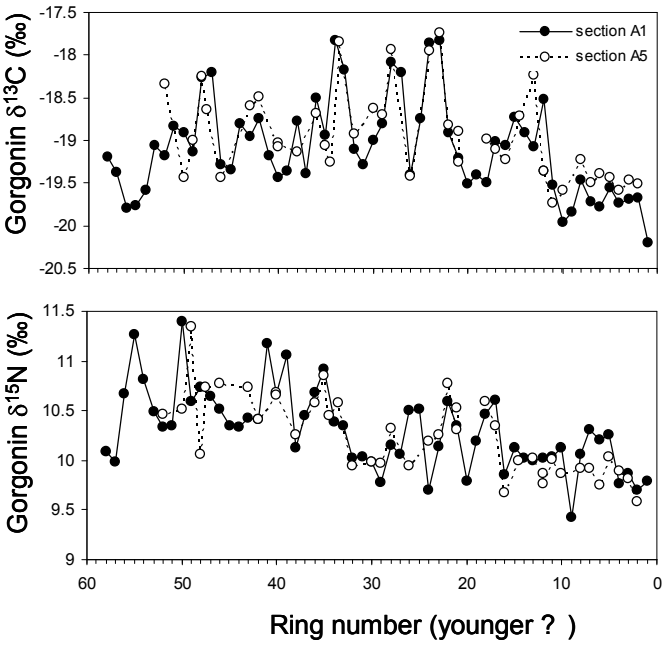

Fig. 4.7: Intra-colony isotopic profiles from two different sections of Colony DFO-2002-con5 (see Fig. 4.2b for location of sections along colony axis).

10

rest. $\delta^{15}N$ was slightly more variable, with values increasing steadily by 0.8 ‰ from the tip to the base of the colony. C:N varied by up to 2 among the different tissue samples. Stable isotope profiles (Fig. 4.7) of gorgonin layers were generated from two sections at the base of the colony, separated by a distance of 3 cm. C:N was not measured. Isotope profiles were virtually identical among the two different sections ($r = 0.69$ $\{\delta^{13}C\}$ and 0.63 $\{\delta^{15}N\}$; $p < .0001$).

4.4.4 Inter-colony isotopic reproducibility

Inter-colony isotopic reproducibility was assessed among three different colonies (Fig. 4.8). For each colony, ring numbers were converted to calendar ages as

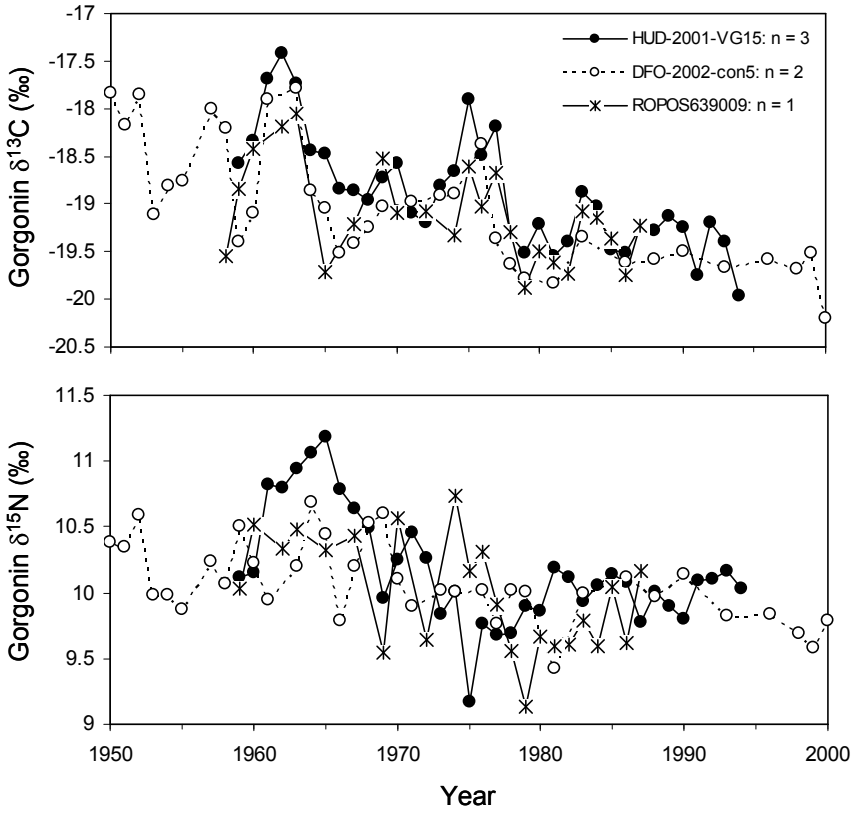

Fig. 4.8: Inter-colony isotopic profiles from three different colonies. Chronology is based on growth ring counts with bomb-^{14}C validation (Sherwood et al. 2005a). Where "n" (number of sections per colony analyzed) was > 1, the average of the profiles is plotted.

described in Sherwood et al., (2005a). Briefly, photographic prints of each section were circulated among three amateur counters, and the average of the three age determinations was calculated. Ring counts were validated by measurements of bomb-^{14}C in each of the sections (Sherwood et al., 2005a). The inter-colony results paralleled intra-colony results, with excellent reproducibility of δ^{13}C, and poorer reproducibility of δ^{15}N (Fig. 4.8). Correlation of δ^{13}C time-series among the different colonies was highly significant ($r = 0.67$ to 0.86; $p < 0.0001$). Correlation of δ^{15}N was significant between colonies HUD-

2001-055-VG15 and ROPOS-639009 ($r = 0.44$; $p < 0.05$), but was insignificant in the other two cases.

4.4.5 Comparison of modern and sub-fossil specimens

The two specimens from ca. 150 and 2000 yrs BP were compared to other corals collected alive from the Northeast Channel (Table 4.2). C:N ratios of these older specimens, 3.4 +/- 0.1 (n = 9), were slightly higher than the modern ones, 3.15 +/- 0.05 (n = 260). The sub-fossil samples were heavier in $\delta^{13}C$' (lipid normalized to account for difference in C:N) by 1.5 ‰ (Fig. 4.9). Part of this difference may be explained by the Suess effect, caused by the depletion of atmospheric ^{13}C from the burning of fossil fuels, with subsequent depletion of oceanic dissolved inorganic carbon (DIC; Quay et al., 1992). The 1.5 ‰ difference between the 150 yr old COHPS-2001-1 and the most recent samples from DFO-2002-con5 is consistent with the decrease in atmospheric $\delta^{13}C$ between the mid 1800s and the present (Francey et al., 1999). The lighter values from ca. 1920, however, exceed the magnitude of the Suess effect. Therefore, there may be other oceanographic and/or trophic level changes affecting $\delta^{13}C$ over shorter timescales. There was also a slight trend towards higher $\delta^{15}N$ with age, with the two sub-fossil specimens having similar values as the oldest layers from DFO-2002-con5 (Fig. 4.9).

4.4.6 $\delta^{15}N$ composition of plankton

In order to assess the TL of *Primnoa resedaeformis* collected from the Northeast Channel (see below) $\delta^{15}N$ at the base of the food web was assessed from measurements of POM_{SUSP}. Unfortunately, the Northeast Channel was not targeted for sampling in years

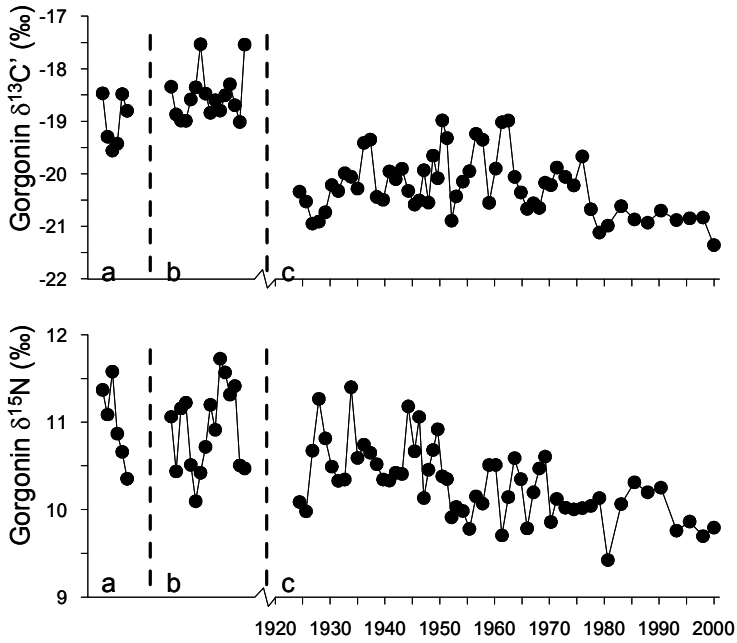

Fig. 4.9: Isotopic profiles from: (a) Colony Fossil-95, ca. 2000 yr old, based on U-series dating (Scott et al. 2003); (b) Colony COHPS-2001-1, ca. 200 yrs old, based on ^{210}Pb-dating; (c) Colony DFO-2002-con5, calendar yrs based on growth ring counts, with bomb-^{14}C validation (Sherwood et al., 2005a).

2000-2003 of the Ecosystems Monitoring Survey (Fig. 4.1). With the exception of the central shoals of Georges Bank, δ^{15}N in surface water POM_{SUSP} was consistent throughout the entire region (4.1 +/- 1.2 ‰, n = 56; Fig. 4.10). We therefore assume that this value is representative of POM_{SUSP} in waters overlying the Northeast Channel.

In August 2004, the Northeast Channel was occupied to collect POM_{SUSP} along a depth transect (Fig. 4.1). Below the euphotic zone δ^{15}N increased rapidly to a maximum of 18.5 ‰ at 215 m depth (Fig. 4.11). While these data represent only one snapshot in

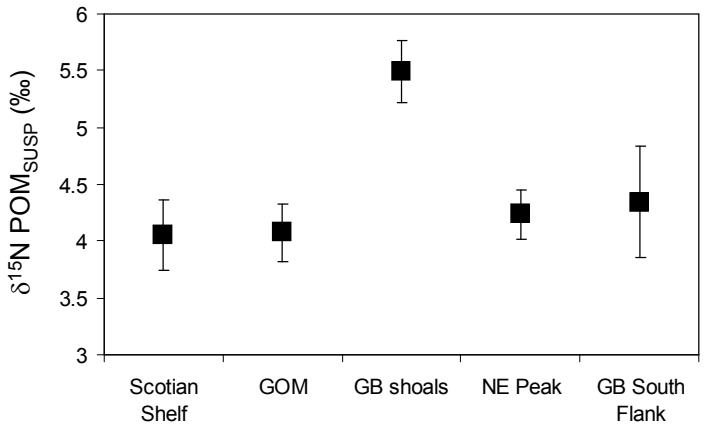

Fig. 4.10: Average (± 1σ) $\delta^{15}N$ of POM_{SUSP} in surface waters of the different areas in the Gulf of Maine/Georges Bank region. Site designations correspond to Fig. 4.1

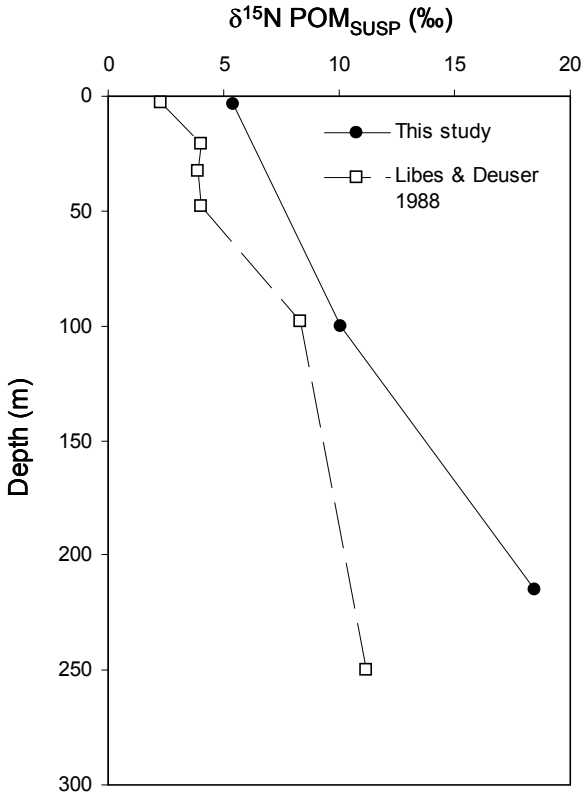

Fig. 4.11: Depth profiles of $\delta^{15}N$ of POM_{SUSP} from the Northeast Channel (this study; see Fig. 4.1 for location), and from Wilkinson Basin inside the Gulf of Maine (Libes and Deuser, 1988)

time, they are consistent with earlier results reported for Wilkinson Basin, located farther inside the Gulf of Maine (Libes and Deuser, 1988).

4.5 DISCUSSION

4.5.1 Trophic level

It has been demonstrated that deep-sea corals form their organic endoskeletons from sinking POM (POM_{SINK}), based on the presence of modern $\Delta^{14}C$ (> 0 ‰) in the gorgonin fraction their skeletons (Griffin and Druffel, 1989; Roark et al., 2005; Heikoop et al., 1998; Sherwood et al., 2005a). Reconstruction of bomb-^{14}C from the skeletons of *Primnoa resedaeformis* collected from the Northeast Channel (Sherwood et al., 2005a) was identical to other proxy records derived from a mollusc shell (Weidman and Jones, 1993) and haddock otoliths (Campana, 1997). Moreover, the timing of the initial rise and peak in bomb-^{14}C was in phase with direct measurements of seawater DIC (Nydal et al., 1998). Therefore, the gorgonin fraction is derived from surface water DIC, transmitted to depth via the plankton food web; but these results do not indicate whether *Primnoa spp.* feed upon sinking phytoplankton, zooplankton or other trophic intermediaries. Because of trophic level fractionation of $\delta^{13}C$ and $\delta^{15}N$, interpretation of time series isotopic profiles requires knowledge of TL.

Further insight to the TL of *Primnoa* spp. is provided by $\delta^{15}N$. This is typically enriched in a consumer relative to its diet by an average enrichment factor of $\Delta\delta^{15}N = 3.4$ ‰ (DeNiro and Epstein, 1981; Minagawa and Wada, 1984; Vander Zanden and

Rasmussen, 2001). The TL of *Primnoa* spp. may therefore be estimated by comparing our data with the isotopic signatures of other organisms of known TL (e.g. Vander Zanden et al., 1997; Polunin et al., 2001). We used primary consumers as the baseline, and calculated TL by the formula: $TL_{consumer} = (\delta^{15}N_{consumer} - \delta^{15}N_{baseline}) / 3.4 + 2$ (Vander Zanden and Rasmussen, 2001). Wherever possible, we used the gorgonin, rather than tissue results, since these integrate seasonal and inter-annual isotopic variations occurring at the base of the food web. Our approach was to reconstruct regionally-specific TL models from literature data.

Primnoa resedaeformis from the Northeast Channel was compared with the TL model of Fry (1988), which was based on taxa collected from nearby Georges Bank. We added to this model isotopic data for POM_{SUSP} (this study) POM_{SINK} (Macko, 1981) and size-fractionated zooplankton (Fry and Quinones, 1994). Most of the invertebrates and fish reported in Fry (1988) and Fry and Quinones (1994) were collected within the 100 m isobath on Georges Bank, where $\delta^{15}N$ of POM_{SUSP} is 1.4 ‰ heavier than in surrounding waters (Fig. 4.10), probably as a result of greater use of regenerated ammonium on the Bank (Ostrom et al., 1997; Wu et al., 1999a). We assume that isotopic enrichment on Georges Bank is transmitted to higher trophic levels. This difference in $\delta^{15}N$ equates to 0.4 trophic levels and must be accounted for in TL model output.

The Northeast Channel/Gulf of Maine $\delta^{15}N$-TL model is shown in Fig. 4.12. Data for the Georges Bank taxa were subtracted by 1.4 ‰. Herbivorous scallops were used for baseline $\delta^{15}N$ (Fry, 1988; 6 - 1.4 = 4.6 ‰). Among live-collected *Primnoa resedaeformis*

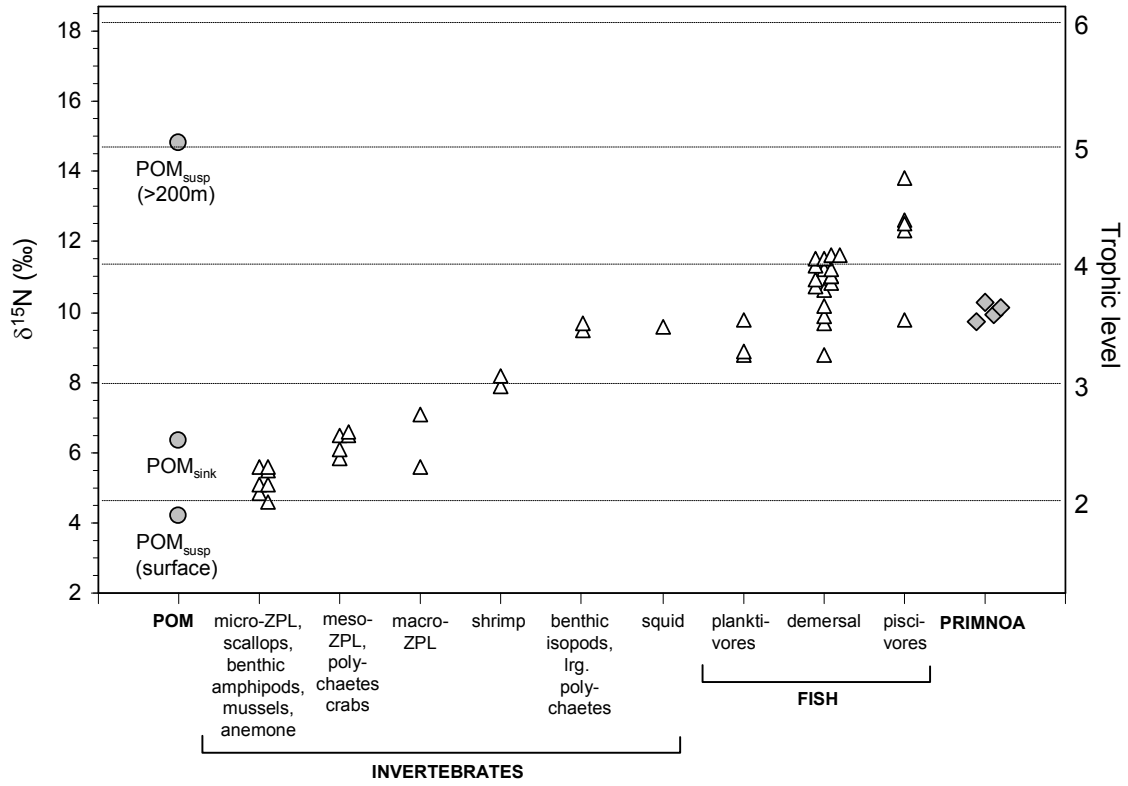

Fig. 4.12: Trophic level (TL)-$\delta^{15}N$ model for the Northeast Channel/Gulf of Maine region (triangles). We subtracted 1.4 ‰ from the data for Georges Bank taxa (data from Fry, 1988; Fry and Quinones, 1994) to account for higher $\delta^{15}N$ on Georges Bank (see Discussion). (Grey circles) Additional data showing surface POM_{SUSP} (this study), deep POM_{SUSP} (average of data from this study and Libes and Deuser, 1988) and POM_{SINK} (based on sediment data from Macko, 1981). (Grey diamonds) *P. resedae-formis* data. TL designations are based on average composition of scallops (TL 2) and $\Delta\delta^{15}N$ = 3.4 ‰. ZPL; zooplankton.

from the Northeast Channel, the inter-colony average $\delta^{15}N$ was 10.0 +/- 0.3 ‰ (n = 5). This value is similar to the $\delta^{15}N$ for large benthic isopods, large polychaetes, and planktivorous fish (Fig. 4.12). The calculated TL is 3.6. This suggests that *P. resedaeformis* is primarily carnivorous. We have also observed that the polyps on *P.*

resedaeformis point down, suggesting that these corals may also feed on resuspended meiofauna.

Another factor which may affect the TL estimate is isotopic modification of particulate matter in deep waters. Significant enrichment of $\delta^{15}N$ below the euphotic zone (Fig. 4.11) rules out the possibility that *Primnoa resedaeformis* feeds on the highly degraded POM_{SUSP} encountered at depth (otherwise $\delta^{15}N$ in *P. resedaeformis* would be much higher; Fig. 4.12). POM_{SINK} may also become isotopically enriched below the euphotic zone, although to a much lesser extent than POM_{SUSP} (Altabet et al., 1988; Altabet et al., 1991; Voss et al., 1996). We estimate that POM_{SINK} in the Northeast Channel has a $\delta^{15}N$ signature of 6.5 ‰ based on sediment data (Macko, 1981) and general similarity in $\delta^{15}N$ between sediments and POM_{SINK} (Altabet and Francois, 1994; Voss et al., 1996; Ostrom et al., 1997). Assuming $\Delta\delta^{15}N = 3.4$, *P. resedaeformis* could feed on POM_{SINK} as well as zooplankton (Fig. 4.12).

Heavier $\delta^{15}N$ in *Primnoa willeyi* from the NE Pacific (12.8 +/- 0.6 ‰, n = 5), when compared to *Primnoa resedaeformis* from the NW Atlantic, may reflect either a difference at the base of the food web or higher TL. We constructed a TL model based on literature $\delta^{15}N$ data from 2 inshore Bays near Juneau (Goering et al., 1990) and Prince William Sound, Alaska (Kline 1999; note: one of our specimens {Smith-51283} was collected *in* Prince William Sound). Baseline $\delta^{15}N$ was set to 8 ‰, using the values reported for herbivorous copepods (*Neocalanus cristatus*; Kline 1999) and bivalves (Goering et al., 1990). Overlap in $\delta^{15}N$ values among similar taxa from these two

Alaskan bays, despite a separation of over 600 km, lends confidence that $\delta^{15}N$ signatures are well conserved within the coastal NE Pacific ecosystem. We calculate a TL of about 3.4 for *P. willeyi*. Measurements of POM_{SINK} from off Vancouver Island ($\delta^{15}N$ = 8-9 ‰, Peña et al., 1999; Wu et al., 1999a) are also consistent with this fraction being a food source for *P. willeyi*. Lighter $\delta^{15}N$ in the sample from Atka Island (9.1 ‰) may be explained by low $\delta^{15}N$ in offshore primary producers (Wu et al., 1997; see below).

It has been shown that coastal ecosystems often exhibit lower $\Delta\delta^{15}N$ than the globally accepted value of 3.4 ‰ (Wu et al., 1997; Sherwood and Rose, 2005). To validate our TL estimates, we also looked at four taxa that were sampled in both the NE Pacific and NW Atlantic: euphausiids, bivalves, pollock, and sole. TL outputs for the two different ecosystems were statistically equal (matched-pairs t-test). Moreover, TL outputs for both ecosystems conform to expectations: bivalves (TL = 2); euphausiids (TL = 2.6); pollock (3.8); sole (3.5 to 3.8). Therefore, our use of $\Delta\delta^{15}N$ = 3.4 ‰ for both Georges Bank and coastal NE Pacific ecosystems does not appear to introduce bias in our model outputs.

In summary, isotopic data support the following three conclusions about the diet of *Primnoa* corals: (1) Presence of modern $\Delta^{14}C$ in *Primnoa resedaeformis* rules out DOC and DIC as a significant carbon source to the gorgonin fraction of the skeleton (Sherwood et al., 2005a); Measurements of $\delta^{15}N$ suggest that (2) zooplankton and/or POM_{SINK} constitute the main diet of *P. resedaeformis* and *Primnoa willeyi*, and (3) the highly degraded fraction of POM_{SUSP} found at depth is not a significant food source. This

is also supported by the finding that the dark, more gorgonin-rich portion of the annual ring couplets in *P. resedaeformis* co-incide with the timing of the spring/summer bloom of phytoplankton and zooplankton (Sherwood, 2002).

Lack of isotopic data for the Sea of Japan and the South Pacific in the literature prevented a similar analysis of the TL of the remaining species. It is quite probable that *Primnoa pacifica* and *Primnoa resedaeformis notialis* share a similar type of diet with *P. resedaeformis* and *P. willeyi,* since all the corals have similar-sized polyps.

As passive suspension feeders, octocorals feed opportunistically on a wide spectrum of plankton size classes, from nanoeukaryotes to zooplankton (Ribes et al., 1999; Orejas, 2003; Ribes et al., 2003). Temperate and boreal asymbiotic species feed mainly on zooplankton and detrital POM in about equal proportion, with smaller plankton (<100 μm) accounting for < 10 % of energy demand (Ribes et al., 1999; Ribes et al., 2003). Among zooplankton, gorgonians ingest smaller, low-motility prey items (Coma et al., 1994; Rossi et al., 2004). Our isotopic data conform to this general pattern, with the exception that the highly degraded POM_{SUSP} found at depth does not appear to be a significant food source. Heterogeneity of prey items may explain the differences in the intra- and inter-colony reproducibility of $\delta^{13}C$ and $\delta^{15}N$. It may be possible that different parts of the colony are more effective at capturing different sized prey items depending on localized current regimes (Coma et al., 1994). Differential feeding on prey size-classes could potentially alter $\delta^{15}N$ signatures, due to strong trophic level fractionation of ^{15}N (Fry and Quinones, 1994). If this is true, then analyses of more

sections per colony and more colonies per site are recommended to get the average $\delta^{15}N$. Since trophic level fractionation of ^{13}C is much weaker (generally < 1 ‰; Vander Zanden and Rasmussen, 2001) differential feeding should exert less influence on $\delta^{13}C$, thereby lending to greater isotopic reproducibility.

4.5.2 Surface-benthic coupling of isotopic signatures

The overall isotopic signature of a food web is determined by bio-physical processes at the level of primary producers. These processes are myriad and complex, especially over shorter timescales. Phytoplankton $\delta^{15}N$ mainly depends on the efficiency of nitrogen utilization (Nakatsuka et al., 1992; Altabet and Francois, 1994; Wu et al., 1997; 1999a) and on the $\delta^{15}N$ signature of the nitrogenous substrate (Ostrom et al., 1997; Altabet et al., 1999). Phytoplankton $\delta^{13}C$ mainly depends on $[CO_{2aq}]$ (Rau et al., 1992; Hoffman et al., 2000), growth rate (Nakatsuka et al., 1992; Hoffman et al., 2000) and cell geometry/plankton species composition (Popp et al., 1998; Fry and Wainright, 1991), as well as the $\delta^{13}C$ signature of the bicarbonate substrate (Cullen et al., 2001). As a result of these myriad factors, there are large isotopic differences between open ocean, slope water, and coastal ecosystems (Wu et al., 1997). Furthermore, different pathways of isotopic fractionation often lead to decoupling of $\delta^{13}C$ and $\delta^{15}N$ in new production (Ostrom et al., 1997; Wu et al., 1999a; 1999b). In Fig. 4.4b, our use of surface water AOU is not meant to imply control on isotopic fractionation, but to give some sense of the different surface productivity regimes where the corals lived. The lightest values were found in the South Pacific, located near a high nutrient-low chlorophyll (HNLC) domain, where despite high $[NO_3]$ and $[CO_{2aq}]$ primary production is limited by micronutrients

such as iron. Similarly low values were observed in a specimen from Atka Island, in the Aleutian Islands, also located near an HNLC domain (Wu et al., 1999b). Heavier values were found in the slope water regions of the NW Atlantic and the Sea of Japan, where primary productivity is typically dominated by blooms of large, fast growing phytoplankton (Mousseau et al., 1996). These blooms lead to nutrient depletion, and heavier $\delta^{13}C$ and $\delta^{15}N$. The heaviest values were in corals from Alaska and British Columbia, consistent with highest productivity rates in these coastal domains. These results demonstrate that isotopic signatures originating with primary producers are transmitted to, and preserved within, the organic endoskeletons of *Primnoa* spp. It is therefore not surprising that $\delta^{13}C$ and $\delta^{15}N$ in Primnoa spp. are both so tightly correlated with AOU (Fig. 4.4b).

4.5.3 Preservation of original isotopic composition

For isotopic trends from gorgonin to have any paleoceanographic utility, there must not be any diagenetic overprinting. In many of the sub-fossil specimens donated to us by fishermen, the gorgonin appeared to be more susceptible to degradation than the inorganic calcite cortex fraction. On the broken axes of these dead colonies, the inner horny axis is often worn down in a smooth cup-shaped depression, while the cortex remains intact. Similarity in C:N, $\delta^{13}C$ and $\delta^{15}N$ between modern and sub-fossil specimens suggests that isotopic signatures are preserved from the time of original formation. This is also supported by identical amino acid abundances between modern and sub-fossil specimens (Sherwood et al., 2006), since diagenesis often leads to the synthesis of microbial biomass with different amino acid and stable isotopic composition

(Macko and Estep, 1984). The degradation observed on sub-fossil specimens appears to be the result of mechanical erosion, probably by the action of suspended sands, rather than organic diagenesis. This finding is consistent with gorgonin being one of the most chemically inert proteins known (Goldberg, 1976). Over millennial timescales, therefore, isotopic abundances in *Primnoa* spp. are preserved, making these corals durable archives of paleoceanographic information.

4.5.4 Paleoceanographic applications

Owing to little trophic level fractionation and excellent intra- and inter-colony reproducibility, $\delta^{13}C$ time-series from *Primnoa* spp. could reliably track variations in surface processes. From Fig. 4.8, it appears that the three colonies of *Primnoa resedaeformis* from the Northeast Channel recorded a peak in $\delta^{13}C$ around the mid-twentieth century, with several decade-scale oscillations. The causes of these variations are not clear; but there may be an important link with known changes in plankton community composition since the 1960s in this region (Sameoto, 2001). On the other hand, evidence of the oceanic Suess effect on the $\delta^{13}C$ composition of modern vs. sub-fossil specimens (Fig. 4.9), and reconstruction of 20th century bomb radiocarbon (Sherwood et al., 2005a) are examples of isotopic variability in source materials recorded in these corals. Therefore, there is evidence that both biological processes (i.e. correlation of $\delta^{13}C$ and $\delta^{15}N$ with AOU) and physical processes (changes in isotopic composition of bicarbonate substrate) are reflected in gorgonin isotopic content. Smaller regional studies with multiple colonies and good chronological control will be required to deconvolute these different factors. Useful information may also be extracted from $\delta^{15}N$ profiles,

provided that time-series variability is large relative to the intra- and inter-colony variability.

The annual nature of ring formation makes *Primnoa* spp. analogous to varved sediment cores, from which much useful paleoceanographic information has been retrieved (e.g. Tunnicliffe, 2000). In similar fashion, annually-resolved isotope time-series have been generated from preserved animal remains, such as fish scales (Wainright et al., 1993) and whale baleen (Schell, 2001). Long lifespans (at least 400 years, probably longer; Risk et al., 2002; Scott et al., 2005) lend to *Primnoa* spp. the advantages of both varved sediment cores (longer, *in situ* time-series) and preserved animal remains (widespread distribution, known TL). Isotopic reconstructions from *Primnoa* spp. could be useful in illustrating temporal variations in marine productivity, as well as tracking the relative importance of top-down vs. bottom-up influences over time (Schell, 2001; Rau et al. 2003; Satterfield IV and Finney, 2002). Oceanographic phenomena that may be recorded include changes in the position of water mass boundaries, upwelling strength, terrestrial nutrient inputs and atmospheric nutrient inputs.

Deep-sea corals could prove to be temporal and spatial recorders of the efficacy of the oceanic biological pump that transfers carbon dioxide from the atmosphere to the deep-ocean. By understanding natural processes that have affected the operation of this pump over century time scales we can better predict the effects of global change and potential engineered approaches such as iron fertilization on oceanic carbon sequestration. The widespread occurrence and diversity of deep-sea corals is only now

being fully appreciated. As more deep-sea corals are discovered in important oceanographic regions the applicability of this potential paleoceanographic archive is likely to increase.

4.6 CONCLUSIONS

1. Measurements of $\delta^{15}N$ indicate that *Primnoa resedaeformis* and *Primnoa willeyi* have a TL of about 3.5. POM_{SINK} and zooplankton appear to constitute the bulk of the diet, whereas DIC, DOC and POM_{SUSP} are not consumed. The TL for *Primnoa pacifica* and *Primnoa resedaeformis notialis* could not be determined, but it is likely that these species feed at a similar TL, based on similar sized polyps.

2. Average $\delta^{13}C$ and $\delta^{15}N$ compositions of the gorgonin fraction were strongly correlated with each other, and with surface water AOU. This demonstrates strong coupling between surface bio-physical processes and stable isotopic compositions in *Primnoa* spp.

3. Isotopic profiles from annual gorgonin rings showed excellent intra-colony and inter-colony reproducibility for $\delta^{13}C$, while for $\delta^{15}N$ the reproducibility was not as good. The latter result may arise from differential feeding upon different sized prey items, depending on localized current regimes; however, more work is needed to address this issue.

4. Similarity in C:N, $\delta^{13}C$ and $\delta^{15}N$ between modern and sub-fossil specimens demonstrates a lack of organic diagenesis in the tough gorgonin fraction. Isotopic

signatures from the time of formation are therefore preserved over millennial timescales, making these corals excellent candidates for retrospective studies of the surface marine environment.

ACKNOWLEDGEMENTS

For providing coral samples, we are thankful to S. Atwood, L. Buhl Mortensen, S. Cairns, D. Gordon, D. Jones, D. Mackas, P. Mortensen, A. Muir, L. Talley, V. Tunnicliffe, and R. Wolkins. J. McKay performed isotopic analyses at GEOTOP. We are grateful to B.Ghaleb for providing radiometric dates. Stable isotopic analyses at UNM were performed by V Atudorei, M.Hess, and Z. Sharp. We thank Jerry Prezioso of NOAA NMFS, Narragansett, RI, for kindly providing POM samples. Lawrence Plug offered valuable help with digital mapping. We also thank 3 anonymous reviewers for suggestions leading to improvement of this manuscript. Funding was provided by an NSERC Strategic Grant to MJR and DBS, an Institute of Geophysics and Planetary Physics, Los Alamos National Laboratory, grant to JMH, and an NSERC postgraduate scholarship to OAS. Radiocarbon analyses were performed under the auspices of the U.S. Department of Energy by the University of California Lawrence Livermore National Laboratory (contract W-7405-Eng-48).

CHAPTER 5

LATE HOLOCENE RADIOCARBON AND ASPARTIC ACID RACEMIZATION DATING OF DEEP-SEA OCTOCORALS

Owen A. Sherwood [1], David B. Scott [1], Michael J. Risk [2]

[1] Centre for Environmental and Marine Geology, Dalhousie University, Halifax, Canada

[2] School of Geography and Geology, McMaster University, Hamilton, Canada

Published as an article in:

Geochimica et Cosmochimica Acta 70: 2806-2814

(June 2006)

5.1 ABSTRACT

Primnoa resedaeformis is a deep-sea gorgonian coral with a 2-part skeleton of calcite and gorgonin (a fibrillar protein), potentially containing long term records of valuable paleo-environmental information. For various reasons, both radiocarbon and U/Th dating of these corals is problematic over the last few centuries. This paper explores aspartic acid racemization dating of the gorgonin fraction in modern and sub-fossil specimens collected from the NW Atlantic Ocean. Radiocarbon dating of the sub-fossil specimen indicates a lifespan of 700 ± 100 years, the longest yet documented for any octocoral. Gorgonin amino acid compositions were identical in the sub-fossil and modern specimens, indicating resistance to organic diagenesis. Similar to bone collagen, the fibrillar protein of gorgonin may impose conformational constraints on the racemization of Asp at low temperatures. The rate of racemization of aspartic acid (D/L-Asp) was similar to previously published results from an 1800 year old anemone (*Gerardia)*. The age equation was: Age (yrs BP 2000 AD) = [(D/L – 0.020 (± .002)) / .0011 (± .0001)]^2 ($r^2 = 0.97$, $p < .001$). The error in an age estimate calculated by D/L-Asp was marginally better than that for ^{14}C dating over the most recent 50-200 years, although the dating error may be improved by inclusion of more samples over a broader time range. These results suggest that D/L-Asp dating may be useful in augmenting ^{14}C dating in cases where ^{14}C calibrations yield 2 or more intercept ages, or in screening samples for further ^{14}C or U/Th dating.

5.2 INTRODUCTION

Deep-sea octocorals often have a two-part skeleton of calcite and gorgonin, a tough, horny protein. Based on $\Delta^{14}C$, $\delta^{13}C$ and $\delta^{15}N$ evidence, the calcite fraction is derived from dissolved inorganic carbon (DIC) at depth, while the gorgonin is derived from recently exported particulate organic matter (POM; Griffin and Druffel, 1989; Druffel et al., 1995; Heikoop et al., 2002; Roark et al., 2005; Sherwood et al., 2005a,b). The gorgonian species *Primnoa resedaeformis* has concentric rings in its axial skeleton that form annually (Andrews et al., 2002; Sherwood et al., 2005a.). This may be true in other octocoral species as well (Thresher et al., 2004). Together, these observations suggest that high temporal-resolution, geochemical-based climate reconstructions of both surface and intermediate/deep water processes may be made from the skeletons of deep-sea octocorals (Heikoop et al., 2002; Thresher et al., 2004; Sherwood et al., 2005a,b).

Obtaining specimens of deep-sea coral for study is not a trivial matter. Financial and logistical demands may render sampling expeditions very difficult. On the other hand, many large, priceless specimens are often available from fishermen and museums. In recent years we have obtained about twenty large specimens of *Primnoa resedaeformis* from long-line fishermen in Nova Scotia. Some of these specimens may contain several hundreds of year's worth of environmental records in their skeletons (Risk et al., 2002). Unfortunately, most of the large specimens were collected dead. The greater apparent availability of dead vs. live specimens in recent decades may be the result of increasing habitat destruction by the dragger fishing fleet since the 1950s (Watling and Norse, 1998;

Hall-Spencer et al., 2002). In addition, the skeletons of *P. resedaeformis* may contain death/re-growth surfaces representing hiatuses in skeletal accretion (Chapter 6).

Since accurate chronology is a fundamental requirement in proxy reconstructions, absolute dating methods are required to exploit the potential climate signals contained in these skeletons. Carbon-14 dating has been used to date sub-fossil octocorals. Risk et al. (2002) used ^{14}C to determine a lifespan of 320 years in a sub-fossil specimen of *P. resedaeformis* dredged from Georges Bank. Druffel et al. (1995) used ^{14}C to determine a lifespan of 1800 years in *Gerardia*, dubbing it the "Bristlecone pine of the deep-sea". *Gerardia* is an anemone, not a coral, but it forms a tough organic endoskeleton much like the gorgonin in *P. resedaeformis*. A major problem with ^{14}C is the inability to resolve dates over the period ca. 1650-1950 AD because of local variations in the marine reservoir effect and the possibility for multiple calibrated ages. Uranium-series dating may also be used to date deep-sea octocorals (Thresher et al., 2004). However, uncertainty in the extent of initial thorium contamination, and low uranium concentration in calcite presents a major problem with this method.

This paper explores the use of amino acid racemization to date the skeletal gorgonin fraction of *P. resedaeformis*. The rate of equilibration of D- and L-handed isomers (racemization) after death of an organism depends on age and temperature. If temperature remains constant, which is more or less expected for the deep-sea, the increase in the D-isomer may be used to calculate age (e.g.: Goodfriend 1992). The approach used here was to calibrate the racemization rate of aspartic acid (Asp) in

known-age samples, then to evaluate whether D/L-Asp would be useful in dating specimens over the last 400 years where ^{14}C dating is problematic.

5.3 MATERIALS AND METHODS

Live-collected and sub-fossil colonies of *Primnoa resedaeformis* were used in this study. Both were collected from the Northeast Channel, a submarine canyon located SW of Halifax, Canada (approx. 65º40'W/ 42º00'N), between 250-475 m depth. The live specimen (DFO2002-con5) was collected by trawl in the summer of 2002 (Sherwood et al., 2005b). The sub-fossil specimen (Fossil-95; Fig 1) was collected by fishermen using long-line gear in 1995. Samples were air-dried following collection. The bases of colony trunks were sectioned with a rock saw, and the sections were ground and polished on a diamond lap wheel and photographed with a digital camera in macro mode.

Radiocarbon and AAR analyses were performed on the gorgonin fractions of Fossil-95 and DFO2002-con5. To isolate the gorgonin, the sections were placed in 0.5 M HCl until complete dissolution of calcite. This took up to 3 weeks. Gorgonin layers were separated by peeling them apart with tweezers and scalpel under a binocular microscope. The position of each layer was carefully marked on the digital photographs while sampling. Samples were placed in 5mm polyethylene vials with 0.5 M HCl for an additional 48 hours, triple rinsed in Milli-Q water and dried for 48 hours in a low temperature oven (~ 50^{o}C).

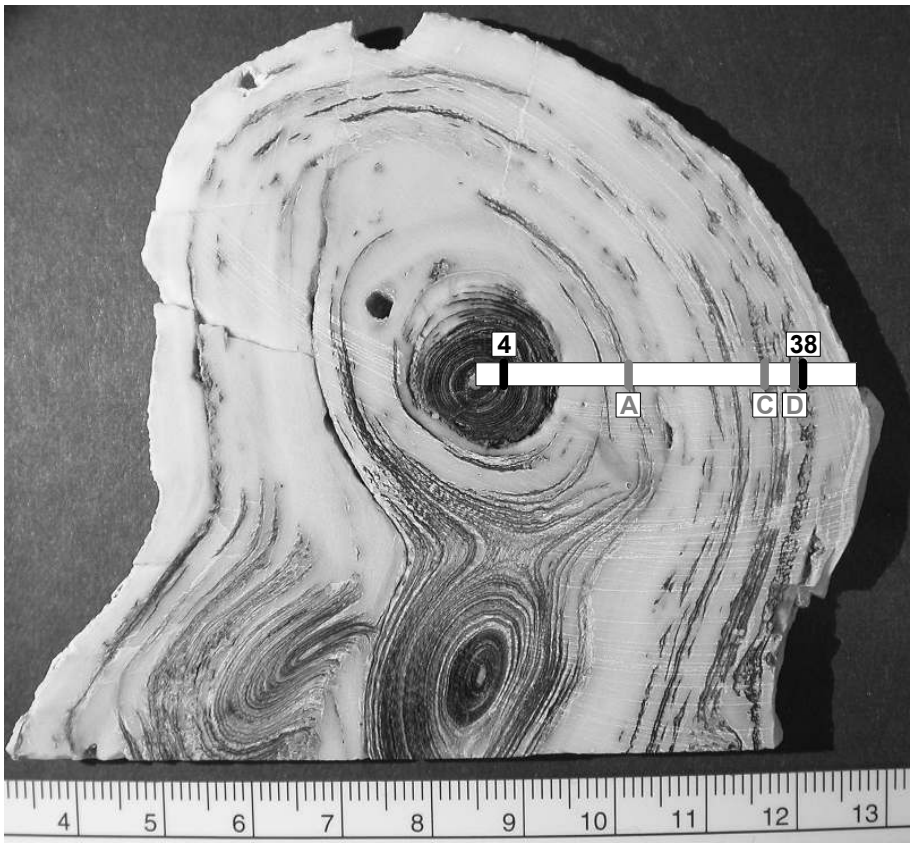

Fig. 5.1: Image of specimen Fossil-95 viewed in cross-section. Black bars and letters show samples isolated for ^{14}C dating. Grey bars and letters show samples isolated for amino acid analysis. Scale on ruler in cm.

Samples for radiocarbon analysis were combusted in individual quartz tubes and reduced to graphite in the presence of iron catalyst. Delta-^{14}C was determined on graphite targets at the Center for AMS. Results include a background and $\delta^{13}C$ correction and are reported as $\Delta^{14}C$ according to Stuiver and Polach (1977).

Amino acid analyses were performed by reverse-phase high performance liquid chromatography with pre-column derivatization following the procedure in Kaufman and

Manley (1998). First, samples were dissolved in 7N HCl over the course of 7 days with intermittent 20 minute intervals in an ultrasonic bath. This expedited dissolution but did not allow the samples to reach a high enough temperature to induce racemization. Samples were hydrolyzed in 7 N HCl, sealed under N_2 and heated to 110^{o}C for 6 hours. The hydrolysates were then desiccated under a N_2 atmosphere at 80 ^{o}C for ~20 minutes, and then rehydrated in 0.01 M HCl with known quantity of L-homo-Arginine (L-hArg) for use as an internal standard. Although initial analyses of Asp yielded poor peak separation, a slower mobile phase flow rate increased resolution and the subsequent analyses were considered reliable. Analytical error, as determined by the range in sample replicates, was 2-4 %.

5.4 RESULTS AND DISCUSSION

5.4.1 Skeletal Chronology

Skeletal chronology in the younger colony, DFO2002-con5, was reported earlier (Sherwood et al., 2005a). Chronology was established on the basis of growth ring counts performed by three amateur counters, and validated by the timing of increase in bomb radiocarbon. The samples used here for amino acid measurements ranged from 1926-2002 yrs AD.

Radiocarbon ages of the sub-fossil specimen, Fossil-95 (Fig 5.1), were calibrated with the program CALIB (Stuiver and Reimer 1993, version 5) using the Marine 04 calibration (Hughen et al., 2004). A correction for local variation in the marine reservoir effect, ΔR, was applied (i.e.: the difference in reservoir age between the local region of

Table 5-1: Calculation of local marine reservoir correction from known-age samples of *P. resedaeformis*. 1 SD errors in brackets

Sample	Ring no.	Ring year [a] (yrs AD)	Pre-1950 age (yrs)	CAMS #	$\Delta^{14}C$ (‰)	^{14}C age (yrs BP 1950)	Model age [b] (yrs BP 1950)	ΔR (yrs)
DFO2002-con5A1	37	1948 (4)	2	97103	-80 (3)	620 (30)	469	151
DFO2002-con5A1	43	1942 (5)	8	97104	-72 (3)	545 (30)	460	85
DFO2002-con5A1	50	1934 (6)	16	97105	-77 (3)	595 (30)	457	138
DFO2002-con5A1	58	1924 (6)	26	97106	-72 (3)	550 (30)	451	99
NED2002-371A	58	1947 (2)	3	111330	-82 (4)	630 (35)	464	166
							Mean	128
							St. dev.	35

[a] Average from 3 amateur ring counters (Sherwood et al., 2005a)
[b] Marine 04 calibrated age (Hughen et al. 2004)

Table 5-2: Radiocarbon ages for the sub-fossil *P. resedaeformis* specimen. 1 s.d. errors in brackets.

Sample	Distance (mm) [a]	CAMS #	$\Delta^{14}C$ (‰)	^{14}C age (yrs BP 1950)	Model age [b] (yrs BP 1950)
Fossil95-D2-38	4.5	111138	-196 (3)	1700 (35)	1125 (65)
Fossil95-D2-4	37	111137	-249 (3)	2245 (40)	1700 (75)

[a] Distance from skeletal margin
[b] ΔR-corrected Marine 04 calibrated age,

interest and the model ocean; Stuiver and Braziunas, 1993). Values of ΔR for Northwest Atlantic shelf waters are available from the Marine Reservoir Correction Database (http://radiocarbon.pa.qub.ac.uk/marine); however, to more accurately correct ^{14}C ages for the Northeast Channel, ^{14}C measurements from known-age specimens of *Primnoa resedaeformis* were used. These measurements span the period 1924-2002 and include both pre- and post- nuclear bomb values (Sherwood et al., 2005a). The pre-1950 values were used to calculate ΔR (e.g.: Surge et al., 2003), which averaged 128 ± 35 years (mean ± st. dev.; Table 1). The large range in ΔR reflects the scatter in pre-bomb $\Delta^{14}C$, and suggests the influence of different water masses over short timescales. The Northeast Channel is located near a sharp gradient between northward Labrador Current waters and southward subtropical gyre waters, which are likely to differ in pre-bomb $\Delta^{14}C$. For comparison, the Marine Reservoir Correction Database reports ΔR estimates of 94 ± 22 years (Georges Bank) and 95 ± 24 years (southern Grand Banks).

Separate annual rings isolated from near the inner and outer skeletal regions of Fossil-95 (Fig 5.1) yielded ΔR-corrected model ages of 1700 ± 75 and 1125 ± 65 years BP, respectively (Table 5.2; 1σ age ranges). The corresponding radial growth rate between samples is 0.06 ± 0.01 mm yr^{-1}. This value is very close to the 0.04 mm yr^{-1} reported earlier in a sub-fossil colony from Georges Bank (Risk et al., 2002). Applying this growth rate from the center to the extreme edge of the colony yields a lifespan of 690 ± 120 years. To our knowledge, this is the longest documented lifespan of any deep or shallow water octocoral.

Table 5.3: Summary of amino acid abundance and D/L data

Sample ID	Sample type	Dist (mm)[a]	Age (yrsAD)	AAL ID	Amino acid abundance (umol/mg)													% wt	D/L-Asp	D/L-Glu	D/L-Val
					Asp	Thr	Ser	Glu	Gly	Ala	Val	Met	Ile	Leu	Tyr	Phe	Arg	Total AA				
DFO2002-con5																						
1	tissue	0	2002 [b]	10859	0.84	0.44	0.55	0.76	0.33	0.57	0.48	0.16	0.42	0.59	0.24	0.36	0.31	6.05	78	.026	.022	0
2	gorgonin	0.1	2000 [b]	10860	1.49	0.41	1.04	0.65	1.36	1.71	0.37	0.07	0.24	0.25	0.24	0.10	0.84	8.74	103	.022	.011	0
10	gorgonin	3.9	1981 [b]	10861	1.07	0.31	0.70	0.47	0.91	1.17	0.33	0.05	0.21	0.18	0.15	0.08	0.62	6.24	74	.027	.014	0
19	gorgonin	6.1	1967 [b]	10862	1.45	0.40	0.94	0.63	1.26	1.58	0.43	0.06	0.27	0.23	0.17	0.10	0.80	8.34	98	.031	.015	0
30	gorgonin	9.0	1951 [b]	10863	1.21	0.31	0.79	0.52	1.02	1.30	0.29	0.04	0.18	0.19	0.13	0.08	0.63	6.71	79	.052 [d]	.011	0
38	gorgonin	10.4	1940 [b]	10864	0.68 [d]	0.18 [d]	0.45 [d]	0.30 [d]	0.56 [d]	0.72 [d]	0.17 [d]	0.02 [d]	0.11 [d]	0.12 [d]	0.07 [d]	0.05 [d]	0.36 [d]	3.77 [d]	44 [d]	.025	.010	0
44	gorgonin	12.6	1927 [b]	10865	1.25	0.35	0.82	0.55	1.06	1.36	0.36	0.04	0.23	0.22	0.13	0.09	0.66	7.15	84	.034	.014	0
Fossil-95																						
A	gorgonin	19	500 [c]	10866	1.02	0.36	0.80	0.53	1.00	1.20	0.38	0.07	0.25	0.24	0.23	0.10	0.69	6.86	82	.06	.014	0
C	gorgonin	11	760 [c]	10867	1.10	0.38	0.80	0.55	1.03	1.22	0.42	0.08	0.27	0.23	0.28	0.10	0.75	7.19	86	.062	.016	0
D	gorgonin	4	820 [c]	10868	0.67 [d]	0.23 [d]	0.48 [d]	0.34 [d]	0.61 [d]	0.73 [d]	0.26 [d]	0.04 [d]	0.17 [d]	0.14 [d]	0.14 [d]	0.07 [d]	0.45 [d]	4.32 [d]	52 [d]	.062	.015	0

[a] Distance from skeletal margin
[b] Age determined by counting annual rings (Sherwood et al., 2005a)
[c] Age determined by applying linear growth rate, as calculated from ΔR-corrected ^{14}C ages from Table 2
[d] Unreliable data; excluded from subsequent calculations

5.4.2 Amino Acid Composition of the Tissue and Gorgonin

The results of all ten amino acid analyses are summarized in Table 3. Following Goodfriend (1997), the percent mass of the organic fraction accounted for by the amino acids was calculated by multiplying the mean molecular weight of each amino acid (weighted by the % composition of each amino acid) by the total molar concentration of all 13 quantified amino acids (Table 3). Values ranged from 70-100 % of the sample mass. In two analyses (AAL #10864 and AAL #10868) amino acid concentrations were systematically lower; on this basis these were judged unreliable and excluded from all subsequent calculations. Thus, the 13 quantified amino acids accounted for, on average, 78 %, 87 % and 84 %, respectively, of the mass of tissue, modern gorgonin and sub-fossil gorgonin.

Fig 5.2 compares amino acid profiles in the tissue and modern and sub-fossil gorgonin. Compared with gorgonin, the tissue was higher in threonine (Thr), glutamic acid (Glu), valine (Val), methionine (Met), isoleucine (Ile), leucine (Leu), tyrosine (Tyr) and phenylalanine (Phe), and lower in aspartic acid (Asp), serine (Ser), glycine (Gly), alanine (Ala) and arginine (Arg). These differences probably relate to the different protein compositions, which is reflected in different C:N values between tissue and gorgonin (7 vs. 3, respectively; Sherwood et al., 2005b).

Compared with the modern gorgonin, the sub-fossil gorgonin had slightly lower amounts of Asp and Ala, and higher amounts of Val, Tyr and Arg (Fig 5.2). These

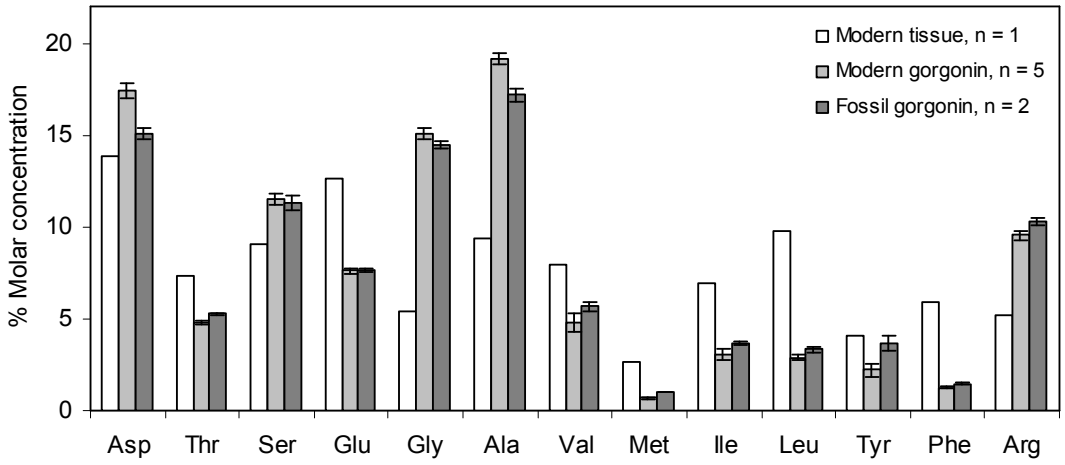

Fig. 5.2: Amino acid composition of the tissue and gorgonin (modern and fossil) fractions of *P. resedaeformis.* Error bars are ± 1 s.d.

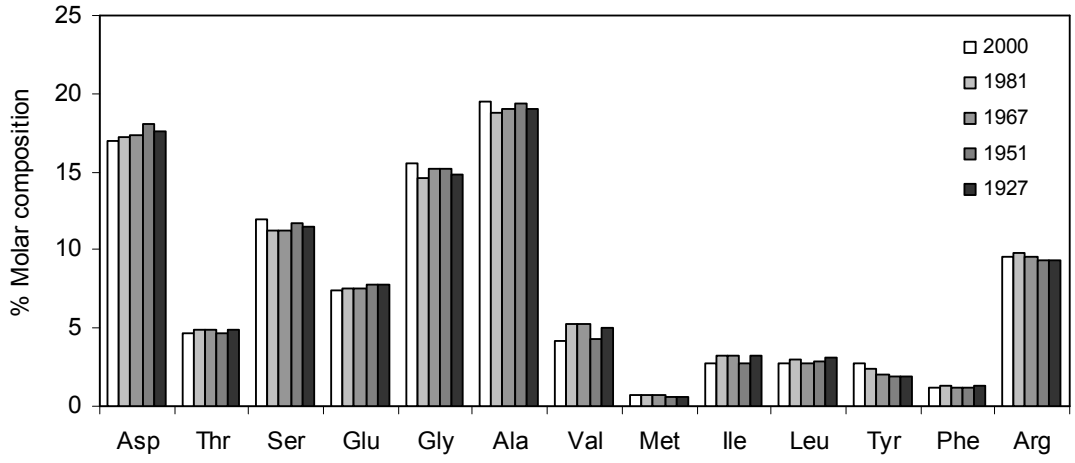

Fig. 5.3: Ontogenetic trends in amino acid composition of the modern gorgonin. Each bar corresponds to an individual annual ring isolated from the skeleton, as indicated by year. Regression analysis yielded no significant increases or decreases in any of the 13 amino acids with age.

differences probably reflect original variability at the time of formation, since there were no differences in the least stable amino acids Thr, Ser, and Met. A similar result was found in the organic endoskeleton of an 1800 yr old *Gerardia* (Goodfriend, 1997).

Fig 5.3 shows ontogenetic trends in amino acid abundances in the modern gorgonin. There were no significant increases or decreases with age of the layer (regression statistics were insignificant for all 13 amino acids). Taken together, the similarity between modern and sub-fossil gorgonin in: 1) % mass accounted for by amino acids, 2) amino acid profiles, and 3) the lack of ontogenetic trends in the modern gorgonin argue for little or no organic diagenesis for at least ca. 1500 years. These findings are consistent with gorgonin being one of the toughest known proteins (Goldberg, 1976).

Gorgonin is thought to be composed of a fibrillar protein supported in a proteinaceous matrix (Lewis et al., 1992). The fibrillar protein was characterized earlier as aromatically cross-linked collagen (Goldberg, 1974, 1976; Szmant-Froelich, 1974). More recently, gorgonin has been characterized as a polyphenol-containing fibrillar protein (H. Ehrlich., private communication). Independent evidence for a fibrillar protein in *P. resedaeformis* is provided here by scanning electron microscopy (Fig 5.4). The voids left by decalcification in acetic acid reveal the fibrillar nature of the remaining organic material. The individual fibres measure approx. 200 nm in diameter, similar to the proteinaceous fibres observed in shallow-water gorgonians (Lewis et al., 1992). Although the exact nature of the gorgonin in *P. resedaeformis* will have to await more

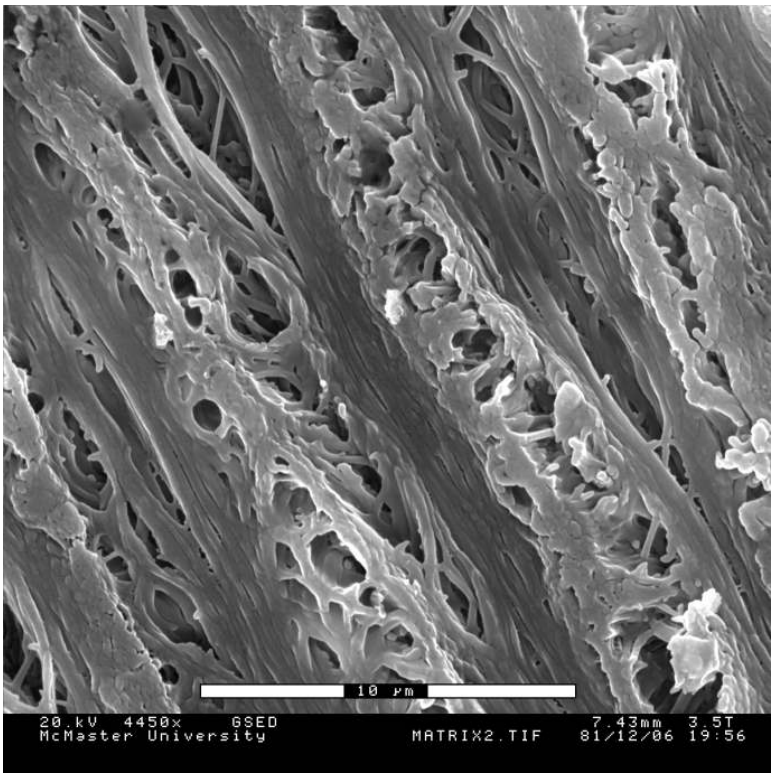

Fig. 5.4: SEM image of acetic acid-etched *P. resedaeformis* viewed in cross-section. The 4 repeating diagonal bands are sub-annual bands (Risk et al. 2002; Sherwood 2002).Fibrillar protein material is oriented both parallel and perpendicular to the plane of view.

detailed study, the presence of fibrillar protein has a significant implication for D/L dating, as discussed below.

5.4.3 D/L Ratios

D/L ratio were measured for Asp, Glu and Val (Table 3; Fig 5.5). For Asp, there was no difference in D/L between modern tissue and gorgonin. There was a significant difference between modern and sub-fossil gorgonin, as expected from the rapid racemization rates of Asp (Goodfriend, 1992). For Glu, D/L was higher in sub-fossil

gorgonin than in modern gorgonin; but the difference was not significant, consistent with slower racemization of Glu. Tissue D/L-Glu was nearly twice that of gorgonin. The reason for this is not clear. D-Val could not be resolved in any of the samples.

Fig 5.6a shows D/L-Asp vs. age for the gorgonin fraction of *Primnoa resedaeformis*. Thirty percent of the total increase occurred over the most recent 75 years, while the remaining 60 % occurred over the remaining 1400 years. This convex-upward pattern is consistent with Asp racemization kinetics in other organisms (e.g.: Mitterer and Kriausakul, 1989; Goodfriend, 1991). Asparagine (Asn) is converted to Asp during the hydrolysis step of sample preparation (Brinton and Bada, 1995), so the measured increase in D-Asp actually represents the combined responses of Asp + Asn (Goodfriend, 1991). Both amino acids are thought to racemize via deamination to an aminosuccinyl residue (Asu; Geiger and Clarke, 1987). Racemization in the Asu residue is some 5 times higher than in free Asp (Radkiewicz et al., 1996). Collins et al. (1999) attribute the non-linear racemization kinetics to the greater tendency for Asn, as compared with Asp, to form Asu residues. Therefore, the earlier phase of rapid racemization in *P. resedaeformis* (Fig 5.6a) is likely dominated by Asn, while the later phase is dominated by Asp.

The data for *Gerardia* collected at ~600 m on Little Bahama Bank are also shown in Fig 5.6a. Values of D/L-Asp for this specimen are from Goodfriend (1997) and corresponding radiocarbon ages are from Druffel et al. (1995). To maintain consistency

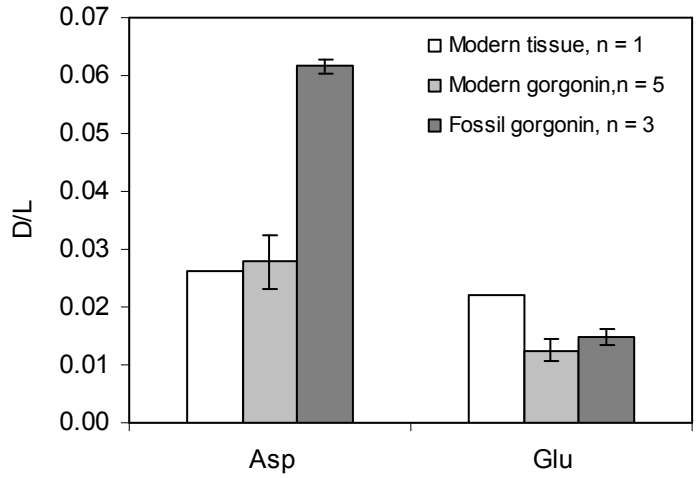

Fig. 5.5: D/L composition of the tissue and gorgonin (modern and fossil) fractions of *P. resedaeformis.* Error bars are ± 1 s.d.

in radiocarbon dating, the ^{14}C ages originally reported in Druffel et al. (1995) were corrected with the Marine04 calibration and a ΔR value of 36 ± 14 (Florida and Bahamas regional average from the Marine Reservoir Correction Database). The D/L values are similar between *P. resedaeformis* and *Gerardia*, although we caution that Goodfriend (1997) used a different sample preparation procedure in obtaining his D/L data, and the organic endoskeleton in *Gerardia* is not mineralized. The lower slope for *Gerardia* (Fig 5.6a) probably reflects the lack of data over the most recent centuries, where Asp racemization is generally fastest.

To linearize racemization rates over the time-period of interest, we tested a variety of transformation functions of D/L (i.e.: ln[(1+D/L)/(1-D/L)]; D/L raised to an exponent >1) and time (square root of time). In all cases, coefficients of determination (r^2) ranged from 0.91 to 0.97 (*P. resedaeformis*) and 0.64 to 0.86 (*Gerardia*). In Fig 5.6b,

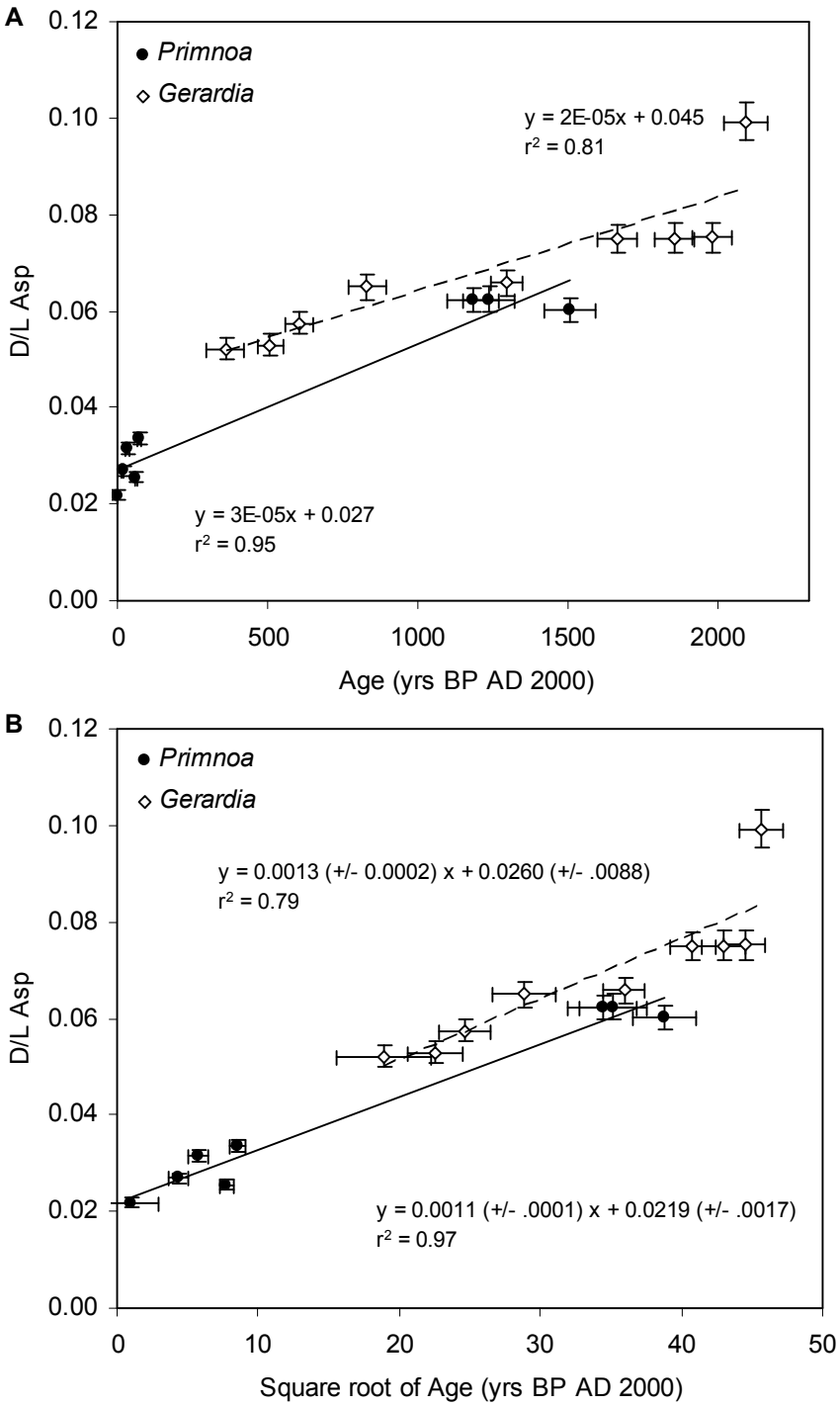

Fig. 5.6: D/L-Asp vs. calendar age (A) and square root of calendar age (B) for *P. resedaeformis* and *Gerardia*. *Gerardia* 14C ages originally reported in Druffel et al. (1995) have been calibrated and corrected for marine reservoir effect (see text). Error bars are ± 1 s.d.

the results for D/L vs. the square root of age are shown because r^2 values are reasonably good both for *P. resedaeformis* (0.97) and *Gerardia* (0.79) and it is easier to visualize the spread of values along the regression across the entire time period. While D/L-Asp values are ~0.007 higher in *Gerardia*, the slopes and intercepts of the two regressions are within 1 standard error of each other. On this basis, we assume that the fit for *P. resedaeformis* reliably estimates D/L values between the two extremes in age represented by the present data. This is an empirical calibration and there is no a priori reason to choose one linearization over another. Recently, Collins et al. (1999) and Collins and Riley (2000) have challenged the practice of treating the net racemization as a "black box", in favor of a modeling approach that accounts for the underlying kinetics of hydrolysis, racemization and decomposition separately. The purpose of the present study, however, was simply to test whether D/L-Asp could be used to resolve ages in the time period ca. 100-400 yrs BP.

Goodfriend (1997) used heating experiments to derive Arrhenius parameters for Asp racemization in *Gerardia*. From his results, the calculated age of the colony was only 250 ± 70 yrs, in conflict with the 1800 yrs determined by ^{14}C (Druffel et al., 1995). Goodfriend (1997) offered 4 explanations for the conflicting age estimates: 1) Possible incorporation of older, ^{14}C -depleted carbon sources in the *Gerardia* skeleton. 2) Non-linearity in the Arrhenius relationship, such that the rate at ambient temperature cannot be reliably extrapolated from rates calculated at high experimental temperatures. 3) Variation in rates among the different layers of skeleton. 4) Change in ambient temperature during the lifetime of the organism. Goodfriend (1997) discussed each of

these possibilities at length and largely discounted the importance of the latter two explanations.

Measurements of bomb-radiocarbon in the recent layers of *Gerardia* (Druffel et al., 1995) as well as in several other species of deep-sea gorgonian (Griffin and Druffel 1989; Roark et al., 2005; Sherwood et al., 2005a) suggest that the proximate source of carbon to the organic endoskeleton is recently exported particulate organic matter (POM). Since bomb radiocarbon was measured in the older (i.e.: mature) layers of *Gerardia*, as well as in younger layers (< 50 yrs) of modern specimens of other gorgonians (Sherwood et al., 2005a), there is no evidence that the organic endoskeleton incorporates a ^{14}C depleted carbon source, such as DIC, dissolved organic carbon or suspended POM found at depth, at any point in the organism's lifetime. This is also supported by the similarity of $\delta^{13}C$ and $\delta^{15}N$ in the same modern and sub-fossil specimens of *P. resedaeformis* presented here (Sherwood et al., 2005b). On the other hand, the ultimate source of carbon could potentially be upwelled DIC or DOC with a depleted ^{14}C signature, upon which POM may grow. The radiocarbon ages measured in *Gerardia* increased linearly with distance from the edge of the skeleton (Druffel et al. 1995). To explain the apparent 1800 yr lifespan in terms of feeding on ^{14}C-depleted POM would require a smooth decrease in upwelling intensity over time, a scenario we find highly unlikely. Therefore, we suggest that Goodfriend's (1997) explanation 1, above, can safely be discounted.

Collins et al. (1999) called into question the practice of estimating racemization rates in collagen by extrapolating from high experimental temperatures. This is because

denaturation temperatures (approx. 70^{o}C) occur between ambient and experimental temperatures (Collins et al., 1999). Below the denaturation temperature, the triple helical structure of collagen imposes a severe conformational constraint on the deamination of Asp + Asn to form Asu, and therefore on the racemization of Asp and Asn. There is little or no racemization within the helical structure of collagen itself, except at the frayed ends of the helix (Collins et al., 1999). Although the organic endoskeleton of *Gerardia* has not been characterized by modern sequencing techniques, it is likely to be a fibrillar protein of some sort, and subject to similar conformational constraints on racemization. The heating experiments on *Gerardia* (Goodfriend, 1997) likely overestimate racemization rates, resulting in younger apparent age (Collins et al., 1999). Thus, the 1800 year age estimate from ^{14}C is probably correct. Similar to *Gerardia* and bone collagen, the fibrillar protein in *P. resedaeformis* may impose a conformational constraint upon Asp + Asn deamination. The observed racemization probably reflects racemization at the degraded ends of protein fibrils, and/or within the associated non-fibrillar protein matrix.

Racemization rate is dependent on temperature as well as time. The present experiment was not designed to evaluate temperature effects, and if the assumption that gorgonin behaves like collagen is correct, then extrapolating racemization rates from Arrhenius parameters determined at high experimental temperatures may be problematic. However, if we assume that racemization kinetics are similar in *P. resedaeformis* and *Gerardia*, then a preliminary evaluation may be made by comparing the two D/L-Asp vs. square root of age relationships (Fig 5.6b). No useful information is provided by the intercepts, or by the fact that *Gerardia* D/L values average 0.007 higher, because a

certain amount of racemization is induced during hydrolysis in the laboratory, and in this case, preparation methods differed. On the other hand, the slopes should not be affected by laboratory procedure. For *P. resedaeformis*, ambient temperature was 7°C (250-500 m average, area SS29 from the Oceanographic Database, Bedford Institute of Oceanography; http://www.mar.dfo-mpo.gc.ca/science/ocean.database). For *Gerardia*, the ambient temperature was 12.5°C (Griffin and Druffel, 1989). Since the slopes were within 1 standard error of each other, differences in racemization rate over a temperature of 6.5°C could not be determined. However, since racemization rate is taxon-specific, it is possible that a taxon effect compensates for, and masks, a temperature effect.

Taking a different approach, the standard error of the regression for *P. resedaeformis* (Fig 5.6b) was 0.0032, or about twice the analytical error in D/L-Asp measurements. Much of this variability may be due to annual-decadal temperature fluctuations, which can exceed ± 2°C in the Northeast Channel between 250-500m. It is probable that Little Ice Age temperatures at this depth were persistently cooler because of southward penetration of the Labrador Current; this phenomenon characterized the 1960s (MERCINA 2001), when NE Channel bottom temperatures were about 2.5°C cooler than the 1950-2000 average. In the analysis below, we assume that the errors in the regression coefficients (Fig 5.6b) reflect temperature effects, and that these temperature effects are accounted for by the overall simulated dating error.

5.4.4 Prospects for D/L-Asp Dating of *P. resedaeformis*

The purpose of this study was to evaluate whether D/L-Asp could be used to date recent (< 400 yrs) colonies of *P. resedaeformis*. From Fig 5.6b, the relationship between D/L-Asp and time is:

$$\text{Age (yrs BP 2000 AD)} = [\ (D/L - 0.020\ (\pm .002)) / .0011\ (\pm .0001)\ ]^{2}$$

$$(r^2 = 0.97,\ p < 0.001) \qquad (1)$$

where the errors in brackets are $1\sigma_x$. Using a spreadsheet, the error in an age calculation was estimated with a Monte Carlo simulation over 1000 iterations (e.g.: Kaufman, 2003). Values of the slope and intercept in equation 1 were applied to specific values of D/L. Each iteration used values drawn at random from normal probability distributions defined by the mean and error in each variable. The $1\sigma_x$ error was used for slope and intercept. Since D/L analyses were not performed on co-eval samples, the 2σ analytical error (± 8 %) was chosen to reflect inter-sample variability in D/L. The 1σ error in a D/L age estimate was calculated for a range of different ages (Fig 5.7). For example, the error for a 100 year old sample is ± 60 years. For comparison, Fig 5.7 also shows local model ^{14}C dating errors, using a ΔR value of 128 ± 35 years, over the same time period. The error associated with a D/L age is marginally better than that of ^{14}C over the last 100-200 years, or where model ^{14}C ages are invalid (50 - 95 years BP AD 2000). Prior to 200 yrs BP, ^{14}C dating provides more precise model ages, while over the most recent 50 years, bomb-^{14}C may be used to constrain age with a high level of precision (Sherwood et al.,

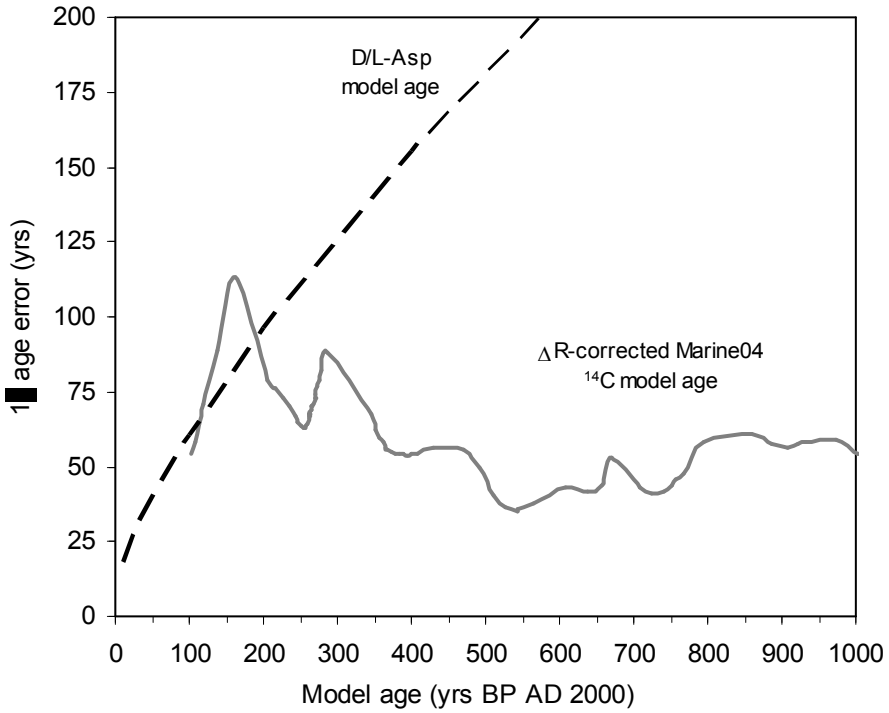

Fig. 5.7: Comparison of 1 s.d. dating errors associated with D/L-Asp and ^{14}C dating methods. D/L-Asp errors calculated with Monte Carlo simulation applied to equation 1 (see text). Marine model ^{14}C age errors calculated with Calib 5.0, using a ^{14}C age error ± 35 years and a ΔR correction of 128 ± 35 years. Model ^{14}C ages < 95 years BP 2000 AD are invalid.

2005a). This comparison is limited by the fact that for model ^{14}C ages, ΔR is assumed to be constant over time. On the other hand, some of the error associated with the D/L age model itself depends on ^{14}C error, as well as analytical error and the effect of variable temperature.

From these preliminary results, the prospects for dating deep-sea coral by D/L-Asp racemization over the last 400 yrs do not look promising. However, analyses of more samples spanning a greater range of ages may better constrain the age equation, and

thereby improve upon dating error. Rates of D/L racemization may also be further constrained by analyzing the fibrillar protein or protein matrix components of gorgonin separately. D/L-Asp dating of *P. resedaeformis* may be useful in screening samples for further ^{14}C or U/Th dating, since D/L determinations are relatively inexpensive and can be performed on minute quantities of sample material. Another approach to using D/L-Asp dating is where a ^{14}C calibration yields 2 or more intercepts. The D/L-Asp data might clearly discern which of the intercepts is more likely.

5.5 CONCLUSIONS

1. Radiocarbon dating of a large sub-fossil specimen of *Primnoa resedaeformis* indicates a lifespan of 700 ± 100 years, the longest documented lifespan of any deep or shallow water octocoral.

2. There were no ontological or long-term trends in amino acid abundances of gorgonin over the last 1500 years. This indicates that the gorgonin may be a durable, long term archive of paleo-environmental information.

3. The increase in D/L-Asp with time is non-linear, as expected from previous studies on other organisms. Similar to bone collagen, the fibrillar protein of gorgonin may impose conformational constraints on the racemization of Asp at low temperatures.

4. Compared with ^{14}C dating, D/L-Asp dating of *P. resedaeformis* may offer marginally better age constraint over the last 50-200 years, but more analyses are required to refine the D/L-Asp vs. time relationship.

ACKNOWLEDGEMENTS

We gratefully acknowledge Sanford Atwood, Derek Jones and Ronnie Wolkins for providing the priceless chunk of fossil coral, and Pal Mortensen, Lena Buhl-Mortensen and Don Gordon for providing the modern specimen. Amino acid analyses were performed by Steve deVogel at INSTAAR. Radiocarbon analyses were performed by Tom Guilderson, under the auspices of the U.S. Department of Energy by the University of California's Lawrence Livermore National Laboratory (W-7405-Eng 48). We thank H. Ehrlich, S. deVogel, D. Kaufman and 2 anonymous reviewers for their valuable comments on the manuscript. This project was funded by a GSA student grant and NSERC postgraduate scholarship to OAS, and by an NSERC Strategic Grant to MJR and DBS.

CHAPTER 6

CARBON-14 RECORDS FROM THE CALCITE PHASE OF DEEP-SEA OCTOCORALS

Owen A. Sherwood [1], Bassam Ghaleb [2], David B. Scott [1], Michael J. Risk [3]

[1] Centre for Environmental and Marine Geology, Dalhousie University, Halifax, Canada

[2] GEOTOP-UQAM-McGill, Montreal, Canada

[3] School of Geography and Geology, McMaster University, Hamilton, Canada

(not yet submitted for publication)

6.1 ABSTRACT

Primnoa resedaeformis is an extraordinarily long-lived, deep-sea octocoral. A massive calcite "crust", formed from dissolved inorganic carbon at depth, comprises the bulk of the skeletons of older colonies. Geochemical measurements from the calcite may therefore provide long term (centuries) records of ambient environmental conditions. This paper explores Pb/Ca and $\Delta^{14}C$ in specimens collected from between 200-400m in the NW Atlantic slopewaters, southwest of Halifax. Growth rings in the calcite crust could not be visualized, therefore special attention was given to the establishment of skeletal chronology with bomb-^{14}C and ^{210}Pb dating methods. Profiles of calcite Pb/Ca were measured in 3 independently dated colonies. Accurate reconstruction of the anthropogenic Pb pulse in the 20th century establishes this property as a useful environmental proxy in *P. resedaeformis*. A profile of calcite $\Delta^{14}C$ provides new evidence for the variability of the ^{14}C reservoir age of upper intermediate waters. Methods presented herein can be extended to other regions and with other octocoral species to obtain estimates of the ^{14}C reservoir age which would otherwise be unavailable.

6.2 INTRODUCTION

Deep-sea, or cold-water corals are attracting increasing attention as new sources of proxy environmental information in cold-water environments. Most studies have focused on scleractinian species, e.g. *Desmophyllum cristagalli* and *Lophelia pertusa*, because of their widespread distribution and great longevity (Smith et al., 1997; Frank et al., 2004; Robinson et al., 2005). Useful proxy information is also recorded in the long-lived skeletons of deep dwelling 'soft' corals; in particular, the gorgonian octocorals (Thresher et al., 2004, Roark et al., 2005, Sherwood et al., 2005a; 2005b) and antipatharians (Williams et al., 2005). Some of these organisms form concentric annual and sub-annual growth rings in their axial skeletons (Risk et al., 2002; Marschal et al., 2004; Sherwood et al., 2005a) that allow for climate reconstructions with unprecedented temporal resolution for cold water environments.

Gorgonian octocorals are particularly interesting as potential climate archives because they form 2-part calcite-protein skeletons. The calcite is formed from ambient dissolved inorganic carbon at depth (DIC) and the gorgonin is derived from recently exported particulate organic carbon (POC; Griffin and Druffel, 1989; Roark et al., 2005; Sherwood et al., 2005a; 2005b). This implies that records of both deep- and surface-water processes could be reconstructed from the same skeletons, in much the same way that benthic-planktic foraminifera are sampled from the same core intervals to reconstruct both deep- and surface-water paleoceanography (Broecker et al., 1990). Our earlier work (Sherwood et al., 2005a; 2005b) has focused on *Primnoa resedaeformis* because it is one of the dominant corals in the Northwest Atlantic slopewaters, and is extremely long-lived

(at least 700 years; Sherwood et al., 2006). The axial skeleton of *P. resedaeformis* contains an inner, horny region, and an outer massive calcite region. The horny region is comprised of annually secreted growth rings. After about 50-100 years of growth, a massive calcite crust or cortex envelops the skeleton. As colonies continue to grow for at least 700 years, the calcite crust comprises the bulk the skeletal mass and thus the bulk of the climate record. Unfortunately, growth rings in the calcite region are more diffuse and difficult to count, at least in specimens from the NW Atlantic, and independent dating techniques are a prerequisite for establishing skeletal chronology.

Studies on potential environmental records contained within the calcite phase of gorgonians are in their infancy. Several authors report a relationship between Mg/Ca and temperature (Weinbauer et al., 2000; Thresher et al., 2004, Bond et al., 2005; Sherwood et al., 2005c); others report inconsistent Mg/Ca profiles across different tracks of the same coral, therefore masking any temperature dependency (Fallon et al., 2005; Allard et al., 2005). Because deep ocean temperature variations are subtle, temperature proxies may not be suitable for testing the fidelity of octocorals as environmental recorders. In this paper, we report on 2 very different geochemical properties, Pb and ^{14}C, which experienced large anthropogenic perturbations over the last century. As growth rings in the calcite region cannot be relied upon as chronometers, we pay careful attention to skeletal chronology using sample stratigraphy, bomb-^{14}C, and ^{210}Pb-dating. Chronological accuracy is verified by the reconstruction of the anthropogenic Pb pulse. Finally, we show that a profile of calcite $\Delta^{14}C$ documents large variability in the ^{14}C reservoir age of upper intermediate waters.

6.3 MATERIALS AND METHODS

Two large stumps of *P. resedaeformis* (Colonies COHPS2001-1 and COHPS2001-2) were collected by fishermen in 2001. The samples were collected from 200 to 400 m in depth (exact depth unknown), from the mouth of the Northeast Channel (approx. 42°00N / 65°50W; Fig. 6.1). Both stumps were dead upon collection, but based on their relatively good condition and lack of extensive encrustation, we originally estimated that these died within a few years of collection. Additional live colonies were collected by the remotely operated submersible ROPOS in August 2001, from depths of 275 to 475 m.

Geochemical analyses were carried out on sections cut from the axial skeletons (Fig. 6.2). For ^{210}Pb and ^{226}Ra analyses, a sample was cut from the side of a section using a low speed saw (Isomet), and this was further cut into 6-8 sub-samples, each weighing about 1 g. The sub-samples were crushed in an agate mortar, and the powder was oxidized in peroxide held at pH 8 by addition of ammonium hydroxide, then washed with de-ionized water and dried at 60°C. Measurement of ^{210}Pb was done by alpha spectrometry of its daughter product, ^{210}Po (Flynn, 1968), while ^{226}Ra was measured by thermal ionization mass spectrometry with isotope dilution (Andrews et al., 1999). Full analytical details are provided in Pons-Branchu et al., 2005. Precision was better than 0.5% on the isotopic ratios.

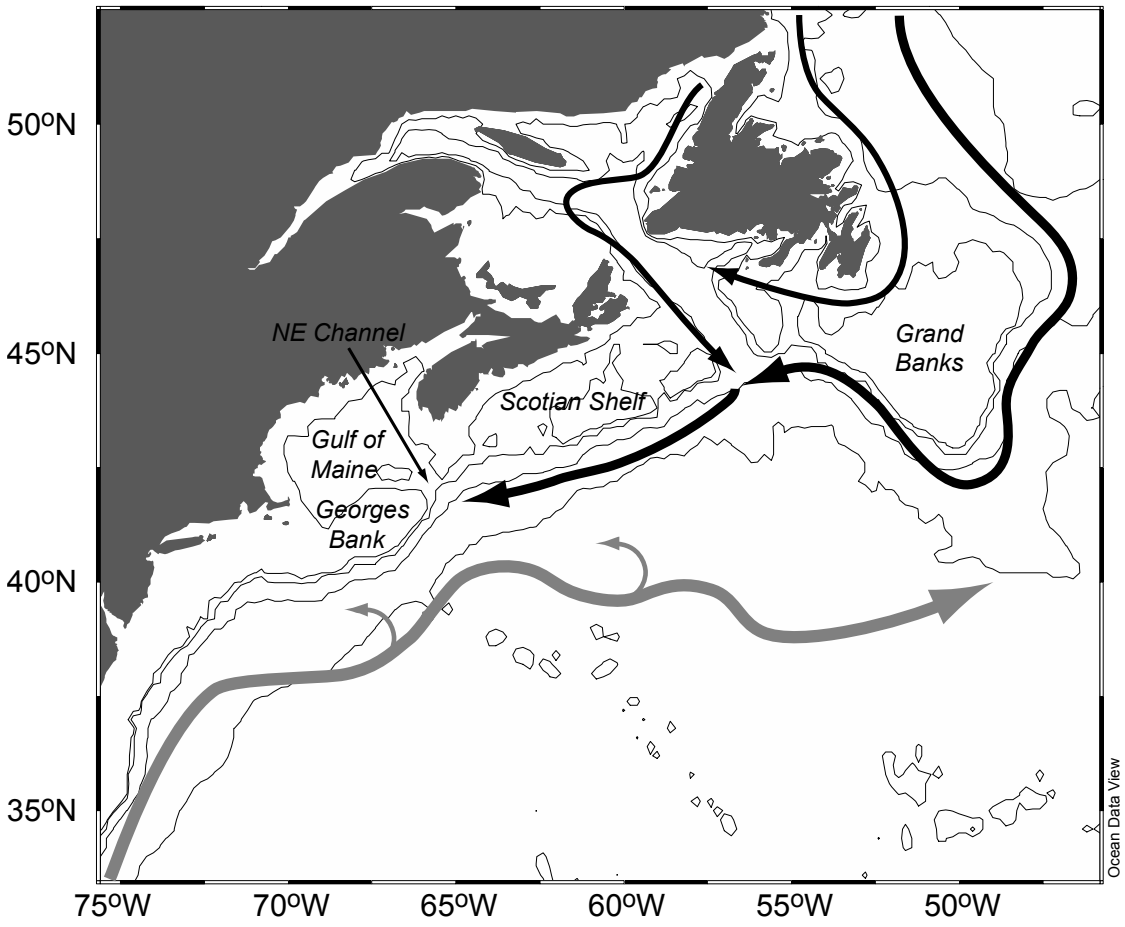

Fig. 6.1: Map of the NW Atlantic study area. Bathymetric contours are 100m, 250m, 2000m, and 4000m. Grey arrows represent Gulf Stream and associated warm core rings. Black arrows represent outer (thicker lines) and inner (thinner lines) axes of the Labrador Current. Corals were collected from the Northeast Channel.

Samples of both gorgonin and massive calcite were analysed for ^{14}C. Isolation of gorgonin samples followed procedures described earlier (Sherwood et al., 2005a). Briefly, layers of gorgonin were isolated by dissolving the sections in 5% HCl for up to 3 weeks, and peeling apart the residual gorgonin layers. To sample the calcite, a computerized micromill (Merchantek) was used. Discrete samples of calcite powder were milled along a radial transect of a section of Colony COHPS2001-1. Individual samples

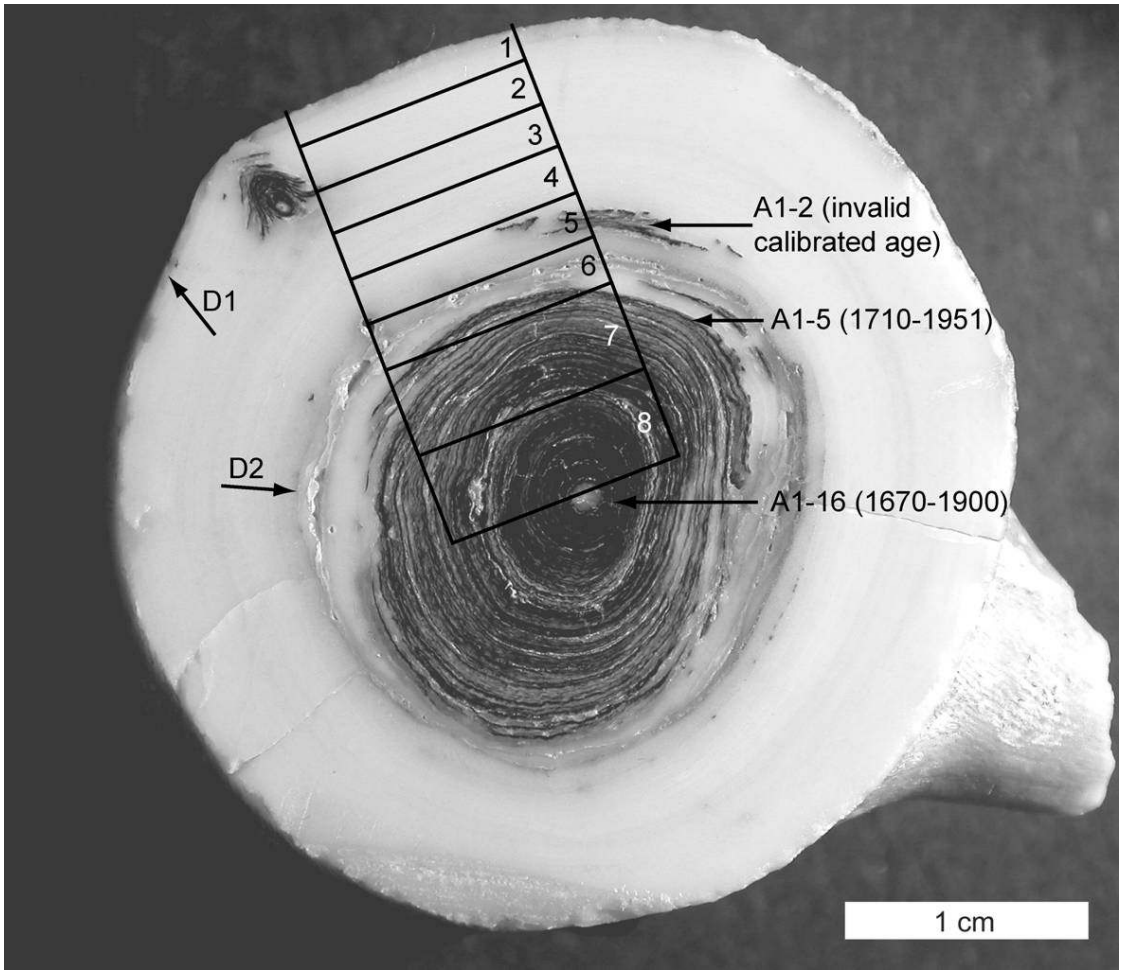

Fig. 6.2: Section of the axial skeleton of Colony COHPS2001-1. Darker region toward centre of section is the "horny axis", composed of annual rings of calcite and gorgonin; lighter region towards outside is the calcite cortex, containing no gorgonin. "D1" and "D2" point to death/re-growth surfaces. Rectangles indicate samples isolated for ^{210}Pb dating. Longer arrows on the right point to locations of gorgonin samples isolated for ^{14}C-dating; CAMS identifier and calibrated 2s min-max ages (in brackets) are shown.

measured 4 mm long, 0.35 mm wide, and 0.4 mm deep, yielding about 1 g of powder. Delta-^{14}C was determined on graphite targets at the Center for AMS. In an initial run, the 1 g of powder was insufficient, and in subsequent runs, the adjacent samples were "doubled up". Results include a background and δ^{13}C correction and are reported as Δ^{14}C according to Stuiver and Polach (1977).

As gorgonin is derived from sinking POM, radiocarbon ages may be calibrated to the surface water ^{14}C history. We used the CALIB program (Stuiver and Reimer, 1993, version 5.0) and the Marine 04 dataset (Hughen et al., 2004). Ages were corrected for local variation in the marine reservoir effect based on previous measurements of the gorgonin of *P. resedaeformis* from the Northeast Channel ($\Delta R = 128 \pm 35$ yr; Sherwood et al., 2006). Use of this value assumes that local water mass effects on $\Delta^{14}C$ of dissolved inorganic carbon have remained constant over time. Because the samples are relatively young (< 400 yrs), a plateau in the radiocarbon calibration led to multiple calibrated ages. Here, calibrated ages are reported as the probability-weighted mean of the 2σ ages, and errors are reported as the 2σ minimum-maximum ranges.

Trace elemental analysis was performed by Laser Ablation ICP-MS. Sections were cleaned by immersion in hot ($90^{o}C$) lithium hypochlorite for one week with periodic ultrasonic agitation, then rinsed in 0.1 % (v/v) HNO_3, followed by triple, 20 minute ultrasonic baths in milli-Q water. This procedure was designed to remove organic and detrital phases; however, the zone of cleaning penetrated to a depth of only 1 mm from the surface of the sections. The cleaned sections were embedded in epoxy and ground and polished on a diamond lap. Polished sections were ultrasonically cleaned in Milli-Q water once again, and wiped with acetone prior to analysis. LA-ICP-MS analyses were performed along radial traverses of the outer calcite cortex region of each section. Analytical parameters are listed in Table 6.1. Isotope abundances of 8 different elements were blank-subtracted, ^{43}Ca-normalized and standardized to NIST 612 glass. Analytical reproducibility was determined by repeating 3 or 4 point analyses at the beginning,

Table 6.1: Analytical parameters used during LA-ICP-MS analysis

Laser conditions	
Type	Nd-YAG
Pulse rate	2 Hz
Power	0.8 mJ
Spot diameter	75 μm
Spot increment	100-150 μm
ICP-MS conditions	
Type	Magnetic sector
Mode	Low resolution, peak jumping
Acquisition delay	30 sec.
Replicates	20
Scan time	15 sec.

Table 6.2: Radiocarbon data and age calibrations

Colony Name	Section ID	CAMS #	$\Delta^{14}C$ (±1σ) (‰)	^{14}C age (± 1σ) (yrs BP)	Calibrated age (yrs AD)
COHPS2001-1	A1-2	111130	-74 (3.5)	565 (35)	Invalid [a,b]
COHPS2001-1	A1-5	111131	-80 (3.5)	620 (35)	1710-1950[a,c]
COHPS2001-1	A1-16	111132	-87 (3.5)	680 (35)	1670-1900 [a]
COHPS2001-1	E2-1	111133	37 (4)	> Modern	1979-2001 [d]
COHPS2001-1	YB2-6	120203	52 (5)	> Modern	1968-1991 [d]
COHPS2001-1	YB2-7	120204	-27 (4)	165 (35)	1962-1964 [d]
COHPS2001-2	D2-43	111134	-82.9 (3.5)	640 (35)	1700-1910 [a]

[a] Ages based on Marine 04 calibration using $\Delta R = 128 \pm 35$ yrs. 2σ min-max ages are reported.
[b] Calibrated age is younger than 1950.
[c] Calibrated age is suspect due to impingement on the end of the calibration dataset
[d] Ages based on intersection with bomb-^{14}C curve; see Fig. 6.3. Min-max intercept ages are reported

middle and end of each traverse, and calculated by the average difference in replicate measurements. We report here only the Pb/Ca results, as this was the only element where the measured variability (> 100%) was large relative to analytical reproducibility (~ 10 %).

6.4 RESULTS

6.4.1 Growth hiatuses

Conspicuous dark bands, described previously in Sherwood (2002), were present in the calcite cortex region of both colonies (Fig. 6.2). The bands contained fine grained siliciclastic material, fungal borings and sponge spicules. These bands represent a hiatus in growth, where the living tissue died and the skeleton was exposed to bioerosion. In each of the dead stumps we identified 2 conspicuous bands, a younger one (D1) near the outside of the colony, and an older one (D2) closer to the centre. These were used as stratigraphic horizons, for correlating geochemical profiles between different sections of the same colony.

Below, we show that D1 and D2 were formed contemporaneously in the 2 independently dated stumps. We did not observe growth hiatuses in younger colonies comprising mostly horny material. Together, these observations suggest that a common environmental trigger leads to death of the basal tissues, but not of the upper branches.

6.4.2 ^{14}C-dating

To constrain absolute chronology, ^{14}C-dating was performed on 6 gorgonin samples isolated from Colony COHPS2001-1 and one sample isolated from Colony COHPS2001-2 (Fig. 6.2 and Table 6.2). For the pre-modern samples, the errors in calibrated ages were very large (> 100 yrs) because of a plateau in the radiocarbon calibration over the last few hundred years. The oldest ages for each colony were 1670-1900 (COHPS2001-1-A1-16) and 1700-1951 (COHPS2001-2-D2-43). For Colony COHPS2001-1, the decrease in age from inside to outside of the colonies was consistent with sample stratigraphy, and indicated an age of possibly up to 300 years.

Three of the youngest samples from COHPS2001-1 were isolated from 1) just before D1, 2) just after D1, and 3) near the outer margin of the skeleton (Fig. 6.3 and Table 6.2). All 3 samples had Δ^{14}C values close to, or greater than 0‰, indicating the influence of bomb-^{14}C. Therefore, ages could be estimated by referencing a local surface water bomb-Δ^{14}C curve based upon previous measurements of the gorgonin of *P. resedaeformis* from the Northeast Channel (Sherwood et al., 2005a) and a clam shell from Georges Bank (Weidman and Jones, 1993). Ages were estimated graphically from the intersection of sample Δ^{14}C (mean $\pm 2\sigma$) intervals on the 95% prediction bands around the reference Δ^{14}C curve. Age estimates for the period 1958-1970 were the most precise because Δ^{14}C was changing rapidly during this interval. The sample from just before D1 (YB2-7) was dated to 1962-1964. The other two samples (YB2-6, E2-1) had maximum ages of 1964 and 1977, respectively; minimum ages could vnot be determined because the Δ^{14}C intervals did not intersect the reference curve at the upper limit.

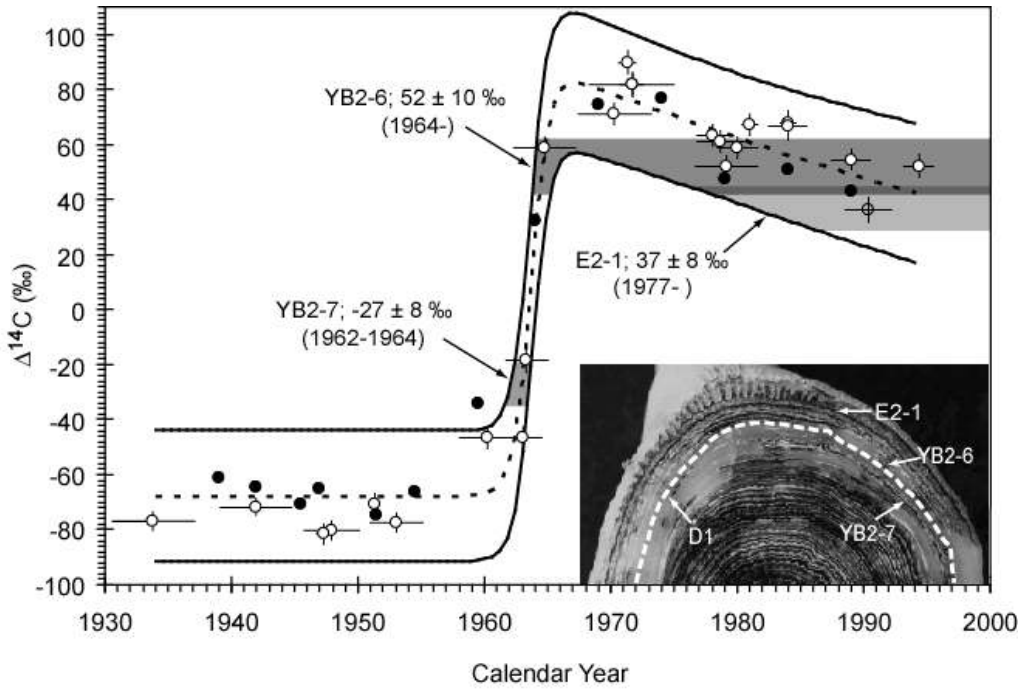

Fig. 6.3: Calibration of bomb-^{14}C data from a younger branch of Colony COHPS2001-1. Inset photograph shows locations of samples relative to D1. Reference curve (---) defined by data from (?) independently dated clam shell (*A. islandica*; Weidman and Jones, 1993) and (?) *Primnoa* colonies (Sherwood et al. 2005a). Error bars, where available, are 1σ. Thick black lines enclose the 95% prediction intervals around the reference curve. Ages estimated by the intersection of Δ^{14}C (± 2σ) data with the reference curve (coloured polygons).

Since the oldest of these three samples was located just before D1 on the section of skeleton from which it was isolated, D1 must have formed around 1965 ± 5.

6.4.3 ^{210}Pb-dating:

Activities of ^{210}Pb ranged from below detection limits to a high of 2 dpm/g, and showed the expected decay from the outer margin towards the center of axial sections

(Table 6.3). Activities of ^{226}Ra were fairly uniform, with a mean (± 1se) of 0.104 ± 0.002 dpm/g. In all but the center-most sub-samples ^{210}Pb:^{226}Ra activity ratios were >1, indicating unsupported or excess ^{210}Pb ($^{210}Pb_{ex}$) was present. In the center-most sub-samples ^{210}Pb had decayed to secular equilibrium with ^{226}Ra, indicating an age of > 110 years, consistent with the ^{14}C-dating.

Following Andrews et al. (2002) the data were linearized by plotted natural-log transformed values of $^{210}Pb_{ex}$ against distance (Fig. 6.4) and growth rates were calculated from:

$$r = \lambda / m \qquad (1)$$

where r is growth rate, m is the slope of the linear regression, and λ is the ^{210}Pb decay constant (0.03067 yr^{-1}). The effect of growth hiatuses on the $^{210}Pb_{ex}$ decay profiles is evident: in both colonies the most recent value appears "compressed" along the horizontal axis (Fig. 6.4). Growth rates calculated from a linear fit on all the values, therefore, would likely underestimate the true growth rate. To address this problem, growth rates were calculated using (1) all data points and (2) only the data between D1 and D2 (Table 6.4). The calculated growth rates (0.074 - 0.180 mm yr^{-1}) were within range of previous studies on deep-sea gorgonians (Andrews et al., 2002; Risk et al., 2002; Thresher et al., 2004). In the first case, the time interval between D1 and D2 is ~120 yrs in both colonies. This suggests an age for D2 of ≥ 155 years (since the age of D1 ≥ 35

Table 6.4: $^{210}Pb_{ex}$-calculated growth rates and time intervals between D1 and D2 (1σ errors in brackets) for Case 1 (all data) and Case 2 (only the data between D1 and D2 used) scenarios.

		Case 1		***Case 2***	
Colony	**Dist. D1-D2 (mm)**	**Growth Rate (mm yr^{-1})**	**Time (yrs)**	**Growth Rate (mm yr^{-1})**	**Time (yrs)**
COHPS2001-1	8.5	0.074 (0.010)	114 (15)	0.122 (0.021)	70 (12)
COHPS2001-2	10.8	0.088 (0.018)	122 (24)	0.180 (0.011)	60 (4)

Table 6.3: Results of ^{210}Pb and ^{226}Ra analyses (in dpm g^{-1};1σ error in brackets; b.d; below detection)

Distance (mm)	**^{210}Pb**	**^{226}Ra**	**$^{210}Pb_{ex}$**
	Colony COHPS2001-1, section K		
0 – 1.6	0.772 (0.044)	0.108 (0.012)[a]	0.664 (0.044)
1.9 – 3.5	0.234 (0.016)	0.108 (0.012)[a]	0.126 (0.016)
3.8 – 5.4	0.218 (0.016)	0.108 (0.012)[a]	0.110 (0.016)
5.7 – 7.3	0.162 (0.014)	0.108 (0.012)[a]	0.054 (0.014)
7.6 – 9.2	0.140 (0.014)	0.108 (0.012)[a]	0.032 (0.014)
9.5 – 11.1	0.115 (0.012)	0.108 (0.012)[a]	0.007 (0.012)
11.4 – 14.9	0.053 (0.006)	0.108 (0.012)[a]	-0.055 (0.006)
15.2 – 18.8	0.064 (0.008)	0.108 (0.012)[a]	-0.044 (0.008)
	Colony COHPS2001-2, section B		
0 – 1.7	1.998 (0.068)	0.103 (0.001)	1.895 (0.068)
2.0 – 4.0	0.363 (0.025)	0.105 (0.011)	0.258 (0.025)
4.3 – 6.7	0.276 (0.021)	0.099 (0.001)	0.177 (0.021)
7.0 – 10.2	0.196 (0.012)	0.096 (0.001)	0.100 (0.012)
10.5 – 14.7	b.d.	0.102 (0.002)	0
15.0 – 20.0	b.d.	0.103 (0.001)	0

(a) Not measured on this section. Average (± half the range) of 5 ^{226}Ra analyses performed on an adjacent section are reported

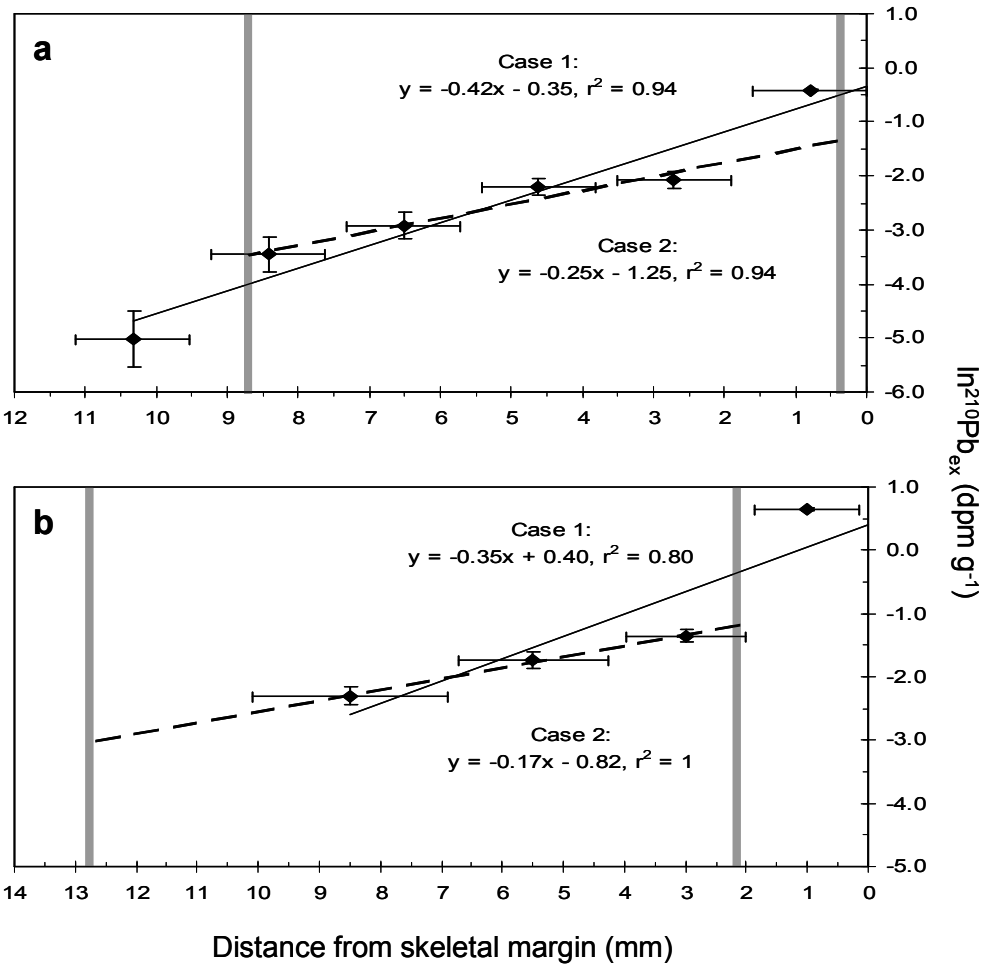

Fig. 6.4: Plots of natural log-transformed $^{210}Pb_{ex}$ vs. distance from the growing edge, (a) COHPS2001-1, (b) COHPS2001-2. Values on abscissa are reversed, so time increases to the left. Horizontal error bars indicate width of skeletal samples. Vertical error bars are 2σ errors in $\ln^{210}Pb_{ex}$.

years, based on bomb-^{14}C constraints on the timing of D1; Fig. 6.3). In the second case the time interval is around 65 yrs, suggesting an age for D2 of ≥ 100 years. The age of D2 must be younger than ~110 yrs, because $^{210}Pb_{ex}$ was detected in this part of the skeleton. Therefore, the second case is a better estimate of the true growth rate.

The duration of the growth hiatus at D1 may be estimated by solving the linear regressions in Fig. 6.4, inputting the most recent value of $^{210}Pb_{ex}$, and converting the length of 'missing skeleton' to a time equivalent. For Colony COHPS2001-1, the duration of the growth hiatus is ~30 years; for Colony COHPS2001-2, it is ~50 years. These values may overestimate the true duration, since growth rates probably slowed before or after the formation of the growth hiatuses. Indeed, it is very unlikely that growth rates were constant, as colonies may twist during their lifetime to remain oriented to prevailing currents (Wainwright and Dillon, 1969); this may explain the scatter about the linear models in Fig 6.3. The scatter may also be explained by variability in the amount of initial $^{210}Pb_{ex}$ over time.

Finally, our ^{210}Pb results suggest that D1 and D2 were formed contemporaneously between the 2 colonies. This is evidenced by similarity in 1) the activity of $\ln^{210}Pb_{ex}$ where the linear fits intersect D1 and D2, and 2) the calculated duration between D1 and D2.

6.4.4 Pb/Ca profiles

Profiles of Pb/Ca are shown in Fig. 6.5. Gaps in the profiles indicate where horny material or growth hiatuses were traversed and corresponding Pb/Ca values were an order of magnitude higher than in the calcite. Shen and Boyle (1988) outlined a procedure of minimizing Pb contamination in reef corals involving a series of oxidative and reductive leaches on crushed samples. Such a rigorous cleaning procedure could not be used here because it was necessary to maintain smooth surfaces on the samples for LA-ICP-MS. It

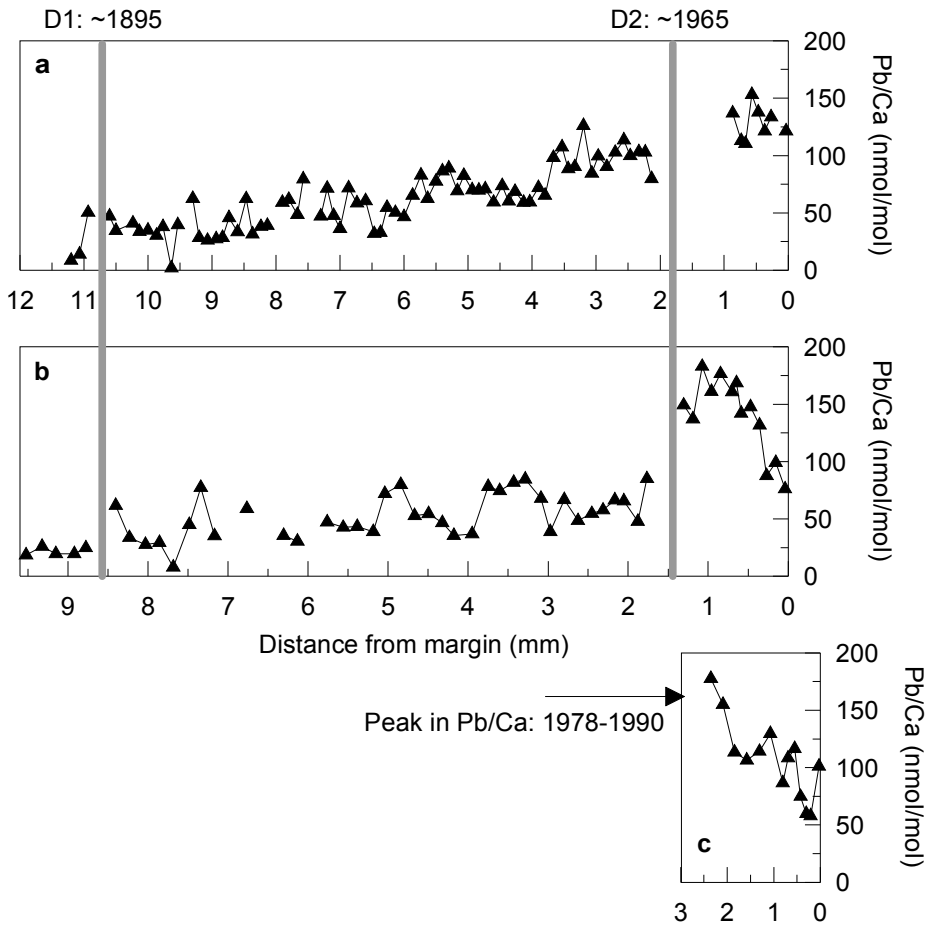

Fig. 6.5: LA-ICP-MS profiles of Pb/Ca measured across the calcite cortex of: (a) COHPS2001-1; (b) COHPS2001-2; (c) ROPOS-637052. Values on abscissa are reversed, so time increases to the left. Error in Pb/Ca is ~10 %. Vertical grey lines indicate positions of D1 and D2 in the 2 older colonies; note similar position of Pb/Ca maxima after D1. The younger colony was collected live in 2001; assuming a growth rate of 0.15 ± 0.1 mm yr^{-1}, Pb/Ca maxima occurred between 1978-1990.

appeared that our procedure was ineffective at removing contaminants associated with horny layers and detrital materials. The Pb/Ca profiles were therefore filtered by evaluating each datum on a case-by-case basis and removing any data that appeared spurious (generally, any data > 4 s.d. from the overall mean). A total of 15% of the data were filtered out.

The Pb/Ca profiles increased gradually from 30 nmol/mol in the oldest skeleton, to a high of 180 nmol/mol in recently formed skeleton, just after D1 (Fig. 6.5). Following this peak, values decreased rapidly to ~80 nmol/mol. The shape of the profiles, and timing of growth hiatuses with respect to Pb/Ca provides further support for contemporaneous formation of D1 and D2 between the two colonies. In colony COHPS2001-2, Pb/Ca increases more slowly before D1, then suddenly increases just after D1; this probably reflects a longer growth hiatus compared to COHPS2001-1.

We also analyzed a small colony of *P. resedaeformis* that was collected alive in 2001 (Colony ROPOS-637052). The Pb/Ca profile from this colony closely matched the most recent intervals in the 2 dead-collected colonies, with a Pb/Ca maximum of 180 nmol/mol, and a decline to 80 nmol/mol near the growing surface (Fig. 6.5c). Assuming a growth rate of 0.15 ± 0.1 mm yr^{-1}, the Pb/Ca maxima occurred between 1978 and 1990. Other live-collected colonies were analyzed, but they were mostly horny in composition, and the Pb/Ca data were deemed unreliable.

The shape of the Pb/Ca profiles is similar to previously published records from aragonitic corals from Bermuda (Shen and Boyle 1987), a calcitic sclerosponge from Bahamas (Lazareth et al., 2000) and bivalve shells from coastal North Carolina (Gillikin et al., 2005). These other records indicate a gradual increase in Pb/Ca since the 1920s, with a peak in the mid-late 1970's, and subsequent decline. The slightly later appearance of a Pb/Ca peak in our corals is consistent with longer residence time of Pb in upper intermediate waters (~10 years) compared with surface waters (~ 2 years; Wu and Boyle,

1997). The range of Pb/Ca measured in *P. resedaeformis* is similar to that of the bivalve record (40 to 230 nmol/mol) and intermediate between the coral (10 to 70 nmol/mol) and sclerosponge records (300 to 1200 nmol/mol). These Pb/Ca trends primarily reflect anthropogenic emissions of lead from the burning of coal and leaded gasoline. Declining Pb to the present day is a result of decreasing anthropogenic emissions as mandated by the Clean Air Act of 1970.

Following Shen and Boyle (1988), Cd and Ba were also examined as geochemical analogues of Pb. There were no similar increases in either of these two elements. Therefore, the Pb/Ca concentrations in Fig. 6.5 appear to reflect lattice-bound, not contaminant Pb.

6.4.5 $\Delta^{14}C$ profiles

To investigate past variations in seawater $\Delta^{14}C$ with *P. resedaeformis*, we measured $\Delta^{14}C$ in along a radial traverse of a section of Colony COHPS2001-1 (Fig. 6.6). Samples were milled from the region of skeleton between D1 and D2, representing the pre-bomb-^{14}C period, and one sample was milled from just after D1, representing the bomb-^{14}C period. The chronology in Fig. 6.6 is based on using D1 (1965 ± 5; Fig. 6.3) as a tie-in point, and the ^{210}Pb-derived duration of growth for the region of skeleton between D1 and D2 (70 ± 12 yrs; Table 6.4). The pre-bomb values fluctuated quasi-decadally between -106 ‰ and -72 ‰ (average -90 ‰). The sample from just after D1 measured -27 ‰, indicating penetration of bomb-^{14}C to depth. Compared with previously published values of surface water $\Delta^{14}C$ based on the gorgonin fraction of *P. resedaeformis*

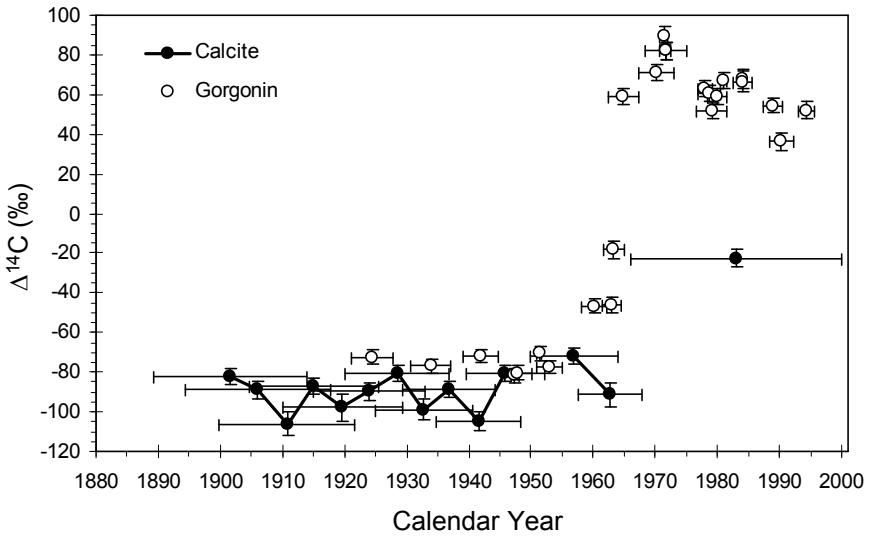

Fig. 6.6: Records of $\Delta^{14}C$ for the Northeast Channel derived from the calcite (this study) and gorgonin (Sherwood et al., 2005a) fractions of *Primnoa resedaeformis*. Pre-bomb calcite record is from the region between D1 and D2 on Colony COHPS2001-1. Chronology based on D1 tie-in point (1965 ± 5; Fig. 6.3) and ^{210}Pb-derived length of time between D1 and D2 (70 ± 12 yrs; Table 6.4).

(Sherwood et al., 2005a), the calcite $\Delta^{14}C$ record is 20 ‰ more depleted (t-test, p 0.001), and the bomb-^{14}C response is lagged by 10-20 years.

Marine reservoir age, R(t), is the difference between the ^{14}C age of a marine sample and the contemporaneous ^{14}C age of the atmosphere (Stuiver and Barziunas, 1993). Analysis of the ^{14}C age of known-age shell or skeletal material deposited prior to bomb ^{14}C contamination is one of the few available means of evaluating R(t). Using the IntCal 04 dataset (Reimer et al., 2004) for the ^{14}C age of the atmosphere, and the calcite ^{14}C age data, the reservoir age of local upper intermediate waters, $R(t)_{200\text{-}400m}$, averages 590 ± 90 yrs (1 s.d.). Using the gorgonin data as a proxy for surface waters (Sherwood et

al., 2005a), the reservoir age of local surface waters, $R(t)_{surface}$, averages 420 ± 30 years. Upper intermediate waters are older, as expected, but exhibit greater variability in reservoir age.

6.5 DISCUSSION

The dating of relatively young octocoral specimens can be problematic. The use of ^{14}C dating is not sufficiently precise over the last few hundred years because of a plateau in the ^{14}C-age calibration. U/Th-dating may provide high precision dates on young corals, but this has only been demonstrated on the aragonite skeletons of scleractinian corals (e.g.: Frank et al., 2004; Robinson et al., 2005). The calcite skeletons of octocorals contain an order magnitude less U than aragonite, and may therefore be more difficult to date (e.g. Thresher et al., 2004). The present study relied on 3 different methods to derive an absolute chronology for the calcite region of *Primnoa resedaeformis*. First, growth hiatuses provided stratigraphic horizons for correlating results obtained on different sections of the same colony. Second, a sample of bomb-^{14}C contaminated gorgonin isolated from just before D1 provided a tie-in point. Finally, ^{210}Pb results provided an estimate of the growth duration between D1 and D2. From these results, the region of skeleton between D1 and D2 formed between 1895 ± 13 and 1965 ± 5. Profiles of skeletal Pb/Ca tracking the anthropogenic input to the environment lend support the accuracy of the skeletal chronological.

It is interesting to note that the timings of D1 (~1965 ± 5) and D2 (~1895 ± 13) coincide, within error, with two extreme cold water events. These events are related to

the southward penetration of Labrador Slope Water (LSW) along the shelf break, displacing Warm Slope Water (WSW) further offshore (Petrie and Drinkwater, 1993; MERCINA, 2001). The younger of the two events lasted for most of the 1960s. The older event, in 1882, was inferred from reports of a mass mortality of burrowing tilefish in the Mid-Atlantic Bight region (Marsh et al., 1999). Virtually nothing is known about the biology and environmental tolerances of *P. resedaeformis*, so it is unclear how a cold event could have led to the temporary death of colonies. Colonies inhabiting the upper slope along the Scotia-Maine margin may be adapted to a relatively narrow range of temperatures (Bryan and Metaxas, in press). Temperature anomalies of -4 ^{o}C associated with LSW (Petrie and Drinkwater 1993) may be sufficient to kill colonies. Alternatively, there is growing evidence that primary productivity is more nutrient-limited in the Scotia-Maine region when LSW is dominant (Petrie and Yeats, 1999; Thomas et al., 2003). Since *P. resedaeformis* feeds on sinking particulate organic matter (Sherwood et al., 2005a), colonies may have starved during the extreme cold water events of 1882 and the 1960s. Both these hypotheses warrant further exploration.

Many previous studies have demonstrated a 1:1 relationship between the Δ^{14}C of coral carbonate and ambient seawater (Druffel and Linick, 1978; Adkins et al., 2002; Roark et al., 2005); this is the basis for reconstructing paleo-Δ^{14}C from independently dated coral colonies (Frank et al., 2004; Robinson et al., 2005). It is also on this basis that the record of Δ^{14}C measured in the calcite phase of *P. resedaeformis* (Fig. 6.6) may be interpreted as a record of seawater Δ^{14}C. Unfortunately, there were no measurements of Δ^{14}C in NW Atlantic slopewaters prior to bomb contamination which could be used for

direct comparison with the *P. resedaeformis* data. Broecker et al. (1960) reported 2 measurements from the Mid-Atlantic Bight area, but these were from 0 m. By the time of the GEOSECS 1972 survey (Stuiver and Ostlund, 1980) bomb-^{14}C had contaminated the upper 800m. The Transient Tracers in the Ocean – North Atlantic (TTNA) survey in 1981 sampled many stations along the continental margin (Fig. 6.7), but again, the upper waters had been contaminated by bomb-^{14}C. Estimates of natural Δ^{14}C in the GLODAP dataset (Key et al., 2004) underestimates the range of natural Δ^{14}C variability measured in *P. resedaeformis,* possibly because the GEOSECS data upon which the natural Δ^{14}C calibration is based were already contaminated above 800m.

In looking at the TTNA dataset (Fig. 6.7), the youngest waters (highest Δ^{14}C) are found in the Labrador Sea. Here, downwelling supplies recently ventilated waters to depth. Even below 3000m, there is evidence of bomb^{14}C contamination at stations 44193 and 44224. At the 2 stations closest to the Northeast Channel (44246 and 44003), the bomb-^{14}C contamination is restricted to the upper 1500m. Below this, the values of Δ^{14}C (-65 ± 10 ‰) are considerably higher than that measured in *P. resedaeformis* (-90 ± 10 ‰). Only the abyssal waters of the central North Atlantic and intermediate waters of the equatorial Atlantic have Δ^{14}C values that overlap with the *P. resedaeformis* data. Therefore, the *P. resedaeformis* data suggest that upwelling of abyssal waters may be an important process along the Scotia-Maine margin (Petrie, 1983). This may help to explain the occurrence of the benthic foraminiferid, *Nuttalides umbonifera* living attached to these corals; this species is an Antarctic water indicator and had not been observed in abundance at this depth previously (Hawkes and Scott, 2005).

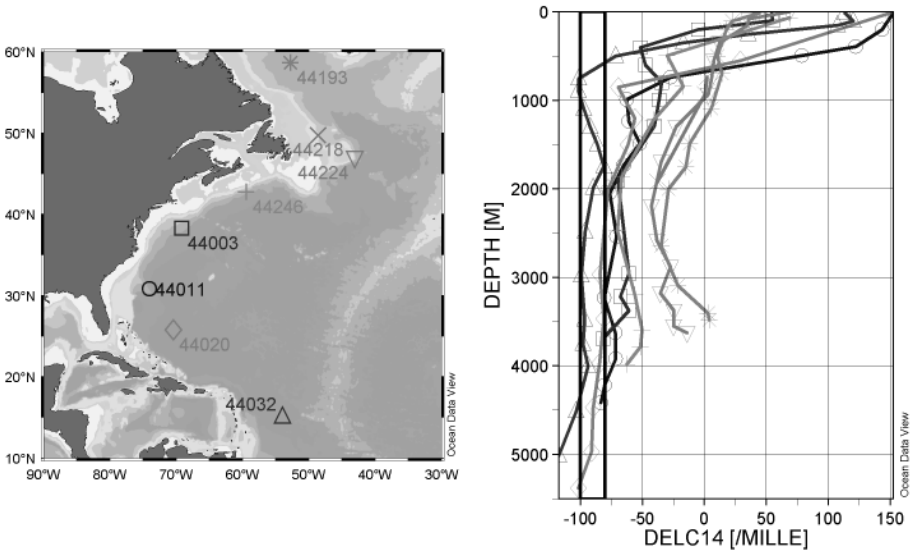

Fig. 6.7: Selected TTNA survey results. Left panel, station locations. Right panel, corresponding profiles of seawater $\Delta^{14}C$. Labrador Sea water samples are younger (higher $\Delta^{14}C$) than more southerly waters. Black rectangle outlines the variability (± 1 sd) measured in the calcite fraction of *P. resedaeformis*.

Advection of WSW vs. LSW may also be important to the $\Delta^{14}C$ composition of slopewater. LSW would be expected to have a $\Delta^{14}C$ composition similar to that of the Labrador Sea (-65 ‰; Stuiver and Ostlund, 1980), where it originates. The water mass characteristics of WSW are largely derived from sub-surface Gulf Stream waters through isopycnal advection and warm core rings and streamers (Csanady and Hamilton, 1988). The water mass underlying the Gulf Stream is sometimes identified as Antarctic Intermediate Water (AAIW), based on nutrient and salinity characteristics (Richardson, 1977; Atkinson, 1983; Csanady and Hamilton, 1988). Mixing with AAIW may impart a more negative $\Delta^{14}C$ signature to WSW, as previously suggested by Tanaka et al. (1990). If this is the case, then the quasi-decadal periodicity in the *P. resedaeformis* profile (Fig.

6.6) may reflect the quasi-decadal periodicity inherent to the interactions of WSW and LSW (Petrie and Drinkwater, 1993; Marsh, 2000; Loder, 2001). Longer records of $\Delta^{14}C$ from older colonies, or patched together from several colonies, could potentially be used to infer past variations in the slopewater system off the Scotia-Maine region. However, further study is needed to assess the extent to which AAIW would be diluted by mixing with WSW.

Variations in $\Delta^{14}C$ composition of LSW itself may also be important to the $\Delta^{14}C$ record in *P. resedaeformis*. Analysis of pre-1950 aged mollusc shows that ^{14}C reservoir ages of Arctic coastal waters can be as old as 800 years (Mangerud and Gulliksen, 1975; Barber et al., 1999). Ice-cover limits the equilibration of surface water with the atmosphere and may explain some of these results. As Arctic waters partly feed LSW, the LSW may be more $\Delta^{14}C$ depleted than would otherwise be expected. If this is the case, then the more negative values in the *P. resedaeformis* record may reflect the presence of LSW rather than WSW.

With such a dynamic oceanographic environment as the Scotia-Maine margin, it is difficult to state unequivocally which process is the most important in determining $\Delta^{14}C$ in *P. resedaeformis*. Nevertheless, the methods presented here can be expanded to other types of octocorals and other locations to provide proxy data where oceanographic data are lacking. The $\Delta^{14}C$ data could also be paired with additional analysis of more conservative water mass tracers (such as $\delta^{18}O$) to provide additional information on water mass circulation.

6.6 CONCLUSIONS

Obviously, the formation of growth hiatuses is an undesirable trait in a proxy environmental recorder. Our dating results suggest that these hiatuses may last decades. Fortunately, these events leave a visible band in the skeleton and are therefore easy to detect. At the very least, growth hiatuses may be useful as stratigraphic horizons, as we have demonstrated here.

In 3 different, independently dated colonies, the pulse of anthropogenic Pb to the oceans was accurately recorded in skeletal calcite. This suggests that skeletal Pb/Ca may be a reliable recorder of ambient Pb concentrations at depth, and may have further paleoceanographic applications in tracking oceanic circulation or upwelling. Given the well-documented increase and phase-out of anthropogenic Pb, we propose that Pb/Ca profiles may be used as an inexpensive, although somewhat less precise analogue to the bomb-^{14}C dating method in deep-sea coral skeletons.

A time-series record of $\Delta^{14}C$, spanning 1895-1965, was generated from the calcite fraction of one of the colonies. The record oscillated on a quasi-decadal scale, between -105 and -70 ‰. These values are interpreted to directly reflect the $\Delta^{14}C$ of upper intermediate waters; however, it is unclear which oceanographic process could have led to the more negative range of values.

ACKNOWLEDGEMENTS

We are gratefully indebted to Derek Jones, Sanford Atwood and the Captain and crew of the CGS *Martha Black* for collecting specimens. Radiocarbon analyses were performed by Thomas Guilderson at LLNL. Kurt Kyser and Don Chipley kindly provided time on the Queens LA-ICP-MS. Brian Petrie and Kumiko Azetsu-Scott offered valuable comments on the physical oceanography. This project was supported by an NSERC strategic grant to MJR and DBS and an NSERC postgraduate scholarship to OAS.

CHAPTER 7

STABLE C AND N ISOTOPIC RECORDS FROM DEEP-SEA OCTOCORALS PARALLEL RECENT CHANGES IN THE SLOPEWATER SYSTEM OFF NOVA SCOTIA

Owen A. Sherwood [1], Moritz Lehmann [2], Kumiko Azetsu-Scott [3],

David Scott [1], Michael Risk [4]

[1] Centre for Environmental and Marine Geology, Dalhousie University, Halifax, Canada

[2] GEOTOP-UQAM-McGill, Montreal, Canada

[3] Bedford Institute of Oceanography, Halifax, Canada

[4] School of Geography and Geology, McMaster University, Hamilton, Canada

7.1 ABSTRACT

The slope waters off Nova Scotia are characterized by modal shifts in the dominance of Labrador Current-derived waters and warm Gulf Stream-derived waters. Observational records show that warm source waters have become increasingly dominant over the last 50 years. Coincident with these changes, a trophic cascade on the Scotian shelf was initiated around 1990 by the overfishing of groundfish. Stable C and N isotopic records from the skeletons of *Primnoa* corals, a proxy for surface water processes, reflect many of these changes. This coral secretes an annually-banded, two-part skeleton of calcite and gorgonin, the latter being a stable protein. The gorgonin is derived from sinking POM, and thus is well suited to studying processes occurring in the euphotic zone over extended time periods. The annual rings of 9 colonies were isolated and analyzed for $\delta^{13}C$ and $\delta^{15}N$ to produce a set of overlapping records covering most of period 1700-2000 AD. An additional record from ~300-800 AD was obtained from a sub-fossil sample. Values of $\delta^{15}N$ were persistently higher most of the last ~2000 years, but declined significantly in the 20th century, with most of the decline coinciding with the observed shift to warmer conditions. While the exact mechanism for the isotopic variability in *Primnoa* remains unclear, results suggest a recent weakening of the Labrador Current may signal a return to mid-Holocene hypsithermal-like conditions.

7.2 INTRODUCTION

Recent studies have emphasized modal shifts in the slopewater region extending from the Mid-Atlantic Bight to the Grand Banks (Petrie and Drinkwater, 1993; Pickart et al., 1999; Loder et al., 2001). During positive modes of this slopewater system, Warm Slope Water (WSW) derived, in part, from the Gulf Stream and Gulf Stream rings, resides southward of the shelf break. During negative states cold/fresh Labrador Slope Water (LSW) advances westward from the Grand Banks, displacing WSW further to the south. The North Atlantic Oscillation (NAO) is thought to have a significant influence on the slopewater system, such that negative NAO anomalies tend to correlate with increased transport of the Labrador Current around the tail of the Grand Banks (Petrie and Drinkwater, 1993). As slopewaters flow onto the shelves via submarine canyons, the relative proportion of WSW vs. LSW has a major influence on shelf hydrography. A widespread cold event on the Scotian shelf and Gulf of Maine associated with negative NAO anomalies persisted through much of the 1960s and again in 1998 (Petrie and Drinkwater, 1993; MERCINA, 2001; Drinkwater et al., 2003; Greene and Pershing, 2003).

Shelf hydrographic conditions relating to the relative dominance of WSW vs. LSW have a major influence on the marine foodweb. Continuous plankton recorder (CPR; MERCINA, 2001) and remote sensing (Thomas et al., 2003) data suggest that warm (cold) states of the slopewater system support higher abundances of phytoplankton. This may be driven by differences in the nutrient composition of the slopewaters, with LSW being relatively nutrient-poor (Petrie and Yeats, 1993; Drinkwater et al., 2003;

Thomas et al., 2003); this reflects a broader pattern of nutrient depletion in the Labrador Sea, relative to the central North Atlantic (Townsend, et al. 2006). Other studies in the Gulf of Maine document positive correlations between NAO, temperature and abundance of *Calanus finmarchicus* (Greene and Pershing, 2000; Conversi et al., 2001; MERCINA 2001). It is not clear, however, whether *Calanus* populations respond directly to changes in primary productivity brought on by the nutrient composition of slopewaters, or to some other mechanism, such as cross-shelf advection (Greene and Pershing, 2000).

Despite the Scotia-Maine region being one of the most intensely surveyed oceanographic realms on earth, routine hydrographic surveys extend back to only about the 1950s. On the other hand, much of the hydrographic variability associated with the NAO occurs over multi-decadal timescales. In addition, the shelf ecosystem has been seriously altered by the well-documented collapse of the ground fishery in the early 1990s (Choi et al., 2004; Bundy, 2005; Frank et al., 2005), which could have modified or obscured any climate-ecosystem interaction over the past few decades. For example, at the base of the food web, Sameoto (2001) documented a decrease in the abundance of large copepods, and an increase in the abundances of smaller copepods and phytoplankton between the periods 1961-1974 and 1991-1998. He discussed several environmental variables that could have led to the changes. More recently, Frank et al. (2005) suggested that changes in the relative abundances of phytoplankton and zooplankton are consistent with a trophic cascade initiated with the removal of demersal piscivores. Clearly, longer-term data from proxy records would allow for a better

understanding of the relative influence of top-down versus bottom-up controls on ecosystem dynamics, as well as on the nature of the slopewater system itself.

Unfortunately, sedimentary core records from this region are notoriously bioturbated, and the effective temporal resolution, despite the relatively high sedimentation rates in shelf basins, is on the order of centuries (Levac, 2001). Previous work on Scotian Shelf cores suggested that a major cooling associated with the incursion of Labrador source waters took place around 2500 years ago (Scott et al., 1984; 1989; Levac, 2001). Further work by Keigwin et al. (2003) suggested that a return to warmer conditions occurred within the last ~150 years. To summarize the present understanding of the slopewater system: in context of the instrumental records, the 1960s were an unusually cold decade; in the context of core records, the 1960s were the vestige of a prolonged 2500 year long cold period.

The deep-sea coral *Primnoa resedaeformis,* one of the dominant gorgonian species along the edge of the Scotian shelf, may be an important new source of proxy climate data (Sherwood et al., 2005a; 2005b). This paper focuses on stable isotopic records from the annually banded horny region of *Primnoa* skeletons. Unlike the calcite, which is derived from dissolved inorganic carbon at depth, the gorgonin is derived from sinking POM and may thus provide annually-resolved records of processes occurring near the base of the food web (Sherwood et al., 2005b). Here, we document similarities in the temporal trends of $\delta^{13}C$ and $\delta^{15}N$, with that of NAO, temperature/salinity and

Calanus abundance over the last 50 years. Over the longer term interval ~300 to 1950 AD, values of $\delta^{15}N$ were consistently higher. Possible causes for this trend are evaluated.

7.3 MATERIALS AND METHODS

7.3.1 Coral collection and processing

Specimens of *P. resedaeformis* were collected from the Northeast Channel (Fig. 7.1) at depths of between 250-475m. This study incorporates data from the five colonies presented earlier (Sherwood et al., 2005b; complete sampling details provided therein), with new data from 3 "recent" (last 100 years), and 5 "subfossil" (~AD 300 - AD 1900) colonies (Table 7.1). Briefly, sections were cut from the colony trunks. The annual gorgonin rings were isolated by dissolving sections in 5% HCl. Stable isotopic analyses of gorgonin were performed by Elemental Analyzer/ Continuous Flow Isotope Ratio Mass Spectrometry at GEOTOP-UQAM-McGill. Isotope ratios are reported in conventional delta notation, where (example for carbon): $\delta^{13}C = [(R_{sample}/R_{standard}) - 1] \times 1000$; and $R = {}^{13}C/{}^{12}C$. Standards used were PDB ($\delta^{13}C$) and air ($\delta^{15}N$). Analytical error, as measured by the standard deviation of duplicate measurements, averaged 0.10 ‰ for $\delta^{13}C$ and $\delta^{15}N$. Where multiple sections per colony were analyzed, the time-series records were averaged for the whole colony. In addition to stable isotopic analyses, some of the gorgonin samples were sent to the Centre for Accelerator Mass Spectrometry for analysis of ^{14}C. Radiocarbon analytical details are provided in Sherwood et al. (2005a).

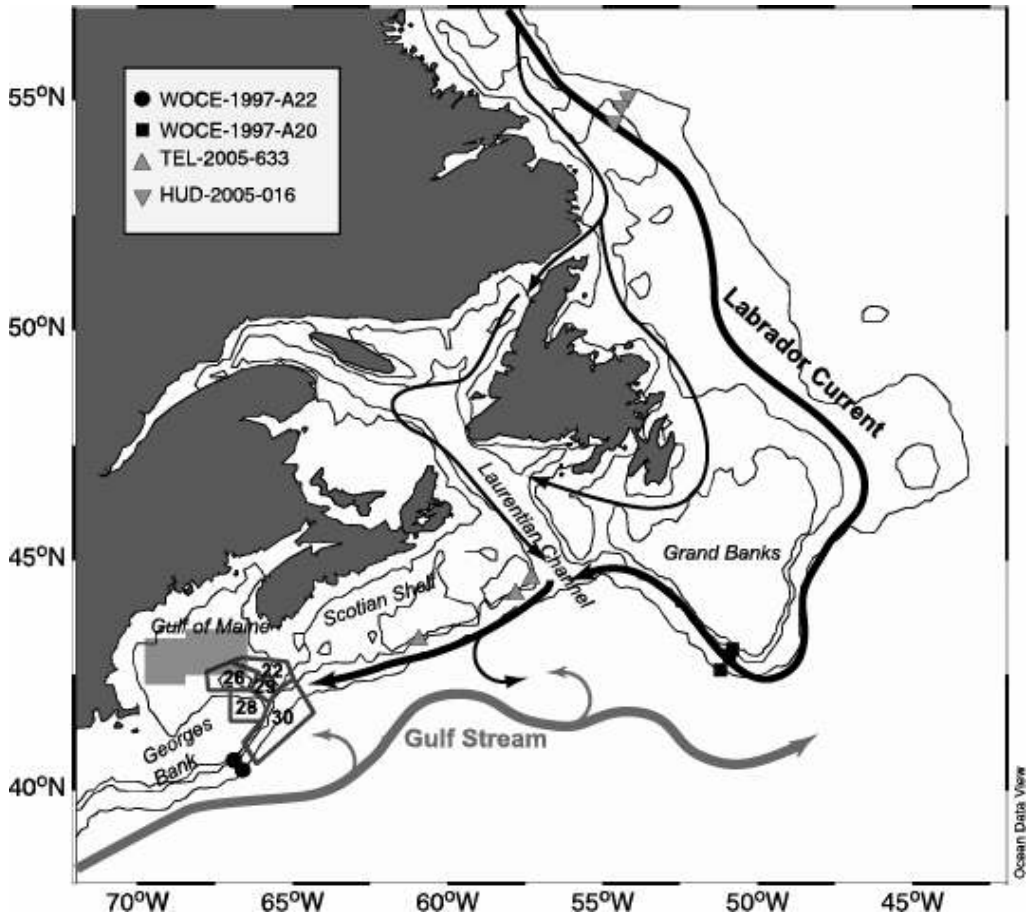

Fig. 7.1: Map of the NW Atlantic showing major current patterns and locations of data used in this study. Black polygons are the areas of hydrographic observations; coral samples were collected from the Northeast Channel, Area SS29. Shaded polygon is the area of CPR observations. Symbols are the locations of selected hydrographic stations discussed in text.

Table 7.1: Summary of dating and isotopic data averaged by coral colony. Age ranges reflect the sums of dating errors (2σ) and colony age spans.

Coral I.D.	Dating method	Age ± ½ range (yrs AD)	$\delta^{13}C \pm sd$ (‰)	$\delta^{15}N \pm sd$ (‰)	N
Fossil-95	^{14}C	480 ± 450	-18.00 ± 0.43	10.93 ± 0.35	39
COHPS2001-1	^{14}C	1800 ± 130	-17.82 ± 0.39	10.91 ± 0.50	15
COHPS2001-2	^{14}C	1830 ± 130	-18.34 ± 0.42	10.75 ± 0.47	37
ROPOS-6400016	^{14}C	1860 ± 140	-17.88 ± 0.46	10.84 ± 0.44	50
DFO2002-con5	Ring counting/bomb-^{14}C	1958 ± 39	-19.05 ± 0.53	10.31 ± 0.37	56
NED2002-371A	Ring counting/bomb-^{14}C	1966 ± 34	-19.20 ± 0.64	10.30 ± 0.45	53
ROPOS-639009	Ring counting/bomb-^{14}C	1973 ± 20	-19.12 ± 0.50	9.99 ± 0.43	24
HUD2001-055-VG15	Ring counting/bomb-^{14}C	1977 ± 20	-18.89 ± 0.60	10.22 ± 0.40	35
ROPOS-6400013	Ring counting/bomb-^{14}C	1989 ± 15	-19.54 ± 0.40	10.20 ± 0.33	26
HUD2000-20-VG2	Ring counting/bomb-^{14}C	1994 ± 8	-19.38 ± 0.28	9.70 ± 0.29	12

7.3.2 Chronology

In most cases, each isotopic analysis was performed on an individual annual ring. Conversion of ring number to calendar year followed 1 of 2 methods (Table 7.1). For recent colonies, calendar years were established as the average of growth ring counts performed by 3 amateur counters, with validation by the bomb-^{14}C method (Sherwood et al., 2005a). For the sub-fossil colonies, one or two of the rings were radiocarbon dated as a tie-in point. Calibration was performed with CALIB software (Stuiver and Reimer, 1993, version 5), using the Marine 04 calibration (Hughen et al., 2004) and a local correction for the marine reservoir effect ($\Delta R = 128 \pm 35$ years; Sherwood et al., 2006). Calibrated ^{14}C dates were calculated as probability-weighted means ± 2σ ranges. Three of the sub-fossil colonies had mean calibrated dates of 1750-1860; corresponding errors of

up to ±120 years reflect a plateau in the radiocarbon calibration between ~1650-1950 AD.

7.3.3 Hydrographic data

The Northeast Channel is a region of extreme currents. Both the shallow and deep currents tend to be directed into the Gulf of Maine on the east side of the channel, and out of the Gulf on the west side (Smith et al., 2001). Selection of hydrographic data for comparison to the isotope records was guided by the likelihood that food sources for *Primnoa* do not necessarily originate within the Northeast Channel, but in surrounding regions as well. Data from 5 pre-defined regions surrounding and including the Northeast Channel (Fig. 7.1) were retrieved from the Bedford Institute of Oceanography hydrographic database (available online at http://www.mar.dfo-mpo.gc.ca/science/ocean.database/data_query.html). Temperature and salinity data were retrieved from 15 ± 15m and 200 ± 50m. The first interval was chosen to reflect high frequency variability associated with atmospheric phenomena, and the second to reflect low frequency variability associated with modal shifts in the slopewater system (Petrie and Drinkwater, 1993). For each region, monthly anomalies of temperature and salinity were computed by subtracting climatological monthly means for the period 1971-2000 from each monthly observation. Annual anomalies were calculated as the mean of the monthly anomalies for each year. Data gaps were filled using linear interpolation. Empirical orthogonal function (EOF) analysis was used to identify the dominant modes of variability among the different regions. In all cases, the leading mode explained between 60-75 % of the total variance. Regional indices of temperature and salinity were

computed as a weighted average, with the records from each region weighted by their respective mode 1 eigenvector weightings. A regional stratification index was computed in a similar manner using differences in density between 0 ± 5m and 50 ± 5m (Drinkwater et al., 2003), however, a leading mode could not be identified.

7.3.4 Nutrient data

Northeast Channel nutrient data were obtained from D. Townsend's "Nut-phyto" dataset, which was acquired in the springtime of 1997-1999 as part of the GLOBEC Georges Bank program (http://globec.whoi.edu/jg/dir/globec/gb/). Stations located within the Northeast Channel were selected and nutrient distributions were plotted with Ocean Data View (ODV) software (Schlitzer, 2004). To evaluate the effect of springtime nutrient drawdown on $\delta^{15}N$ of phytoplankton, monthly values of vertically integrated nitrate and nitrite (NO_3+NO_2) at 50m depth were calculated, using, where necessary, a polynomial fit of integrated NO_3+NO_2 vs. depth.

Additional data on the carbon dioxide ($[CO_2]_{aq}$) and isotopic ($\delta^{13}C$) content of warm and cold slopewaters was obtained from the Global Ocean Data Analysis Project (GLODAP; Key et al., 2004). A subset of these data was collected during World Ocean Circulation Experiment (WOCE) meridional transects of the NW Atlantic. Cruise A20 (~52^{o}W) sampled cold slopewater south of the Grand Banks. Cruise A22 (~66^{o}W) sampled warm slopewater south of Georges Bank (Fig. 7.1).

In May-June 2005 water samples for measurement of the $\delta^{15}N$ of nitrate ($\delta^{15}N_{NO3}$) were collected opportunistically during routine hydrographic surveys conducted by the Bedford Institute of Oceanography. Samples were collected from the upper slope regions (Fig. 7.1) of 1) the Labrador Shelf (54.8°N / 54.5°W) and 2) the Scotian Shelf, south of Banquereau Bank (44.5°N / 57.5°W) and Emerald Bank (43.3°N / 61.1°W). Water was sampled with the CTD rosette every 50m between 0 - 400m (or deepest). Sub-samples were collected into pre-washed (5% HCl and deionized water) 60 ml polyethylene bottles and frozen immediately upon collection. Measurement of $\delta^{15}N_{NO3}$ followed the bacterial denitrifier method (Sigman et al., 2001). Briefly, sample nitrate is converted to nitrous oxide (N_2O) by denitrifying bacteria that lack N_2O reductase activity. Isotopic analysis was then performed on the N_2O gas by Continuous Flow Isotope Ratio Mass Spectrometry at GEOTOP-UQAM-McGill.

7.3.5 Statistical analysis

To investigate potential sources of isotopic variability, linear correlations of the *Primnoa* $\delta^{13}C$ and $\delta^{15}N$ records with the various hydrographic and climatic records were performed. The latter data include the winter North Atlantic Oscillation Index (Hurrell et al., 2001) and an index of Continuous Plankton Recorder *Calanus* abundance in the central Gulf of Maine (MERCINA, 2001) which we assume to be broadly representative of productivity for the region including the Northeast Channel. Most of the timeseries were significantly autocorrelated at 1-2 year lags, which could lead to spurious correlations between timeseries when one is naturally lagged with respect to the other. In addition, for the isotope timeseries we estimate a chronological uncertainty of ~2 years.

Although there are methods to deal with the problems of both autocorrelation (Pyper and Peterman, 1998) and chronological error (Worm and Myers, 2003), we have taken a simpler approach by binning the timeseries into appropriate size bins (3 years). The statistical test is more conservative owing to one third fewer degrees of freedom. We also reason that binning averages out the chronological error while preserving low frequency variability, which is our main interest.

7.4 RESULTS

7.4.1 Long term trends

To avoid misrepresenting temporal relationships among the imprecisely dated 1750-1900 AD colonies, colony averages were plotted instead of the complete time-series records (Fig. 7.2). For most of the near 2000 yr long record, $\delta^{13}C$ and $\delta^{15}N$ were relatively constant. Then, in the 20^{th} century, both $\delta^{13}C$ and $\delta^{15}N$ decreased markedly. The decline in $\delta^{13}C$ parallels the Suess effect, i.e. the decrease in atmospheric $\delta^{13}C$ caused by the burning of fossil fuels. Based on proxy records (Bohm et al., 2002; Swart et al., 2002) and direct measurements (Kortzinger and Quay, 2003) the $\delta^{13}C$ perturbation in upper North Atlantic waters is lagged by roughly a decade relative to the atmosphere. A reference $\delta^{13}C$ curve, derived from Antarctic ice cores (Francey et al., 1999) is therefore plotted with a 10-year lag in Fig. 7.2. Taking into account the Suess effect, there was little apparent difference in modern vs. subfossil values of $\delta^{13}C$. In contrast to $\delta^{13}C$, there is no atmospheric effect on $\delta^{15}N$ of seawater. Therefore, we interpret the $\delta^{15}N$ record as a significant decline of about 1 ‰.

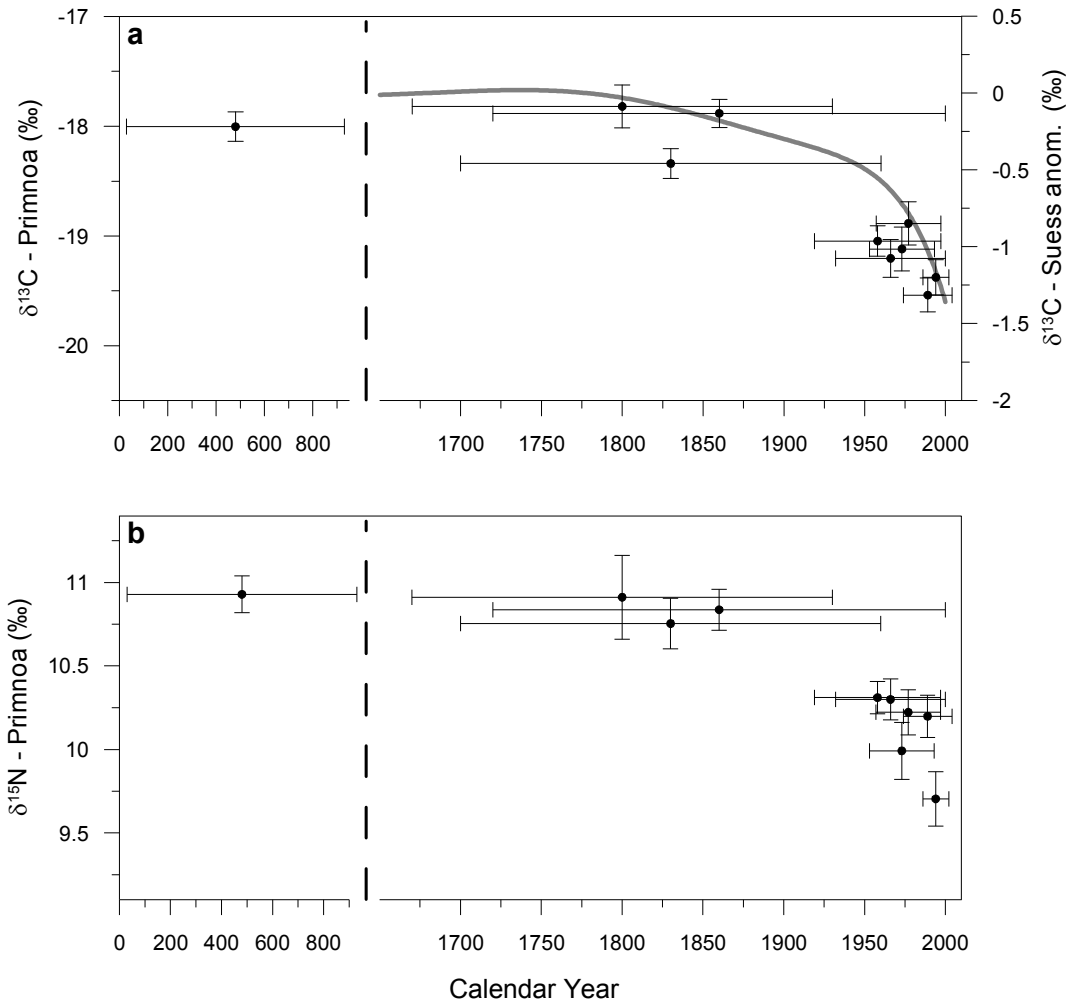

Fig 7.2: Long-term trends in $\delta^{13}C$ (a) and $\delta^{15}N$ (b) averaged by coral colony. Horizontal error bars are 2σ min-max ages. Vertical error bars are 95 % confidence limits. Grey curve in (a) is the Suess anomaly for the North Atlantic, derived from a polynomial smoothing of the atmospheric record (Francey et al., 1999) and lagged by 10 years to reflect North Atlantic surface water response (see text for rationale).

7.4.2 Recent trends

Isotopic records from the 6 recent colonies are shown in Fig. 7.3. The overlapping records showed excellent reproducibility for $\delta^{13}C$. A mean $\delta^{13}C$ curve, taken as the mean of all measurements in each year, exhibited a weak but statistically significant decline (linear regression: $r^2 = 0.09$; $p < .01$). After normalizing the mean $\delta^{13}C$ record for the Suess anomaly, the decline was no longer significant ($r^2 = 0.00$, $p = 0.6$). For $\delta^{15}N$ the reproducibility was somewhat poorer, but a decreasing trend was significant ($r^2 = 0.74$, $p<.000$). Values of $\delta^{15}N$ towards the earlier part of the 1900s were similar to those of the sub-fossil colonies (~10.7 ‰). The major decline occurred around 1980, with a shift to values of around 9.7 ‰.

7.4.3 Correlation with environmental records

Records of selected environmental variables and $\delta^{13}C$ and $\delta^{15}N$ are compared in Fig. 7.4. The first 3 records (winter NAO index, T-200m and *Calanus* abundance) are reproduced from MERCINA (2001), but with T-200m recalculated for the vicinity of the Northeast Channel. Persistent negative (positive) anomalies characterized the environmental records for most of the period before (after) 1971. A major drop in the NAO index in 1996 also was also related to negative temperature and *Calanus* anomalies in 1998. The $\delta^{13}C$ and $\delta^{15}N$ anomalies exhibited the reverse trends, with more positive (negative) values before (after) the early 1970s. The isotopic records did not register positive values around 1998; however, short-term events of <2 years are smoothed out by averaging and chronological error.

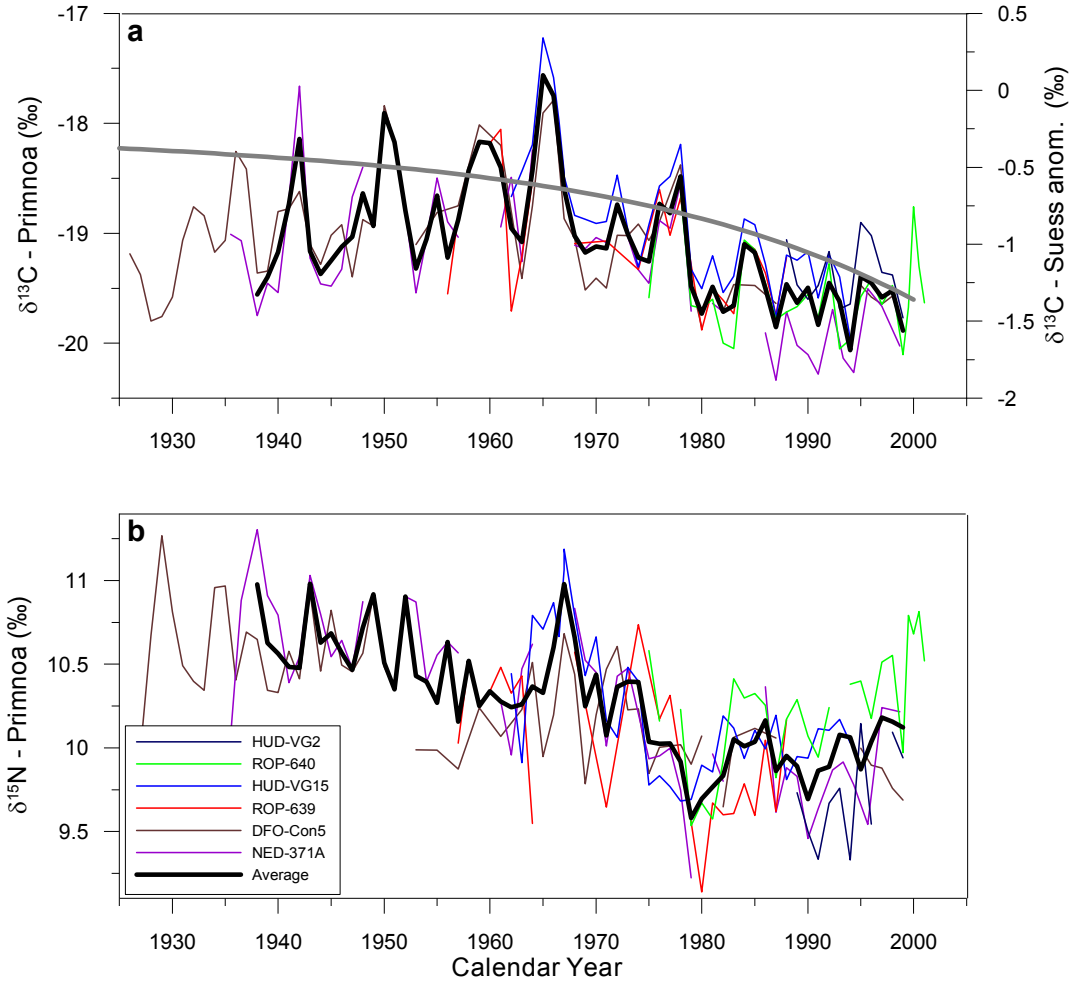

Fig 7.3: Isotopic records from 6 recent colonies. Analytical error ~ ± 0.1‰. Estimated dating error ~ ± 2 years. Grey curve in (a) is the Suess anomaly

A correlation matrix of all environmental and isotopic records is shown in Fig. 7.5. The environmental data are mutually correlated, the general interpretation being that negative NAO phases lead to an increase in the westward transport of the Labrador Current, bringing cold and fresh LSW into the Scotia-Maine region (Petrie and Drinkwater, 1993). Being low in nutrients (Petrie and Yeats, 1999) the LSW supports

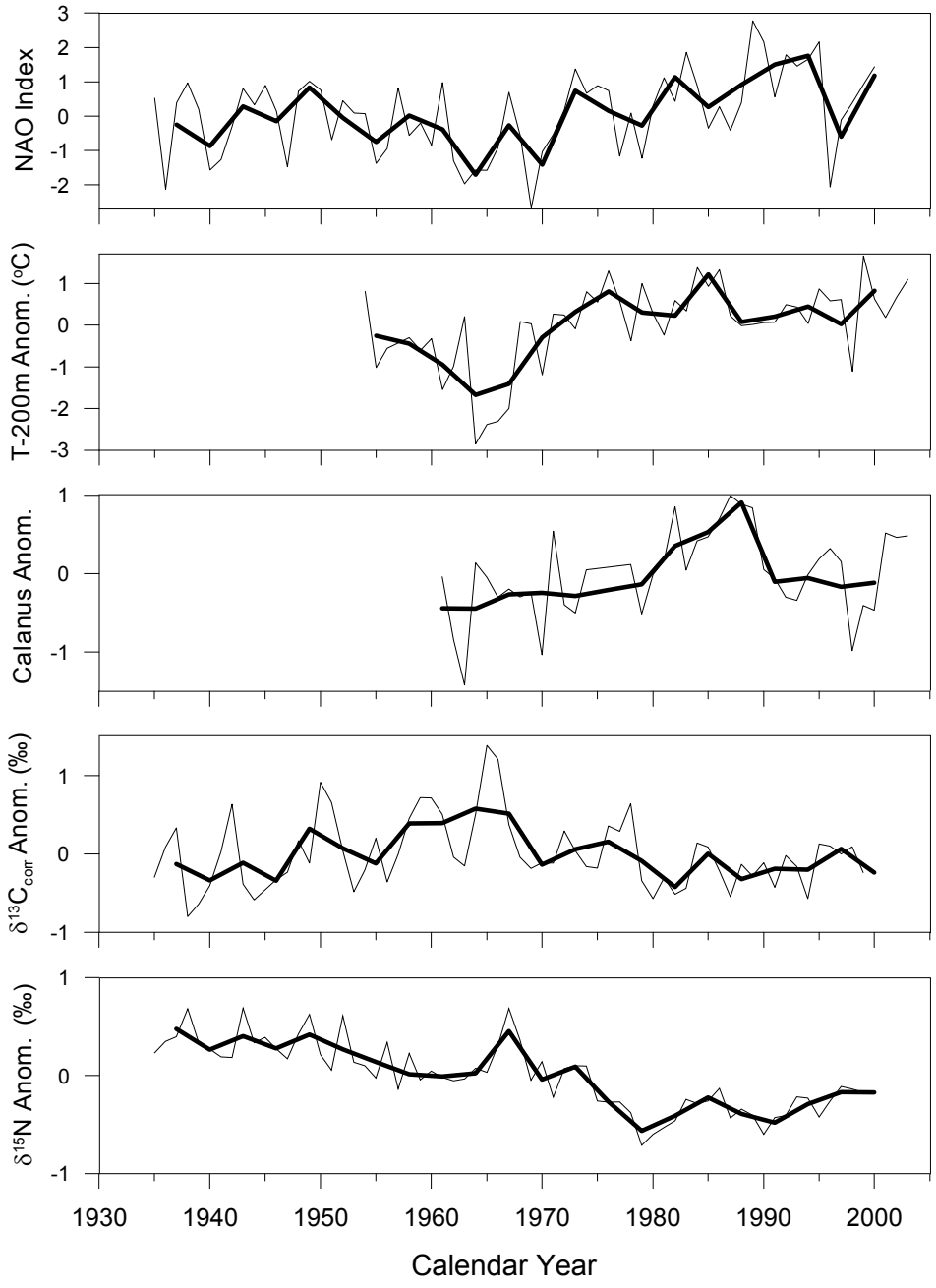

Fig 7.4: Timeseries anomalies of the winter (DJFM) NAO, regional temperature at 200m depth, *Calanus* abundance (MERCINA 2001), and average $\delta^{13}C$ and $\delta^{15}N$ records from *Primnoa*. $\delta^{13}C$ record corrected for the Suess effect. Thin lines are annual averages, bold lines are 3 yr decimations

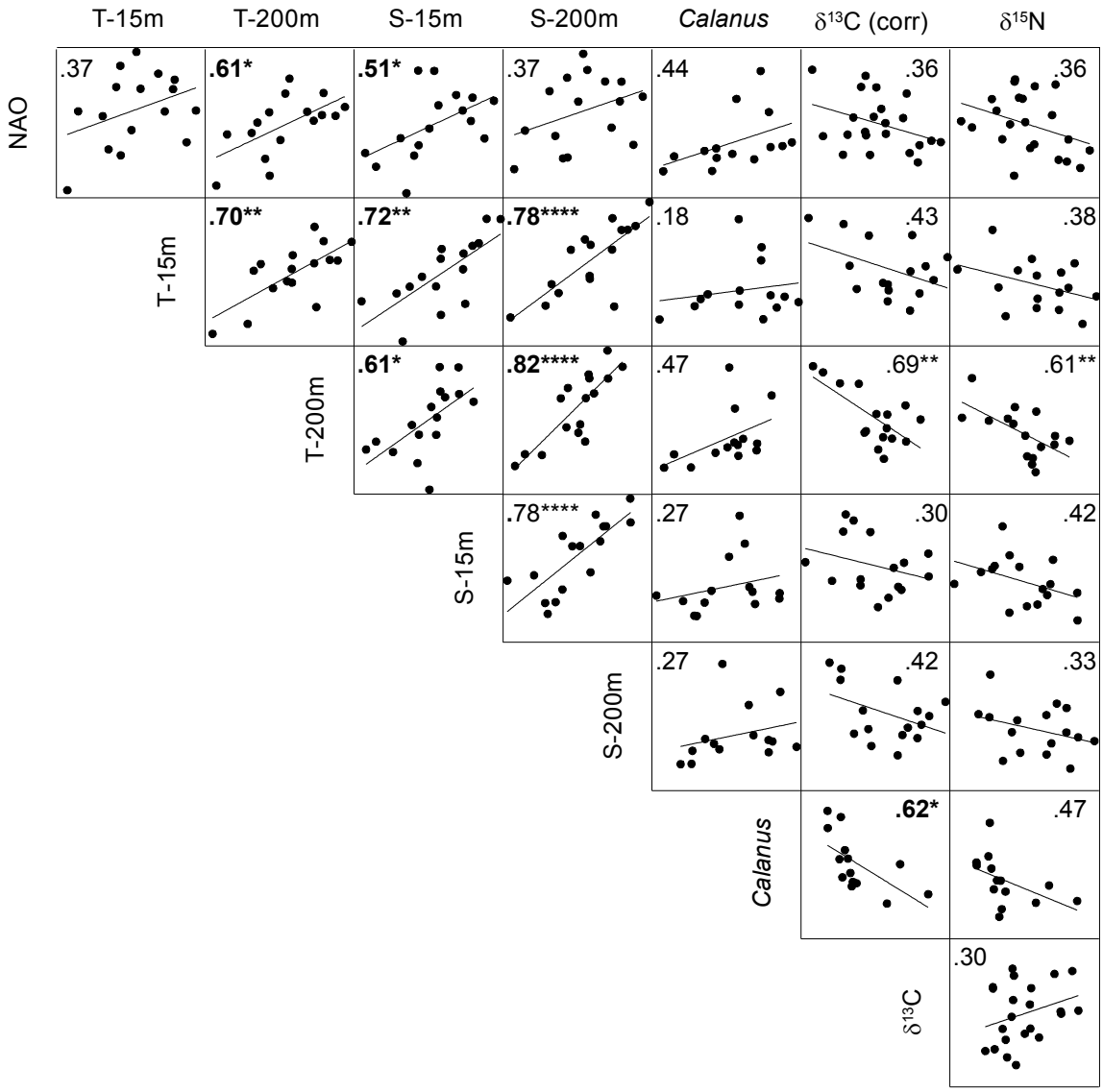

Fig 7.5: Correlation matrix of anomalies of environmental variables and *Primnoa* $\delta^{13}C$ (corrected for Suess effect) and $\delta^{15}N$. Records were decimated into 3 year bins before correlation. Numbers in boxes are Spearman's rank r, with significant correlations in bold. Significance levels are: * 0.05, ** 0.01, *** 0.001, ****.0001

reduced productivity of phytoplankton (Thomas et al., 2003) and possibly also *Calanus* (MERCINA, 2001). Note the positive correlations between shallow (15±15m) and deep (200±50m) temperature and salinity. These data suggest that both Labrador Slope Water (LSW), concentrated >150 m in depth, and Labrador Shelf Water (LShW), concentrated < 150 m in depth (Houghton and Fairbanks, 2001) are associated with westward advances of the Labrador Current. The $\delta^{13}C$ and $\delta^{15}N$ records, overall, were anticorrelated with the environmental records. For $\delta^{13}C$ there were significant anticorrelations with T-200m and *Calanus* abundance. For $\delta^{15}N$, there was a significant anticorrelation with T-200m. Finally, $\delta^{13}C$ and $\delta^{15}N$ were positively correlated, but the correlation was not significant.

7.4.4 Northeast Channel nutrient distribution

Fig. 7.6 shows the distribution of temperature, salinity, nutrients and chlorophyll in the Northeast Channel (area SS29 in the BIO database) for the period 1997-1999. Conditions in 1997/1999 versus those of 1998 represent warm and cold states, respectively of the slopewater system (Greene and Pershing, 2003; Drinkwater et al., 2003). Using the T-S classification of Houghton and Fairbanks (2001), the cold/fresh waters in 1998 represent LShW from 50-150m and LSW > 150m. Reduced concentrations of nutrients and chlorophyll characterize 1998, as previously observed (Petrie and Yeats, 1999; MERCINA, 2001; Thomas et al., 2003).

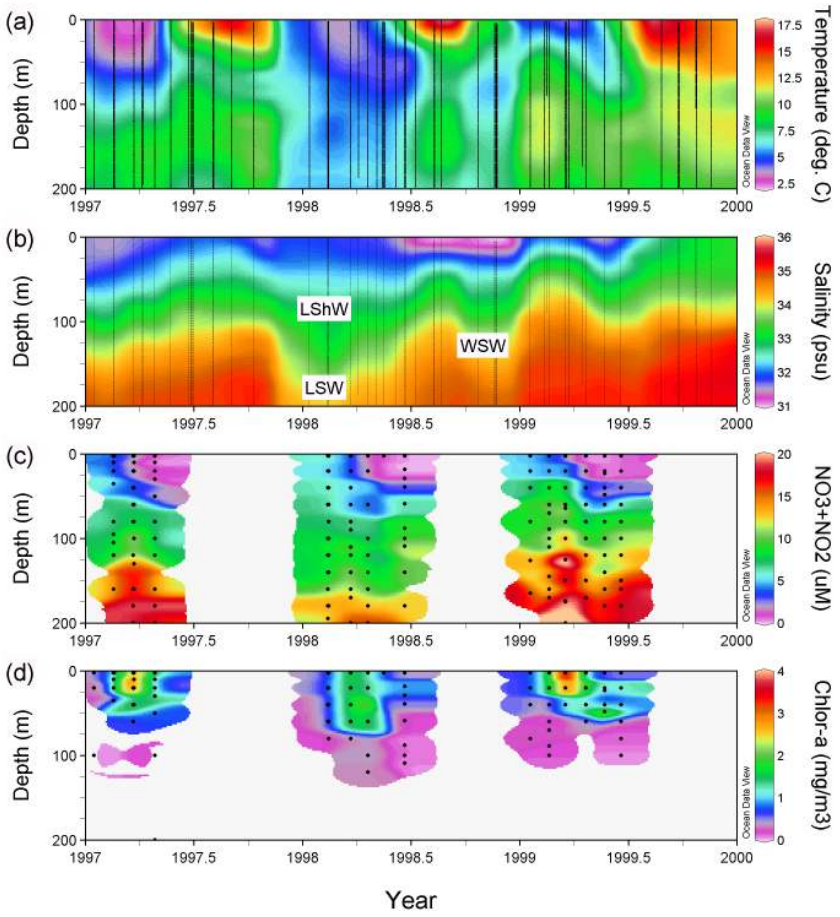

Fig 7.6: Depth-Time patterns in temperature (a), salinity (b), NO_3+NO_2 (c) and Chlorophyll-a (d) for the Northeast Channel (region 29). Nutrient and chlorophyll data from D. Towsend. Note cold/fresh event in 1998, coincident with lower nutrients and chlorophyll.

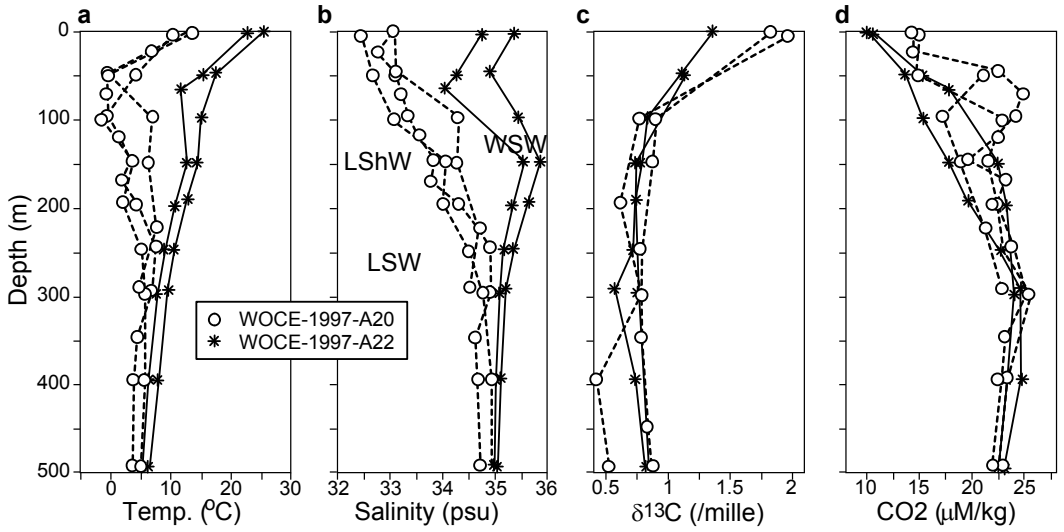

Fig. 7.7: Depth profiles of (a) temperature, (b) salinity, (c) $\delta^{13}C$ and (d) $[CO_2]_{aq}$ from WOCE cruises A20 (south of Grand Banks) and A22 (south of Georges Banks). See Fig. 7.1 for locations of stations. Note cold/fresh waters off Grand Banks, and warmer/saltier waters off Georges Bank.

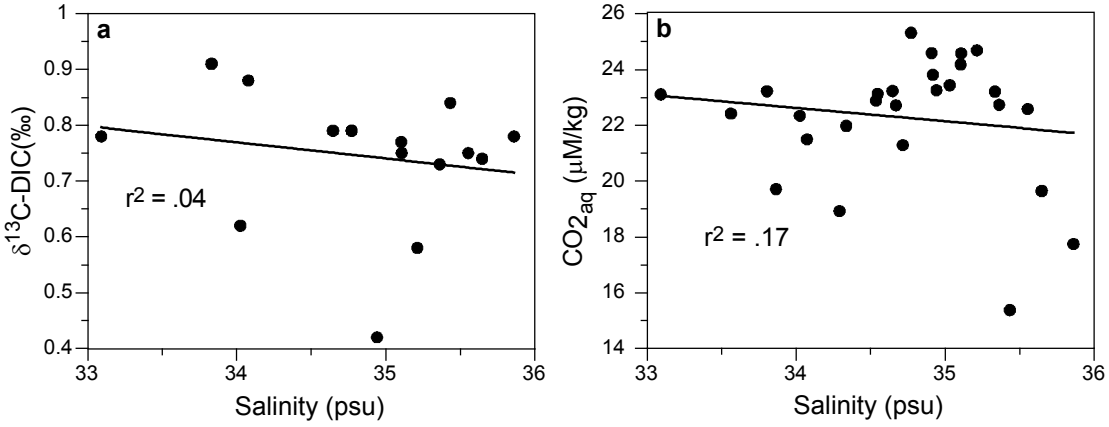

Fig. 7.8: Regressions of (a) $\delta^{13}C$ of seawater and (b) CO_{2aq} against salinity using the WOCE data from Fig. 7.7. Data from upper 100 m excluded. Neither regression is significant.

7.4.5 Isotopic composition of source nutrients

δ^{13}C-DIC:

WOCE cruises A20 (south of Grand Banks) and A22 (south of Georges Bank; Fig. 7.1) were the only available sources of slopewater $\delta^{13}C$ data. Temperature and salinity profiles (Fig. 7.7 a,b) from slopewater stations (i.e. bottom depth < 2500m) clearly show the cold/fresh LSW and LShW off Grand Banks, and warmer/saltier WSW off Georges Bank. Water mass designations follow T-S properties of Houghton and Fairbanks (2001). Profiles of $\delta^{13}C$ reveal no differences between the water masses (Fig. 7.7c). Also shown (Fig. 7.7d) are profiles of $[CO_2]_{aq}$. In the discussion that follows, $[CO_2]_{aq}$ is considered as a potential factor in determining $\delta^{13}C$ in phytoplankton. Slightly higher $[CO_2]_{aq}$ was measured in the LShW. Taking salinity as an independent, conservative delineator of LSW, LShW and WSW, however, there do not appear to be statistically significant differences in $\delta^{13}C$ or $[CO_2]_{aq}$ of the different water masses (Fig. 7.8).

δ^{15}N-NO_3:

Water samples collected opportunistically from the Labrador and Eastern Scotian shelves were measured for $\delta^{15}N_{NO3}$ (Fig. 7.1). Samples were located more towards the shelf compared with the WOCE cruises, so the 2 datasets are not exactly comparable. Nevertheless, profiles of temperature and salinity (Fig. 7.9a,b) clearly show cold/fresh LSW and LShW off the Labrador Shelf and at 1 station off Banquereau Bank, near the Laurentian Channel. The 2 other stations from further westward along the Scotian shelf were occupied by warmer/saltier WSW. As collections were made in summer, euphotic

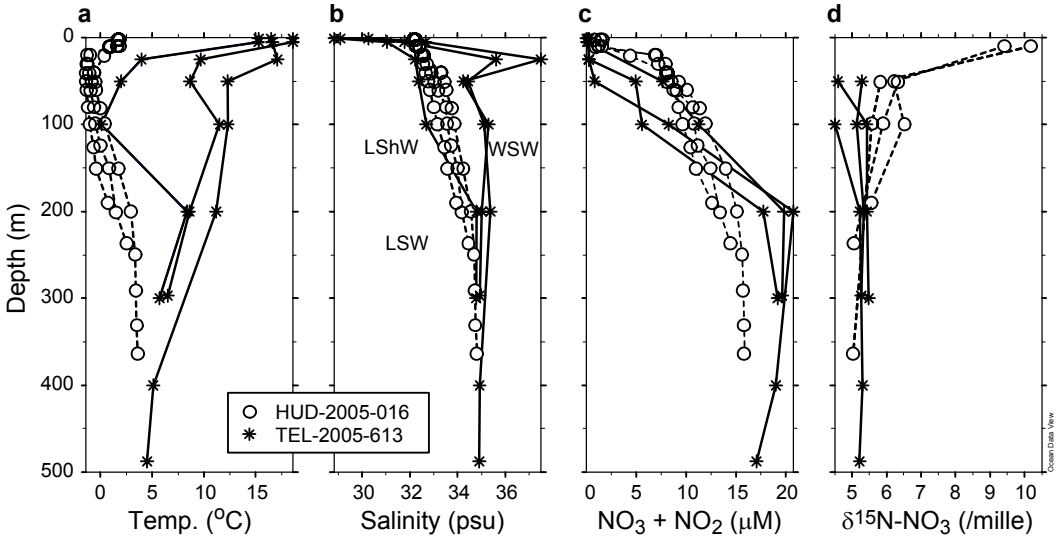

Fig. 7.9: Depth profiles of (a) temperature, (b) salinity, (c), NO_3+NO_2 and (d) $\delta^{15}N_{NO3}$ measured during the Hudson and Teleost cruises. See Fig. 7.1 for station locations. Labrador source waters were detected at one of the Teleost stations (near Banquereau Bank) and at the Hudson stations off Labrador. At all stations, NO_3+NO_2 was exhausted by the spring bloom.

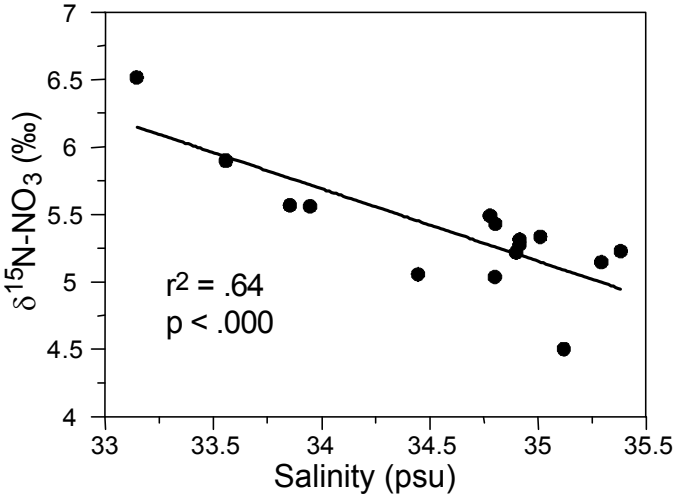

Figure 7.10: Regression of $\delta^{15}N_{NO3}$ vs. salinity using the Hudson and Teleost data from Fig. 7.9. Values from upper 100m excluded due to isotopic enrichment by phytoplankton uptake.

zone NO_3+NO_2 was exhausted by the spring bloom (Fig. 7.9c). Profiles of $\delta^{15}N_{NO3}$ were heavier along the Labrador shelf (Fig. 7.9d). The heaviest values, up to 10 ‰ in the upper 50m, reflect isotopic enrichment of residual nitrate. At Scotian Shelf stations, there was insufficient nitrate in the upper 50m to measure $\delta^{15}N_{NO3}$. The subsurface waters appear to be isotopically lighter in the Scotian Shelf samples. Below 200m, all the profiles of $\delta^{15}N_{NO3}$ converge on the global deep water mean ~5 ‰ (Sigman et al., 2000). Regression of $\delta^{15}N_{NO3}$ on salinity was negative and significant ($r^2 = 0.43$; $p < 0.01$; Fig. 7.9). The LShW appears to be the source of heavier nitrate, there being no discernable difference in the $\delta^{15}N_{NO3}$ of LSW vs. WSW. From mass balance considerations, the smaller volume of LShW, relative to LSW and WSW, would be more readily stripped of NO_3+NO_2, with corresponding increase in isotopic composition of the residual nutrient.

7.5 DISCUSSION

In the discussion that follows, we consider the possible reasons for the observed correlations of $\delta^{13}C$ and $\delta^{15}N$ with the environmental variables. For each of $\delta^{13}C$ and $\delta^{15}N$, we consider isotopic fractionations that may originate 1) among source nutrients, 2) during growth of phytoplankton, 3) during trophic transfer, or 4) during sinking of POM through the water column. Our discussion focuses on the isotopic consequences of the warm vs. cold source waters, since $\delta^{13}C$ and $\delta^{15}N$ broadly correlate with the relative dominance of these water masses over the 50 years of instrumental records.

7.5.1 Possible causes of $\delta^{13}C$ variability

$\delta^{13}C$-DIC:

Based on the WOCE data (Figs. 7.7 and 7.8), there were no significant differences in the $\delta^{13}C$ composition of warm vs. cold source waters. Assuming that $\delta^{13}C$ is conserved during transit of the Labrador Current to the Northeast Channel, differences in seawater $\delta^{13}C$ do not support the observed variability in the *Primnoa* $\delta^{13}C$ records.

Phytoplankton effects:

Isotopic fractionation during growth of phytoplankton is frustratingly complex and variable. While earlier research emphasized $[CO_2]_{aq}$ in determining phytoplankton $\delta^{13}C$ (Jasper et al., 1994; Rau, 1994) more recent studies point to growth rate, cell geometry, nutrient and light limitation and active carbon uptake (as opposed to passive diffusion) as equally, if not more, important (see reviews in Freeman et al., 2001; Laws et al., 2002). Looking again at the WOCE data, differences in $[CO2]_{aq}$ do not support the variability measured in *Primnoa*. In all likelihood, some combination of biological factors such as growth rate and species composition contributes to most, if not all, of the observed variability in the $\delta^{13}C$ records. A study on Georges Bank highlighted unusually high $\delta^{13}C$ in diatoms (Fry and Wainwright, 1991). Hence, a decline in the relative abundance of diatoms:dinoflagellates, as observed over most of the North Atlantic (Leterme et al., 2005) could potentially account for a decline in $\delta^{13}C$ since the 1960s. Likewise, a decrease in phytoplankton growth rate, perhaps associated with some combination of nutrient concentration and vertical mixing could account for the decline.

Unfortunately, it is not possible with the available data to quantitatively evaluate the relative importance of these different processes.

Trophic effects:

Trophic fractionation of $\delta^{13}C$ averages about 1 ‰ per trophic level (DeNiro and Epstein, 1978; Fry and Sherr, 1984). Based on previous studies into the diets of shallow water gorgonians (e.g.: Ribes et al., 1999), and $\delta^{15}N$ evidence (Sherwood et al., 2005b), it is possible that *Primnoa* consumes both sinking POM and zooplankton. By extension, *Primnoa* could shift between more phytoplankton-rich to more zooplankton-rich diets over time. However, assuming that the maximum prey size is limited to the diameter of polyps (4mm), the largest zooplankton in the *Primnoa* diet should be limited to mesozooplankton. The difference in apparent trophic level between mesozooplankton and sinking POM is negligible (Sherwood et al., 2005b); hence, a trophic effect should not contribute to variability in the $\delta^{13}C$ records. However, more complex plankton foodwebs, involving multiple transfers from, say, nanophytoplankton to microzooplankton to mesozooplankton, may accumulate multiple trophic fractionations and become significant (Wu et al., 1999a).

Microbial degradation:

Microbial degradation of sinking POM can exert a fractionation effect on $\delta^{13}C$ (Macko and Estep, 1984; Lehmann et al., 2002). Some sediment trap experiments document enrichment of up to 1-2 ‰ in the sinking flux (Wu et al., 1999a; Lourey et al., 2004) while others document no change with depth (Ostrom et al., 1997; Woodworth et

al., 2004). Our earlier work on $\Delta^{14}C$ and $\delta^{15}N$ in *Primnoa* indicates that refractory POM is not consumed (Sherwood et al., 2005a; 2005b). Elsewhere, in the Labrador Sea, isotopic composition of 12 different species of soft corals exhibited no depth effect between 50-1500m (Sherwood, Edinger, et al., unpubl.). Thus, soft corals exhibit a preference for "fresh" POM of higher nutritional value. On these grounds it is unlikely that interannual variability in food "freshness" could account for the $\delta^{13}C$ variability.

In summary, differences in the $\delta^{13}C$ and $[CO_2]_{aq}$ of warm vs. cold source waters do not support the observed variability in the *Primnoa* $\delta^{13}C$ records. Most of the interannual variability in *Primnoa* $\delta^{13}C$ probably arises during growth of phytoplankton in surface waters. The number of trophic intermediaries between phytoplankton and *Primnoa* may also be important on interannual timescales. The relative dominance of warm vs. cold source waters could potentially influence either of these processes, through modification of the physical (i.e. vertical mixing) or chemical (nutrients) conditions.

7.5.2 Possible causes of $\delta^{15}N$ variability

$\delta^{15}N$-NO_3:

Salinity anomalies of up to -0.9 characterize cold events associated with LSW/LShW (Fig. 7.6). Regression of $\delta^{15}N_{NO3}$ vs. salinity (Fig. 7.10) predicts corresponding increases in $\delta^{15}N_{NO3}$ of about 0.5 ‰. Additional support for differences in $\delta^{15}N_{NO3}$ between warm and cold source waters may be observed in a comparison of $\delta^{15}N$ of sediments and various invertebrate and fish species from the Gulf of Maine and Labrador shelf (Fig. 7.11). These data confirm that a systematic offset in $\delta^{15}N$ of 1.1 ‰,

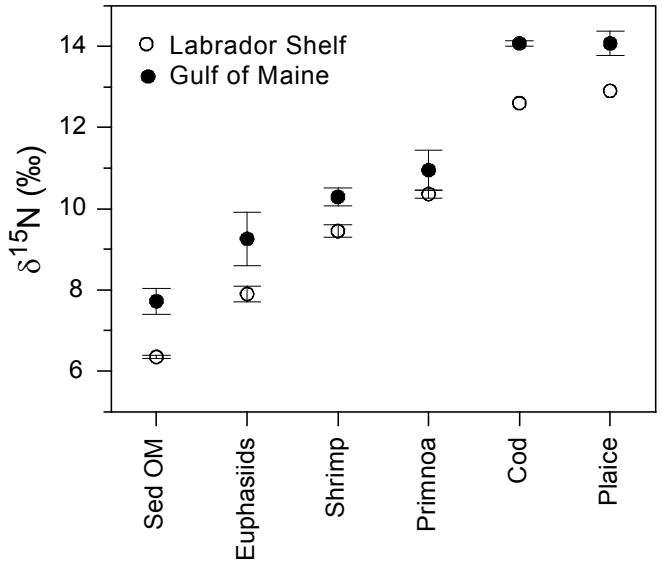

Fig. 7.11: $\delta^{15}N$ values for sedimentary organic matter (Macko, 1981; Muzuka and Hilliare-Marcel, 1990), *Primnoa* tissue (Sherwood et al., 2005b) and representive invertebrates and fish from Labrador (Sherwood and Rose, 2005) and Gulf of Maine (Fry, 1988). Error bars (where available) are ±1 se.

extends upward through the food web. The difference in $\delta^{15}N_{NO3}$ of 0.5-1.1 ‰ is similar in magnitude to the recent decline in the *Primnoa* $\delta^{15}N$ record (1 ‰) since around 1980. We therefore conclude that differences in $\delta^{15}N_{NO3}$ are sufficient to account for correlation of *Primnoa* $\delta^{15}N$ with the relative dominance of warm vs. cold source waters.

Nutrient utilization:

Variations in the $\delta^{15}N$ of phytoplankton are commonly attributed to nutrient utilization efficiency, such that, when nitrate utilization is incomplete, ^{14}N is

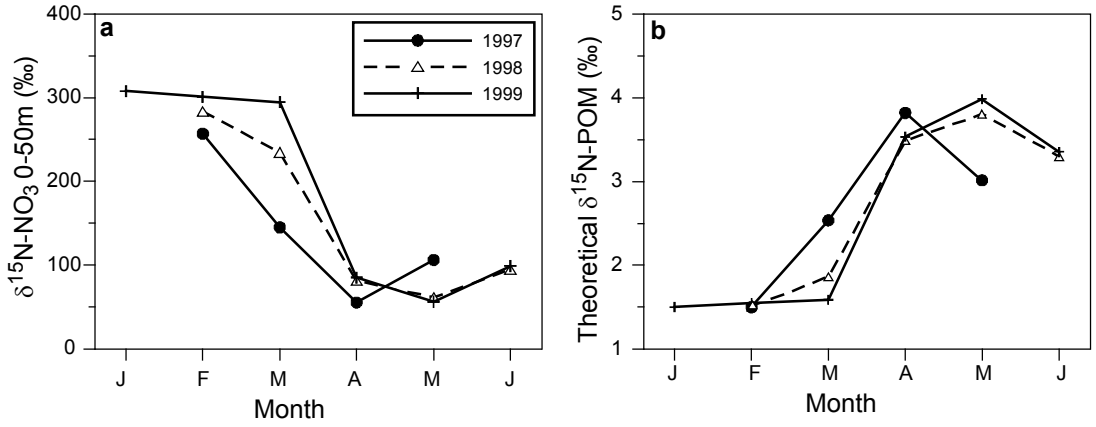

Fig. 7.12: (a) Comparison of nutrient drawdown in upper 50m in cold (1998) vs. warm (1997/1999) states of the slopewater system. Rate of drawdown is no faster in 1998 than in 1997 or 1999. Final concentrations are similar in all years. Nutrient data from D. Townsend. (b) Theoretical effect on $\delta^{15}N_{POM}$ using equation 1 in text.

preferentially assimilated, leading to isotopically depleted biomass (Nakatsuka et al. 1992, Altabet and Francois, 1994, Wu et al., 1997; 1999a). To examine whether lower nutrients and productivity affect $\delta^{15}N_{POM}$, springtime nutrient drawdown was evaluated between 1998 and 1999 (Fig. 7.12a). By May of both years, vertically integrated (0-50m) NO_3+NO_2 was consumed to near exhaustion. Corresponding values of $\delta^{15}N_{POM}$ for each month were modeled with a Rayleigh-type fractionation equation (Mariotti et al., 1981):

$$\delta^{15}N_{POM} = \delta^{15}N_{NO3} - \varepsilon\,(\ln f)[f/(1-f)] \qquad (1)$$

where: $\delta^{15}N_{NO3}$ is the isotopic composition of source nutrients before drawdown (5.5 ‰), ε is phytoplankton fractionation constant (5 ‰), and f = the fraction of initial nutrient remaining. Equation 1 represents the accumulated product, which is appropriate for

sinking POM. Theoretical values of $\delta^{15}N_{POM}$ were identical between years, with values in May approaching 4 ‰ (Fig. 7.12b). It is worth noting that similar values were measured in POM throughout the Gulf of Maine (Sherwood et al., 2005b), thus, our choice of values for $\delta^{15}N_{NO3}$ and ε is credible. Inter-specific differences in ε among phytoplankton (Needoba et al., 2003) should have little impact on our calculations, since nutrient utilization neared completion. Overall, it appears that differences in initial nutrient concentration between warm and cold states of the slopewater system do not support the long term variability in $\delta^{15}N$, because nutrients are ultimately consumed to the point where values of $\delta^{15}N_{POM}$ converge on that of $\delta^{15}N_{NO3}$.

Trophic level:

In an earlier paper (Sherwood et al., 2005b), we speculated that trophic fractionation of $\delta^{15}N$ (~3.4 ‰ / trophic level) may account for poorer intra- and inter-colony reproducibility of $\delta^{15}N$, relative to $\delta^{13}C$. For instance, different parts of colonies may be more effective at capturing different prey size classes. In surface waters, the complexity of the planktic food web could have a significant impact on $\delta^{15}N$ in *Primnoa*. Sherwood et al. (2005b) documented higher $\delta^{15}N$ on Georges Bank compared with the surrounding Gulf of Maine, apparently due to recycling of nutrients within the mixed layer (Townsend and Pettigrew, 1997). As stated in a previous section, although sinking POM and mesozooplankton have about the same apparent trophic level, multiple trophic intermediaries between primary production and *Primnoa* could potentially contribute significantly to the $\delta^{15}N$ variability.

Microbial degradation:

The $\delta^{15}N$ of POM increases by about 3.4 ‰ as it initially sinks out of the euphotic zone, but, it generally does not change much as it continues to sink (Altabet 1988; Altabet et al., 1991; Ostrom et al., 1997). Previous arguments concerning the impact of food "freshness" on $\delta^{13}C$ apply to $\delta^{15}N$ as well. Hence, it is unlikely that variations in food freshness account for observed variations in *Primnoa* $\delta^{15}N$.

In summary, the most likely sources of $\delta^{15}N$ variability are differences in $\delta^{15}N_{NO3}$ between warm and cold source waters, and possibly also differences in trophic complexity between warm and cold states.

7.5.3: Sub-fossil diagenesis

In a previous study we detected slightly higher lipid content in a subset of the sub-fossil colonies presented here (Sherwood et al., 2005b). As lipids tend to be lighter in $\delta^{13}C$ (DeNiro and Epstein, 1978), the subfossil values may be slightly more enriched (about 0.5 ‰) relative to the recent values. It is not clear what led to the higher C:N values in the sub-fossil colonies; samples were visibly free of allochthonous material and amino acid analyses suggest no organic diagenesis in the protein fraction of the gorgonin (Sherwood et al., 2006). As C:N was not measured in all of the colonies, the long term trends in $\delta^{13}C$ should be interpreted with caution.

7.5.4: $\delta^{15}N$ record: slopewater shift, or trophic cascade?

The *Primnoa* $\delta^{15}N$ record exhibited a significant decline over the 20th century with the major decline occurring around 1980 (Fig. 7.3). Over the last 50 years, $\delta^{15}N$ was significantly anticorrelated with temperature at 200m (Fig. 7.5). On this basis, along with apparently higher $\delta^{15}N$ in nitrate, sediments, and various organisms (Fig. 7.10, 7.11), we conclude that higher values of $\delta^{15}N$ in the past could be an indication that Labrador source waters (LSW and LShW) were more predominant during most of the last 2000 years than they have been more recently. This finding is supported by previous studies indicating that a "neoglacial" period off Nova Scotia was initiated around 2500 years ago by invasion of Labrador source waters (Scott et al., 1984; 1989; Levac, 2001). Keigwin et al. (2003) suggested that a rapid return to warmer conditions occurred sometime within the last 150 years. The resolution of the Keigwin et al. (2003) study was limited by bioturbation in the core. Our records suggest that this change occurred very recently and coincides with a prolonged positive phase of the NAO since around 1971. Recent trends in the slopewater system may therefore signal an anthropogenic-induced return to hypsithermal-like conditions

While a shift to warmer source waters may explain the $\delta^{15}N$ decline, the impact of a trophic cascade warrants further investigation. From the 1970s to the 1990s, the Eastern Scotian shelf shifted from an ecosystem dominated by large benthic fish, to one dominated by smaller pelagic fish (Choi et al., 2004; Bundy, 2005). Temporal trends in the biomass of fish, seals, benthic invertebrates, zooplankton and phytoplankton are consistent with a trophic cascade initiated by overfishing of large benthic piscivores

(Frank et al., 2005). Among plankton, there was a relative increase in the ratio of phytoplankton and small zooplankton vs. larger zooplankton, including *Calanus* copepods (Sameoto, 2001; Frank et al., 2005). The transition in the plankton community occurred sometime between 1974 and 1991, during a gap in Continuous Plankton Recorder observations (Sameoto, 2001). However, it is unclear whether the change in the plankton community was triggered by bottom-up, or top-down forces. Similar temporal patterns were observed in the Gulf of Maine, but the increase in phytoplankton and small zooplankton was attributed to bottom-up forces, namely, an increase in autumn stratification (Pershing et al., subm.).

An increase in the ratio of phytoplankton and small zooplankton vs. larger zooplankton could potentially explain the decline in the Primnoa $\delta^{15}N$ record, insofar as zooplankton tend to be isotopically heavier (Fry and Quiñones, 1994). Several lines of evidence argue against this hypothesis. 1) As stated earlier, it is unlikely that *Primnoa* eat large zooplankton, because they are considerably larger than *Primnoa* polyp diameters (4 mm), and animals can only ingest what they can fit in their mouths. Previous $\delta^{15}N$ evidence is also inconsistent with a diet of large zooplankton (Sherwood et al., 2005b). 2) While there was a gap in the Continuous Plankton recorder observations from 1974-1991, biomass data suggest that the major regime shift in the Scotian shelf ecosystem occurred around 1990 (Frank et al., 2005). Assuming that conditions on the Eastern Scotian Shelf extended to the Western Scotian Shelf and Gulf of Maine, then the regime shift was delayed by about a decade relative to the decline in *Primnoa* $\delta^{15}N$ around 1980 (Fig. 7.3).

3) An ecosystem model of the Eastern Scotian Shelf suggests that trophic level of benthic invertebrates remained unchanged through collapse of the groundfishery (Bundy, 2005).

Examination of potential causes of $\delta^{15}N$ variability in *Primnoa* suggests that several different factors could account for the long-term variability. Which explanation do we favor? The $\delta^{15}N_{NO3}$ hypothesis offers a more parsimonious explanation, but this may be because it was more readily quantifiable in the present study. In reality, the bulk isotopic analysis presented here is a "blunt tool" with which to probe paleoceanographic variability. Future studies, no doubt, will focus on compound specific analyses. For instance, the $\delta^{15}N$ of phenylalanine does not increase with trophic level, while that of glutamic acid increases by about 7 ‰ (McClelland and Montoya, 2002). Separate analysis of these amino acids could therefore be used to distinguish changes relating to $\delta^{15}N_{NO3}$ from changes relating to trophic complexity. We suggest that such studies could be used to unravel competing effects of trophic level and isotopic signature of source waters.

7.6 CONCLUSIONS

1. Records of $\delta^{13}C$ and $\delta^{15}N$ measured in the gorgonin fraction of 6 different *Primnoa* colonies from the Northeast Channel exhibited excellent reproducibility, indicating that these parameters respond in a consistent manner to environmental processes occurring in surface waters.

2. Records of $\delta^{13}C$ and $\delta^{15}N$ were broadly anticorrelated with the records of NAO, temperature, salinity and productivity. The common underlying cause of hydrographic and biological variability is the relative dominance of cold source waters associated with the Labrador Current and warm source waters associated with the Gulf Stream.

3. The long-term $\delta^{13}C$ record declined from -18 ‰ during most of the last 2000 years, to -19.5 ‰ during the latter half of the 20^{th} century, an amount consistent with the oceanic Suess effect. The cause of the high frequency interannual variability remains unknown.

4. The long-term $\delta^{15}N$ record declined from 10.7 ‰ during most of the last 2000 years, to 9.7 ‰ during 20^{th} century. The magnitude of the decline is consistent with a shift from $\delta^{15}N_{NO3}$-heavier Labrador source waters, to isotopically lighter Gulf Stream-derived waters. The recent shift to warmer source waters may signal an anthropogenic-induced shift to hypsithermal-like conditions.

5. A trophic cascade, leading to an increase in the proportion of isotopically lighter phytoplankton in the coral's diet, offers an alternative, less parsimonious explanation.

Future compound-specific isotope analysis could be used to sort out different factors leading to isotopic variability in *Primnoa* and other soft corals.

ACKNOWLEDGEMENTS

We thank Derek Jones and Sanford Atwood for providing the sub-fossil specimens, and Don Gordon, Pal Mortensen and the Captain and crew of the CGS *Martha Black* for the recent specimens. Radiocarbon analyses were performed by Tom Guilderson at LLNL. Special thanks to Jennifer McKay at GEOTOP for processing the large number of stable isotopic analyses. Kevin Pauly kindly collected water samples. Thanks also to Andrew Pershing for providing the *Calanus* data. This manuscript was greatly improved by the suggestions of Evan Edinger.

CHAPTER 8

GENERAL CONCLUSIONS

Proxy records from *Primnoa* and other annually-banded gorgonian corals offer unprecedented new opportunities to gain insights into paleoceanographic variability. The work presented in this thesis documents that:

1) *Primnoa resedaeformis* secretes annual growth rings of organic gorgonin that may be isolated and analyzed chemically to obtain proxy data on past environments.

2) The stable isotopic composition of gorgonin rings in *Primnoa* is related to a variety of processes occurring in surface waters, including the isotopic composition of source nutrients, and plankton productivity.

3) Life-spans of individual colonies may exceed 700 years, making *Primnoa* one of the oldest animals in the sea.

4) Useful proxy environmental data may be obtained from both the calcite and gorgonin fractions of colonies. Measurements of $\Delta^{14}C$ from the calcite fraction are particularly useful, as they are directly related to the $\Delta^{14}C$ of ambient water masses.

5) For colonies collected off Nova Scotia, proxy records from *Primnoa* indicate that the recent shift to warmer conditions since 1970 is largely anomalous with respect to the last 2000 years.

6) The paleoceanographic potential of octocorals has just barely been tapped. Future studies on a wider variety of specimens will no doubt shed new light into climate-ocean interactions over long time periods.

REFERENCES

Adkins, J.F., Boyle, E.A. 1997. Changing atmospheric $\Delta^{14}C$ and the record of deep water paleoventilation ages. Paleoceanography. 12, 337-344.

Adkins, J.F., Cheng, H., Boyle E.A., Druffel, E.R.M., Edwards, R.L., 1998. Deep-sea coral evidence for rapid change in ventilation of the deep North Atlantic 15,400 years ago. Science. 280, 725-728.

Adkins, J.F., Griffin, S., Kashgarian, M., Cheng, H., Druffel, E.R.M., Boyle, E.A., Edwards, R.L., Shen, C.-C., 2002. Radiocarbon dating of deep-sea corals. Radiocarbon. 44: 567-580.

Adkins, J.F., Boyle, E.A., Curry, W.B., Lutringer, A., 2003. Stable isotopes in deep-sea corals and a new mechanism for "vital effects". Geochimica et Cosmochimica Acta. 67, 1129-1143.

Adkins, J.F., Henderson, G.M., Wang, S.-L., O'Shea, S., Mokadem, F., 2004. Growth rates of the deep-sea scleractinian *Desmophyllum cristagalli* and *Enallopsammia rostrata*. Earth and Planetary Science Letters. 227, 481-490.

Allard, G., Sinclair, D.J., Williams, B., Hillaire-Marcel, C., Ross, S., Risk, M. 2005. Dendochronology in bamboo? Geochemical profiles and reproducibility in a specimen of the deep water bamboo coral *Keratoisis* spp. Proc. 3rd International Symposium on Deep-Sea Corals. Miami, USA, pp. 204.

Andrews, A. H., Coale, K.H., Nowicki, J.L., Lundstrom, C., Palacz, Z., Burton, E.J., Cailliet, G.M. 1999. Application of an ion-exchange separation technique and thermal ionization mass spectrometry to ^{226}Ra determination in otoliths for radiometric age determination of long-lived fishes. Canadian Journal of Fisheries and Aquatic Sciences. 56, 1329–1338.

Andrews, A.H., Cordes, E.E., Mahoney, M.M., Munk, K., Coale, K.H., Cailliet, G.M., Heifitz, J., 2002. Age, growth and radiometric age validation of a deep-sea, habitat-forming gorgonian (*Primnoa resedaeformis*) from the Gulf of Alaska. Hydrobiologia. 471, 101-110.

Andrews, A.H., Cailliet, G.M., Kerr, L.A., Coale, K.H., Lundstrom, C., DeVogelaere, A.P. 2005. Investigations of the age and growth for three deep-sea corals from the Davidson Seamount off central California. In: Freiwald, A., Roberts, J.M. (Eds.), Cold-Water Corals and Ecosystems. Springer, Berlin, pp. 1021-1038.

Altabet, M.A. 1988. Variations in nitrogen isotopic composition between sinking and suspended particles: implications for nitrogen cycling and particle transformation in the open ocean. Deep-Sea Research. 35, 535-554.

Altabet, M.A., McCarthy J.J. 1985. Temporal and spatial variations in the natural abundance of ^{15}N in PON from a warm-core ring. Deep-Sea Research. 32, 755-772.

Altabet, M.A., Francois, R. 1994. Sedimentary nitrogen isotopic ratio as a recorder for surface ocean nitrate utilization. Global Biogeochemical Cycles. 8, 103-116.

Altabet, M.A., Deuser W.G., Honjo, S. 1991. Seasonal and depth-related changes in the source of sinking particles in the North Atlantic. Nature. 354, 136-139.

Altabet, M.A., Francois, R., Murray, D.W., Prell, W.L. 1995. Climate-related variations in denitrification in the Arabian Sea from sediment $^{15}N/^{14}N$ ratios. Nature. 373, 506-508.

Altabet, M.A., Pilskaln, C., Thunell, R., Pride, C., Sigman, D., Chavez, F., Francois, R. 1999. The nitrogen isotope biogeochemistry of sinking particles from the margin of the eastern North Pacific. Deep-Sea Research. 46, 655-679.

Atkinson, L.P. 1983. Distribution of Antarctic Intermediate Water over the Blake Plateau. Journal of Geophysical Research. 88 (C8), 4699-4704.

Barber, D.C., Dyke, A., Hillaire-Marcel, C., Jennings, A.E., Andrews, J.T., Kerwin, M.W., Bilodeau, G., McNeely, R., Southon, J., Morehead, M.D., Gagnon, J.-M. 1999. Forcing the cold event of 8200 years ago by catastrophic drainage of Laurentide lakes. Nature. 400, 344-348.

Bard, E., Fairbanks, R.G., Hamelin, B., Zindler, A., Chi Trach, H. 1991. Uranium-234 anomalies in corals older than 150000 years. Geochimica et Cosmochimica Acta. 55, 2385-2390.

Bard, E., Arnold, M., Fairbanks, R.G., Hamelin, B. 1993. ^{230}Th-^{234}U and ^{14}C ages obtained by mass spectrometry on corals. Radiocarbon. 35, 191-199.

Barnes, D.J., 1970. Coral skeletons: An explanation of their growth and structure. Science. 170, 1305-1308.

Bauer, J.E., Druffel, E.R.M., Wolgast, D.M., Griffin, S. 2002. Temporal and regional variability in sources and cycling of DOC and POC in the northwest Atlantic continental shelf and slope. Deep-Sea Research. (II). 49, 4387-4419.

Beuck, L., Freiwald, A., 2005. Bioerosion patterns in a deep-water Lophelia pertusa thicket (Propeller Mound, northern Porcupine Seabight.) In: Freiwald, A., Roberts, J.M. (Eds.), Cold-water Corals and Ecosystems. Springer, Berlin, pp. 915-936.

Boerboom, C.M., Smith, J.E., Risk, M.J., 1998. Bioerosion and micritisation in the deep-sea coral *Desmophyllum cristagalli*. Historical Biology. 13, 53-60.

Bohm, F., Haase-Schramm, A., Eisenhauer, A., Dullo, W.C., Joachimski, M.M., Lehnert, H., Reitner, J. 2002. Evidence for preindustrial variations in the marine surface water

carbonate system from coralline sponges. Geochemistry Geophysics Geosystems. 3(3): 1019, doi:10.1029/2001GC000264.

Bond, Z.A., Cohen, A.L., Smith, S.R., Jenkins, W.J., 2005. Growth and composition of high-Mg calcite in the skeleton of a Bermudian gorgonian (*Plexaurella dichotoma*): Potential for paleothermometry. Geochemistry Geophysics Geosystems. 6, Q08010, doi:10.1029/2005GC000911.

Bosley, K.L., Wainright, S.C. 1999. Effects of preservation and acidification on the stable isotope ratios (^{15}N:^{14}N, ^{13}C:^{12}C) of two species of marine animals. Canadian Journal of Fisheries and Aquatic Sciences. 56, 2181–2185.

Breeze, H., Davis, D.S., Butler, M., Kostylev, V. 1997. Distribution and status of deep sea corals off Nova Scotia. Ecology Action Centre, Marine Issues Committee Special Publication Number 1, 58 pp.

Brinton, K.L.F., Bada, J.L 1995. Comment on "Aspartic acid racemization and protein diagenesis in corals over the last 350 years" by G.A. Goodfriend, P.E. Hare, and E.R.M. Druffel. Geochimica et Cosmochimica Acta. 59, 415-416.

Broecker, W.S., Gerard, R., Ewing, M., Heezen, B.C. 1960. Natural radiocarbon in the Atlantic Ocean. Journal of Geophysical Research. 65(a), 2903-2931.

Broecker, W.S., Klas, M., Clark, E., Trumbore, S., Bonani, G., Wolfli, W., Ivy, S. 1990. Accelerator mass spectrometric measurements on foraminifera shells from deep sea cores. Radiocarbon. 32, 119-133.

Bromley, R.G. 2005. Preliminary study of bioerosion in the deep-water coral Lophelia, Pleistocene, Rhodes, Greece. In: Freiwald, A., Roberts, J.M. (Eds.), Cold-water Corals and Ecosystems. Springer, Berlin, pp. 895-914.

Bryan, T.L., Metaxas, A. Predicting suitable habitat for deep-water coral in the families *Paragorgiidae* and *Primnoidae* on the Atlantic and Pacific continental margins of North America. Marine Ecology Progress Series. (in press).

Bryan, W.B., Hill, D., 1941. Spherulitic crystallization as a mechanism of skeletal growth in the hexacorals. Proceedings of the Royal Society of Queensland. 52, 78-91.

Bryden, H.L., Longworth, H.R., Cunningham, S.A. 2005. Slowing of the Atlantic meridional overturing circulation at 25^{o}N. Nature. 438: 655-657.

Bundy, A. 2005. Structure and functioning of the eastern Scotian Shelf ecosystem before and after the collapse of groundfish stocks in the early 1990s. Canadian Journal of Fisheries and Aquatic Sciences. 62: 1453-1473.

Cairns, S.D. l981. Marine flora and fauna of the northeastern United States. Scleractinia. NOAA Technical Report. NMFS Circular. 438: l4 pp.

Campana, S.E. 1997. Use of radiocarbon from nuclear fallout as a dated marker in the otoliths of haddock *Melanogrammus aeglefinus*. Marine Ecology Progress Series. 150, 49–56.

Carriquiry, J.D., Risk, M.J., 1988. Timing and temperature record from stable isotopes of the 1982-1983 El Niño warming event in Eastern Pacific corals. Palaios. 3, 359-364.

Cheng, H., Adkins, J.A., Edwards, R.L., Boyle, E.A., 2000. U-Th dating of deep-sea corals. Geochimica et Cosmochimica Acta. 64, 2401-2416.

Choi, J.S., Frank, K.T., Legget, W.C., Drinkwater, K. 2004. Transition to an alternate state in a continental shelf ecosystem. Canadian Journal of Fisheries and Aquatic Sciences. 61, 505-510.

Cline, J.D., Kaplan, I.R. 1975. Isotopic fractionation of dissolved nitrate during denitrification in the eastern tropical north Pacific Ocean. Marine Chemistry. 3, 271-299.

Cohen, A.L., McConnaughey, T.A., 2003. Geochemical perspectives on coral mineralization. Reviews in Mineralogy and Geochemistry. 54, 151-187.

Cohen, A.L., Lundälv, T., Thorrold, S.R., Corliss, B.H., Smith, S.R., George, R.Y. Sr/Ca variability in the skeleton of a cold-water scleractinian, *Lophelia pertusa*. Manuscript submitted to Geochemistry, Geophysics, Geosystems.

Collins, M.J., Waite, E.R., van Duin, A.C.T. 1999. Predicting protein decomposition: the case of aspartic-acid racemization kinetics. Philosophical Transactions of the Royal Society of London. B. 354: 51-64.

Collins, M.J., Riley, M.S. 2000. Amino acid racemization in biominerals: the impact of protein degradation and loss. In: *Perspectives in Amino Acid and Protein Geochemistry* (eds. G.A., Goodfriend, M.J. Collins, M.L. Fogel, S.A. Macko, and J.F. Wehmiller). Oxford Univ. Press, New York. pp. 120-142.

Coma, R., Gili, J.M., Zabala, M., Riera, T. 1994. Feeding and prey capture cycles in the aposymbiontic gorgonian *Paramuricea clavata* Marine Ecology Progress Series. 115, 257-270.

Constanz, B.R. 1986. Coral skeleton construction: A physicochemically dominated process. Palaois. 1, 152-157.

Conversi, A., Piontkovski, S., Hameed, S. 2001. Seasonal and interannual dynamics of *Calanus finmarchicus* in the Gulf of Maine (Northeastern US shelf) with reference to the North Atlantic Oscillation. Deep-Sea Research II. 48: 519-530

Csanady, G.T., Hamilton, P. 1988. Circulation of slopewater. Continental Shelf

Research. 8, 565-624.

Cuif, J.-P., Dauphin, Y., 2005. The two-step mode of growth in the scleractinian coral skeletons from the microscale to the overall scale. Journal of Structural Biology. 150, 319-331.

Cullen, J.T., Rosenthal, Y., Falkowski, P.G. 2001. The effect of anthropogenic CO_2 on the carbon isotope composition of marine phytoplankton. Limnology and Oceanography. 46, 996-998.

DeNiro M.J., Epstein, S. 1978. Influence of diet on the distribution of carbon isotopes in animals. Geochimica et Cosmochimica Acta. 42, 495–506.

DeNiro, M.J., Epstein, S. 1981. Influence of diet on the distribution of nitrogen isotopes in animals. Geochimica et Cosmochimica Acta. 45, 341–351.

Drinkwater, K.F.B., Petrie, B., Smith, P.C. 2003. Climate variability on the Scotian Shelf during the 1990s. ICES Marine Science Symposium. 219, 40-49.

Druffel, E.R.M. 1989. Decade time scale variability of ventilation in the North Atlantic: High precision measurements of bomb radiocarbon in banded corals. Journal of Geophysical Research. 94, 3271-3285.

Druffel, E.M., Linick, T.W. 1978. Radiocarbon in annual coral rings of Florida. Geophysical Reseach Letters. 5(11): 913-916.

Druffel, E.R.M., King, L.L., Belastock, R.A., Buesseler, K.O. 1990. Growth rate of a deep-sea coral using ^{210}Pb and other isotopes. Geochimica et Cosmochimica Acta. 54, 1493-1500.

Druffel, E.R.M., Griffin, S., Witter, A., Nelson, E., Southon, J., Kashgarian, M., Vogel, J., 1995. *Gerardia*: Bristlecone pine of the deep-sea? Geochimica et Cosmochimica Acta. 59, 5031-5036.

Edwards, R.L., Beck, W.J., Burr, G.S., Donahue, D.J., Chappell, J.M.A., Bloom, A.L., Druffel, E.R.M., Taylor, F.W. 1993. A large drop in atmospheric $^{14}C/^{12}C$ and reduced melting in the Younger Dryas, documented with ^{230}Th ages of corals. Science. 260, 962-967.

Edwards, R.L., Gallup, C.D., Cheng, H. 2003. Uranium-series dating of marine and lacustrine carbonates. Reviews in Mineralogy and Geochemistry. 52, 363-405.

Emiliani, C., Hudson J.H., Shinn E.A., George R.Y., Lidz, B. 1978. Oxygen and carbon isotopic growth record in a reef coral from the Florida Keys and a deep-sea coral from Blake Plateau. Science. 202, 627-629.

Epstein, S., Buchsbaum, R., Lowenstam, H.A., Urey, H.C. 1953. Revised carbonate-water isotopic temperature scale. Bulletin of the Geological Society of America 64, 1315-1325.

Etnoyer, P., Morgan, L. 2003. Occurrences of habitat-forming deep sea corals in the Northeast Pacific Ocean. Report to NOAA Office of Habitat Conservation. Marine Conservation Biology Institute, Redmond Washington. 31 pp.

Fallon, S.J., White, J.C., McCulloch, M.T., 2002. Porites corals as recorders of mining and environmental impacts: Misima Island, Papua New Guinea. Geochimica et Cosmochimica Acta. 66, 45-62.

Fallon, S.J., Roark, E.B., Guilderson, T.P., Dunbar, R.B., Weber, P. 2005. Elemental imaging and proxy development in the deep sea coral, *Corallium secundrum*.

Proceedings of the 3rd International Symposium on Deep-Sea Corals. Miami, USA, pp. 187.

Flynn, W. W., 1968. The determination of low levels of polonium-210 in environmental materials. Analytica Chimica Acta. 43, 221–227.

Fosså, J.H., Mortensen, P.B., Furevik, D.M. 2002. The deep-water coral *Lophelia pertusa* in Norwegian waters: distribution and fishery impacts. Hydrobiologia. 471: 1-12.

Francey, R.J., Allison, C.E., Etheridge, D.M., Trudinger, C.M., Enting, I.G., Leuenberger, M., Langenfelds, R.L., Michel, E., Steele, L.P. 1999. A 1000 year high precision record of $\delta^{13}C$ in atmospheric CO_2. Tellus. 51B, 170-193.

Frank, K.T., Petrie, B., Choi, J.S., Legget, W.C. 2005. Trophic cascades in a formerly cod-dominated ecosystem. Science. 308, 1621-1623.

Frank, N., Paterne, M., Ayliffe, L., van Weering, T., Henriet, J.-P., Blamart, D., 2004. Eastern North Atlantic deep-sea corals: tracing upper intermediate water $\Delta^{14}C$ during the Holocene. Earth and Planetary Science Letters. 219, 297-309.

Frank, N., Lutringer, A., Paterne, M., Blamart, D., Henriet, J.P., van Rooij, D., van Weering, T.C.E. 2005. Deep-water corals of the northeastern Atlantic margin: carbonate mound evolution and upper intermediate water ventilation during the Holocene. In: Freiwald, A., Roberts, J.M. (Eds.), Cold-Water Corals and Ecosystems. Springer, Berlin, pp. 113-133.

Freeman, K. H. 2001. Isotopic biogeochemistry of marine carbon. Reviews in Mineralogy and Geochemistry. 43, 579-605.

Fry, B. 1988. Food web structure on Georges Bank from stable C, N, and S isotopic compositions. Limnology and Oceanography. 33, 1182–1190.

Fry, B., Sherr, E.B. 1984. $\delta^{13}C$ measurements as indicators of carbon flow in marine and freshwater ecosystems. Contributions to Marine Science. 27, 13–47.

Fry, B., Wainright, S.C. 1991. Diatom sources of ^{13}C-rich carbon in marine food webs. Marine Ecology Progress Series. 76, 149-157.

Fry, B., Quiñones, R.N. 1994. Biomass spectra and stable isotope indicators of trophic level in zooplankton of the northwest Atlantic. Marine Ecology Progress Series. 112, 201-204.

Furla, P., Bénazet-Tambutté, S., Jaubert, J., Allemand, D., 1998. Diffusional permeability of dissolved inorganic carbon through the isolated oral epithelial layers of the sea anemone, *Anemonia viridis*. Journal of Experimental Marine Biology and Ecology. 230, 71-88.

Gagnon, A.C., Adkins, J.F., 2005. Multiple proxy "vital effects" in a deep-sea coral. Proceedings of the 3rd International Symposium on Deep-Sea Corals. Miami, USA, pp. 188.

Ganeshram, R.S., Pederson, T.F., Calvert, S.E., Murray, J.W. 1995. Large changes in oceanic nutrient inventories from glacial to interglacial periods. Nature. 376, 755-757.

Geiger, T., Clarke, S. 1987. Deamidation, isomerization, and racemization at asparaginyl and aspartyl residues in peptides. Succinimide-linked reactions that contribute to protein degradation. Journal of Biological Chemistry 262, 785-794.

Gilliken, D.P., Dehairs, F., Baeyens, W., Navez, J., Lorrain, A., André, L. 2005. Inter-and intra-annual variations of Pb/Ca ratios in clam shells (*Mercenaria mercenaria*): A record of anthropogenic lead pollution? Marine Pollution Bulletin. 50, 1530-1540.

Gladfelter, E.H. 1982. Skeletal development in *Acropora cervicornis*: I. Patterns of calcium carbonate accretion in the axial corallite. Coral Reefs. 1, 45-51.

Goering, J., Alexander, V., Haubenstock, N. 1990. Seasonal variability of stable carbon and nitrogen isotope ratios of organisms in a North Pacific bay. Estuarine Coastal and Shelf Science. 30, 239–260.

Goldberg, W.M. 1974. Evidence of a sclerotized collagen from the skeleton of a gorgonian coral. Comparative Biochemistry and Physiology. 49B, 525-529.

Goldberg, W.M. 1976. Comparative study of the chemistry and structure of gorgonian and antipatharian coral skeletons. Marine Biology. 35, 253-267.

Goldberg, W.M. 1991. Chemistry and structure of skeletal growth rings in the black coral *Antipathes fiordenis* (Cnidaria, Antipatharia). Hydrobiologia. 217/216, 403-409.

Goldstein, S.J., Lea, D.W., Chakraborty, S., Kashgarian, M., Murrell, M.T. 2001. Uranium-series and radiocarbon geochronology of deep-sea corals: implications for Southern Ocean ventilation rates and the oceanic carbon cycle. Earth and Planetary Science Letters. 193, 167-182.

Goodfriend G.A. 1991. Patterns of racemization and epimerization of amino acids in land snails over the course of the Holocene. Geochimica et Cosmochimica Acta. 55, 293-302.

Goodfriend, G.A. 1992. Rapid racemization of aspartic acid in mollusc shells and the potential for dating over recent centuries. Nature. 357, 399-401.

Goodfriend, G.A., 1997. Aspartic acid racemization and amino acid composition of the organic endoskeleton of the deep-water colonial anemone *Gerardia*: Determination of longevity from kinetic experiments. Geochimica et Cosmochimica Acta. 61, 1931-1939.

Goreau, T.F., 1959. The physiology of skeletal formation in corals I. A method for measuring the rate of calcium deposition by corals under different conditions. Biological Bulletin. 116, 59-75.

Grasshoff, M., Zibrowius, H., 1983. Kalkkrusten auf Achsen von Hornkorallen. Senckenbergiana Maritima. 15, 111-145.

Greene, C.H., Pershing, A.J. 2000. The response of Calanus finmarchicus populations to climate variability in the Northwest Atlantic: basin-scale forcing associated with the North Atlantic Oscillation. ICES Journal of Marine Science. 57, 1536-1544.

Greene, C.H., Pershing, A.J. 2003. The flip-side of the North Atlantic Oscillation and modal shifts in slope-water circulation patterns. Limnology and Oceanography. 48, 319-322.

Griffin, S., Druffel, E.R.M., 1989. Sources of carbon to deep-sea corals. Radiocarbon. 31, 533-543.

Grigg, R.W. 1974. Growth rings: annual periodicity in two gorgonian corals. Ecology. 55, 876-881.

Grossman, E.L., Ku, T-L., 1986. Oxygen and carbon isotope fractionation in biogenic aragonite: Temperature effects: Chemical Geology. (Isotope Geoscience Section) 59, 59-74.

Hall-Spencer, J., Allain, V., Fosså, J.H. 2002. Trawling damage to Northeast Atlantic ancient coral reefs. Proceedings of the Royal Society of London. 269 (1490), 507-11.

Haug, G.H., Pederson, T.F., Sigman, D.M., Calvert, S.E., Nielsen, B., Peterson, L.C. 1998. Glacial/interglacial variations in production and nitrogen fixation in the Cariaco Basin during the last 580 kyr. Paleoceanography. 13, 427-432.

Hawkes, A., Scott, D.B., 2005. *Primnoa resedaeformis* habitat characterization using an associate assemblage of attached benthic foraminifera. In: Freiwald, A., Roberts, J.M. (Eds.), Cold-water Corals and Ecosystems. Springer, Berlin. pp. 881-894.

Heikoop, J.M., Tsujita C.J and M.J. Risk. 1996. Corals as proxy recorders of volcanic activity: Banda Api, Indonesia. Palaois. 11: 286-292.

Heikoop, J.M., Risk, M.J., Lazier, A.V., Schwarcz, H.P. 1998. $\delta^{18}O$ and $\delta^{13}C$ signatures of a deep-sea gorgonian coral from the Atlantic coast of Canada. EOS. 79 (supplement 17), S179.

Heikoop, J.M., Hickmott, D.D., Risk, M.J., Shearer, C.K., Atudorei, V. 2002. Potential climate signals from the deep-sea gorgonian coral *Primnoa resedaeformis*. Hydrobiologia. 471, 117-124.

Henderson, G.M. 2002. Seawater ($^{234}U/^{238}U$) during the last 800 thousand years. Earth and Planetary Science Letters. 199, 97-110.

Hendy E.J., Gagan M.K., Alibert C.A., McCulloch M.T., Lough J.M., Isdale, P.J., 2002. Abrupt decrease in tropical Pacific sea surface salinity at end of Little Ice Age. Science. 295, 1511-1514.

Hoffman, M., Wolf-Gladrow, D.A., Takahashi, T., Sutherland, S.C., Six, K.D., Maier-Reimer, E. 2000. Stable carbon isotope distribution of particulate organic matter in the ocean: a model study. Marine Chemistry. 72, 131-150.

Houghton, R.W., Fairbanks, R.G. 2001. Water sources for Georges Bank. Deep-Sea Research. II. 48, 95-114.

Hughen, K.A., Baillie, M.G.L., Bard, E., Bayliss, A., Beck, J.W., Bertrand, C.J.H., Blackwell, P.G., Buck, C.E., Burr, G.S., Cutler, K.B., Damon, P.E., Edwards, R.L., Fairbanks, R.G., Friedrich, M., Guilderson, T.P., Kromer, B., McCormac, F.G., Manning, S.W., Bronk Ramsey, C., Reimer, P.J., Reimer, R.W., Remmele, S., Southon, J.R., Stuiver, M., Talamo, S., Taylor, F.W., van der Plicht, J., Weyhenmeyer, C.E. 2004. Marine 04 Marine radiocarbon age calibration, 26 - 0 ka BP. Radiocarbon. 46, 1059-1086.

Hurrell, J.W., Kushnir, Y., Visbeck, M. 2001. The North Atlantic Oscillation. Science. 291: 603-605.

IPCC (Intergovernmental Panel on Climate Change) 2001. Climate Change: The Scientific Basis. Cambridge Univ. Press, Cambridge. 880 pp.

Jasper, J.P., Hayes, J.M., Mix, A.C., Prahl, F.G. 1994. Photosynthetic fractionation of ^{13}C and concentrations of dissolved CO_2 in the central equatorial Pacific during the last 255,000 years. Paleoceanography. 9, 781-798.

Johnston, I.S. 1980. The ultrastructure of skeletogenesis in hermatypic corals. International Review of Cytology 67, 171-214.

Kalish, J.M. 1993. Pre- and post-bomb radiocarbon in fish otoliths. Earth and Planetary Science Letters. 114, 549-554.

Kaufman, D.S., Manley, W.F. 1998. A new procedure for determining DL amino acid ratios in fossils using reverse phase liquid chromatography. Quaternary Geochronology. 17, 987-1000.

Kaufman, D. 2003. Dating deep-lake sediments by using amino acid racemization in fossil ostracodes. Geology. 31, 1049-1052.

Keigwin, L.D., Sachs, J.P., Rosenthal, Y. 2003. A 1600-year history of the Labrador Current off Nova Scotia. Climate Dynamics. 21, 53-62.

Keil, R.G., Fogel, M.L. 2001. Reworking of amino acid in marine sediments: Stable carbon isotopic composition of amino acids in sediments along the Washington coast. Limnology and Oceanography. 46, 14-23.

Kerr, L.A., Andrews, A.H., Munk, K., Coale, K.H., Frantz, B.R., Cailliet, G.M., Brown, T.A. 2005. Age validation of quillback rockfish (*Sebastes maliger*) using bomb radiocarbon. Fishery Bulletin. 103, 97-107.

Key, R.M. 2001. Radiocarbon. In: Steele, J., Thorpe, S., Turekian, K. (Eds.), Encyclopedia of Ocean Sciences. Academic Press, London, pp. 2338-2353.

Key, R.M., Kozyr, A., Lee, K., Wanninkhof, R., Bullister, J.L., Feely, R.A., Millero, F.J., Mordy, C., Peng, T.-H. 2004. A global ocean carbon climatology: Results from Global Data Analysis Project (GLODAP). Global Biogeochemical Cycles. 18, GB4031. doi:10.1029/2004GB002247.

Kline, T.C. 1999. Temporal and spatial variability of $^{13}C/^{12}C$ and $^{15}N/^{14}N$ in pelagic biota of Prince William Sound, Alaska. Canadian Journal of Fisheries and Aquatic Sciences. 56 (supp 1), 94-117.

Knapp, A.N., Sigman, D.M., Lipschultz, F. 2005. N isotopic composition of dissolved organic nitrogen and nitrate at the Bermuda Atlantic time-series site. Global Biogeochemical Cycles. 19, GB1018. doi:10.1029/2004GB002320.

Knutsen, D.W., Buddemeier, R.W., Smith, S.V. 1972. Coral chronometers: Seasonal growth bands in reef corals. Science. 177, 270-272.

Kortzinger, A., Quay, P.D. 2003. Relationship between anthropogenic CO_2 and the ^{13}C Suess effect in the North Atlantic Ocean. Global Biogeochemical Cycles. 17(1), 1005. doi:10.1029/2001GB001427.

Kroopnick, P. 1985. The distribution of ^{13}C of $\sum CO_2$ in the world oceans. Deep-Sea Research. 32, 57-84.

Laws, E.A., Popp, B.N., Cassar, N., Tanimoto, J. 2002. ^{13}C discrimination patterns in oceanic phytoplankton: likely influence of CO_2 concentrating mechanisms, and implications for palaeoreconstructions. Functional Plant Biology. 29, 323–333.

Lazareth, C.E., Willenz, P., Navez, J., Keppens, E., Dehairs, F., Andre´, L., 2000. Sclerosponges as a new potential recorder of environmental changes: Lead in *Ceratoporella nicholsoni*. Geology. 28, 515–518.

Lazier, A.V., Smith, J.E., Risk, M.J., 1999. The skeletal structure of *Desmophyllum cristagalli*: the use of deep-water corals in sclerochronology. Lethaia. 32, 119-130.

Lehmann, M.F., Bernasconi, S.M., Barbieri, A., McKenzie, J.A. 2002. Preservation of organic matter and alteration of its carbon and nitrogen isotope composition during simulated and in situ early sedimentary diagenesis. Geochimica et Cosmochimica Acta. 66, 3573-3584.

Leterme, S.C., Edwards, M., Seuront, L., Attrill, M.J., Reid, P.C., John, A.W.G. 2005. Decadal basin-scale changes in diatoms, dinoflagellates, and phytoplankton color across the North Atlantic. Limnology and Oceanography. 50, 1244-1253.

Levac, E. 2001. High resolution Holocene palynological record from the Scotian Shelf. Marine Micropaleontology. 43, 179-197.

Levitus, S., Boyer, T. 1994. World Ocean Atlas 1994, Volume 2: Oxygen. NOAA Atlas NESDIS 2, U.S. Department of Commerce, Washington, D.C.

Lewis, J.C., Barnowski, T.F., Telesnicki, G.J., 1992. Characteristics of carbonates of gorgonian axes. Biological Bulletin. 183, 278-296.

Libes, S.M., Deuser, W.G. 1988. The isotope geochemistry of particulate nitrogen in the Peru Upwelling Area and the Gulf of Maine. Deep-Sea Research. 35, 517-533.

Linnaeus, C. 1758. Systema naturae. Editio decima, reformata. 1. Holmiae: Impensis Direct. Laurentii Salvii. pp. i-iv + 1-824

Loder, J.W., Shore, J.A., Hannah, C.G., Petrie, B.D. 2001. Decadal-scale hydrographic and circulation variability in the Scotia-Maine region. Deep-Sea Research. II. 48, 3-35.

Lomitschka, M., Mangini, A. 1999. Precise Th/U-dating of small and heavily coated samples of deep sea corals. Earth and Planetary Science Letters. 170, 391-401.

Lourey, M.J., Trull, T.W., Sigman, D.M., 2004. Sensitivity of delta N-15 of nitrate, surface suspended and deep sinking particulate nitrogen to seasonal nitrate depletion in the Southern Ocean. Global Biogeochemical Cycles. 17(3), 1081.

Ludwig, K.R., Titterington, D.M. 1994. Calculation of ^{230}Th/U isochrons, ages and errors. Geochimica et Cosmochimica Acta. 58, 5031-5042.

Lutringer, A., Blamart, D., Frank, N., Labeyrie, L. 2005. Paleotemperatures from deep-sea corals: scale effects. In: Freiwald, A., Roberts, J.M. (Eds.), Cold-Water Corals and Ecosystems. Springer, Berlin, pp. 1081-1096.

Macintyre, I.G., Bayer, F.M., Logan, M.A., Skinner, H.C.W. 2000. Possible vestige of early phosphatic biomineralization in gorgonian octocorals (Coelenterata). Geology. 28, 455-458.

MacIsaac, K., Bourbonnais, C., Kenchington, E., Gordon D.C. Jr. Gass, S. 2001. Observations on the occurrence and habitat preference of corals in Atlantic Canada. In: J.H.M. Willison et al. (Eds.) Proceedings of the First International Symposium on Deep-Sea Corals, Ecology Action Centre and Nova Scotia Museum, Halifax, NS, pp. 58-75.

Macko, S.A. 1981. Stable nitrogen isotope ratios as tracers of organic geochemical processes. PhD thesis, Univ Texas, Austin. 182 pp.

Macko, S.A., Estep, M.L. 1984. Microbial alteration of stable nitrogen and carbon isotopic compositions of organic matter. Organic Geochemistry. 6, 787-790.

Mangerud, J., Gulliksen, S. 1975. Apparent radiocarbon ages of recent marine shells from Norway, Spitsbergen, and Arctic Canada. Quaternary Research. 5, 263-273.

Mangini, A., Lomitschka, M., Eichstadter, R., Frank, N., Vogler, S. 1998. Coral provides way to age deep water. Nature. 392, 347-348.

Mariotti, A., Germon, J.C., Hubert, P., Kaiser, P., Letolle, R., Tardieux, A., Tardieux, P. 1981. Experimental determination of nitrogen kinetic isotope fractionation: some principles; illustration for the denitrification and nitrification processes. Plant and Soil. 62, 413-430.

Marschal, C., Garrabou, J., Harmelin, J.G., Pichon, M., 2004. A new method for measuring growth and age in the precious red coral *Corallium rubrum* (L.). Coral Reefs. 23, 423-432.

Marsh, R., Petrie, B., Weidman, C.R., Dickson, R.R., Loder, J.W., Hannah, C.G., Frank, K., Drinkwater, K. 1999. The 1882 tilefish kill – cold event in shelf waters off the north-eastern United States? Fisheries Oceanography. 8 (1), 29-49.

Marsh, R. 2000. Modeling changes in North Atlantic circulation under the NAO-minimum wind forcing of 1877-1881. Atmosphere-Ocean. 38, 367-393.

McConnaughey, T., McRoy, C.P. 1979. Food web structure and the fractionation of carbon isotopes in the Bering Sea. Marine Biology. 53, 257-262.

McConnaughey, T.A., 1989a. ^{13}C and ^{18}O isotope disequilibria in biological carbonates. 1. Patterns. Geochimica et Cosmochimica Acta. 53, 151-162.

McConnaughey, T.A., 1989b. ^{13}C and ^{18}O isotope disequilibria in biological carbonates. 2. In vitro simulation of kinetic isotope effects. Geochimica et Cosmochimica Acta. 53, 163-171.

McConnughey, T.A., 2003. Sub-equilibrium oxygen-18 and carbon-13 levels in biological carbonates: carbonate and kinetic models. Coral Reefs. 22, 316-327.

McClelland, J.W., Montoya, J.P. 2002. Trophic relationships and the nitrogen isotopic composition of amino acids in plankton. Ecology. 83, 2173–2180.

MERCINA (Marine Ecosystems Responses to Climate In the North Atlantic working group). Pershing, A.J., Greene, C.H., Hannah, C., Mountain, D.G., Sameoto, D., Head, E., Jossi, J.W., Benfield, M.C., Reid, P.C., Durbin, T.G. 2001. Oceanographic responses to climate in the Northwest Atlantic. Oceanography. 14, 76-82.

Minagawa, M., Wada, E. 1984. Stepwise enrichment of $\delta^{15}N$ along food chains: further evidence and the relation between ^{15}N and animal age. Geochimica et Cosmochimica Acta. 48, 1135–1140.

Mitterer, R.M., Kriausakul, N. 1989. Calculation of amino acid racemization rates based on apparent parabolic kinetics. Quaternary Science Reviews. 8, 353-357.

Montagna, P., McCulloch, M., Taviani, M., Remia, A., Rouse, G. 2005. High-resolution trace element compositions in deep-water scleractinian corals (*Desmophyllum dianthus*) from the Mediterranean Sea and the Great Australian Bight. In: Freiwald, A., Roberts, J.M. (Eds.), Cold-Water Corals and Ecosystems. Springer, Berlin, pp. 1109-1126.

Mortensen, P.B., Rapp, H.T., 1998. Oxygen and carbon isotope ratios related to growth line patterns in skeletons of Lophelia pertusa (L.) (Anthozoa, Sclleractinia): Implications for determination of linear extension rates. Sarsia. 83, 433-446.

Mousseau, L., Legendre, L., Fortier, L. 1996. Dynamics of size-fractionated phytoplankton and trophic pathways on the Scotian Shelf and at the shelf break, Northwest Atlantic. Aquatic Microbial Ecology. 10, 149-163.

Muzuka, A.N.N., Hillaire-Marcel, C. 1999. Burial rates of organic matter along the eastern Canadian margin and stable isotope constraints on its origin and diagenetic evolution. Marine Geology. 160: 251-270.

Nakatsuka, T., Handa, N., Wada, E., Wong, C.S. 1992. The dynamic changes of stable isotopic ratios of nitrogen and carbon in suspended and sedimented particulate organic matter during a phytoplankton bloom. Journal of Marine Research. 50, 267–296.

Needoba, J.A., Waser, N.A., Harrison, P.J., Calvert, S.E. 2003. Nitrogen isotope fractionation in 12 species of marine phytoplankton during growth on nitrate. Marine Ecology Progress Series. 255, 81-91.

Nydal, R., Brenkert, A.L. (ed), Boden, T.A. (ed) 1998. Carbon-14 measurements in surface water CO_2 from the Atlantic, Indian and Pacific Oceans, 1965-1994. ORNL/CDIAC-104, NDP-057A. Carbon dioxide information analysis center, Oak Ridge National Laboratory, Oak Ridge, Tennessee.

Orejas, C., Gili, J.M., Arntz, W. 2003. Role of small-plankton communities in the diet of two Antarctic octocorals (*Primnoisis antarctica* and *Primnoella* sp.). Marine Ecology Progress Series. 250, 105-116.

Ostrom, N.E., Macko, S.A., Deibel, D., Thompson, R.J. 1997. Seasonal variation in the stable carbon and nitrogen isotope biogeochemistry of a coastal cold ocean environment. Geochimica et Cosmochimica Acta. 61, 2929-2942.

Overpeck, J.T., Otto-Bleisner, B.L., Miller, G.H., Muhs, D.R., Alley, R.A., Kiehl, J.T. 2006. Paleoclimatic evidence for future ice-sheet instability and rapid sea-level rise. Science. 1747-1750.

Peña, M.A., Denman, K.L., Calvert, S.A., Thomson, R.E., Forbes, J.R. 1999. The seasonal cycle in sinking particle fluxes off Vancouver Island, British Columbia. Deep-Sea Research. II. 46, 2969-2992.

Pershing, A.J., Greene, C.H., Durbin, E.G., Head, E.J., Hakkinen, S., Mountain, D.G., Jossi, J.W., Runge, J.A., Bailey, B.A., Brodziak, J., Green, J.R., Incze, L.S., Kane, J., Kenney, R.D., O'Brien, L., Overholtz, W.J., Patrician, M.R., Pringle, J.M., Roberts, Y.L., Sameoto, D. Remote forcing of marine ecosystem dynamics in the Northwest Atlantic. Manuscript submitted to Science

Petrie, B. 1983. Current response at the shelf break to transient wind forcing. Journal of Geophysical Research. 88 (C14), 9567-9578.

Petrie, B., Drinkwater, K. 1993. Temperature and salinity variability on the Scotian Shelf and in the Gulf of Maine 1945-1990. Journal of Geophysical Research. 98 (C11), 20079-20089.

Petrie, B., Yeats, P. 1999. Annual and interannual variability of nutrients and their estimated fluxes in the Scotian Shelf – Gulf of Maine region. Canadian Journal of Fisheries and Aquatic Sciences. 57, 2536-2546.

Pickart, R.S., McKee, T.K., Torres, D.J., Harrington, S.A. 1999. Mean structure and interannual variability of the slopewater system south of Newfoundland. Journal of Physical Oceanography. 29, 2541-2558.

Polunin, N.V.C., Morales-Nin, B., Pawsey, W.E., Cartes, J.E., Pinnegar, J.K., Moranta, J. 2001. Feeding relationships in Mediterranean bathyal assemblages elucidated by stable nitrogen and carbon isotope data. Marine Ecology Progress Series. 220, 13-23.

Pons-Branchu, E., Hillaire-Marcel C., Deschamps P., Ghaleb B., Sinclair, D.J. 2005. Early diagenesis impact on precise U-series dating of deep-sea corals: Example of a 100–200-year old *Lophelia pertusa* sample from the northeast Atlantic. Geochimica et Cosmochimica Acta. 69, 4865-4879.

Popp, B.N., Laws, E.A., Bidigare, R.R., Dore, J.E., Hanson, K.L., Wakeham, S.G. 1998. Effect of phytoplankton cell geometry on carbon isotopic fractionation. Geochimica et Cosmochimica Acta. 62(1), 69–77.

Pyper, B.J., Peterman, R.M. 1998. Comparison of methods to account for autocorrelation in corrlelation analyses of fish data. Canadian Journal of Fisheries and Aquatic Sciences. 55, 2127-2140.

Quay, P., Tilbrook, B., Wong, C. 1992. Oceanic uptake of fossil fuel CO_2: Carbon-13 evidence. Science. 256, 74-79.

Radkiewicz, J.L., Zipse, H., Clarke, S. Houk, K.N. 1996. Accelerated racemization of aspartic acid and asparagine residues via succinimide intermediates: an ab initio theoretical exploration of mechanism. J. Am. Chem. Soc. 118, 9148-9155.

Rau, G.H., Takahashi, T., Des Marais, D.J., Repeta, D.J., Martin, J.H. 1992. The relationship between $\delta^{13}C$ of organic matter and [CO_2 (aq)] in ocean surface water: data from a JGOFS site in the northeast Atlantic Ocean and a model. Geochimica et Cosmochimica Acta. 56, 1413–1419.

Rau, G.H. 1994. Variations in sedimentary organic $\delta^{13}C$ as a proxy for past changes in ocean and atmospheric [CO2]. In: Zahn, R., Kamiski, M., Labeyrie, L.D., Pedersen, T.F. (Eds.), Carbon Cycling in the Glacial Ocean Constraints on the Ocean's Role in Global Climate Change. Springer, Berlin, pp. 307-322.

Rau, G.H., Ohman, M.D., Pierrot-Bults, A. 2003. Linking nitrogen dynamics to climate variability off central California: a 51 year record based on $^{15}N/^{14}N$ in CalCOFI zooplankton. Deep-Sea Research. II. 50, 2431-2447.

Reimer, P.J., Baillie, M.G.L., Bard, E., Bayliss, A., Beck, J.W., Bertrand, C.J.H., Blackwell, P.G., Buck, C.E., Burr, G.S., Cutler, K.B., Damon, P.E., Edwards, R.L., Fairbanks, R.G., Friedrich, M., Guilderson, T.P., Hogg, A.G., Hughen, K.A., Kromer, B., McCormac, F.G., Manning, S.W., Ramsey, C.B., Reimer, R.W., Remmele, S., Southon, J.R., Stuiver, M., Talamo, S., Taylor, F.W., van der Plicht, J., Weyhenmeyer, C.E. 2004. IntCal04 Terrestrial radiocarbon age calibration, 26 - 0 ka BP. Radiocarbon. 46, 1029-1058.

Remia, A., Taviani, M. 2004. Shallow-buried Pleistocene Madrepora-coral mounds on a muddy continental slope. Tuscan Archipelago, NE Tyrrhenian Sea. Facies. 50, doi: 10.1007/s10347-004-0029-2.

Ribes, M., Coma, R., Gili, J.M. 1999. Heterogeneous feeding in benthic suspension feeders: the natural diet and grazing rate of the temperate gorgonian *Paramuricea clavata* (Cnidaria: Octocorallia) over a year cycle. Marine Ecology Progress Series. 183, 125-137.

Ribes, M., Coma, R., Rossi, S. 2003. Natural feeding of the temperate asymbiotic octocoral-gorgonian *Leptogorgia sarmentosa* (Cnidaria: Octocorallia). Marine Ecology Progress Series. 254, 141-150.

Richardson, P.L. 1977. On the crossover between the Gulf Stream and the Western Boundary Undercurrent. Deep-Sea Research. 24, 139-159.

Risk, M.J., Heikoop, J.M., Snow, M.G., Beukens, R., 2002. Lifespans and growth patterns of two deep-sea corals: *Primnoa resedaeformis* and *Desmophyllum cristagalli*. Hydrobiologia. 471, 125-131.

Risk, M.J., Hall-Spenser, J. and B. Williams. 2005. Climate records from the Faroe-Shetland Channel using *Lophelia pertusa* (Linnaeus, 1758). In: Freiwald, A., Roberts, J.M. (Eds.), Cold-Water Corals and Ecosystems. Springer, Berlin, pp. 1097-1108.

Roark, E.B., Guilderson, T.P., Flood-Page, S., Dunbar, R.B., Ingram, B.L., Fallon, S.J., McCulloch, M., 2005. Radiocarbon-based ages and growth rates of bamboo corals from the Gulf of Alaska. Geophysical Research Letters. 32, L04606. doi:10.1029/2004GL021919.

Robinson, L.F., Adkins, J.F., Keigwin, L.D., Southon, J., Fernandez, D.P., Wang, S.-L., Scheirer, D.S. 2005. Radiocarbon variability in the Western North Atlantic during the Holocene. Science. 310, 1469-1473.

Robinson, L.F., Adkins, J.F., Fernandez, D.P., Burnett, D.S., Wang, S.-L., Gagnon, A.C., Krakauer, N. 2006. Primary U distribution in scleractinian corals and its implications for U series dating. Geochemistry Geophysics Geosystems. 7, Q05022.

Rollion-Bard, C., Blamart, D., Cuif, J.-P., 2003. Microanalysis of C and O isotopes of azooxanthellate and zooxanthellate corals by ion microprobe. Coral Reefs. 22, 405-415.

Rossi, S., Ribes, M., Coma, R., Gili, J-M. 2004. Temporal variability in zooplankton prey capture rate of the passive suspension feeder *Leptogorgia sarmentosa* (Cnidaria: Octocorallia), a case study. Marine Biology. 144, 89-99.

Saino, T., Hattori, A. 1987. Geographical variation in the water column distribution of suspended particulate organic nitrogen and its ^{15}N natural abundance in the Pacific and its marginal seas. Deep-Sea Research. I. 34, 807-827.

Sameoto, D. 2001. Decadal changes in phytoplankton color index and selected calanoid copepods in continuous plankton recorder data from the Scotian Shelf. Canadian Journal of Fisheries and Aquatic Sciences. 58, 749-761.

Sarnthein, M., Winn, K., Jung, S.J.A., Duplessy, J.-C., Labeyrie, L., Erlenkeuser, H., Ganssen, G. 1994. Changes in east Atlantic deepwater circulation over the last 30,000 years: Eight time slice reconstructions. Paleoceanography. 9, 209-267.

Satterfield, F.R. IV, Finney, B.P. 2002. Stable isotope analysis of Pacific salmon: insight into trophic status and oceanographic conditions over the last 30 years. Progress in Oceanography. 53, 231-246.

Schell, D.M. 2000. Declining carrying capacity in the Bering Sea: isotopic evidence from whale baleen. Limnology and Oceanography. 45, 459–462.

Schlitzer, R., 2004. Ocean Data View, http://www.awi-bremerhaven.de/GEO/ODV.

Schröder-Ritzrau, A., Mangini, A., Lomitschka, M. 2003. Deep-sea corals evidence periodic reduced ventilation in the North Atlantic during the LGM/Holocene transition. Earth and Planetary Science Letters. 216, 399-410.

Schröder-Ritzrau, A., Freiwald, A., Mangini, A. (2005) U/Th-dating of deep-water corals from the eastern North Atlantic and the weatern Mediterranean Sea. In: Freiwald, A., Roberts, J.M. (Eds.), Cold-Water Corals and Ecosystems. Springer, Berlin, pp. 157-172.

Scott, D.B., Mudie, P.J., Vilks, G., Younger, C. 1984. Latest Pleistocene-Holocene paleoceanographic trends on the continental margin of eastern Canada: foraminiferal, dinoflagellate and pollen evidence. Marine Micropaleontology. 9, 181-218.

Scott, D.B., Baki, V., Younger, C. 1989. Late Pleistocene-Holocene paleoceanographic changes on the eastern Canadian continental margin. Palaeogeography Palaeoclimatology Palaeoecology. 74, 279-295.

Scott, D.B., Risk, M.J., 2003. End moraines on the upper Scotian Slope: Relationship to deep-sea coral and fish habitats. Abstracts of the 2nd International Symposium on Deep-Sea Corals, Erlangen, Germany. p. 78.

Shackleton, N.J. 1967, Oxygen isotope analyses and Pleistocene temperatures reassessed. Nature. 215, 15–17.

Shen, G.T., Boyle, E.A. 1987. Lead in corals—reconstruction of historical industrial fluxes to the surface ocean. Earth and Planetary Science Letters. 82, 289–304.

Shen, G.T., Boyle, E.A. 1988. Determination of lead, cadmium, and other trace metals in annually-banded corals. Chemical Geology. 67, 47-62.

Sherwood, G.D., Rose, G.A. 2005. Stable isotope analysis of some representative fish and invertebrates of the Newfoundland and Labrador continental shelf food web. Estuarine Coastal and Shelf Science. 63, 537-549.

Sherwood, O.A. 2002. The deep-sea gorgonian coral *Primnoa resedaeformis* as an oceanographic monitor. M.Sc. thesis, McMaster University, Hamilton, Canada. 65 pp.

Sherwood, O.A., Scott, D.B., Risk, M.J., Guilderson, T.P. 2005a. Radiocarbon evidence for annual growth rings in the deep-sea octocoral *Primnoa resedaeformis*. Marine Ecology Progress Series. 301. 129-134.

Sherwood, O.A., Heikoop, J.M., Scott, D.B., Risk, M.J., Guilderson, T.P., McKinney, R.A. 2005b. Stable isotopic composition of deep-sea gorgonian corals *Primnoa* spp.: a new archive of surface processes. Marine Ecology Progress Series. 301, 135-148.

Sherwood, O.A., Heikoop, J.M., Sinclair, D.J., Scott, D.B., Risk, M.J., Shearer, C., Azetsu-Scott, K. 2005c. Skeletal Mg/Ca in Primnoa resedaeformis: relationship to temperature? In: Freiwald, A., Roberts, J.M. (Eds.), Cold-Water Corals and Ecosystems. Springer, Berlin, pp. 1061-1079.

Sherwood, O.A., Scott, D.B., Risk, M.J. 2006. Late Holocene radiocarbon and aspartic acid racemization dating of deep-sea octocorals. Geochimica et Cosmochimica Acta. 70, 2806-2814.

Shirai, K., Kusakabe, M., Nakai, S., Ishii, T., Watanabe, T., Hiyagon, H., Sano, Y., 2005. Deep-sea coral geochemistry: Implication for the vital effect. Chemical Geology. 224, 212-222.

Sigman, D.M., Altabet, M.A., McCorkle, D.C., Francois, R., Fischer, G. 2000. The $\delta^{15}N$ of nitrate in the Southern Ocean: Nitrogen cycling and circulation in the ocean interior. Journal of Geophysical Research. 105(C8), 19599-19614.

Sigman, D.M., Casciotti, K.L., Andreani, M., Barford, C., Galanter, M., Bohlke, J.K. 2001. A bacterial method for the nitrogen isotopic analysis of nitrate in seawater and freshwater. Analytical Chemistry. 73, 4145-4153.

Sinclair, D.J., 2005.Correlated trace element "vital effects" in tropical corals: A new geochemical tool for probing biomineralization. Geochimica et Cosmochimica Acta. 69, 3265-3284.

Sinclair, D.J., Sherwood, O.A., Risk, M.J., Hillaire-Marcel, C., Tubrett, M., Sylvester, P., McCulloch, M., Kinsley, L. 2005. Testing the reproducibility of Mg/Ca profiles in the deep-water coral *Primnoa resedaeformis*: putting the proxy through its paces. In: Freiwald, A., Roberts, J.M. (Eds.), Cold-Water Corals and Ecosystems. Springer, Berlin, pp. 1039-1060.

Sinclair, D.J., Williams, B., Risk, M.J., McCulloch, M.T. Trace-element "vital effects" - a ubiquitous feature of scleractinian coral skeletons. Manuscript submitted to Science, Dec 2005.

Sinclair, D.J., Risk, M.J. A numerical model of trace-element co-precipitation in a physicochemical calcification system: Application to coral biomineralization and trace element 'vital effects'. Geochimica et Cosmochimica Acta. (in press).

Smith, J.E., Risk, M.J., Schwarcz, H.P., McConnaughey, T.A., 1997. Rapid climate change in the North Atlantic during the Younger Dryas recorded by deep-sea corals. Nature. 386, 818-820.

Smith, J.E., Schwarcz, H.P., Risk, M.J., McConnaughey T.A., and N. Keller. 2000. Paleotemperatures from deep-sea corals: overcoming "vital effects". Palaois. 15, 25-32.

Smith, J.E., Schwarcz, H.P., Risk, M.J. 2002. Patterns of isotopic disequilibria in azooxanthellate coral skeletons. Hydrobiologia. 471, 111-115.

Smith, P.C., Houghton, R.W., Fairbanks, R.G., Mountain, D.G. 2001. Interannual variability of boundary fuxes and water mass properties in the Gulf of Maine and on Georges Bank: 1993-97. Deep-Sea Research. II. 48, 37-70.

Sorauf, J.E., Jell, J.S., 1977. Structure and incremental growth in the ahermatypic coral *Desmophyllum cristagalli* from the North Atlantic. Palaeontology. 20, 1-19.

Stuiver, M., Polach, H.A. 1977. Discussion: Reporting of ^{14}C data. Radiocarbon. 19, 355-363.

Stuiver, M., Braziunas, T.F. 1993. Modeling atmospheric ^{14}C influences and ^{14}C ages of marine samples to 10,000 BC. Radiocarbon, 35, 137-189.

Stuiver, M. Reimer, P.J. 1993. Extended ^{14}C database and revised CALIB radiocarbon calibration program. Radiocarbon. 35, 215-230. (version 5 available online at http://radiocaron.pa.qub.ac.uk/calib/).

Stuiver, M., Quay, P.D., Ostlund, H.G. 1983. Abyssal C-14 distribution and the age of the world oceans. Science. 219. 849-851.

Surge, D.M., Lohmann, K.C., Goodfriend, G.A. 2003. Reconstructing estuarine conditions: oyster shells as recorders of environmental change, Southwest Florida. Estuarine Coastal and Shelf Science. 57: 737-756.

Swart, P.K., Hubbard, J.A.E.B. 1982. Uranium in scleractinian coral skeletons. Coral Reefs. 1: 13-19.

Swart, P.K., Thorrold, S., Eisenhauer, A., Rosenheim, B., Harrison, C.G.A., Grammer, M., Latkoczy, C. 2002. Intra-annual variation in the stable oxygen and carbon and trace element composition of sclerosponges. Paleoceanography. 17(3), 1029/2000PA000622.

Szmant-Froelich, A. 1974. Structure, iodination, and growth of the axial skeletons of *Muricea californica* and *M. fruticosa* (Coelenterata: Gorgonacea). Marine Biology. 27, 299-306.

Tanaka, N., Monaghan, M.C., Turekian, K.K. 1990. $\Delta^{14}C$ balance for the Gulf of Maine, Long Island Sound and the Middle Atlantic Bight: Evidence for the extent of Antarctic Intermediate Water contribution. Journal of Marine Research. 48, 75-87.

Teichert, C., 1958. Cold- and deep-water coral banks. AAPG Bulletin. 42, 1064-1082.

Thomas, A.C., Townsend, D.W., Weatherbee, R. 2003. Satellite-measured phytoplankton variability in the Gulf of Maine. Continental Shelf Research. 23, 971-989.

Thresher, R., Rintoul, S.R., Koslow, J.A., Weidman, C., Adkins, J., Proctor, C., 2004. Oceanic evidence of climate change in southern Australia over the last three centuries. Geophysical Reseach Letters. 31, L07212. doi:10.1029/2003GL018869.

Thunell, R.C., Sigman, D.M., Muller-Karger, F., Astor, Y., Varela, R. 2004. Nitrogen isotope dynamics of the Cariaco Basin, Venezuela. Global Biogeochemical Cycles. 18, GB3001. doi:10.1029/2003GB002185.

Tieszen, L.L., Boutton, T.W., Tesdahl, K.G., Slade, N.A. 1983. Fractionation and turnover of stable carbon isotopes in animal tissues: implications for ^{13}C analysis of diet. Oecologia. 57, 32–37.

Titschak, J., Freiwald, A. 2005. Growth, deposition and facies of Pleistocene bathyal coral communities from Rhodes, Greece. In: Freiwald, A., Roberts, J.M. (Eds.), Cold-Water Corals and Ecosystems. Springer, Berlin, pp. 41-59.

Townsend, D.W., Pettigrew, N.R. 1997. Nitrogen limitation of secondary production on Georges Bank. J. Plankton Res. 19, 221-235.

Townsend, D.W., Thomas, A.C., Mayer, L.M., Thomas, M., Quinlan, J. 2006. Oceanography of the Northwest Atlantic Continental Shelf. In: Robinson, A.R. and K.H. Brink (eds). The Sea, Volume 14, Harvard University Press. pp. 119-168.

Tudhope, A.W., Chilcott, C.P., McCulloch, M.T., Cook, E.R., Chappell, J., Ellam, R.M., Lea, D.W., Lough, J.M., Shimmield, G.B., 2001. Variability in the El Niño-Southern oscillation through a glacial-interglacial cycle. Science. 291, 1511-1517.

Tunnicliffe, V. 2000. A fine-scale record of 130 years of organic carbon deposition in an anoxic fjord, Saanich Inlet, British Columbia. Limnology and Oceanography. 45, 1380-1387.

Vander Zanden, M.J., Cabana, G., Rasmussen, J.B. 1997. Comparing trophic position of freshwater fish calculated using stable nitrogen isotope ratios ($\delta^{15}N$) and literature dietary data. Canadian Journal of Fisheries and Aquatic Sciences. 54, 1142–1158.

Vander Zanden, M.J., Rasmussen, J.B. 2001. Variation in $\delta^{15}N$ and $\delta^{13}C$ trophic fractionation: Implications for aquatic food web studies. Limnology and Oceanography. 46, 2061-2066.

Voss. M., Altabet, M.A., Bodungen. B.V. 1996. $\delta^{15}N$ in sedimenting particles as indicator of euphotic zone processes. Deep-Sea Research. I. 43, 33-47.

Wainwright, S.A., Dillon, J. 1969. On the orientation of sea fans (genus Gorgonia). Biological Bulletin. 136, 130-139.

Wainright, S.C., Fogarty, M.J., Greenfield, R.C., Fry, B. 1993. Long-term changes in the Georges Bank food web: trends in stable isotopic compositions of fish scales. Marine Biology. 115, 481-493.

Ward-Paige, C.A., Risk, M.J., Sherwood, O.A. 2005. Reconstruction of nitrogen sources on coral reefs: $\delta^{15}N$ and $\delta^{13}C$ in gorgonians from the Florida Reef Tract. Marine Ecology Progress Series. 296, 155–163.

Watling, L., Norse, E.A. 1998. Disturbance of the seabed by mobile fishing gear: a comparison to forest clearcutting. Conservation Biology. 12(6), 1180-1197.

Weber J.N. 1973. Deep-sea scleractinian coral: isotopic composition of skeleton. Deep-Sea Research. II, 901-909.

Weidman, C.R., Jones, G.A. 1993. A shell-derived time history of bomb ^{14}C on Georges Bank and its Labrador Sea implications. Journal of Geophysical Research. 98 (C8), 14577-14588.

Weinbauer, M.G., Brandstätter, F., Velimirov, B. 2000. On the potential use of magnesium and strontium concentrations as ecological indicators in the calcite skeleton of the red coral (*Corallium rubrum*). Marine Biology. 137: 801-809.

Williams, B., Risk M.J., Sulak K., Ross S. and R. Stone. 2005. Deep-water Antipatharians and Gorgonians: proxies of biogeochemical processes. Proceedings of the 3rd International Symposium on Deep-Sea Corals. Miami, USA, pp. 70.

Wisshak, M., Freiwald, A., Lundälv, T., Gektidis, M., 2005. The physical niche of the bathyal *Lophelia pertusa* in a non-bathyal setting: environmental controls and

paleoecological implications In: Freiwald, A., Roberts, J.M. (Eds.), Cold-Water Corals and Ecosystems. Springer, Berlin, pp. 979-100.

Woodworth, M., Goni, M., Tappa, E., Tedesco, K., Thunell, R., Astor, Y., Varela, R., Diaz-Ramos, J.R., Muller-Karger, F. 2004. Oceanographic controls on the carbon isotopic compositions of sinking particles from the Cariaco basin. Deep-Sea Research. I. 51, 1955-1974.

Worm, B., Myers, R.A. 2003. Meta-analysis of cod-shrimp interactions reveals top-down control in oceanic food webs. Ecology. 84, 162-173.

Wu, J., Boyle, E.A. 1997. Lead in the western North Atlantic Ocean: completed response to leaded gasoline phaseout. Geochimica et Cosmochimica Acta. 61, 3279-3283.

Wu, J., Calvert, S.E., Wong, C.S. 1997. Nitrogen isotope variations in the subarctic northeast Pacific: relationships to nitrate utilization and trophic structure. Deep-Sea Research. I. 44, 287-314.

Wu, J., Calvert, S.E., Wong, C.S. 1999a. Carbon and nitrogen isotope ratios in sedimenting particulate organic matter at an upwelling site off Vancouver Island. Estuarine Coastal and Shelf Science. 48, 193–203.

Wu, J., Calvert, S.E., Wong, C.S., Whitney, F.A. 1999b. Carbon and nitrogen isotopic composition of sedimenting particulate material at Station Papa in the subarctic northeast Pacific. Deep-Sea Research. II. 46, 2793-2832.

Appendix A
Photographs of Coral Sections

COHPS2001-2

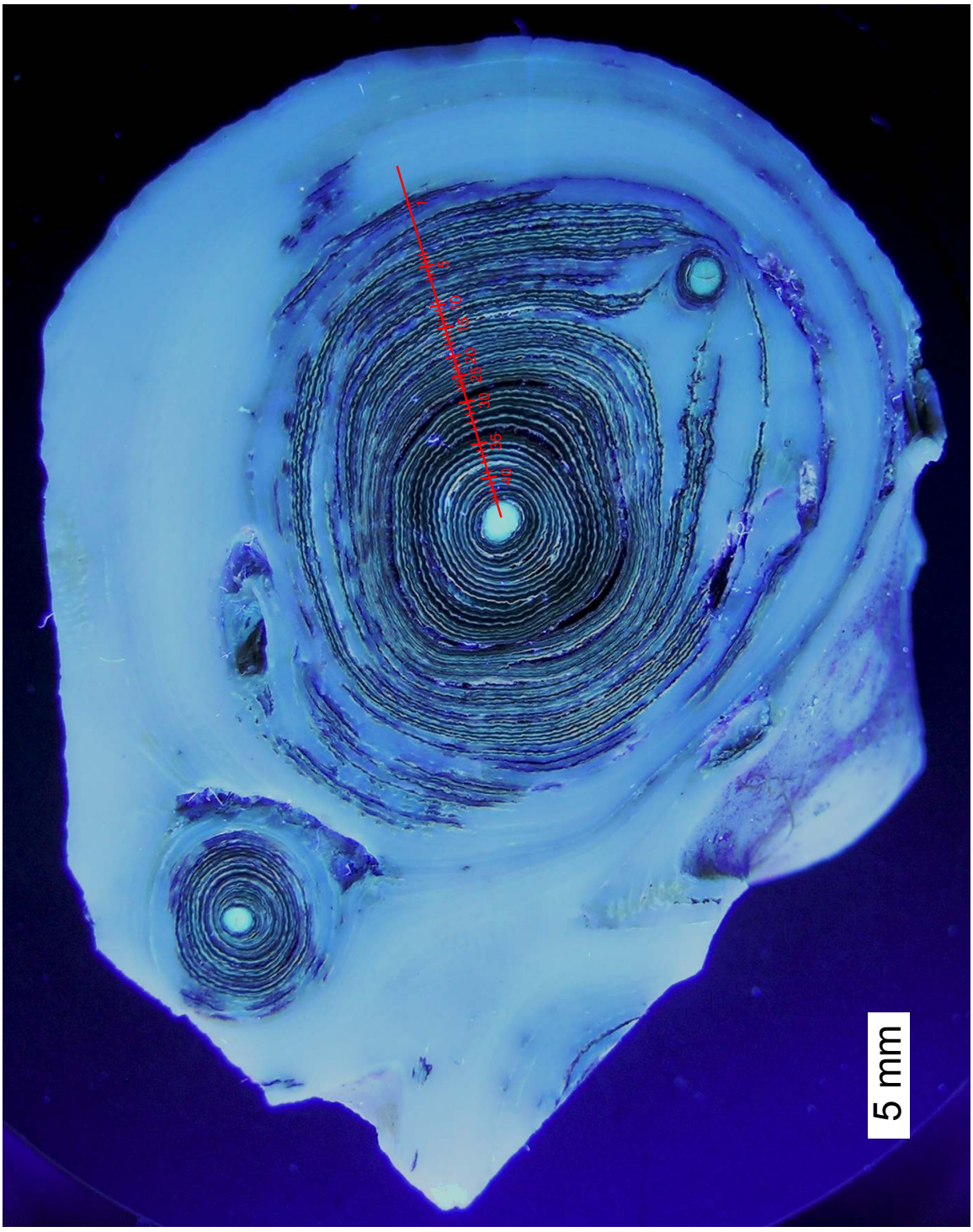

DFO-2002-con5-A4

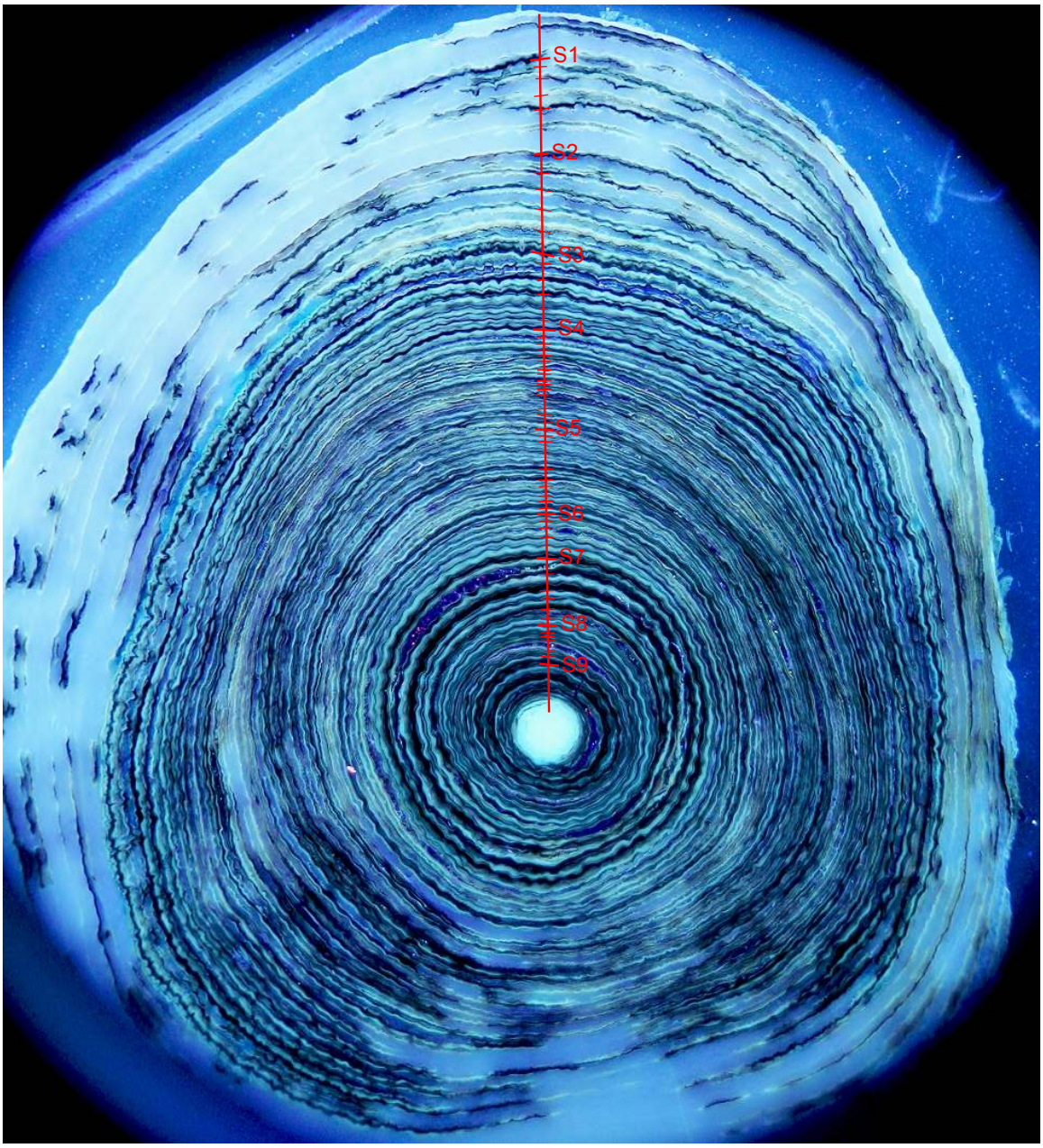

Fossil-95

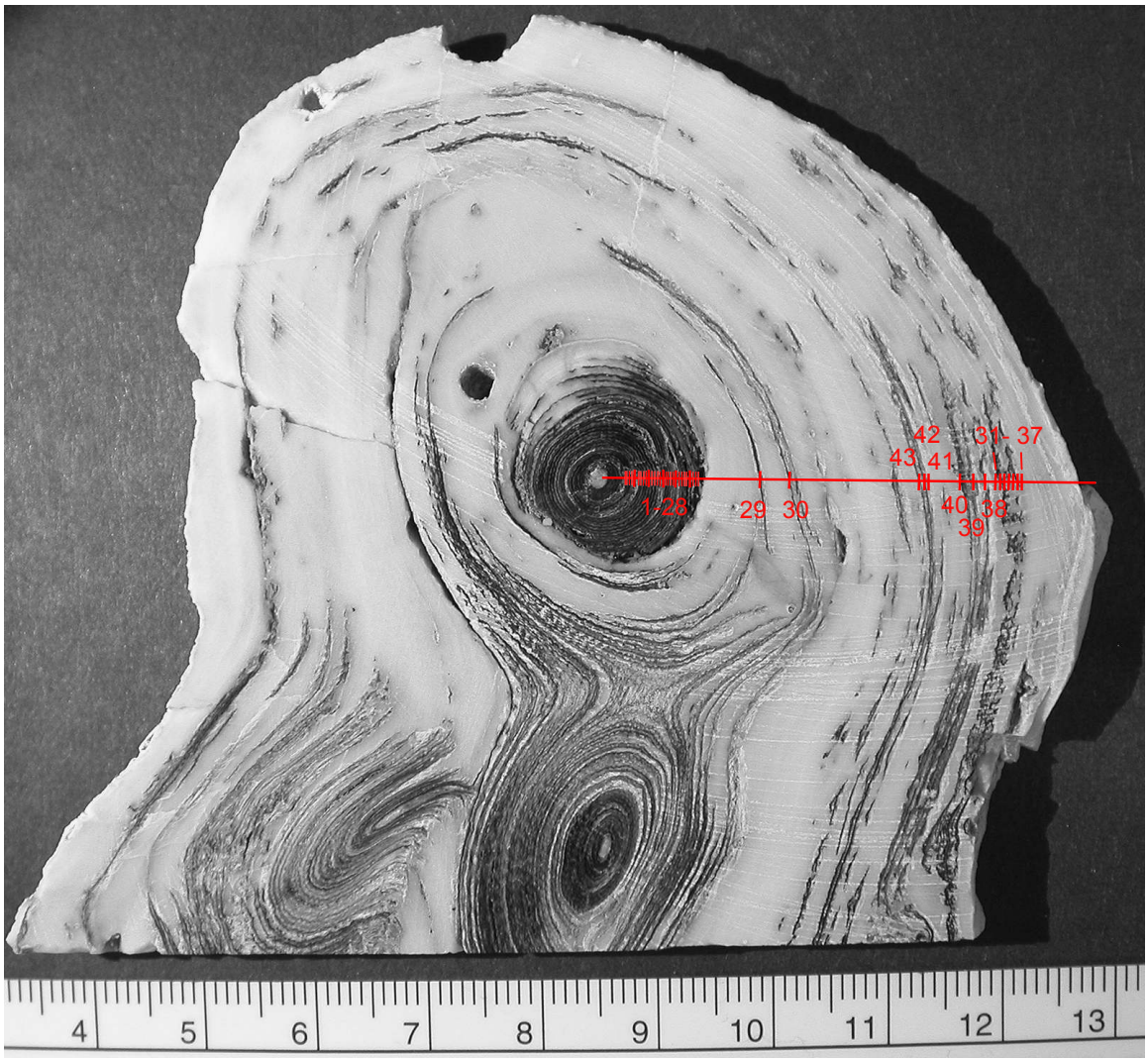

HUD-2000-020-VG2-E

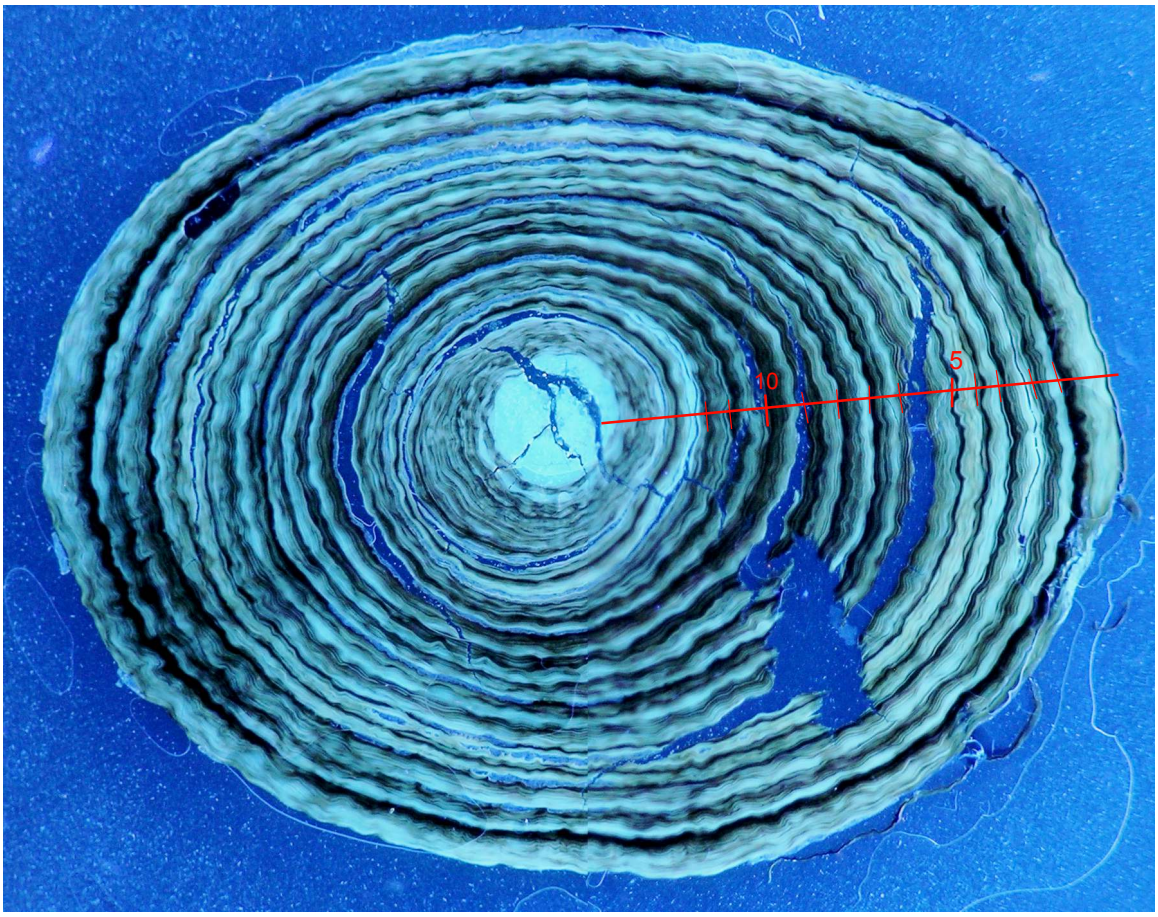

HUD-2001-VG15-A1

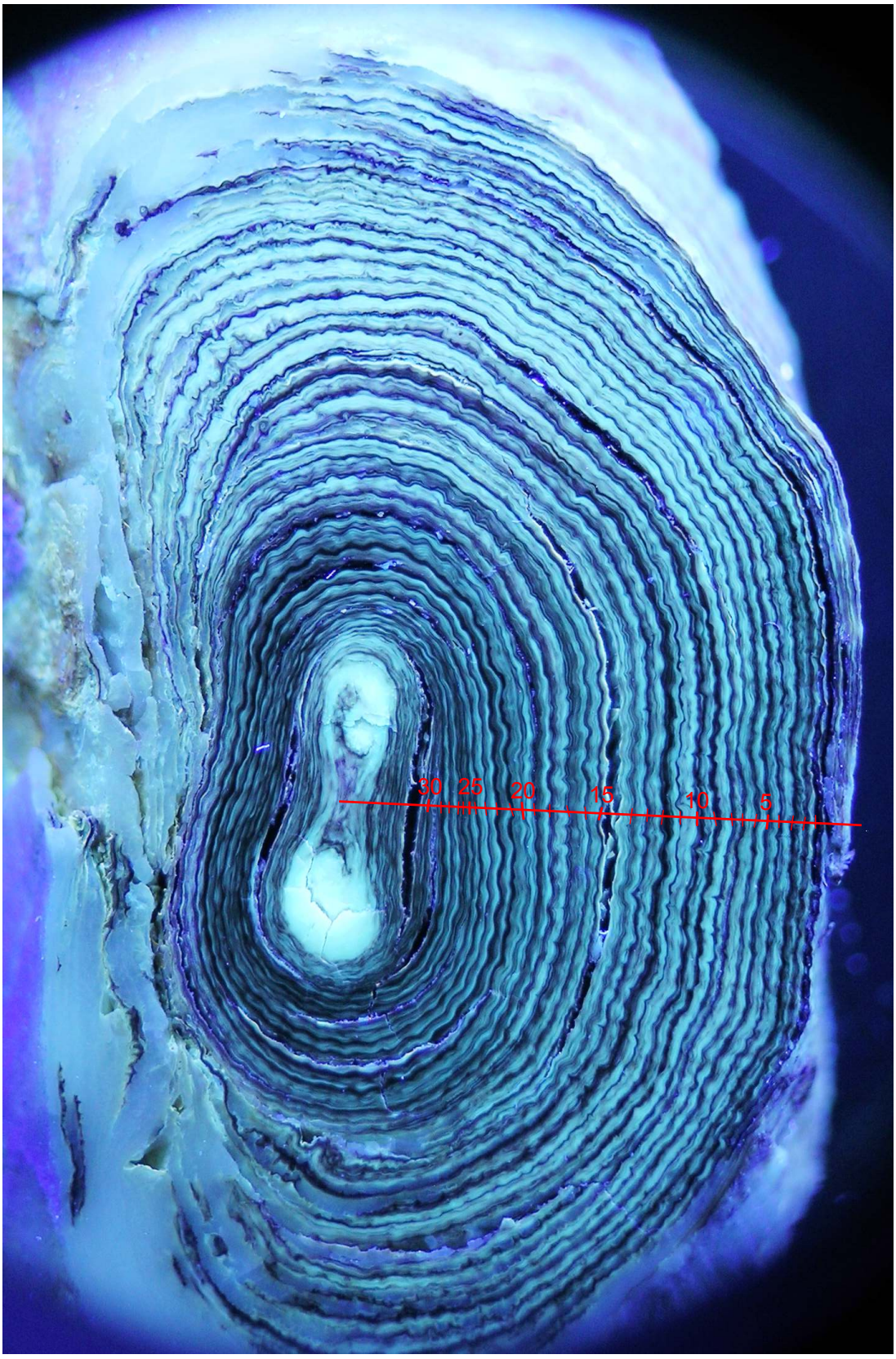

NED-2002-37-1A

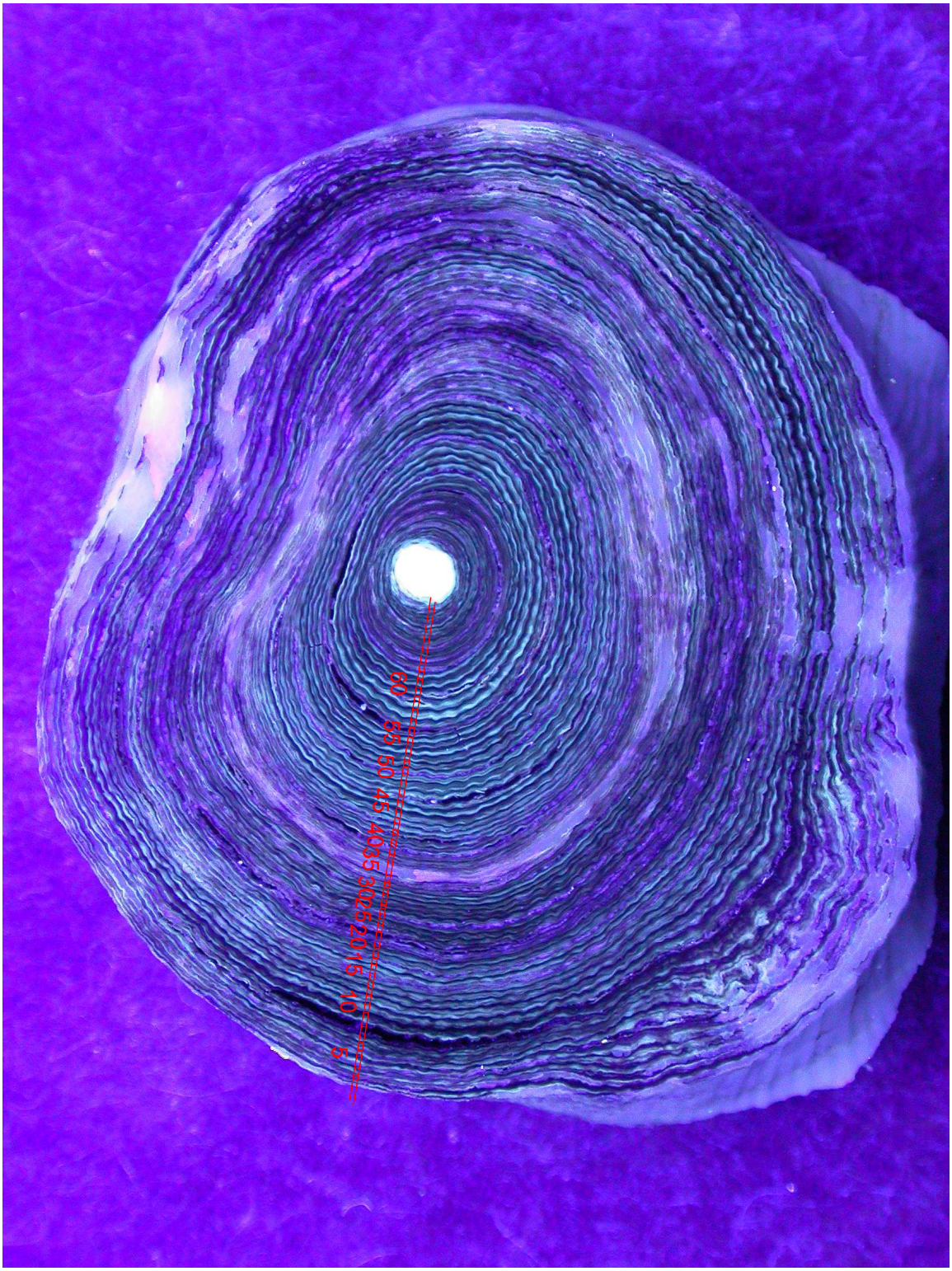

ROPOS 639009-C4

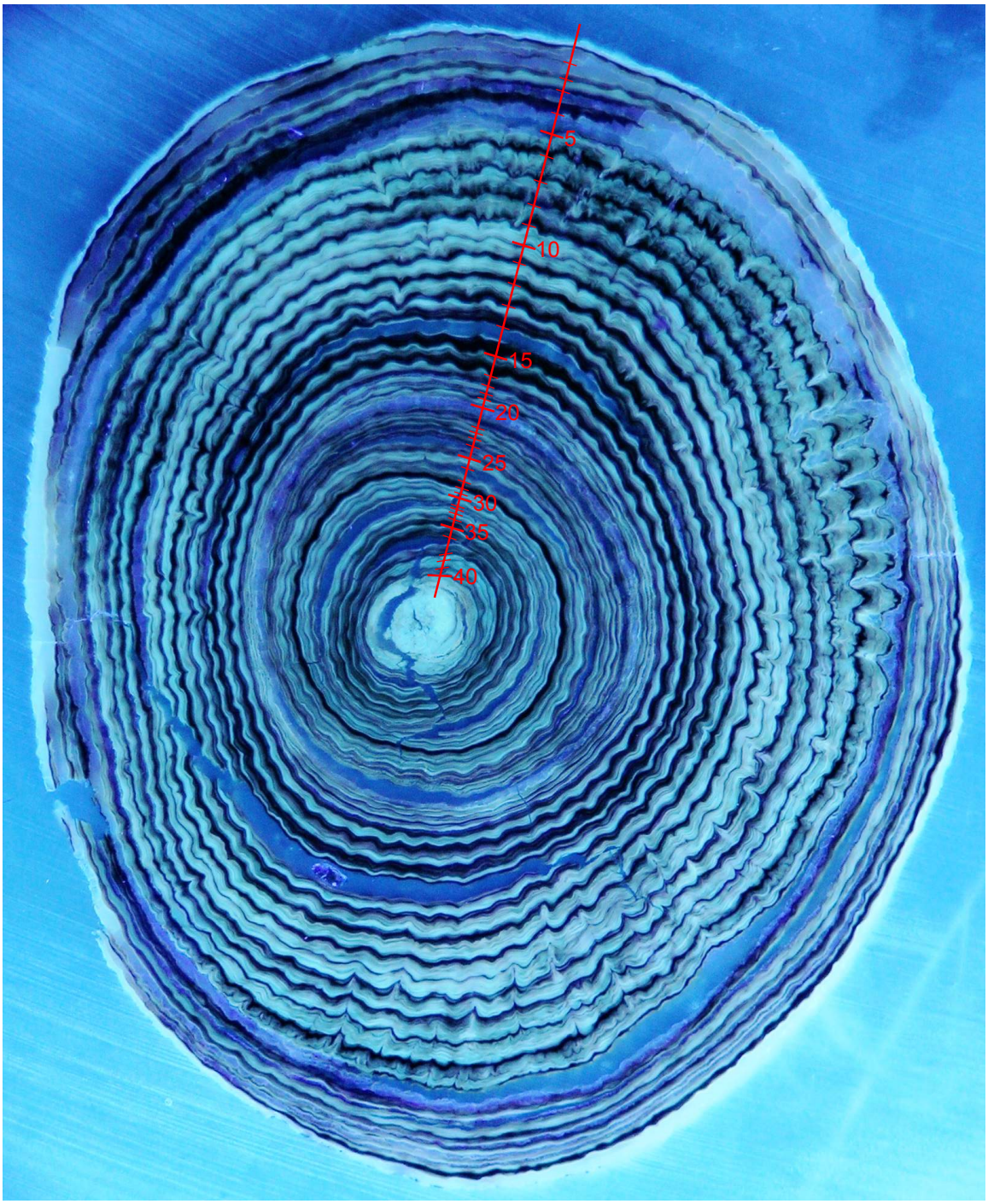

ROPOS 6400013-E1

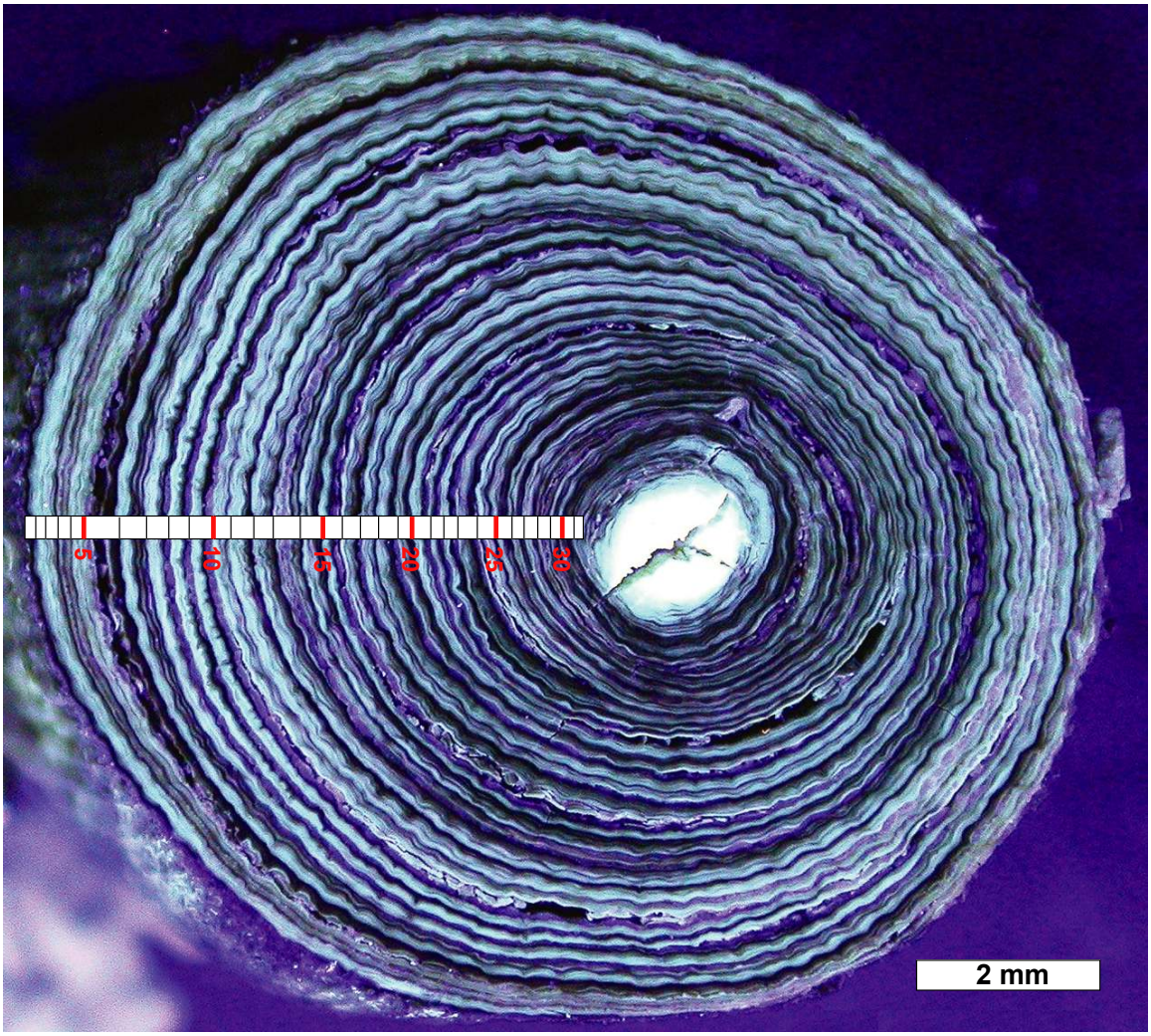

R6400016-A

Appendix B
C-14 Data

CENTER FOR ACCELERATOR MASS SPECTROMETRY
Lawrence Livermore National Laboratory

1) $\delta^{13}C$ values are the assumed values according to Stuiver and Polach (Radiocarbon, v. 19, p.355, 1977) when given without decimal places. Values measured for the material itself are given with a single decimal place.
2) The quoted age is in radiocarbon years using the Libby half life of 5568 years and following the conventions of Stuiver and Polach (ibid.).
3) Radiocarbon concentration is given as fraction Modern, $\Delta^{14}C$, and conventional radiocarbon age.
4) Sample preparation backgrounds have been subtracted, based on measurements of samples of 14C-free coal.

CAMS #	Sample Name	d13C	Fraction Modern	±	Δ14C	±	14C age	±
DATE:	June 8 2003							
97097	con5A1 005b	-17	1.043	0.004	36.360	4.487	>Modern	
97098	con5A1 010b	-17	1.059	0.004	51.802	4.029	>Modern	
97099	con5A1 016b	-17	1.078	0.004	71.279	3.957	>Modern	
97100	con5A1 021b	-17	1.066	0.004	58.969	3.825	>Modern	
97101	con5A1 025b	-17	0.959	0.003	-46.747	3.450	335	30
97102	con5A1 031b	-17	0.929	0.003	-77.316	3.312	595	30
97103	con5A1 037b	-17	0.926	0.003	-80.310	3.316	620	30
97104	con5A1 043b	-17	0.934	0.003	-71.589	3.349	545	30
97105	con5A1 050b	-17	0.929	0.003	-77.042	3.391	595	30
97106	con5A1 058b	-17	0.934	0.003	-72.262	3.411	550 581	30
DATE:	June 23 2003							
97759	E02 #1&2	0	0.924	0.004	-82.296	4.219	640	40
97760	E02 #3&4	0	0.917	0.004	-89.050	4.323	700	40
97761	E02 #5&6	0	0.900	0.006	-106.231	5.921	850	60
97762	E02 #7&8	0	0.919	0.004	-86.856	3.946	680	35
97763	E02 #9&10	0	0.908	0.007	-97.715	6.769	770	60
97764	E02 #11&12	0	0.916	0.004	-89.855	4.390	705	40
97765	E02 #13&14	0	0.925	0.004	-80.597	4.130	625	40
97766	E02 #15&16	0	0.907	0.005	-98.934	5.380	785	50
97767	E02 #17&18	0	0.917	0.004	-88.500	4.064	695	40
97768	E02 #19&20	0	0.901	0.004	-104.705	4.487	835	40
97769	E02 #21&22	0	0.925	0.004	-80.766	4.100	625	40
97771	E02 #25-28	0	0.934	0.004	-71.879	3.686	550	35
97772	E02 #29	0	0.914	0.006	-91.360	6.173	720	60

97773	E02 #39&40	0	0.984	0.004	-22.663	4.371	135	40
DATE:	Nov 3 2004							
111130	COHPS2001-1A1-2	-17	0.932	0.004	-74.178	3.529	565	35
111131	COHPS2001-1A1-5	-17	0.926	0.004	-80.324	3.504	620	35
111132	COHPS2001-1A1-16	-17	0.919	0.003	-87.207	3.478	680	35
111133	COHPS2001-1E2-1	-17	1.043	0.004	36.471	3.948	>Modern	
111134	COHPS2001-2D2-43	-17	0.923	0.003	-82.861	3.495	640	35
111135	COHPS2003-1A2-35	-17	0.936	0.004	-70.072	3.544	530	35
111136	COHPS2003-2A2-39	-17	0.929	0.003	-77.388	3.239	595	30
111137	Fossil95-D2-4	-17	0.756	0.003	-248.527	3.408	2245	40
111138	Fossil95-D2-38	-17	0.809	0.003	-196.245	3.057	1700	35
111139	HUDVG13-22	-17	1.066	0.004	58.816	4.081	>Modern	
111140	HUDVG15-A3-10	-17	1.074	0.004	67.085	4.053	>Modern	
111141	R6400013-E1-15	-17	1.061	0.004	54.348	3.698	>Modern	
111142	HUDVG15-A3-19	-17	1.097	0.004	89.910	4.140	>Modern	
111143	HUDVG15-A3-26 28	-17	0.988	0.005	-18.247	4.505	95	40
DATE:	Nov 21 2004							
111328	NED2002-371A-1	-17	1.039	0.004	32.608	4.497	>Modern	
111329	NED2002-371A-16	-17	1.075	0.005	67.674	4.808	>Modern	
111330	NED2002-371A-58	-17	0.924	0.004	-81.710	3.513	630	35
111331	NED2002-37-51-25	-17	1.070	0.004	63.180	4.064	>Modern	
DATE:	Dec 6 2004							
111623	R639009C4-19	-17	1.089	0.004	81.977	4.060	>Modern	
111624	R639009C4-27 28	-17	0.960	0.004	-46.458	3.970	330	35
111625	R639009C4-40	-17	0.936	0.003	-70.472	3.492	535	30
111626	R6400013-E1-10	-17	1.059	0.004	52.132	4.172	>Modern	
111627	R6400013-E1-20	-17	1.074	0.005	66.674	5.367	>Modern	
111628	R6400013-E1-25	-17	1.068	0.004	60.913	3.984	>Modern	
111629	R6400013-E1-31	-17	1.089	0.004	81.999	4.421	>Modern	
111630	R6400016-1A3-55	-17	0.925	0.004	-80.880	3.973	625	35
DATE:	Nov 22 2005							
120203	COHPS2001 14B2 6	-17	1.059	0.004	52.255	4.478	>Modern	
120204	COHPS2001 14B2 7	-17	0.980	0.004	-26.979	3.771	165	35

Appendix C
Stable Isotope and C:N Data

GEOTOP STABLE ISOTOPE AND C:N RESULTS
GORGONIN SAMPLES FOR TIMESERIES RECORDS:

COHPS2001-1A1

Band ID	d13C	d15N	C:N
1	-19.03	10.50	3.43
2	-18.04	10.43	nd
2	-18.16	10.53	nd
5	-16.75	10.47	nd
6-7	-18.22	10.50	nd
8-9	-17.91	11.41	nd
10-12	-17.51	11.32	nd
13-15	-17.72	11.57	nd
S1, S1-1,-2,-3	-18.01	11.73	nd
S2+2, +3	-17.81	10.91	nd
S2, S2+1	-18.05	11.20	3.31
S2-1, -2, -3	-17.68	10.72	nd
S3+2, +3	-16.74	10.42	nd
S3+2, +3	-16.90	10.44	nd
S3, S3+1	-17.56	10.10	nd
S3-1	-17.79	10.51	nd
S4+1, +2, +3	-18.20	11.22	nd
S4	-18.20	11.16	nd
S4-1	-18.08	10.44	nd
S4-2	-17.55	11.06	3.50
S4-2rep	-17.78	11.37	nd

COHPS2001-2D2

Band no.	d13C	d15N	C:N
1	-18.47	11.09	nd
2	-18.64	10.72	nd
3	-18.80	11.14	nd
4	-19.02	10.60	nd
5	-18.95	10.72	nd
6,7	-17.49	10.37	nd
8	-18.22	10.53	nd
9	-18.37	11.08	nd
10	-18.54	11.13	nd
11	-17.82	11.72	nd
12,13	-18.01	10.65	nd
14	-18.16	10.58	nd
15,16	-18.50	11.36	nd
17	-17.85	10.51	nd
18	-18.13	10.53	nd
19,20	-18.12	11.13	nd
21,22	-17.32	11.11	nd
23	-17.94	11.55	nd
24	-18.01	11.30	nd

25	-18.40	11.47	nd	
26	-18.32	11.43	nd	
27,28	-18.09	11.55	nd	
28,30	-18.93	10.81	nd	
31	-18.87	10.78	nd	
32	-18.67	10.48	nd	
33	-18.00	10.26	nd	
34	-18.62	10.10	nd	
35	-17.81	9.90	nd	
36	-18.54	10.02	nd	
37	-19.03	10.42	nd	
38	-18.48	10.47	nd	
39	-18.45	10.41	nd	
40	-18.28	10.45	nd	
41	-18.84	10.52	nd	
42	-17.93	10.48	nd	
43	-18.13	10.31	nd	
44	-18.80	10.23	nd	

DFO2002- con5A1

Band no.	d13C	d15N	C:N	Equiv. Index Band
1	-20.21	9.79	nd	
2	-19.68	9.70	nd	
3	-19.70	9.86	nd	
4	-19.73	9.76	nd	
5	-19.55	10.25	nd	S2
6	-19.78	10.20	nd	
7	-19.72	10.31	nd	
8	-19.46	10.06	nd	
9	-19.84	9.42	nd	
10	-19.97	10.13	nd	S3
11	-19.52	10.04	nd	
12	-18.52	10.02	nd	
13	-19.07	10.00	nd	
14	-18.91	10.02	nd	
15	-18.73	10.12	nd	S4
16	-19.06	9.86	nd	
17	-19.02	10.61	nd	
18	-19.50	10.47	nd	
19	-19.41	10.20	nd	
20	-19.52	9.78	nd	
21	-19.20	10.35	nd	
22	-18.91	10.59	nd	
23	-17.84	10.14	nd	
24	-17.87	9.71	nd	
25	-18.75	10.51	nd	
26	-19.40	10.51	nd	
27	-18.20	10.07	nd	
28	-18.09	10.15	nd	
29	-18.80	9.78	nd	
30	-19.00	9.98	nd	
31	-19.28	10.03	nd	S5
32	-19.11	10.02	nd	

33	-18.17	10.35	nd	
34	-17.83	10.38	nd	
35	-18.93	10.92	nd	
36	-18.50	10.68	nd	
37	-19.40	10.46	nd	
38	-18.78	10.13	nd	
39	-19.36	11.06	nd	
40	-19.43	10.67	nd	S6
41	-19.17	11.18	nd	
42	-18.75	10.41	nd	
43	-18.95	10.42	nd	
44	-18.80	10.33	nd	
45	-19.34	10.34	nd	S7
46	-19.29	10.52	nd	
47	-18.20	10.65	nd	
48	-18.26	10.74	nd	
49	-19.13	10.59	nd	
50	-18.91	11.40	nd	
51	-18.84	10.34	nd	S8
52	-19.18	10.33	nd	
53	-19.06	10.49	nd	
54	-19.58	10.81	nd	
55	-19.76	11.27	nd	
56	-19.80	10.67	nd	
57	-19.38	9.98	nd	
58	-19.19	10.09	nd	

DFO2002- con5A5

Band no.	d13C	d15N	C:N	Equiv. Index Band
3	-19.51	9.58	nd	
4	-19.46	9.82	nd	
5	-19.59	9.89	nd	
6	-19.43	10.03	nd	S2
7	-19.40	9.75	nd	
8	-19.50	9.92	nd	
9	-19.23	9.92	nd	
11	-19.58	9.87	nd	S3
12	-19.74	10.01	nd	
13	-19.37	9.76	nd	
13rep	-19.37	9.86	nd	
14	-18.24	10.02	nd	
15	-18.72	10.00	nd	
16	-19.22	9.67	nd	S4
17	-19.10	10.34	nd	
18	-18.98	10.60	nd	
20	-18.89	10.53	nd	
20rep	-19.25	10.31	nd	
21	-18.82	10.78	nd	
22	-17.75	10.25	nd	
23	-17.95	10.19	nd	
24	-19.42	9.95	nd	
25	-17.94	10.33	nd	

26	-18.70	9.97	nd	
27	-18.63	9.98	nd	
28	-18.93	9.95	nd	S5
29	-17.85	10.58	nd	
31	-19.25	10.45	nd	
32	-19.06	10.86	nd	
33	-18.68	10.58	nd	
34	-19.13	10.25	nd	S6
35	-19.03	10.68	nd	
35rep	-19.07	10.66	nd	
36	-18.49	10.42	nd	
37	-18.60	10.73	nd	
39	-19.44	10.78	nd	S7
40	-18.64	10.73	nd	
41	-18.25	10.07	nd	
42	-19.00	11.35	nd	S8
43	-19.44	10.52	nd	
45	-18.34	10.47	nd	

FOSSIL95

Band no.	d13C	d15N	C:N
1,2	-18.64	10.64	nd
3	-18.33	10.88	nd
5	-17.29	10.80	nd
6	-18.82	10.67	nd
7	-18.38	10.90	nd
8	-18.38	10.95	nd
9	-18.26	11.12	nd
10	-17.61	10.40	nd
11	-17.77	10.64	nd
12	-17.88	10.63	nd
13	-18.20	10.69	nd
14	-18.30	10.93	nd
15,16	-18.69	10.86	nd
17	-18.51	10.75	nd
18	-18.33	10.89	nd
19	-18.20	10.60	nd
20	-17.57	10.79	nd
21	-18.33	10.36	nd
22	-18.38	10.82	nd
23	-17.69	10.62	nd
24	-17.47	10.93	nd
25	-17.65	10.97	nd
27	-17.51	11.40	nd
28	-18.21	11.67	nd
29	-18.21	11.54	nd
30	-17.95	11.48	nd
43	-17.95	11.18	nd
42	-17.93	11.04	nd
41	-17.36	10.41	nd
40	-18.12	11.11	nd
39	-17.15	11.42	nd
38	-17.44	10.92	nd

31	-17.53	11.13	nd
32	-17.71	11.35	nd
33	-18.06	11.69	nd
34	-18.14	11.06	nd
35	-18.69	11.09	nd
36	-17.67	10.34	nd
37	-17.85	10.53	nd

HUD2000- 20-VG2- E1

Band no.	d13C	d15N	C:N
1	-19.77	9.94	3.09
2	-19.38	10.09	3.11
3	-19.36	9.02	3.17
3rep	-19.38	9.24	nd
4	-19.02	9.54	3.14
5	-18.90	10.14	3.22
6	-19.65	9.33	3.12
7	-19.69	9.76	3.20
8	-19.17	9.67	3.20
9	-19.48	9.33	3.23
10	-19.60	9.50	3.19
11	-19.47	9.73	3.17
12	-19.06	8.21	nd

HUD2001-055- VG15-C1

Band no.	d13C	d15N	C:N	Equiv. Band no. on A1
1	-19.61	10.64	3.20	-2
1rep	-19.67	10.54	nd	-2
2	-19.11	10.52	3.17	-1
2rep	-19.11	10.19	nd	-1
3	-19.80	10.34	3.21	0
4	-19.26	10.17	3.17	1
5	-19.16	10.15	3.19	1
6	-19.37	10.54	3.13	2
7	-19.32	10.13	3.12	3
8	-19.73	10.42	3.16	4
9	-19.24	10.36	3.14	5
10	-19.04	10.61	3.14	6
11	-18.87	10.21	3.12	7
12	-19.37	10.56	3.11	8
12rep	-19.31	10.88	nd	8
13	-19.40	10.61	3.15	9
14	-19.23	10.33	3.15	10
15	-19.43	10.70	3.14	11
16	-19.35	10.35	3.17	12
17	-18.01	10.64	3.13	13
18	-18.22	10.42	3.13	14
19	-18.49	10.90	3.10	15
20	-18.75	10.27	3.11	15
21	-19.05	10.13	3.1	16
22	-19.35	10.88	3.12	17
23	-18.66	11.01	3.17	18
24	-18.34	10.44	3.1	19

25	-18.87	11.06	3.12	20
26	-18.84	10.84	3.13	21
27	-23.98	10.71	3.14	23
28	-18.56	11.61	3.08	24
29	-18.33	11.51	3.16	25
30	-17.49	11.23	3.16	26
31	-17.17	11.08	3.13	27
32	-18.11	11.30	3.1	28
33	-18.40	10.03	3.11	29
34	-18.67	10.44	3.14	30

HUD2001-055- VG15- D1

Band no.	d13C	d15N	C:N	Equiv. Band no. on A1
1	-19.27	10.15	3.21	0
2	-19.05	10.22	3.20	1
3	-19.19	9.97	3.18	2
4	-19.07	10.07	3.13	3
5	-19.83	10.41	3.12	4
5rep	-19.70	10.63	nd	4
6	-19.25	9.97	3.13	5
7	-18.95	10.44	3.16	7
8	-19.46	10.17	3.16	8
9	-19.51	10.41	3.15	9
10	-19.17	10.13	3.16	10
11	-19.56	9.81	3.13	11
12	-19.35	9.75	3.15	12
13	-18.40	9.31	3.15	13
13rep	-18.39	9.68	nd	13
14	-18.49	9.48	3.14	14
15	-18.78	9.54	3.13	15
16	-18.93	9.65	3.13	16
17	-19.31	10.41	3.12	17
18	-18.92	10.47	3.13	18
19	-18.42	9.66	3.10	19
20	-18.99	9.84	3.12	20
21	-18.98	10.49	3.10	21
22	-18.87	10.43	3.10	22
23	-18.84	10.87	3.16	23
24	-18.41	10.76	3.13	24
25	-18.56	10.62	3.17	25
26	-17.98	10.67	3.15	26
27	-17.67	10.51	3.15	27
28	-17.27	10.33	3.15	28
29	-18.28	10.28	3.12	29
30	-18.47	9.79	3.16	30

HUD2001-055- VG15- E1

Band no.	d13C	d15N	C:N	Equiv. Band no. on A1
1	-19.96	10.03	3.21	-3
2	-19.18	9.70	3.13	-2
3	-19.28	9.69	3.14	-1
4	-19.70	9.85	3.15	0

4rep	-19.75	10.09	nd	0
5	-19.24	9.43	3.13	1
6	-18.94	9.40	3.16	2
7	-19.41	9.27	3.16	2
8	-19.20	9.23	3.17	3
9	-19.74	9.74	3.12	4
10	-19.36	9.64	3.13	5
11	-18.81	9.60	3.18	6
12	-18.79	9.15	3.15	7
13	-19.35	9.63	3.15	8
14	-19.71	9.56	3.17	9
15	-19.21	9.11	3.20	10
16	-19.53	9.18	3.17	11
17	-19.29	8.98	3.19	12
18	-18.16	9.10	3.18	13
19	-18.74	9.41	3.16	14
20	-17.90	9.17	3.16	15
21	-18.73	9.57	3.16	15
22	-18.81	9.52	3.16	16
23	-18.76	9.59	3.16	16
24	-19.28	9.55	3.13	17
25	-19.24	10.26	3.14	17
26	-19.62	9.90	3.15	18
27	-19.01	10.03	3.12	18
28	-18.66	10.09	3.20	19
29	-18.82	9.59	3.20	20

NED2002-37-1A

Band no.	d13C	d15N	C:N
1	-20.03	10.22	nd
2	-19.67	10.24	nd
3	-19.50	9.54	nd
4	-20.27	9.78	nd
5	-20.14	9.92	nd
6	-19.69	9.87	nd
7	-20.28	9.64	nd
8	-20.10	9.46	nd
9	-20.02	9.83	nd
10	-19.71	9.88	nd
11	-20.34	9.62	nd
12	-19.91	10.36	nd
13	-19.38	10.02	nd
14	-19.71	9.80	nd
15	-19.64	9.96	nd
16	-19.71	9.22	nd
18	-18.55	9.75	nd
20	-18.96	10.00	nd
21	-18.89	9.95	nd
22	-19.45	9.93	nd
23	-19.33	10.20	nd
24	-19.03	10.48	nd
25	-18.73	10.43	nd
26	-19.09	10.01	nd

27	-19.04	10.45	nd
28	-19.14	10.52	nd
29	-19.11	10.83	nd
30,31	-17.64	10.67	nd
32,33	-18.24	10.62	nd
34	-19.26	10.47	nd
35	-18.49	9.96	nd
36	-18.94	10.28	nd
38	-18.32	10.26	nd
40	-19.04	10.57	nd
41	-18.89	10.63	nd
42	-18.50	10.55	nd
43	-19.05	10.39	nd
44	-19.54	10.87	nd
45	-18.79	10.90	nd
47	-17.97	10.53	nd
49	-18.40	10.87	nd
50	-18.67	10.47	nd
51	-19.33	10.64	nd
52	-19.48	10.54	nd
53	-19.46	10.80	nd
54	-19.23	11.03	nd
55	-17.66	10.54	nd
56	-18.70	10.39	nd
57	-19.54	10.79	nd
58	-19.46	10.91	nd
59	-19.75	11.30	nd
60,61	-19.07	10.88	nd
62	-19.01	10.07	nd
63	-19.35	9.90	nd
64	-19.50	10.21	nd
65	-18.75	10.25	nd

ROPOS 639009-C4

Band no.	d13C	d15N	C:N	Equiv. Band no. on C4
1	-19.22	10.17	3.17	6
2	-19.74	9.62	3.13	7
3	-19.36	10.05	3.17	8
4	-19.15	9.60	3.14	9
5	-19.08	9.79	3.12	10
6	-19.73	9.61	3.06	11
6rep	-19.52	9.87	nd	11 rep
7	-19.61	9.60	3.15	12
8	-19.50	9.67	3.21	13
9	-19.88	9.14	3.16	14
10	-19.29	9.56	3.18	15
11	-18.68	9.91	3.16	16
12	-19.02	10.31	3.15	17
12rep	-18.98	10.30	nd	18
13	-18.60	10.17	3.16	19
14	-19.33	10.74	3.15	21
15	-19.07	9.65	3.27	23
16	-19.09	10.57	3.23	24

17	-18.53	9.55	3.15	25
18	-19.21	10.43	3.15	27
19	-19.71	10.33	3.23	28
20	-18.06	10.48	3.17	29
21	-18.18	10.34	3.19	30
22	nd	nd	3.18	31
23	-18.43	10.52	3.21	32
24	-18.85	10.03	3.19	33
25	-19.55	8.82	3.20	34

ROPOS6400013-E1

Band no.	d13C	d15N	C:N
1	-20.87	10.39	nd
2	-19.63	10.52	nd
3	-19.30	10.82	nd
4	-18.76	10.68	nd
5	-19.67	10.79	nd
6	-20.10	9.97	nd
7	-19.48	10.55	nd
8	-19.65	10.51	nd
9	-19.42	10.18	nd
10	-19.58	10.40	nd
11	-19.96	10.38	nd
12	-20.05	nd	nd
13	-19.28	10.24	nd
14	-19.77	9.94	nd
15	-19.56	10.07	nd
16	-19.67	10.29	nd
17	-19.72	10.17	nd
18	-19.78	9.82	nd
19	-19.45	10.25	nd
20	-19.15	10.32	nd
21	-19.06	10.30	nd
22	-20.05	10.41	nd
23	-20.00	9.92	nd
24	-19.60	9.57	nd
25	-19.68	9.67	nd
26	-19.66	9.53	nd
27	-18.62	10.23	nd
28,29	-18.72	10.16	nd
30	-19.59	10.58	nd

ROPOS6400016

Band no.	d13C	d15N	C:N
1	-18.65	10.17	nd
2	-18.32	10.39	nd
3	-17.63	10.30	nd
4	-18.49	10.59	nd
5,6	-17.51	10.82	nd
7	-17.27	11.51	nd
8	-17.67	11.25	nd
9	-17.35	11.01	nd
10	-17.55	11.01	nd

11	-17.26	11.34	nd
12	-18.32	10.60	nd
13,14	-18.25	11.16	nd
15,16	-17.86	10.47	nd
17,18	-17.08	11.40	nd
19,20	-17.89	10.98	nd
21,22	-18.08	11.11	nd
23	-17.79	11.27	nd
24	-18.83	10.73	nd
25	-18.79	10.72	nd
26	-18.70	10.37	nd
27	-18.17	10.81	nd
28	-18.12	11.04	nd
29,30	-17.98	11.33	nd
31	-17.72	11.38	nd
32	-17.90	11.43	nd
33	-17.63	10.96	nd
34	-17.88	10.96	nd
35	-17.98	11.50	nd
36	-17.36	10.89	nd
37	-17.79	10.81	nd
38	-17.57	10.79	nd
39	-18.09	10.66	nd
40	-18.20	11.09	nd
41	-17.93	10.79	nd
42	-17.83	11.26	nd
43	-17.75	11.37	nd
44,45	-18.05	11.59	nd
46,47	-18.41	11.24	nd
48,49	-17.99	10.49	nd
50,51	-18.04	10.85	nd
52	-16.83	10.89	nd
53	-17.51	10.63	nd
54	-17.96	10.63	nd
55	-17.40	10.41	nd
56	-17.14	10.11	nd
57	-17.81	9.56	nd
58	-17.04	10.41	nd
59	-18.13	10.20	nd
60	-18.12	10.48	nd
61	-18.50	10.06	nd

GEOTOP STABLE ISOTOPE AND C:N RESULTS
TISSUE AND OTHER SAMPLES:

Specimen	Fraction	Sample no.	d13C	d15N	C:N
NE Channel samples:					
ROPOS 637052	tissue	1	-23.559	10.348	nd
ROPOS 637052	tissue	1 rep	-23.477	10.528	nd
ROPOS 637052	tissue	2	-23.61	10.33	7.96
ROPOS 637052	tissue	3	-23.69	10.22	7.16
ROPOS 637052	tissue	4	-23.72	10.10	7.98

FOSSIL95	gorgonin	layerB	-18.08	10.35	3.53
FOSSIL95	gorgonin	layerD1	-17.76	10.66	3.54
FOSSIL95	gorgonin	layerD2	-18.71	10.87	3.46
FOSSIL95	gorgonin	layerD3	-18.84	11.58	3.36
FOSSIL95	gorgonin	layerD4	-18.57	11.09	3.47
FOSSIL95	gorgonin	layerD5	-17.75	11.37	3.41
R639009	tissue	tiss1	-23.74	10.08	7.49
R639009	tissue	tiss2	-24.13	10.18	7.74
R639009	tissue	tiss3	-23.88	10.11	7.13
DFO-2002-con5	tissue	2 cm	-23.99	10.14	6.46
DFO-2002-con5	tissue	10 cm	-24.07	10.52	8.53
DFO-2002-con5	tissue	20 cm	-23.35	10.76	6.72
DFO-2002-con5	tissue	30 cm	-24.07	10.51	7.31
DFO-2002-con5	tissue	50 cm	-23.86	10.96	7.22
Smithsonian samples:					
4142	tissue	1	-19.51	12.79	4.75
4544	tissue	1	-18.62	10.45	3.33
52199	tissue	1	-14.93	12.53	4.06
52199	tissue	1 rep	-18.24	nd	nd
56993	tissue	1	-21.00	10.77	4.49
56993	tissue	1 rep	-21.40	10.60	nd
56993	tissue	2	-21.69	10.59	4.57
56993	tissue	3	-20.87	10.72	4.50
58171	tissue	1	-22.33	7.66	4.13
58171	tissue	2	-21.73	7.89	4.12
58171	tissue	3	-22.09	7.73	4.12
15875	gorgonin	1	-19.10	10.70	3.33
15875	gorgonin	2	-19.52	11.35	3.47
1010257	tissue	1	-23.76	9.30	7.37
1010257	tissue	2	-23.78	9.26	6.56
1010257	tissue	3	-23.72	8.89	6.74
1010257	tissue	3 rep	-23.81	8.90	nd
1010785	tissue	1	-19.38	12.70	6.40
1010785	tissue	2	-19.42	12.95	6.30
1010785	tissue	3	-19.66	12.61	5.97
Other Pacific/Japan Samples:					
QC98	tissue	1	-20.97	13.40	7.07
QC98	tissue	2	-21.37	13.13	7.75
QC98	tissue	3	-21.17	13.25	8.20
QC98	gorgonin	1	-17.87	12.66	3.21
QC98	gorgonin	2	-18.11	12.75	3.27
QC98	gorgonin	3	-17.81	13.04	3.19
OHOTSK	tissue	1	-22.32	13.03	4.90
OHOTSK	tissue	1 rep	-22.49	12.96	nd
OHOTSK	tissue	2	-22.54	12.73	4.85
OHOTSK	gorgonin	1	-19.38	10.71	3.20
OHOTSK	gorgonin	2	-19.54	10.19	3.24
KIS 2002	tissue	1	-19.42	13.80	5.72
KIS 2002	gorgonin	outer1	-16.67	12.71	3.39

KIS 2002	gorgonin	outer2	-16.26	12.16	3.21
KIS 2002	gorgonin	outer3	-15.46	11.94	3.23
KIS 2002	gorgonin	middle1	-16.23	12.40	3.25
KIS 2002	gorgonin	middle2	-15.97	12.38	3.21
KIS 2002	gorgonin	inner1	-15.91	12.49	3.23
KIS 2002	gorgonin	inner1 rep	-16.04	12.34	nd
KIS 2002	gorgonin	inner2	-16.12	11.68	3.29

Appendix D

Hydrographic and $\delta^{15}N$ data from Hudson and Teleost cruises

Cruise	Date d/m/y	Line/Set	Stn	Long. dd	Lat. dd	Bottle ID	Depth	Sal psu	Temp deg. C	Sigma-T	NO3/NO2 microMole	Silicate microMole	Phosphate microMole	d15N-NO3 per mille
HUD2005016	6/2/2005	143	7	-54.287	54.955	286039	364	34.800	3.600	27.671	15.812	9.343	1.025	5.035
HUD2005016	6/2/2005	143	7	-54.287	54.955	286040	331	34.745	3.507	27.635	15.825	9.753	1.023	NaN
HUD2005016	6/2/2005	143	7	-54.287	54.955	286041	291	34.717	3.440	27.620	15.740	9.812	1.029	NaN
HUD2005016	6/2/2005	143	7	-54.287	54.955	286042	250	34.686	3.347	27.603	15.633	9.895	1.022	NaN
HUD2005016	6/2/2005	143	7	-54.287	54.955	286043	200	34.556	2.928	27.539	15.125	10.183	1.014	NaN
HUD2005016	6/2/2005	143	7	-54.287	54.955	286044	151	34.240	1.747	27.383	14.003	10.218	0.990	NaN
HUD2005016	6/2/2005	143	7	-54.287	54.955	286045	99	33.854	0.431	27.158	11.946	10.334	0.944	5.567
HUD2005016	6/2/2005	143	7	-54.287	54.955	286046	81	33.736	0.006	27.086	11.384	10.602	0.943	NaN
HUD2005016	6/2/2005	143	7	-54.287	54.955	286047	60	33.521	-0.409	26.931	10.088	10.505	0.905	NaN
HUD2005016	6/2/2005	143	7	-54.287	54.955	286048	51	33.445	-0.481	26.873	9.280	10.228	0.877	5.817
HUD2005016	6/2/2005	143	7	-54.287	54.955	286050	40	33.316	-0.598	26.773	8.134	9.732	0.845	NaN
HUD2005016	6/2/2005	143	7	-54.287	54.955	286051	21	32.604	0.363	26.154	4.361	7.230	0.672	NaN
HUD2005016	6/2/2005	143	7	-54.287	54.955	286052	10	32.249	1.881	25.777	1.551	6.646	0.464	10.190
HUD2005016	6/2/2005	143	7	-54.287	54.955	286053	2	32.256	1.855	25.784	1.389	6.599	0.451	NaN
HUD2005016	6/2/2005	147	6	-54.475	54.756	286054	237	34.446	2.516	27.487	14.437	10.759	1.029	5.055
HUD2005016	6/2/2005	147	6	-54.475	54.756	286055	201	34.167	1.510	27.342	13.411	10.720	1.002	NaN
HUD2005016	6/2/2005	147	6	-54.475	54.756	286056	150	33.977	0.835	27.233	12.438	10.409	0.975	NaN
HUD2005016	6/2/2005	147	6	-54.475	54.756	286057	124	33.727	-0.026	27.080	11.158	10.371	0.954	NaN
HUD2005016	6/2/2005	147	6	-54.475	54.756	286058	99	33.558	-0.476	26.964	10.814	10.487	0.961	5.897
HUD2005016	6/2/2005	147	6	-54.475	54.756	286059	80	33.508	-0.584	26.928	10.643	10.481	0.953	NaN
HUD2005016	6/2/2005	147	6	-54.475	54.756	286060	61	33.196	-0.959	26.690	9.020	10.212	0.920	NaN
HUD2005016	6/2/2005	147	6	-54.475	54.756	286061	51	33.027	-0.861	26.550	8.127	9.279	0.892	6.332
HUD2005016	6/2/2005	147	6	-54.475	54.756	286062	41	32.892	-1.098	26.448	8.131	9.194	0.906	NaN
HUD2005016	6/2/2005	147	6	-54.475	54.756	286063	30	32.699	-1.225	26.295	7.925	8.942	0.893	NaN
HUD2005016	6/2/2005	147	6	-54.475	54.756	286064	20	32.582	-0.998	26.194	6.975	7.621	0.843	NaN
HUD2005016	6/2/2005	147	6	-54.475	54.756	286065	10	32.381	0.872	25.947	NaN	NaN	NaN	NaN
HUD2005016	6/2/2005	147	6	-54.475	54.756	286067	11	32.375	0.910	25.940	0.902	3.115	0.412	NaN
HUD2005016	6/2/2005	147	6	-54.475	54.756	286068	2	32.158	1.756	25.713	1.605	5.695	0.456	NaN
HUD2005016	6/2/2005	154	5	-54.757	54.492	286073	190	33.947	0.741	27.216	12.606	10.885	0.994	5.558
HUD2005016	6/2/2005	154	5	-54.757	54.492	286074	151	33.580	-0.416	26.980	10.993	10.467	0.952	NaN
HUD2005016	6/2/2005	154	5	-54.757	54.492	286075	126	33.448	-0.662	26.883	10.458	10.255	0.958	NaN
HUD2005016	6/2/2005	154	5	-54.757	54.492	286076	100	33.146	-1.028	26.652	9.648	10.335	0.963	6.517
HUD2005016	6/2/2005	154	5	-54.757	54.492	286077	80	33.006	-1.172	26.543	9.232	10.378	0.951	NaN
HUD2005016	6/2/2005	154	5	-54.757	54.492	286078	60	32.833	-1.310	26.407	8.771	10.092	0.941	NaN

Cruise	Date d/m/y	Line/Set	Stn	Long. dd	Lat. dd	Bottle ID	Depth	Sal psu	Temp deg. C	Sigma-T	NO3/NO2 microMole	Silicate microMole	Phosphate microMole	d15N-NO3 per mille
HUD2005016	6/2/2005	154	5	-54.757	54.492	286079	50	32.762	-1.371	26.351	8.509	9.871	0.944	6.221
HUD2005016	6/2/2005	154	5	-54.757	54.492	286080	41	32.664	-1.383	26.272	8.021	9.192	0.924	NaN
HUD2005016	6/2/2005	154	5	-54.757	54.492	286081	30	32.548	-1.344	26.177	7.182	8.686	0.883	NaN
HUD2005016	6/2/2005	154	5	-54.757	54.492	286082	20	32.485	-1.289	26.124	6.854	8.589	0.869	NaN
HUD2005016	6/2/2005	154	5	-54.757	54.492	286083	10	32.249	1.614	25.795	1.152	5.281	0.466	9.420
HUD2005016	6/2/2005	154	5	-54.757	54.492	286085	2	32.225	1.759	25.766	0.795	5.217	0.439	NaN
Teleost-633	7/18/2005	48	36	-57.262	44.713	274608	300	34.777	5.706	27.414	19.223	18.524	1.459	5.490
Teleost-633	7/18/2005	48	36	-57.262	44.713	274609	200	34.803	8.388	27.061	17.756	11.753	1.321	5.430
Teleost-633	7/18/2005	48	36	-57.262	44.713	274610	100	32.680	0.085	26.230	5.538	4.866	1.078	5.420
Teleost-633	7/18/2005	48	36	-57.262	44.713	274611	50	32.355	1.957	25.856	4.926	4.268	0.885	4.588
Teleost-633	7/18/2005	48	36	-57.262	44.713	274612	25	32.220	3.984	25.577	0.235	0.512	0.500	NaN
Teleost-633	7/18/2005	48	36	-57.262	44.713	274613	5	31.054	15.258	22.878	0.185	0.329	0.369	NaN
Teleost-633	7/26/2005	48	36	-57.262	44.713	274614	1	28.833	15.276	21.168	0.187	0.300	0.357	NaN
Teleost-633	7/19/2005	50	202	-57.765	44.274	274619	488	34.899	4.519	27.651	17.061	10.855	1.187	5.218
Teleost-633	7/19/2005	50	202	-57.765	44.274	274620	400	34.915	5.096	27.597	19.018	12.573	1.325	5.312
Teleost-633	7/19/2005	50	202	-57.765	44.274	274621	200	35.382	11.175	27.042	20.788	10.713	1.340	5.226
Teleost-633	7/19/2005	50	202	-57.765	44.274	274622	100	35.120	12.307	26.624	8.262	3.736	0.732	4.499
Teleost-633	7/19/2005	50	202	-57.765	44.274	274623	50	34.425	12.280	26.089	0.778	1.811	0.408	NaN
Teleost-633	7/19/2005	50	202	-57.765	44.274	274624	25	35.617	17.112	25.962	0.231	1.644	0.174	NaN
Teleost-633	7/19/2005	50	202	-57.765	44.274	274625	5	31.763	16.620	23.120	0.214	0.423	0.279	NaN
Teleost-633	7/19/2005	50	202	-57.765	44.274	274626	1	29.083	16.503	21.093	0.216	0.355	0.255	NaN
Teleost-633	7/25/2005	106	923	-61.112	43.262	274835	297	34.915	6.497	27.421	19.643	13.974	1.350	5.275
Teleost-633	7/25/2005	106	923	-61.112	43.262	274836	200	35.011	8.583	27.193	19.834	13.266	1.349	5.333
Teleost-633	7/25/2005	106	923	-61.112	43.262	274837	100	35.293	11.518	26.909	11.266	5.890	0.841	5.145
Teleost-633	7/25/2005	106	923	-61.112	43.262	274838	50	34.242	8.672	26.577	7.651	4.602	0.773	5.282
Teleost-633	7/25/2005	106	923	-61.112	43.262	274839	25	37.500	9.672	28.964	NaN	NaN	NaN	NaN
Teleost-633	7/25/2005	106	923	-61.112	43.262	274840	5	32.661	18.594	23.337	0.031	0.629	0.199	NaN
Teleost-633	7/25/2005	106	923	-61.112	43.262	274841	1	30.260	18.574	21.509	0.006	0.569	0.195	NaN

Appendix E
Copyright Permissions Letters

ELSEVIER

17 May 2006 Our ref: CT/mm/may 06.J014

Mr Owen Sherwood
Dalhousie University
osherwood@dal.ca

Dear Mr Sherwood

GEOCHIMICA ET COSMOCHIMICA ACTA, *Accepted for publication, Sherwood, "Late Holocene radiocarbon…"*

As per your letter dated 15 May 2006, we hereby grant you permission to reprint the aforementioned material at no charge **in your thesis** subject to the following conditions:

1. If any part of the material to be used (for example, figures) has appeared in our publication with credit or acknowledgement to another source, permission must also be sought from that source. If such permission is not obtained then that material may not be included in your publication/copies.

2. Suitable acknowledgment to the source must be made, either as a footnote or in a reference list at the end of your publication, as follows:

   "Reprinted from Publication title, Vol number, Author(s), Title of article, Pages No., Copyright (Year), with permission from Elsevier".

3. Reproduction of this material is confined to the purpose for which permission is hereby given.

4. This permission is granted for non-exclusive world **English** rights only. For other languages please reapply separately for each one required. Permission excludes use in an electronic form. Should you have a specific electronic project in mind please reapply for permission.

5. This includes permission for the Library and Archives of Canada to supply single copies, on demand, of the complete thesis. Should your thesis be published commercially, please reapply for permission.

Yours sincerely

C. Truter

Clare Truter
Deputy Rights Manager, S&T

Date: Wed, 17 May 2006 08:42:55 +0200 [03:42:55 AM ADT]
From: John Austin <john@int-res.com>Add to Address book (john@int-res.com)
To: OSHERWOO@dal.ca
Subject: Fwd: Copyright agreement - form attached
Part(s): Download All Attachments (in .zip file)
Headers: Show All Headers

Publisher permission is herewith granted for the purpose described below
provided adequate acknowledgement is made to the original source of publication.
Helga Witt
Administrative Director
Inter-Research, Science Center

> X-ATTACHEXT: DOC
> X-SpamCatcher-Score: 2 [X]
> Date: Mon, 15 May 2006 13:41:49 -0300
> From: Owen Sherwood <OSHERWOO@DAL.CA>
> To: john@int-res.com
> Subject: Copyright agreement - form attached
>
> May 15, 2006
>
>Marine Ecology Progress Series
>Ecology Institute
>Oldendorf/Luhe
>Germany
>
>Dear MEPS,
>I am preparing my PhD thesis for submission to the Faculty of Graduate Studies at Dalhousie
>University, Halifax, Nova Scotia, Canada. I am seeking your permission to include a manuscript version of >the following papers as a chapter in the thesis:
>
>Radiocarbon evidence for annual growth rings in the deep-sea octocoral Primnoa resedaeformis. By: OA >Sherwood, DB Scott, MJ Risk, TP Guilderson. Mar Ecol Prog Ser 301:129-134 (2005).
>
>Stable isotopic composition of deep-sea gorgonian corals *Primnoa* spp.: a new archive of surface >processes. OA Sherwood, JM Heikoop, DB Scot, MJ Risk, TP Guilderson, RA McKinney. Mar Ecol Prog >Ser 301:135-148 (2005).
>
>Canadian graduate theses are reproduced by the Library and Archives of Canada (formerly National >Library of Canada) through a non-exclusive, world-wide license to reproduce, loan, distribute, or sell >theses. I am also seeking your permission for the material described above to be reproduced and distributed >by the LAC(NLC). Further details about the LAC(NLC) thesis program are available on the LAC(NLC) >website (www.nlc-bnc.ca). Full publication details and a copy of this permission letter will be included in >the thesis.
>
>Yours sincerely,
>Owen Sherwood
--
--
Inter-Research Science Centre
Nordbuente 23,
21385 Oldendorf/Luhe,
Germany

Tel: (+49) (4132) 7127 Email: john@int-res.com
Fax: (+49) (4132) 8883 www.int-res.com